

**Identification and characterization of tissue-resident
memory T cells in humans**

Brahma Vencel Kumar

Submitted in partial fulfillment of the
requirements for the degree
of Doctor of Philosophy
under the Executive Committee
of the Graduate School of Arts and Sciences

COLUMBIA UNIVERSITY

2018

©2017

Brahma Vencel Kumar

All rights reserved

ABSTRACT

Identification and characterization of tissue-resident memory T cells in humans

Brahma Vencel Kumar

Memory T cells are critical for maintaining lifelong immunity by protecting against reinfection with previously encountered pathogens. In recent years, a subset of memory T cells termed tissue-resident memory T cells (TRM) has emerged as the primary mediator of protection at many tissue sites. Numerous studies in mice have demonstrated that TRM accelerate pathogen clearance compared with other subsets of memory T cells. The defining characteristic of TRM is that they are retained within tissues and do not circulate in the blood. The lack of TRM in blood has proved to be a barrier for investigating the role of TRM in healthy humans. As a result, there are many outstanding questions about TRM biology in humans, including which phenotypic markers identify TRM, if TRM represent a unique memory subset, as well as defining transcriptional and functional characteristics of this subset.

Through a unique collaboration with the local organ procurement agency, we obtained samples from >15 tissue sites from healthy organ donors of all ages. We found that the surface marker CD69 was expressed by memory CD4⁺ and CD8⁺ T cells in multiple tissues including spleen and other lymphoid tissues, lung, and intestines, but not in blood, suggesting that this marker may identify TRM in human tissues. We identify a core transcriptional signature that distinguishes CD69⁺ memory T cells in tissues from CD69⁻ memory T cells in tissues and blood with key homologies to the transcriptional profile of TRM in mice, suggesting that CD69 expression identifies TRM in humans. We show that human TRM have a distinct profile of adhesion and migration markers, and a unique dual functional capacity encompassing effector

cytokine production but also the upregulation of inhibitory markers and the ability to produce IL-10 upon stimulation. These results suggest unique adaptations for TRM to maintain long-term residence within tissues and carry out pathogen clearance.

We found substantial heterogeneity within human TRM in lymphoid and mucosal tissue sites, including a substantial fraction (40-60%) of TRM in various human tissues with the ability to efflux fluorescent dyes. These efflux(+) TRM had phenotypic and transcriptional characteristics associated with quiescence, including expression of immunomodulatory markers, reduced expression of exhaustion markers, and reduced turnover at steady state. Upon TCR stimulation, efflux(+) TRM produced lower levels of proinflammatory cytokines and cytotoxic molecules but had a superior ability to proliferate compared with efflux(-) TRM. However, efflux(+) also had an enhanced capacity for IL-17 production along with transcriptional features of IL-17 signaling following stimulation. Overall, these studies establish universal properties of human TRM and hint at the function of distinct TRM subsets in mediating tissue immunity.

TABLE OF CONTENTS

LIST OF FIGURES	iii
LIST OF TABLES	vi
LIST OF ABBREVIATIONS	vii
ACKNOWLEDGEMENTS	viii
DEDICATION	x
CHAPTER 1: Introduction	1
Section 1.1: Overview of the T cell response to infection.....	1
Section 1.2: Human T cell development and maintenance of naïve T cells	7
Section 1.3: T cell activation and subset differentiation.....	13
Section 1.4: Memory T cells.....	17
Section 1.5: Tissue-resident memory T cells (TRM).....	21
Section 1.6: Thesis aims.....	40
CHAPTER 2: Materials and methods	44
Section 2.1: Acquisition and isolation of T cells from human tissues.....	44
Section 2.2: Flow cytometric analysis of human T cells.....	49
Section 2.3: Functional Assays.....	53
Section 2.4: Whole transcriptome profiling by RNA Sequencing.....	54
Section 2.5: Imaging of human lymphoid tissues.....	63
Section 2.6: Statistical tests.....	64
CHAPTER 3: Human Tissue-Resident Memory T Cells Are Defined by Core Transcriptional and Functional Signatures in Lymphoid and Mucosal Sites	65
Section 3.1: Introduction.....	66

Section 3.2: Results.....	66
Section 3.3: Discussion.....	118
CHAPTER 4: Dye efflux capacity defines a functionally distinct subset of human CD8⁺ tissue resident memory cells.....	123
Section 4.1: Introduction.....	124
Section 4.2: Results.....	126
Section 4.3: Discussion.....	164
CHAPTER 5: Conclusions.....	167
REFERENCES.....	180
APPENDICES.....	199
Appendix A. The functional profile of naïve and memory T cells with aging.....	199
Appendix B. Functional properties of CD103 ⁺ vs CD103 ⁻ human TRM.....	207
Appendix C. Imaging of frozen sections of human lymph nodes.....	210
Appendix D. Accepted Abstracts.....	216
Appendix E. Abstracts of contributing author manuscripts.....	218
Appendix F. Curriculum Vitae.....	222

LIST OF FIGURES

- Figure 1.1. Overview of the T cell development and response to infection.
- Figure 1.2. Distribution of TRM phenotype cells in human tissues.
- Figure 2.1. Tissue sites received from organ donors.
- Figure 2.2. RNA-Sequencing workflow used in this study.
- Figure 3.1. CD69⁺ memory T cells are prevalent in tissues and do not show features of activation.
- Figure 3.2. Sorting strategy for RNA Sequencing.
- Figure 3.3. CD69 expression defines a transcriptionally distinct memory subset in humans with features of tissue residency.
- Figure 3.4. PCA of randomly selected genes.
- Figure 3.5. A core gene signature defines tissue CD69⁺ memory T cells distinct from circulating CD69⁻ cells in tissues and blood.
- Figure 3.6. Expression of CD49a, CD103, and CXCR6.
- Figure 3.7. Expression of PD-1, CD101, and CX3CR1.
- Figure 3.8. Comparison of the human and mouse TRM transcriptome.
- Figure 3.9. T-bet and Eomes expression by human memory T cells.
- Figure 3.10. TCR repertoire overlap.
- Figure 3.11. TCR clonal analysis, turnover, and function of CD69⁺ and CD69⁻ cells.
- Figure 3.12. Transcript levels of cytokines in TRM and TEM
- Figure 3.13. Cytokine production by CD103⁺ and CD103⁻ human CD69⁺ memory T cells.
- Figure 3.14. Lineage and tissue-specific transcription and phenotypic profiles in human CD69⁺ memory T cells.

Figure 3.15. Tissue- and lineage- specific genes.

Figure 3.16. CCR9 Expression in CD69⁺ and CD69⁻ memory T cells.

Figure 3.17. TRM are a phenotypically distinct subset across multiple tissues.

Figure 3.18. t-SNE analysis of TRM and TEM from additional donor.

Figure 3.19. A core signature of human TRM.

Figure 4.1. Identification of Memory T cell subsets in Humans.

Figure 4.2. A subset of memory CD8⁺ T cells across human tissues effluxes fluorescent dyes.

Figure 4.3. Dye efflux yields populations with high and low mitochondrial fluorescence staining.

Figure 4.4. CD8⁺ TRM have heightened capacity for dye efflux across human tissues.

Figure 4.5. MAIT cells are a minor subpopulation of CD69⁺ human memory CD8⁺ T cells.

Figure 4.6. Efflux(+) TRM have unique transcriptional properties.

Figure 4.7. Fold Changes of Additional Gene Categories.

Figure 4.8. Efflux(+) TRM exhibit a resting phenotype at steady-state.

Figure 4.9. Additional phenotypic analysis of efflux(+) CD8⁺ TRM.

Figure 4.10. The transcriptional response of TRM to stimulation.

Figure 4.11. Dissecting the transcriptional response to stimulation by efflux status.

Figure 4.12. Dye efflux marks functionally distinct subsets of TRM.

Figure 4.13. T-bet and Eomes expression

Figure 5.1. Distribution and characteristics of TRM in human tissues.

Figure 5.2. Proposed cooperativity of TRM subsets.

Figure 5.3. Human TRM have core and subset-specific features.

Figure A.A.1. Naïve T cells retain function with age.

Figure A.A.2. IL-4 and IL-10 Production by Naïve and Memory T cells

Figure A.B.1. Localization of CD69⁺ and CD69⁻ T cells within human lymph nodes.

Figure A.C.1. Elevated CRTAM expression by human lung TRM.

Figure A.C.2. Crtam is expressed exclusively by Lung TRM in mice.

Figure A.C.3. Schematic of OT-II Flu Memory Model

LIST OF TABLES

Table 1.1. Overview of major T cell subsets in humans.

Table 2.1. List of antibodies used in flow cytometry.

Table 3.1. List of all donors used in this study.

Table 3.2. RNA-Seq QC Summary.

Table 3.3. Details about genes in core signature.

Table 3.4. Significant pathways common to all CD69+ subsets.

Table 4.1. RNA-Seq QC Summary.

Table A.A.1. Tabular data for all cytokines measured in this study.

List of Abbreviations

TRM: Tissue-resident memory T cells.

TEM: Effector memory T cells. Defined by the phenotype CD45RA-CCR7-.

TCM: Central memory T cells. Defined by the phenotype CD45RA-CCR7+.

LN: lymph node.

BM: bone marrow.

CBA: Cytometric bead array. This is the name of a kit used to measure cytokine levels in supernatants.

PMA: phorbol myristate acetate. This is used in conjunction with ionomycin to stimulate T cells.

ACKNOWLEDGEMENTS

I have had an amazing experience during my PhD and for that I would first like to thank my mentor, Dr. Donna Farber. I was given the opportunity to work on cutting-edge projects and also the complete freedom to pursue any ideas that interested me. Dr. Farber provided the scientific guidance and resources for me to be successful in this process, and she has always been very supportive and encouraging, even when there were no positive developments in my projects. I am thankful to have been able to conduct my research in a lab that is highly collaborative and friendly, and I have always felt that Dr. Farber and all members of the lab are fully invested in my scientific success and personal well-being. It was thanks to this environment that I always felt highly motivated and truly enjoyed doing science, and was able to learn many new techniques by working together with other lab members. I am extremely grateful for the experience I have had, for the skills I have learned, and for the future successes I will have as a result of my experiences here.

I am grateful to have been part of a collaboration through which I am able to study human immunology by using tissues obtained from healthy organ donors. For this, I would like to thank our collaborators at the local organ procurement agency, LiveOnNY, for making this possible as well as the organs donors and their families for their generous donations to science. This collaboration was also made possible by Dr. Dustin Carpenter and Dr. Takashi Senda, our on-call surgeons, who worked tirelessly through the night many times to harvest donor tissues.

I am very fortunate to have been a part of two collaborative projects. First off, I worked closely with Dr. Wenji Ma and Dr. Yufeng Shen, who played a major role in the analysis of RNA-Sequencing data presented in Chapter 3. That project, and the publication that resulted from it, would not have been possible without the efforts of Dr. Ma and Dr. Shen. Next, I have been working closely with Radomir Kratchmarov and Dr. Steven Reiner on a project investigating a

population of T cells that can efflux fluorescent dyes (Chapter 4). This project would not have been possible without Radomir, who helped generate with the original idea for this project and performed many of the experiments.

I would like to thank the members of my thesis committee: Dr. Megan Sykes, Dr. Peter Sims, and Dr. Uttiya Basu, as well as most recently Dr. Arnold Han. The committee members have given me valuable advice and guidance throughout my PhD that has helped improve my projects and helped me develop as a scientist. I would also like to thank Zaia Sivo, Senior Program Manager of the Integrated Graduate Program, and Dr. Patrice Spitalnik, Dr. Ron Liem, Dr. Steven Reiner, and Jeffrey Brandt of the MD/PhD program, for supporting me throughout my time at Columbia.

I would like to thank Dr. Attila Bacsi and Dr. Kitti Pazmandi of the University of Debrecen, Hungary. Prior to starting in the MD/PhD program at Columbia, I worked under the supervision of Drs. Bacsi and Pazmandi. This was my first experience doing bench science full-time, and under their guidance I learned many of the laboratory skills that were instrumental to my success as a graduate student.

I am grateful to have worked together with all members of the Farber Lab. I would first like to mention Michelle Miron, who sat next to me for these past few years. Michelle has helped me with all of my projects and has always been there to talk when I need scientific advice or personal support. I would also like to thank Daniel Paik for scientific advice, moral support, and friendship. I would like to thank Joe Thome, a former graduate student, who mentored me during my summer rotation and at the beginning of my PhD.

I would like to thank my family for always supporting me and playing a critical role in my successes. Finally, I would like to thank my girlfriend Rita, who has encouraged and reassured me through this whole process.

DEDICATION

This work is dedicated to the millions of patients who suffer from immune mediated disease with no cure, in the hope that this small advance in human immunology may contribute to the body of knowledge that can improve clinical outcomes.

CHAPTER 1: Introduction

Adapted and expanded significantly from: **Kumar, B.V.**, Connors, T., and Farber D.L. (2017)

Human T cells and immune responses: impact of place and time. *Immunity*. Accepted.

Section 1.1: Overview of T cell immunity in humans

T lymphocytes, or T cells, are part of the adaptive immune system and play a major role in combatting pathogens via a variety of mechanisms including killing of infected cells, coordination of immune responses, and secretion of anti-viral cytokines. T cells also play an important role in protecting against tumors and maintaining immune self-tolerance, and further are implicated as major drivers of many inflammatory and autoimmune diseases. In order to carry out these diverse functions, T cells exist as many different subtypes, with each subtype having unique characteristics and a distinct role in the immune response.

T cells development occurs in the thymus, where progenitors originating from the bone marrow develop into mature naïve T cells that together are capable of recognizing millions of diverse antigens. These naïve T cells populate virtually all tissues sites of the human body early in life, and upon infection, naïve T cells that are specific for an invading pathogen become activated and expand into a large population of effector T cells [1, 2]. This marks the first phase of the T cell immune response: clonal expansion. This large pool of effector T cells eliminates the invading pathogen from the body via diverse mechanisms. The next phase of the T cell response is the contraction phase, during which the majority of the effector T cells that were generated to combat infection die by apoptosis [1, 2]. The third and final phase of the T cell response is memory generation, in which a small fraction of the effectors generated differentiate into a variety of memory subsets. An overview of this process, as well as basic events in T cell development, is

shown in Figure 1.1. These memory T cells protect the body against subsequent encounters with the same pathogen. Memory T cells are extremely long-lived and can protect the body for years or even decades after the initial infection.

The establishment and maintenance of immune responses, homeostasis, and memory depends on T cells. T cells express a receptor with the potential to recognize diverse antigens from pathogens, tumors, and the environment, and also maintain immunological memory and self-tolerance. T cells are also implicated as major drivers of many inflammatory and autoimmune diseases. The *in vivo* functional role of T cells in immunity and immunopathology and the underlying mechanisms involved have been largely elucidated from mouse models, and have led to the development and advancement of immune-based cures and immunotherapies in humans [3, 4]. However, the power and utility of mouse models to test hypotheses depends on reducing the scope of inquiry to one type of infection or disease perturbation over a defined time period in sterile, pathogen-free conditions. By contrast, humans are continuously exposed to multiple benign and pathogenic microorganisms, harbor chronic pathogens, yet can survive for many decades free of major infections even in advanced years [5].

Additionally, the role of T cells in the immune response is not uniform throughout the human body. Recent studies from both mice and humans have shown that anatomic localization is intimately linked to T cell function and that each tissue has a unique immune microenvironment [6-9]. Different T cell subsets are maintained in different tissues, and immune responses are highly compartmentalized. An example of this is a subset of memory T cells termed tissue-resident memory T cells (TRM) that do not circulate out their tissue of residence, and these cells are the primary mediators of protection against infection at many sites [10]. By maintaining TRM specific for pathogens that are encountered in a particular tissue, the immune system is able to clear

pathogens efficiently without expending resources to maintain unnecessary populations. Thus, to understand the role of T cells in humans it is critical to examine T cells within a variety of tissues and not just blood, which only contains 2-3% of the total T cell complement [11, 12]. To address this, our laboratory has established a collaboration with LiveOnNY, the local organ procurement agency, through which we receive samples from >15 tissues from healthy organ donors across all ages. This unique tissue resource has enabled investigation of T cells not found in the blood and has driven novel insights about *in situ* responses within tissues [13-19].

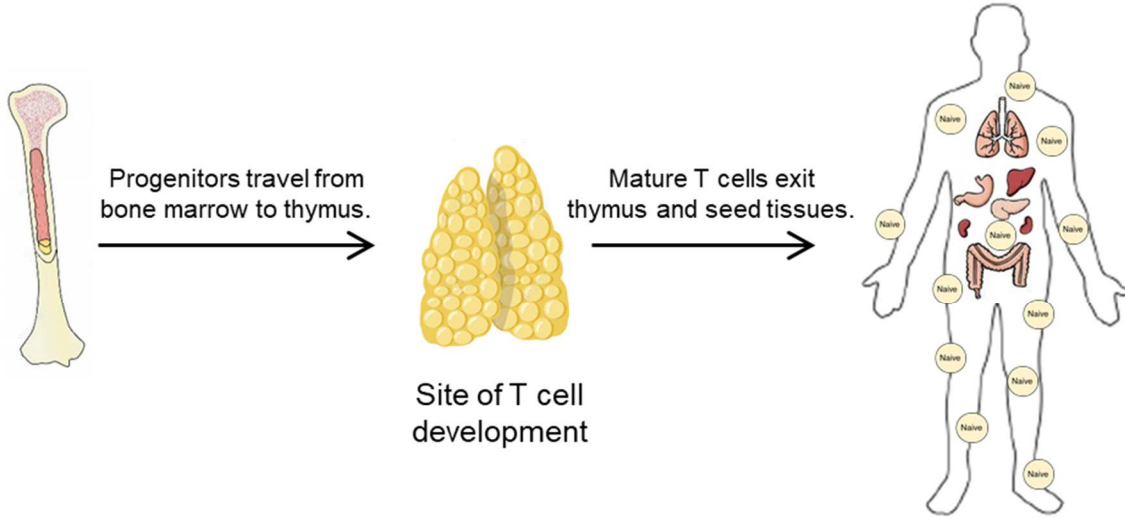
Figure 1.1. Overview of the T cell development and response to infection.

(A) Overview of T cell development. T cell precursors emerge from the bone marrow and travel to the thymus, which is the primary site of T cell development. In the thymus, the cells undergo TCR rearrangement and positive and negative selection to generate mature naïve T cells. These naïve T cells emerged from the thymus and seed virtually all tissues of the body in early life.

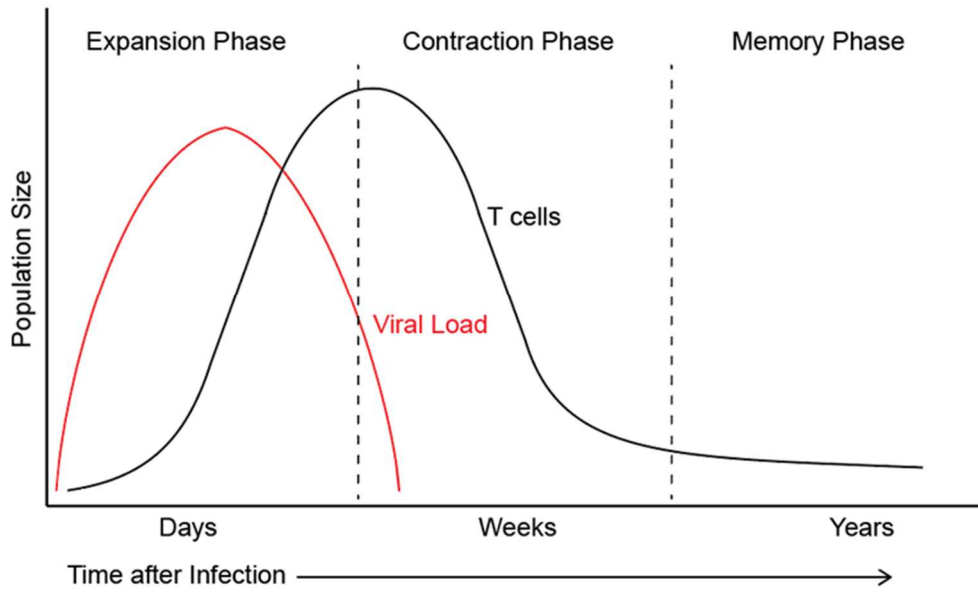
(B-C) Overview of the T cell response to infection. **(B)** Kinetics of the T cell response to infection. Following infection, there are 3 phases of the T cell response to infection: the expansion phase, during which activated cells proliferate to generate effectors; the contraction phase, during which effectors die following infection clearance; and the memory phase, during which memory T cells form and remain in the body for time periods up to years or decades. **(C)** A naïve T cell is first activated upon recognition of cognate antigen and appropriate costimulatory signals presented by dendritic cells. Activated naïve cells expand into a large population of effector cells which help clear the infection. Following infection, the majority of effector T cells die by apoptosis while a small fraction persist in the form of various memory T cell subsets which all have unique tissue distributions.

Note: some organ images taken from Google Image search results.

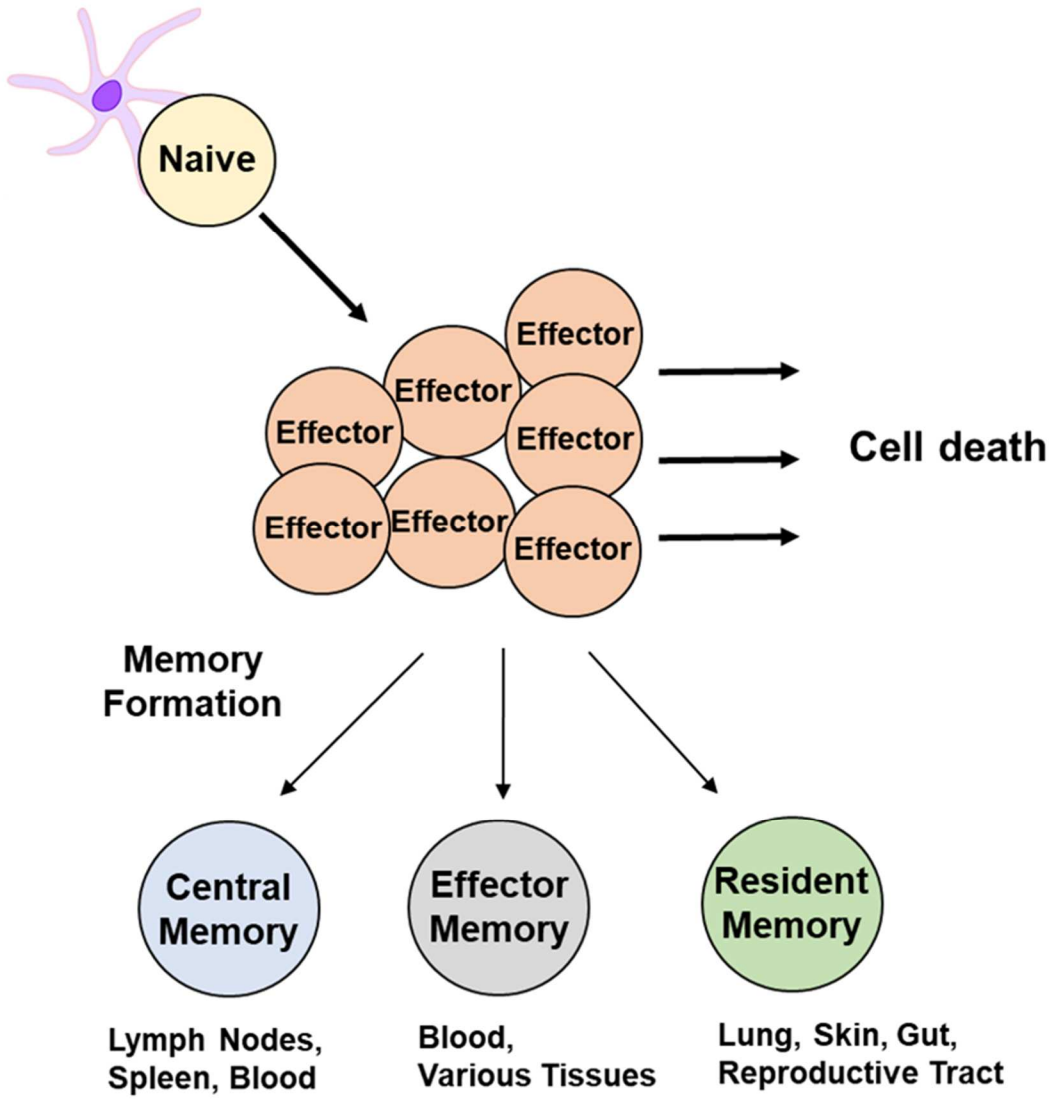
A.



B.



C.



Section 1.2: Human T cell development and maintenance of naïve T cells

Thymopoiesis

The thymus is the primary site of T cell development, where progenitors from the bone marrow lacking CD4⁺ and CD8⁺ coreceptor expression undergo TCR rearrangement to generate CD4⁺CD8⁺ double positive (DP) thymocytes [20]. DP cells undergo selection giving rise to CD4⁺ or CD8⁺ single positive (SP) thymocytes that ultimately emerge into the periphery as naïve T cells exhibiting CD45RA⁺CCR7⁺ phenotypes. This process can generate an enormous repertoire of naïve T cells with up to 100 million different specificities in humans [21]. A less frequent, but critical subset of CD4⁺CD25⁺ cells expressing the Foxp3 transcription factor designated regulatory T cells (Tregs) [22] represents 9-10% of human CD4⁺ SP thymocytes [23], and also expresses naïve CD45RA⁺CCR7⁺ phenotypes [24]. Tregs are responsible for restraining immune responses to maintain tolerance to self-antigens and prevent autoimmunity. Most of our knowledge of thymopoiesis, on the genesis of new T cells and mechanisms for their selection and development derive from studies in mouse models using thymectomy, bone marrow reconstitution, and genetic manipulation [25, 26]. In humans, similar manipulations are not possible; however, “natural” experiments involving thymectomy and thymic transplantation and studies of recent thymic emigrants (RTE) provide key insights into human thymopoiesis and how it differs from mice.

Unlike mice who are born lymphopenic, with T cells populating secondary lymphoid organs only at the end of gestation, humans are born with a full complement of T cells [27]. In utero, human T cell progenitors are detected in the fetal thymus as early as 9 weeks of gestation, with mature T cells appearing in the thymus by 12-13 weeks and the spleen and lymph nodes by 24 weeks of gestation [28]. Human Tregs also develop early in fetal life and are detected in the thymus at 12 weeks and in lymph nodes at 14 weeks [29, 30]. It was established some time ago

that neonatal thymectomy in mice results in both profound immunodeficiency and multi-organ lymphocytic infiltration [31, 32], due to defects in development of both naïve T cells and Tregs, respectively [33]. Neonatal thymectomy in humans is performed during cardiac surgery to repair congenital abnormalities, and these patients (many now in their third-to-fourth decade of life) do not experience increased incidence of infections [34, 35]. Adults who underwent neonatal thymectomy remain healthy despite having more extensive declines in naïve T cell frequencies with age compared to control individuals [36, 37]. Moreover, neonatally thymectomized adults show no increases in the incidence of autoimmunity or allergy compared to aged-matched controls [38], consistent with their maintenance of normal blood Treg frequencies and numbers [39]. By contrast, infants born with a congenital defect in Treg development (based on deletion or mutation of the *Foxp3* transcription factor) present with Immune dysregulation, Polyendocrinopathy, Enteropathy, X-linked (IPEX) syndrome manifested by systemic autoimmunity and multi-organ infiltrates [40]. Therefore, the critical events in T cell development commence prior to birth in humans, and humans are born with a T cell complement sufficient to effect anti-pathogen immunity and immunoregulation.

T cell development in the thymus involves rigorous selection events as determined in mouse models with newly generated DP thymocytes undergoing positive selection for self HLA recognition based on interactions with thymic epithelial cells (non-hematopoietic) and negative selection to remove strongly self-reactive clones through interactions with thymic DC [20]. Tregs undergo a different type of selection, and tend to be more self-reactive [41]. It is unclear whether thymic selection events occur similarly in humans, but novel insights have emerged from studies of thymus transplantation, a rare surgery used to successfully reconstitute the T cell compartment in infants with complete DiGeorge syndrome who are born lacking a functional thymus [42].

Pioneering work of Dr. Louise Markert and colleagues showed that transplantation of completely allogeneic thymus tissues from unrelated infants resulted in thymopoiesis, generation of polyclonal functional naïve T cells and anti-pathogen immunity, enabling these individuals who otherwise would have died of infections to survive [43, 44]. Interestingly, thymic recipients are tolerant of self and the thymic transplant (they require no immunosuppression) and also generate Tregs with diverse repertoires [43, 45], suggesting unique flexibility of the early neonatal period for tolerance induction. Based on mouse studies, the generation of functional immunity requires positive selection on thymic epithelial cells (TEC); however, in human thymic transplants the TEC are of donor origin, yet functional T cells emerge that can respond to antigens presented by the host antigen presenting cells (APCs) [46]. Whether human thymocyte selection is more permissive than mouse, occurring based on interactions with donor epithelium and/or recipient thymic APC is not known but suggests that rules for selection in mice do not apply wholly to humans.

How long does thymopoiesis persist in humans? The thymus is largest at birth, and age related changes in the thymus including a reduction in thymic volume, loss of epithelial cells, increase in perivascular space, and replacement of thymic tissue by fat begin relatively early in life [47]. Thymic function can be assessed in peripheral T cells based on CD31 surface expression [48, 49] and measuring TCR excision circles (TREC) as products of rearrangement, which are both indicators of recent thymic emigrants [50, 51]. There are well-documented decreases in CD31 expression and TREC content of peripheral blood T cells with age [48, 52, 53]. The greatest decline in thymopoiesis was generally believed to occur during puberty; however, more recent studies suggest that this steep reduction may occur later in life. In human thymic tissue obtained from organ donors aged several months to >70 years, DP thymocytes (indicating ongoing selection) were detected at the expected frequency (60-80%) in active thymus tissue from donors <40 years

of age, while few DP cells were detected in thymus tissues of adults >40 years of age [15]. Similarly, TREC levels of naïve T cells derived from human spleen and LN of these donors exhibited a steep reduction in individuals over 40 years of age [15], also observed in earlier studies quantitating TREC in peripheral blood naïve T cells [53]. Residual thymic activity can still persist beyond the fifth decade of life, as RTE-like cells can be detected in peripheral blood [52] and in renal transplant recipients following T cell depletion therapy [54]. Taken together, these findings indicate a profound age-related decline in thymic function after the fourth decade of life. Persistence of residual active thymus tissue may produce new T cells under lympho-depleting conditions and be amenable to regeneration therapies to rejuvenate the human immune system.

Naïve and Treg cell maintenance

In light of declining thymic output, how do individuals maintain a functional and diverse naïve T cell repertoire for responding to new antigens? Studies examining T cell turnover in human volunteers and mice administered deuterated water demonstrated important differences between the two species regarding thymopoiesis and naïve T cell maintenance. In both young and old mice, the majority of naïve T cells derive from thymic output, with minimal peripheral division of naïve T cells, while in humans, the majority of naïve T cells derived from peripheral turnover, even in younger adults with active thymic output [55, 56]. These studies also showed that while the average life span of mouse naïve T cells is only 6-10 weeks, in humans, individual naïve T cells can persist 5-10 years [55, 56]. The intrinsic long lifespan and turnover of human naïve T cells can account for their persistence well into old age.

A mechanistic view of human naïve T cell maintenance has emerged from newer studies using high throughput DNA sequencing for assessing TCR repertoires and through study of naïve

T cells in tissue sites. TCR sequencing can measure clonal diversity and quantitate expanded clones. Human naïve T cells exhibit a highly diverse TCR encompassing up to 100 million different specificities [21]. Naïve phenotype cells in the blood of elderly individuals (70-85 years old) still maintain a diverse repertoire of unique TCR amino acid sequences that, while reduced compared to that of young adults [21], suggests that humans are capable of responding to novel antigens even at advanced ages. Studies from our laboratory examining naïve T cells in circulation and multiple tissue sites has enabled a novel assessment of how naïve T cells are maintained over the lifespan, from infancy to old age [15, 16, 18]. Naïve T cells comprise a significant proportion (20-50%) of total T cells within multiple lymph nodes for decades after the cessation of functional thymic output and even into the seventh and eighth decade of life. Naïve T cells also maintain functionality with age, with no apparent functional differences between naïve T cells from younger individuals with active thymic output and older individuals with no thymic output [15]. TCR repertoire analysis of lymphoid naïve and memory T cells via CDR3 sequencing revealed high diversity (and corresponding low clonality) of CD4⁺ and CD8⁺ naïve T cells compared to the corresponding memory subset in spleen and multiple LN [15], indicating that naïve T cells in tissues maintain their capacity to respond to diverse antigens.

Tregs also emerge from the thymus and exist in high frequencies in tissues during early life; however their persistence and frequency differs from naïve T cells. The early establishment of Tregs in utero is followed by elevated levels in early life with up to 10-30% of all CD4⁺ T cells in blood, lymphoid tissue, and mucosal sites being Tregs compared to less than 5% in adults [16, 57]. Despite differences in overall frequency, pediatric and adult Tregs share similar features. Tregs maintain a TCR repertoire entirely distinct from corresponding non-Treg populations, with minimal overlap of TCR amino acid sequences between these subsets in umbilical cord blood and in adult

peripheral blood [58]. These results also suggest distinct thymic selection involved in development of Tregs from naïve T cells in humans. At all ages, Tregs in blood and lymphoid tissues are CD45RA+CCR7+, indicating a naïve phenotype, while Tregs in mucosal sites are CD45RA- and express CD45RO, like conventional memory T cells [16]. Functionally, pediatric Tregs in LN can express increased levels of FoxP3 compared to adult LN Tregs [16]; however, more studies are needed to assess how early life Tregs differ from those which persist in later life.

The decline in Treg frequency in humans begins earlier in childhood than the decline in conventional naïve populations [16], suggesting both thymic and peripheral mechanisms at play. Studies in mice along with complementary analyses in humans indicates that age-associated reductions in Treg generation is due to interactions between thymic output, peripheral induction and maintenance. In mice, mature Tregs migrate back to the thymus and suppress thymic production of Tregs but not conventional naïve T cells [59]. Mature Tregs were also detected in human pediatric thymii [59], suggesting a similar mechanism controlling Treg production in humans. Compared with naïve T cells, human Tregs exhibit higher turnover, as measured by Ki67 expression [16, 39], which along with reduced thymic output could also contribute to their reduced frequency with age. Treg frequency may also be affected by changes in Dendritic cell (DC) populations. Recent studies showed that human fetal dendritic cells could promote Treg induction and inhibit pro-inflammatory cytokine production more readily than adult DCs [60]. Together, these results suggest multiple interacting mechanisms for control of Treg frequencies after childhood, consistent with the optimal window for tolerance induction occurring early in life.

Section 1.3: T cell activation and subset differentiation

Naïve T cells become activated primarily by dendritic cells, and this activation requires presentation of both antigen/MHC ligands and costimulatory molecules for engagement of the T cell receptor (TCR) and the CD28 costimulatory receptor, respectively. This initiates a complex signaling cascade within the naïve T cell that results in IL-2 production, proliferation, and differentiation to effector populations [61]. These effector populations carry out pathogen clearance and can be divided in many subsets, each with unique functional roles.

Effector CD4⁺ T cells, or T helper (Th) cells, have diverse functions including promoting antibody secretion by B cells [62], helping the development of CD8⁺ effector T cells (also known as cytotoxic T lymphocytes or CTLs) [63], and direct pathogen clearance [64]. T helper subtypes are delineated based on function including Th1, Th2, Th17, T follicular helper (Tfh), and induced Tregs, as well as expanding array of subtypes such as Th9 and Th22 [65, 66]. These T helper subsets are crucial to the immune response, with each having a unique role; Th1 cells produce IFN- γ to promote responses against intracellular pathogens and Th2 cells produce IL-4 for B cell help and immune responses against extracellular pathogens. Tregs exert their suppressor functions by secreting inhibitory cytokines (IL-10, TGF- β , and IL-35), stimulating apoptotic pathways, inducing metabolic disruption via cytokine deprivation, and modulation of DC maturation and function [67]. Different signals promote the development of different Th subsets, and key transcription factors have been identified that are associated with each subset. These key transcription factors are: T-bet for Th1 cells, GATA3 for Th2 cells, ROR γ t for Th17, AhR for Th22 cells, and FoxP3 for Tregs [65]. It should also be noted that while the classification of CD4⁺ effector cells into discrete Th1/Th2/Th17 subsets can apply in a general way, there is considerable functional heterogeneity and plasticity within Th subsets [66, 68]. For example, populations of

CD4⁺ effector cells can secrete multiple cytokines characteristic of more than one subtype, and under certain conditions Th cells can switch their pattern of cytokine secretion [66, 68].

Activated CD8⁺ T cells differentiate into cytotoxic T cells (CTLs), which secrete high levels of IFN- γ and TNF and acquire cytotoxic capacities, expressing perforin and granzyme, with the ability to directly kill infected cells [69]. Functionally, CTLs kill infected cells by inducing the target cells to undergo apoptosis. This takes place when CTLs recognized MHC bound cognate antigen on the surface of the target cell, and then release granules containing cytotoxic molecules like perforin, which creates holes in the membrane of the target cells, and granzymes, which are enzymes that can induce apoptosis in the target cell after diffusing through pores created by perforin. Additionally, granzyme may directly inhibit the production of viral proteins [70] and directly kill intracellular bacteria by targeting the electron transport chain to produce reactive oxygen species that are lethal to the bacteria [71]. Overall however, the actions and lifespan of these effector cells are generally short-lived *in vivo* in humans, with a subset of previously activated cells undergoing further differentiation to persist as long-lived resting memory T cells.

A number of transcription factors play an important role in the development of CTLs. T-bet and eomesodermin (eomes) are two T-box transcription factors that play critical roles in mediating CTL formation and function, and these transcription factors also control CD8⁺ memory T cell function and development [72, 73]. The expression of T-bet and eomes is somewhat reciprocal, with high T-bet expression driving effector function and terminal differentiation and high eomes expression being associated with memory formation and longevity [72, 73]. TCF-1 is another transcription factor that plays an important role in controlling T cell fate. Specifically, TCF-1 is expressed at high levels by naïve T cells but needs to be downregulated in CTLs to allow for effector function [74-76]. Finally, expression of the transcription factor IRF4 is required for

effector CD8⁺ T cell differentiation [77-79]. While these represent a few key transcription factors that influence T cell differentiation, several other transcription factors also cooperate to determine CD8⁺ T cell fates [73].

In humans, studying the dynamics of T cell activation and differentiation to effector and memory T cell fates requires specific cohorts that are challenged and followed over time. Elegant studies using the live-attenuated Yellow fever virus vaccination (YFV-7D) show activated CD4⁺ and CD8⁺T cells co-expressing CD38 and HLA-DR detectable in the blood within 2-3 days; YFV-specific CD8⁺ T cells are subsequently detectable in blood and exhibit peak responses after 14-21 days [80-83]. As in mouse infection models, the kinetics of the T cell response is delayed relative to infectious viral titers, with the magnitude of the effector CD8⁺ T cell response correlating with initial viral load [80]. This virus-induced effector response contracts rapidly, returning to near baseline levels by 30 days [80-82]. Virus-specific memory T cells subsequently persist in frequencies reduced from the effector response (5-6%) [82, 84, 85], yet are detectable 25 years after vaccination [85, 86]. Similar kinetics of effector expansion and memory development were observed following smallpox (vaccinia) and influenza vaccination [82], with vaccinia-specific memory T cells detected after many decades [87]. Together, these studies indicate that human effector T cell expansion, contraction, and memory formation following viral infection is similar in kinetics and magnitude to many acute viruses investigated in mice.

While the majority of effector T cells contract rapidly and are not present in significant proportions at steady state in humans, a population of terminal effector cells (TEMRA) exhibiting CD45RA⁺CCR7⁻ phenotypes can persist in circulation. TEMRA cells are mostly present within the CD8⁺T cell lineage, exhibit high capacity for IFN- γ production and low proliferative capacity, and their frequency in blood is correlated with persistent CMV infection [88]. The proportion of

CD8⁺ TEMRA cells in blood and bone marrow increases with age, specifically in CMV seropositive donors [14, 89], suggesting a role for TEMRA in persistent infections. CD4⁺ TEMRA cells are rarely detected, but expansion of CD4⁺ TEMRA cells with cytotoxic function occurs in individuals infected with Dengue virus and is associated with protection [90]. These findings suggest that certain viruses trigger terminal effector differentiation, which is important for protection or long-term control. Interestingly, TEMRA cells appear to be particular to human T cells, with no clear correlate in mouse infection models.

Section 1.4: Memory T cells

As detailed in the previous sections, the majority of effector T cells contract following pathogen clearance but a limited fraction (approximately 5%) persist long-term as memory T cells, which at steady state represent the predominant T cell population that exists in virtually all human tissue sites and blood. Human memory T cells are classically distinguished from naïve T cells by the expression of CD45RO and the lack of CD45RA expression [91, 92]. Memory T cells are classically divided into two primary subtypes based on the expression homing receptors into central memory (TCM), which express CCR7, and effector-memory (TEM), which are CCR7- [93]. Stem-cell memory (TSCM) is an additional, more recently described T cell subset that exists in low frequencies, and can be identified by the phenotype CD45RA+CCR7+CD95+CD122+ [94]. Finally, tissue-resident memory T cells (TRM) are another recently identified subset of memory T cells that exist in high proportions within tissues [10] and will be covered in detail in the next section of this chapter.

Functionally, both TCM and TEM are both capable of producing IL-2 and effector cytokines upon stimulation. However, TCM exhibit properties more similar to naïve T cells, including gene expression and homing receptor profile, high proliferative capacity, and ability to produce elevated levels of IL-2, while TEM have a greater ability to produce effector cytokines such as TNF and IFN- γ and have greater cytotoxic capabilities [6, 93-95]. TSCM are a relatively rare subset with high proliferative and self-renewal capabilities, but no effector function [94]. TSCM resemble naïve T cells based on the phenotype CCR7+CD45RA+, but also by the fact that they express CD62L and have high levels of the costimulatory receptors CD28 and CD27. These phenotypic and functional properties of these and other major T cell subsets are covered in Table 1.1.

Within the adult human, each memory subset has a unique tissue distribution. Via a unique tissue resource, recent studies from our laboratory have analyzed T cell subsets in tissues over six decades of adult life and revealed that TEM were the predominant T cell population in lungs, small and large intestines, spleen, and blood, and represented 30-50% of the T cell complement in multiple lymph nodes [14, 17, 18]. By contrast, in most healthy adults naïve T cells were primarily found in blood, spleen, and lymph nodes, although still at lower frequencies than memory T cells. For CD4⁺T cells, TCM cells were present in similar frequencies (average 20%) in lymphoid sites with lower frequencies in mucosal tissues, and there were few TEMRA phenotype cells. For CD8⁺T cells, significant fractions (~30%) of TEMRA cells were found within blood and blood-rich tissues (spleen, bone marrow, and lung) but not in other sites. Studies from our lab found negligible (approximately 5% for most tissues) CD8⁺ TCM-phenotype cells in any site [14, 18]; other studies also found low but somewhat higher (~20%) frequencies of TCM within the CD8⁺ T cell lineage in peripheral blood [93, 96, 97]. Overall however, most subset frequencies were quite stable across highly diverse donors, suggesting tissue-specific compartmentalization of human T cell subsets.

The developmental relationship between T cell subsets is the subset of ongoing research. Models for the linear and bifurcated generation of human memory T cell subsets have been previously inferred from functional analysis, differentiation markers, and analysis of cell division [98]. However, recent studies using epigenetic and transcriptional analysis have provided new insights into the differentiation hierarchy of memory T cells. For CD4⁺ T cells, epigenomic profiling based on assessment of methylation status, DNA accessibility, and histone modifications revealed a progressive loss of DNA methylation of key genes that control memory development in the order naïve – TCM – TEM – TEMRA [99]. The authors observed a similar progression in

terms of transcriptional profile and telomere length. A linear progression of differentiation for human CD8⁺ T cells in the order naïve—TSCM—TCM—TEM was suggested by methylation analysis and chromatin accessibility [100, 101]. Compared with naïve T cells, TEM had the most number of differentially methylated regions and TSCM had the least, with TCM falling in between. The different CD4⁺ and CD8⁺ memory T cell subsets all contained specific elements of effector cells such as demethylation of effector genes (e.g., IFN- γ), suggesting an effector precursor and supporting a linear differentiation model [99-101].

Table 1.1. Overview of major T cell subsets in humans

	Naïve	Central Memory (TCM)	Effector Memory (TEM)	Stem cell memory (TSCM)	TEMRA
Phenotype	CD45RA+ CCR7+	CD45RA- CCR7+	CD45RA- CCR7-	CD45RA+ CCR7+ CD122+ CD95+	CD45RA+ CCR7-
Predominant Location	Lymphoid tissues, blood	Lymphoid tissues, blood (CD4 ⁺ cells)	All sites, highest in barrier tissues.	Blood, other sites?	Blood, spleen, lungs (CD8 ⁺ cells)
Proliferative Capacity	+++	++	+	+++	-
Effector Function (IFN-γ, TNF, cytotoxicity)	-	+	++	-	+++
IL-2 Production	++	++	+	++	+/-

Section 1.5: Tissue-resident memory T cells (TRM)

Overview of TRM

Memory T cells were originally divided into central and effector memory subsets which patrolled lymphoid and peripheral tissues, respectively [93]. However, this analysis was done in blood and a number of studies were unable to reconcile these findings in tissues, leading to the designation of another subset called tissue-resident memory T cells (TRM), which exists solely within tissues and does not recirculate [10, 102]. TRM have been described in virtually every tissue studied, including barrier sites such as skin, gut, lung, and reproductive tract, organs such as liver and kidney, secondary lymphoid organs, exocrine sites such as pancreas and salivary glands, and brain [10, 103-113]. Functionally, TRM mediate rapid *in situ* protection against diverse viral, bacterial, and parasite infections, and are more effective than circulating memory T cells in pathogen clearance [103, 105-107, 114-116]. In fact, TRM can clear pathogens without any contribution from circulatory T cells or antibodies. The clinical importance of TRM is further underscored by the fact that protective TRM can be generated in response to vaccination and cancer [117-120], and in addition to having protective roles, TRM can be pathogenic and are implicated in many human diseases [121, 122].

The existence of TRM and demonstration that these TRM enhance protection was demonstrated a number of years ago for both CD8⁺ [107, 123] and CD4⁺ [105] lineages. Since that time, many studies as well as reviews on TRM have focused on CD8⁺ TRM [10, 102]. However, several additional studies have proven the existence of bona fide CD4⁺ TRM, which like their CD8⁺ counterparts, are also important for optimal protective responses [111, 115, 118, 124-127]. In mice, TRM can be identified using parabiosis assays [103, 104, 128], *in vivo* antibody labeling [105, 124, 129], or by using photoconversion of T cells to track migration [111, 127, 130].

Phenotypically, TRM can be distinguished from circulating memory T cells based on the expression of CD69 [10, 124, 129], a surface marker which promotes retention through sequestration of S1PR1 [131, 132], and for certain subsets of CD8⁺ TRM by the expression of CD103 [10, 133].

Phenotypic and transcriptional properties of TRM

A number of studies have established that TRM are a distinct subset from circulating memory T cells based on phenotypic and transcriptional properties. At first glance, TRM have some similarities to TEM in that TRM do not express CCR7 or CD62L, which are two key markers used to delineate memory subsets [10]. However, a key difference between TEM and TRM shown by numerous studies is that CD4⁺ and CD8⁺ TRM from both barrier and lymphoid tissues upregulate the cell surface marker CD69 [103, 105, 109-112, 134-136]. CD69 promotes tissue-retention by leading to the downregulation of sphingosine-1 phosphate receptor 1 (S1PR1), a receptor which promotes tissue egress and migration towards sphingosine-1 phosphate found in the blood and lymph [131, 132, 137, 138]. In fact, it has even been shown that downregulation of S1PR1 (and its associated transcription factor KLF2) is required for TRM formation, and that forced S1PR1 expression inhibits TRM generation [139]. CD103, a cell surface integrin which binds E-cadherin on epithelial cells, is also commonly used as a marker of CD8⁺ TRM [10]. However, CD8⁺ TRM lacking CD103 expression have also been described, and it has been shown that CD103⁺ and CD103⁻ TRM are developmentally distinct subsets [10, 133]. Further, CD4⁺ TRM do not highly express CD103. Therefore, at present, CD69 appears to be the most reliable phenotypic marker of CD4⁺ and CD8⁺ TRM in mice, short of methods such as *in vivo* labelling or parabiosis.

Transcriptional profiling comparing CD8⁺ TRM with circulatory T cells in mice has been done via microarray [108, 110, 140] and RNA sequencing [109]. (RNA-Sequencing has a superior ability to detect low abundance transcripts and a greater dynamic range compared with microarray [141].) These studies have shown that TRM are a transcriptionally distinct subset compared with circulating memory T cells (either TEM or TCM). This result reinforces the designation of TRM as a separate memory subset. A number of key features of TRM can be determined by comparing the results of these studies. However, a core gene signature of TRM remains to be established as these studies that performed gene expression profiling of TRM used different infection models, different tissue sites, and sometimes different TRM subsets (i.e. CD103⁺ vs CD103⁻ TRM). Further, these studies have compared TRM from a barrier site to circulating memory from the spleen [108-110]. As tissue microenvironments can have powerful effects on T cells [134], differentially expressed genes in these studies might include those that result from tissue differences rather than TRM vs. TEM/TCM differences. Finally, no published studies have performed whole transcriptome profiling of CD4⁺ TRM or of TRM from lymphoid tissues.

These studies that performed gene expression profiling of TRM confirmed the downregulation of S1PR1 and also showed that TRM may downregulate other sphingosine-1-phosphate receptors such as S1PR4 and S1PR5. Further, these studies showed that TRM downregulate of KLF2 as well as the related transcription factor KLF3. Overall, these results confirm S1PR1 downregulation as a critical way that TRM are able to avoid egress cues and maintain residence. TRM have also been shown to have differential expression of other homing receptors and certain adhesion markers. Examples include downregulation of SELL (encoding CD62L) [139, 140, 142] and CXCR4 [109], and upregulation of CXCR6 [109, 142] and ITGA1 (encoding the adhesion marker CD49a) [108, 110]. These results reinforce that unique migratory

properties of TRM may be required to maintain tissue residence. These studies further uncovered notable transcriptional differences related to T cell function (e.g. upregulation of transcripts encoding cytokines and cytotoxic molecules by TRM), and these will be detailed in the later section that covers TRM function. These studies have also identified differences between TRM and circulatory memory T cells with respect to transcription factors. The roles of these transcription factors will be discussed in the section on TRM generation and maintenance. Overall, however, the key results from studies performing transcriptional profiling of TRM indicate that TRM are a transcriptionally distinct subset from TEM and TCM, with unique functional and phenotypic properties and unique transcriptional regulators.

TRM function and protective responses to pathogens

It is well established that TRM are the primary mediators of pathogen clearance at many tissue sites and that TRM accelerate pathogen clearance compared with circulating memory T cells [10]. For example, one study generated CD8⁺ memory T cells in response to vaccinia virus skin infection, and the authors showed using a parabiosis model that TRM were superior to TCM in clearing a subsequent infection [103]. In fact, previously infected mice containing TRM but whose TCM were depleted (using FTY720) were still able to clear infection, but mice containing only TCM were unable to clear infection [103]. Another study found that protection against skin HSV infection was correlated with the number of skin CD8⁺ TRM but not with the number of circulating memory T cells [143]. CD4⁺ TRM appear to have similar characteristics; in a study from our lab, mice containing CD4⁺ TRM in the lung enjoyed greater protection against influenza infection (as measured by weight loss and survival) compared with mice containing circulatory memory T cells [105]. Enhanced protection by TRM has been demonstrated in several other studies [107, 108,

144, 145], including in studies where protective TRM were generated by vaccination [117, 118, 146, 147]. The mechanisms for this superior protection appear to result from: 1. Proximity to the site of infection which allows faster response compared with circulating T cells which would have to be recruited, and 2. Cell intrinsic abilities which give TRM the ability to be superior defenders. These cell intrinsic abilities including unique functional properties, including increased expression of a number of genes involved in function including transcripts encoding granzyme B, TNF, and IFN- γ [108-110, 140, 148]. Some of these studies also showed that TRM upregulate the transcription factor IRF4 [108, 109], which is an important mediator of T cell effector function [77-79]. These transcriptional properties strongly suggest unique functional properties of TRM and that TRM are “poised” for rapid effector function upon stimulation, and the ability of CD8⁺ TRM to produce these cytokines has also been validated [10]. While transcriptional profiling of CD4⁺ TRM has not been done, studies suggest that these cells are also capable of secreting IFN- γ [126, 149], as well as TNF and IL-2 [126].

Numerous studies have investigated the cell-intrinsic functional properties of CD8⁺ TRM that allow pathogen clearance. Broadly, it appears that the function of TRM can be divided into two main roles: 1. Direct effector function mediated by TRM, and 2. a “sound the alarm” function, whereby TRM are sentinels that recruit T cells and other leukocytes to the site of infection. These properties are not always mutually exclusive, and “sound the alarm” function has been reported in a few recent high profile articles [114, 150, 151]. Upon reactivation, TRM induced VCAM-1 expression on endothelial cells via IFN- γ production, allowing for the recruitment of circulating lymphocytes, induced dendritic cell maturation via TNF production, and induced NK cell activation via IL-2 production [114, 135]. One of these studies performed transcriptional profiling of skin tissue near TRM upon secondary challenge and found that TRM induce an antiviral state

in surrounding cells via IFN- γ production [150]. These surrounding cells upregulated a number of genes involved in anti-pathogen responses, and in fact this TRM-mediated effect was sufficient to protect against an antigenically unrelated pathogen. Direct effector function by TRM is apparent by fact that TRM are able to clear pathogens without any contribution from circulating T cells (such as when an agent is administered to deplete circulating leukocytes) [103, 106, 118]. The fact that protection after circulating leukocyte depletion exists even against heterosubtypic strains of influenza implies that it is mediated by TRM rather than antibodies which were formed during the primary response [118]. To carry out these effector functions, TRM must come into contact with and recognize invading pathogens. Two studies examining TRM motility have shown TRM patrol the epidermis and have a unique dendritic morphology (as opposed to the amoeboid shape of circulating T cells), whereby dendrites are continuously extended and retracted to sample the local environment [152, 153]. Upon recognition of antigen, these patrolling TRM reduced their motility to stay in the area of infection [153]. Overall, these data suggest that mouse TRM continuously patrol regions of prior infection and upon antigen encounter, mediate protection via direct effector function as well as by recruiting other leukocytes from circulation.

TRM in human tissues

While the majority of studies on TRM have been conducted in mice, the presence of TRM (or at least TRM-phenotype cells) within multiple human tissues has also been demonstrated [140, 142, 154-159]. For example, transplant patients who were administered alemtuzumab, an agent which depletes all circulating T cells, still retained T cells in their skin [154, 155]. The retained memory T cells expressed CD69, similar to TRM in mice. Further, analysis of memory T cells from healthy organ donors in our lab revealed that CD69 is expressed by the majority of memory

T cells in multiple tissues sites including mucosal sites, lymphoid sites, and exocrine tissues such as salivary glands, while blood memory T cells are largely CD69⁻ [18]. Some additional studies have identified memory T cells expressing the TRM markers CD69 or CD103 in human tissues, suggesting the presence of TRM [158, 159]. Nonetheless, it has not been formally established that CD69 identifies TRM in humans, nor have any other phenotypic markers been established that reliably identify TRM in human tissues. Phenotypically, these TRM phenotype cells appear to have certain common features with TRM in mice. These include downregulation of S1PR1 transcriptionally [160], low CD62L expression [158, 159], low CCR7 expression [155, 160], and upregulation of CD49a [159]. Further, similar to mice, it appears that both CD103⁺ and CD103⁻ subsets of TRM exist within the skin [155]. Overall, these limited studies suggest the presence of TRM in human tissues with features analogous to mouse TRM. However, additional studies are needed to establish core phenotypic properties of human TRM.

Several lines of evidence suggest that these TRM have a protective role in humans analogous to their established roles in mice. Patients given alemtuzumab, an agent which depletes circulating T cells while preserving TRM, do not have higher rates of infections [154], suggesting memory T cells residing within tissues adequately control ongoing and new infections. Two studies examining responses to herpes simplex virus (HSV), which is used as a model system for studying TRM in mice [107, 161], identified long-lived CD8⁺ $\alpha\alpha$ resident T cells that were formed following infection in humans [160, 162]. These TRM clustered around infected cells, expressed cytolytic molecules and upregulated antiviral genes, and were associated with control of symptoms. TRM in other tissues also display enhanced specificity for site-specific pathogens, including influenza-specific CD8⁺T cells within the lung TRM subset [124, 159], hepatitis B virus (HBV)-specific CD8⁺ T cells within liver CD69⁺ memory T cells [163], and EBV specific CD8⁺

TRM in the spleen and tonsils [157]. The tissue distribution of T cells specific for systemic viruses that infect and/or persist in multiple sites is more complex. CMV-specific T cells exhibit different distribution patterns with predominance in either blood, bone marrow (majority of donors), or lung and lung lymph nodes, with higher frequencies of total and activated virus specific T cells being associating with lower viral loads [14]. Bone marrow was also found to be enriched compared to blood for specificities to multiple systemic pathogens [164], suggesting compartmentalization of long-lived memory populations in the bone marrow. Finally, it has been shown that human TRM from the lung, GI tract, and other sites are capable of producing multiple effector and pro-inflammatory cytokines including IFN- γ , TNF α , and IL-17 [142, 158, 159]. Taken together, these findings suggest that human TRM are generated at sites of infection, and upon pathogen encounter, TRM exhibit cytotoxic abilities, produce anti-viral cytokines like IFN- γ , and recruit other leukocytes to the site of inflammation.

While TRM are critical for protection at many sites, emerging evidence strongly suggests that TRM can also be pathogenic and that TRM are implicated in a number of human illnesses (for detailed reviews, see [121, 122]). In the skin for example, studies suggest that TRM contribute to the pathogenesis of several skin disease including psoriasis, vitiligo, mycosis fungoides (MF), and fixed drug eruption. The clinical characteristics of these diseases strongly suggest TRM involvement: lesions occur within a fixed area rather than being diffuse; lesions recur at exactly the same location, suggesting that the T cells have not circulated; and the onset of inflammation tends to occur very rapidly after antigen exposure, suggesting that the T cells contributing to inflammation are already located within the tissue [121]. Further, these conditions tend to worsen over time [121], which is consistent with the fact that TRM accumulate with repeated antigen exposure (see prior sections).

In MF, T cells from lesioned skin do not express CCR7 or CD62L, consistent with a TRM phenotype, while T cells from conditions that affect the skin diffusely do express these markers of circulating T cells [154, 165]. In psoriasis, E-selectin blockade, which inhibits T cell migration into the skin, does not lead to resolution of symptoms [166], suggesting that TRM are mediating the disease rather than circulating T cells that enter the skin from the blood. Further, psoriatic lesions developed when non-lesioned skin from psoriasis patients was transferred onto immunodeficient mice [167], suggesting that pathogenic TRM were contained within the skin and that lesions can develop without any recruitment from circulation. Finally, a recent article that examined T cells from biopsies of psoriasis and vitiligo lesions showed that CD8⁺CD103⁺ TRM producing IL-17 (which drives the development of psoriasis) were overrepresented in psoriatic lesions, while TRM producing IFN- γ and expressing cytotoxic molecules (which together drive the development of vitiligo) were overrepresented in vitiligo lesions [168].

These skin diseases represent illnesses where the involvement of TRM is well-characterized. However, there are many other diseases where evidence suggests TRM involvement, although further studies are needed to conclusively determine this. These include gut diseases such as Crohn's, brain diseases such as multiple sclerosis and schizophrenia, rheumatoid arthritis, and asthma and allergic airways disease to name a few [121, 122]. Ongoing studies will elucidate the roles of TRM in these and potentially additional conditions; however, at present there is sufficient evidence to state that TRM have a critical role in human disease in addition to protection against invading pathogens.

TRM generation and maintenance

It is well established in mice that TRM generation occurs in response to infection at many different tissue sites, and this is true for both CD4⁺ and CD8⁺ TRM in barrier, lymphoid, and other tissues [10, 103, 105-110, 112]. The current literature suggests that CD8⁺ TRM develop from effector T cells that enter the affected tissue early during infection, and once inside the tissue a number of signals promote the development of a CD103⁺ TRM phenotype and prevent tissue egress [10, 102, 148]. In the skin for example, peak influx of TRM precursors occurs around 1 week post infection, and these effector cells transition into fully developed TRM by about day 30, including acquiring CD69 and CD103 expression and progressively diverging from other memory subsets transcriptionally [110, 140]. Another study showed that only early effector cells and not memory T cells have the ability to enter the intestinal mucosa, and these early effectors were the cells that developed into TRM in the gut [123]. The authors also showed that in humans only early effectors expressed gut homing molecules following yellow fever vaccination, suggesting that in both humans and mice there is a limited time window when TRM precursors have the ability to seed tissues. This concept is reinforced by other studies showing that TRM are maintained without the need for replenishment from circulating memory T cells [124, 126]. The ability of effector T cells to enter a particular tissue may depend on homing receptors such as $\alpha 4\beta 7$ in the case of the intestine, and the anatomic location of the draining lymph node has a large influence on which homing molecules effector T cells express [122]. Inflammatory signals generated at the site of infection may also have a role in recruiting effector T cells into the tissue [169, 170].

Which cells are the precursors to the TRM? One study that examined the development of CD8⁺CD103⁺ TRM in multiple tissue sites demonstrated that these TRM arose from KLRG1^{low} precursors that entered the epithelium during early infection [110]. A number of other studies have

confirmed low KLRG1 expression on CD8⁺ TRM, both in mice and humans [136, 142, 169]. Finally, one study found that TRM and TCM subsets in mice had completely overlapping TCR repertoires [171], suggesting that naïve cells gave rise to TCM and TRM in parallel. This further suggests that TRM arise from cells that have gone through the effector phase, as direct differentiation from naïve to TRM or TCM would not produce the result of overlapping TCR repertoires.

Once in the tissue, effector T cells respond to signals that drive the development of a TRM phenotype, including upregulation of CD69 and CD103. It was established some time ago that TGF- β can drive CD103 expression [172], and a number of further studies have confirmed that TGF- β promotes CD103 upregulation and TRM development [106, 110, 136, 139, 169, 173, 174]. It should be noted however that TGF- β may only be important for CD103⁺ TRM, as CD103⁻ TRM have been shown to develop in a TGF- β independent manner and represent a distinct subset [133]. While CD103⁺ CD8⁺ TRM exist in epithelial layers, CD103⁻ CD8⁺ TRM exist below in the lamina propria layer where they cluster with CD4⁺ T cells and macrophages and show signs of TCR engagement [113, 133]. This suggests that these cell clusters may provide signals for CD103⁻ TRM retention and/or formation, while CD103 TRM in the epithelium are more dependent on TGF- β [175]. Finally, other cytokines that can induce CD103 expression include TNF, IL-15, and IL-33 [110, 139], and other factors that can drive CD69 upregulation include TNF and type I interferons [122].

Aside from KLF2, which has a role in regulating T cell migration by controlling the expression of S1PR1 (as described above), several transcription factors have been found to be differentially expressed by TRM and/or important for the formation of TRM. The transcription factors T-bet and Eomes, which are key controllers of TCM and TEM development [72], may also

play important roles in TRM development [148]. For example, CD103⁺TRM in the skin, gut, lung, and brain all have reduced expression of T-bet and Eomes compared with circulating memory T cells [108, 110, 140]. In fact, one recent study showed the progressive downregulation of these transcription factors during the development of CD8⁺CD103⁺ TRM, and further that forced expression of either Eomes or T-bet inhibited TRM formation [106]. Downregulation of T-bet enabled responses to TGF- β [106], which has been shown to promote the expression of CD103 and in some cases CD69 [110, 136, 139, 173, 174]. However, while downregulation of both T-bet and Eomes occurred during TRM formation, some residual T-bet expression still was required to maintain TRM populations (by maintaining CD122 expression to be able to respond to IL-15 signals), while Eomes was completely downregulated [106]. Another recent study similarly found that T-bet downregulation was necessary for promoting TRM development by allowing responsiveness to TGF- β [169]. The role that T-bet and Eomes play in human TRM development and maintenance is the subject of ongoing research.

Recently, the transcription factor homolog of BLIMP-1 in T cells (Hobit) was shown to play a key role in TRM development in mice [109]. The authors show that Hobit is highly expressed by TRM at all sites (but not by circulatory memory T cells), and that Hobit deficiency resulted in reduced TRM formation mice [109]. Blimp1 was another transcription factor the authors investigated, and while Blimp1 deficiency by itself did not impair TRM formation, combined Blimp1 and Hobit deficiency acted in a synergistic manner and resulted in significant inhibition of TRM development following infection [109]. The authors showed these results held in several infection models in different tissues and that Hobit and Blimp1 also mediate tissue residency for other cells types like NK cells and NKT cells, suggesting that these are universal

mediators of tissue residency. The role these transcription factors play in human TRM development is not known.

So far, this section has focused on how TRM precursors develop into mature TRM as well as the signals and transcriptional regulators involved in this process. It has also been shown that CD4⁺ T cell help is critical for the generation of protective CD8⁺CD103⁺ TRM in the lung following influenza infection in mice [169]. This effect was dependent on IFN- γ produced by the CD4⁺ cells, and, in the absence of CD4⁺ T cells help, CD8⁺ TRM precursors failed to localize to the epithelium and did not downregulate of T-bet. These results are consistent with another study which showed that CD4⁺ T cells were important for driving the migration of CD8⁺ effector T cells into the infected tissue site [170]. Because the CD4⁺ T cells entered the lung approximately 1 day prior to CD8⁺ T cells in the first study [169], the IFN- γ produced by CD4⁺ T cells is likely what drove the recruitment of CD8⁺ effectors. In support, it was shown that IFN- γ promotes the production of CXCR3 ligands [170], and CXCR3 drives CD8⁺ T cell entry into the lung [176]. When CD8⁺ precursors fail to localize properly to the epithelium, they are not exposed to signals such as TGF- β which induce CD103⁺ upregulation and TRM development. Overall, these studies highlight the critical role CD4⁺ T cells play in the recruitment of CD8⁺ effectors to the infection site and promotion of CD8⁺ TRM development.

Less is known about CD4⁺ TRM generation, although it is well established that protective CD4⁺ TRM are also generated in response to virus [105, 118, 124, 126]. While these studies did not directly examine mechanisms of CD4⁺ TRM generation, our laboratory examined the kinetics of the CD4⁺ T cell response to influenza in the lung and showed a large initial increase in non-resident cells following infection followed by the development of CD4⁺ TRM over the course of a few weeks [124], similar to dynamics established for CD8⁺ TRM. The absolute numbers of the

CD4⁺ TRM in the lung diminished as time passed following infection; however, CD4⁺ TRM were still detected 120 days after a single infection [124], indicating long-term maintenance in the absence of ongoing infection/inflammation. Further, these studies have revealed other interesting aspects of CD4⁺ TRM. In terms of localization, CD4⁺ TRM in the reproductive tract appear to persist in the lamina propria layer (as opposed to the epithelial layer) where they exist in memory lymphocyte clusters (MLCs) along with CD103-CD8⁺ TRM, DCs, and macrophages [126, 175]. Chemokines secreted by macrophages within the MLCs help retain the CD4⁺ TRM [126]. In the lung, CD4⁺ TRM form clusters around the airways while circulating CD4⁺ memory T cells are spread more diffusely through the parenchyma [124]. Overall, these studies suggest that the kinetics and long-term persistence of CD4⁺ TRM is similar to CD8⁺ TRM, but that CD4⁺ and CD8⁺ TRM may respond to different signals for development and/or maintenance.

While TRM have typically been studied in the context of infection, it should also be noted that TRM can be generated in response to other stimuli such as vaccination. In one study, the authors generated HSV-specific TRM in the genital tract by using a vaccination strategy that involved infecting the mice with HSV at a distant skin site and then applying topical chemokines to the genital tract to bring effector T cells to that site [117]. This effectively pulled effector T cells into the genital tract, leading to the development of CD8⁺ TRM that were protective against subsequent HSV infection. Interestingly, there was no inflammation in the genital tract during the initial vaccination as measured by increased numbers of other leukocytes such as DCs, NK cells, granulocytes, or monocytes [117]. Overall, this study demonstrates a vaccination strategy that can generate protective TRM in the complete absence of local inflammation or antigen. Another study from our laboratory showed that CD4⁺ and CD8⁺ TRM protective against influenza could be generated by live attenuated virus vaccination [118]. While TRM generation in this study did

involve response to live virus, this strategy further highlights the possibility of generating protective TRM without the inflammatory damage associated with a typical primary response. Overall, these studies highlight the potential for harnessing TRM for clinical purposes to protect against infections where protection cannot be adequately achieved with conventional antibody-based vaccines.

TRM have been shown to accumulate with increasing antigen exposure [103, 111, 147]. For example, while a single infection or inflammatory insult in the skin results in only localized TRM formation [143, 177], repeated insults lead to widespread TRM formation including at previously unaffected sites as well as greater densities of TRM at the site of infection [103, 147]. Because protection is correlated with density of TRM and because TRM need to be present within a relatively local area to defend against reinfection, these data suggest that multiple pathogen exposures may be required to establish widespread and effective protection against secondary infection. Further, these data may provide an explanation for why higher proportions of TRM phenotype cells are found in human tissues compared with mice, particularly in lymphoid tissue sites, as the human tissues investigated have been experienced years or several decades of continuous and diverse pathogen exposures. Finally, there is also evidence in both humans and mice that TRM formation is developmentally regulated. A recent study from our laboratory showed reduced formation of TRM in the lungs of infant mice compared with adult mice following influenza infection [178]. This effect was T cell intrinsic, as adoptively transferred infant T cells had a reduced ability to establish TRM in adult hosts. Another study from our lab showed reduced CD103 expression by TRM in infants compared with children [16]. This could either be a result of decreased antigen exposure, T cell intrinsic defects in TRM general in infants, or both. Overall,

however, it is clear that both antigen exposure and development play an important role in TRM formation.

Numerous studies have demonstrated that TRM can persist long-term in tissues without ongoing infection [103, 123, 124, 143], and studies have examined the signals that promote this TRM maintenance and survival within the tissue. Interestingly, there is evidence that TRM can be generated and maintained in the absence of antigen and that these TRM are protective against subsequent infection [117, 143, 174]. However, these studies focused on CD8⁺ TRM in epithelial sites, and signaling requirements for TRM in different sites may be different. The signaling requirements for CD4⁺ TRM may also be different, as the one study mentioned did not find long term retention of CD4⁺ cells in the genital tract when there was no inflammation or antigen, unlike for CD8⁺ TRM [117]. CD4⁺ TRM may be maintained by memory lymphocyte clusters, as mentioned above, in which CD4⁺ TRM exist below the epithelium in clusters with antigen presenting cells and CD8⁺ TRM. Within these clusters, CD4⁺ TRM receive ongoing signals in the form of chemokines and low grade antigen from macrophages, which may promote their long term survival and maintenance [175].

The homeostatic signals for TRM maintenance have not yet been defined. One study found that IL-15 signals are required for TRM formation [110], and another study found that residual T-bet expression was required for longer term TRM survival via maintaining CD122 expression (which is a receptor for IL-15) [106]. Together, these findings suggest that IL-15 is critical for both generation and maintenance of TRM, at least for CD8⁺ TRM in barrier tissues and in mice. However, another study found that IL-15 was not required for the generation or maintenance of CD8⁺ TRM populations in secondary lymphoid tissues [112]. Therefore, it is not clear whether maintenance signals for TRM differ from those required for TEM or TCM persistence, which

require IL-7 and IL-15 for long-term maintenance [179]. It is also not known whether maintenance requirements of TRM differ in barrier vs. lymphoid tissues. Finally, there is also evidence that aryl hydrocarbon receptor signaling may be important for the maintenance of CD8⁺ TRM populations in the skin [152].

A recent article reported that uptake of exogenous free fatty acids via the transporters FABP4 and FABP5 is necessary for CD8⁺ TRM survival in vivo [140]. In the setting of FABP4 and FABP5 deficiency, TRM survival was impaired. However, FABP4 and FABP5 deficiency also resulted in reduced TRM numbers at early time points, suggesting the importance of these transporters both for TRM generation and long-term maintenance. Notably, CD8⁺ TRM from human skin also exhibited increased expression of FABP4 and FABP5 [140], suggesting that preferential use of free fatty acids may be a universal property of CD8⁺ TRM in barrier sites.

Tissue residency in other T cells subsets

Tissue residence may not be unique to memory T cells. There is evidence that naïve T cells can persist in tissues, and particularly within lymph nodes. Clonal analysis of naïve T cells in spleen and lymph nodes of individuals revealed no overlap between the TCR repertoires of naïve T cells from different lymphoid sites, regardless of age [15]. Even naïve T cell clones that were modestly expanded were largely limited to a single lymphoid site, in contrast with expanded memory populations which showed high overlap between sites [15]. These data suggest that naïve T cells take up long term residence in lymph nodes where they can expand *in situ*, with lymph nodes serving as reservoirs for their maintenance. Given that naïve T cells lack expression of canonical TRM markers, we propose that retention mechanisms for naïve T cells in lymph nodes may be more dependent on cytokine signaling rather than specific cell-cell interactions.

The concept of tissue residency has also been described for Tregs. In mice, tissue Tregs in fat, lung, and muscle serve key roles in metabolic homeostasis and tissue repair and exhibit distinct phenotypes and transcriptional profiles compared with lymphoid Tregs [180]. In human tissues, a proportion of Tregs (40-50%) express the TRM marker CD69 [16]. Tregs residing in human skin also express skin-homing receptors CLA, CCR4, and CCR6 [181]. Increased proportions of Tregs which differentially produce IL-17 have been identified in psoriatic skin lesions compared to unaffected skin [182], suggesting roles for Tregs in controlling local homeostasis. Tregs have also been identified in human fat, with decreased Tregs correlating with obesity [183]. Human tissue Tregs in lymph nodes may preserve homeostasis as their depletion results in increased T cell proliferation and cytokine production *ex vivo* [16, 184]. More studies are required to dissect the importance and functional role of human tissue Tregs in maintaining homeostasis.

Outstanding Questions about TRM

Overall, current research suggests that therapeutic modulation of TRM can have broad implications for infectious disease therapy, vaccination, autoimmunity, and cancer, and this has sparked considerable research on TRM in recent years. However, there are still a number of unanswered questions about TRM biology. For example, the developmental relationship between TRM and other memory subsets is unclear, and it is also not known if TRM represent a terminally differentiated subset with the inability to proliferate. Further, the majority of studies on TRM are conducted in mice and examine responses in barrier tissues, and therefore the characteristics of TRM in lymphoid tissues and in humans are not well-defined. In humans, reliable phenotypic markers of TRM have not been established. Further, the transcriptional and functional characteristics that define TRM in humans is not known, as well as how these properties vary for

CD4⁺ and CD8⁺ TRM and for TRM from different tissues. In fact, at the start of this research, transcriptional profiling had not been performed comparing human TRM to other memory subsets, or on TRM from lymphoid tissues. Finally, interpretation of TRM studies is further complicated by the fact that TRM are heterogeneous; different groups of TRM have been described based on function, homing receptor profiles, and cell surface phenotype, and some of these TRM subtypes are developmentally distinct and have unique subatomic localizations [133, 155, 168, 185]. Therefore, data about one subset of TRM cannot always be extrapolated to another TRM subset. Overall, the aims of this thesis seek to fill several gaps in our current understanding of human TRM, as described in the next section.

Section 1.6: Thesis aims

AIM 1: Define phenotypic, functional, and transcriptional signatures of human TRM.

As described above, while many aspects of TRM biology are well-characterized in mice, major gaps exist in our understanding of human TRM. First off, reliable phenotypic markers of TRM in humans have not been established. It is also not known whether TRM represent a distinct memory subset in humans, with unifying transcriptional, phenotypic, or functional characteristics for CD4⁺ and CD8⁺ from different tissues. In fact, even in mice CD4⁺ TRM and TRM from lymphoid sites have not been completely characterized; in particular, whole transcriptome profiling of these subsets has not been performed. *We hypothesize that human TRM can be identified by the expression of CD69, and that human TRM represent a distinct memory subset with unique transcriptional, phenotypic, and functional properties relative to circulating memory subsets.* In order to address this, there are five specific subaims:

1. Investigate the distribution of CD69 and CD103 expression by memory T cells across human tissues.
2. Determine if CD69 expression identifies human TRM.
3. Identify transcriptional, phenotypic, and functional properties of human TRM from spleen and lung tissues, and for both CD4⁺ and CD8⁺ lineages.
4. Compare the transcriptional properties of human and mouse TRM
5. Establish a core gene signature that is common to TRM from multiple tissue sites, CD4⁺ and CD8⁺ lineages, and mouse and human species.

Here, we demonstrate that CD69 is exclusively expressed by memory T cells in tissues and that CD69⁺ memory T cells do not show features of activation. Transcriptionally, CD69⁺ memory

T cells in tissues share key homologies to mouse TRM and were distinct from CD69- memory T cells in tissues, which were similar to circulating blood TEM. Together, these data suggest that TRM are contained within the CD69+ fraction of memory T cells in tissues while CD69- memory T cells in tissues are circulating. Next, we identify a core transcriptional profile of 31 genes that defines the human TRM subset in lung and spleen and is common to both CD4⁺ and CD8⁺ TRM. We also show that TRM in mice also have differential expression of these genes, suggesting that this core signature identifies universal properties of the TRM subset. Based on this core signature, TRM in humans had a unique profile of adhesion and homing molecules, including upregulation of specific integrins and downregulation of specific homing receptors that mediate tissue egress. Functionally, while CD4⁺ and CD8⁺ human TRM in multiple sites had an enhanced ability to produce certain effector cytokines, these TRM also exhibited increased expression of inhibitory molecules such as PD-1, produced higher levels of the anti-inflammatory cytokine IL-10, and exhibited reduced proliferation compared with circulating TEM, suggesting a dual functional role encompassing protection and regulation. Overall, these results establish that human TRM identified by CD69 expression are transcriptionally, functionally, and phenotypically distinct from their circulating counterparts.

AIM 2: Investigate the functional and transcriptional bases for human TRM heterogeneity.

Our data from the first aim suggested substantial heterogeneity within the human TRM subset, both functionally and phenotypically [186]. This finding is consistent with prior studies in both mice and humans, showing that functionally and phenotypically distinct subsets of TRM exist, with different subsets have different developmental pathways, transcriptional profiles, subanatomic locations, and roles in protection and disease [10, 108, 133, 155, 168]. Therefore,

even though as a whole TRM represent a subset with critical roles in pathogen clearance and human disease, understanding how different TRM subsets function is vital before clinical strategies targeting TRM can be implemented.

Heterogeneity based on the ability to efflux fluorescent dyes has not been characterized with the human TRM subset. However, the importance of this trait is underscored by that fact that the capacity to efflux fluorescent dyes is associated with increased self-renewal properties for hematopoietic stem cells [187, 188]. As numerous studies have reported that TRM can persist long-term in tissues, an efflux(+) subset may present of a subset of TRM poised for longevity and serve as a reservoir for renewal of other TRM subsets. Notably, the ability to efflux dyes has been demonstrated T cells, both in mucosal-associated invariant T cells (MAIT) [189, 190] as well as non-MAIT T cells in tissues such as bone marrow and intestines [191, 192]. *We hypothesize that TRM with the ability to efflux dyes exist in both lymphoid and mucosal tissues, and that efflux(+) TRM represent a functionally distinct subset of TRM.* There are four specific subaims:

1. Determine if efflux(+) memory T cells exist within healthy human tissues.
2. Establish the unique phenotypic properties of the efflux(+) subset.
3. Establish the unique functional properties of the efflux(+) subset, including cytokine producing and cytotoxic abilities, proliferative capabilities, and responses to homeostatic cytokines.
4. Characterize the transcriptional profile of efflux(+) TRM, and determine how efflux (+) TRM respond transcriptionally to stimulation.

In this study, we describe a functionally distinct subset of human CD8⁺ TRM defined by the capacity to efflux fluorescent dyes that are not MAIT T cells. Efflux(+) TRM were found in

multiple tissue sites including spleen, lymph nodes, lung, and bone marrow. Compared with efflux(-) TRM, efflux(+) TRM showed evidence of reduced proliferative turnover (as measured by Ki67), increased CD127 expression, and decreased expression of activation (HLA-DR) and exhaustion markers (PD-1, CTLA-4), suggesting that efflux(+) TRM exist in a more quiescent and less activated state within tissues. Transcriptional profiling supported these results, with differential expression of genes controlling the cell cycle, and further suggested that efflux(+) TRM have a unique profile of adhesion and migration markers that promotes long-term retention. Functionally, efflux(+) TRM produced reduced quantities of inflammatory cytokines and underwent less cytotoxic degranulation after stimulation compared with efflux(-) TRM. Moreover, efflux(+) TRM had higher proliferative capacity after stimulation and exhibited greater responses to IL-7 signaling. Interestingly, efflux(+) TRM had an enhanced capacity for IL-17 production and showed evidence of IL-17 signaling transcriptionally. Together, these results establish efflux(+) and efflux(-) TRM are unique subsets that may exhibit non-redundant functions during the immune response. Specifically, efflux(+) TRM may have a program that promotes longevity and retention and therefore serve as a reservoir of TRM capable of proliferation upon infection, while efflux(-) TRM may be poised for secretion of effector cytokines and for direct cytotoxic function to rapidly clear pathogens.

CHAPTER 2: Materials and Methods

Section 2.1: Acquisition and isolation of T cells from human tissues

Acquisition of human tissue samples from organ donors

Human tissues were obtained from deceased organ donors at the time of organ acquisition for clinical transplantation through an approved research protocol and material transfer agreement with LiveOnNY, the organ procurement organization for the New York metropolitan area. All donors were free of chronic disease and cancer, Hepatitis B, and Hepatitis C, and were HIV-negative. Isolation of tissues from deceased organ donors does not qualify as “human subjects” research, as confirmed by the Columbia University IRB. For isolation of blood from living volunteers, blood was drawn via venipuncture from consented volunteers, as approved by the Columbia University IRB.

The procedure for acquiring tissue samples from research consented organ donors involves coordinating the activities of transplant surgeons, transplant coordinators, our laboratory’s on-call surgeons, and laboratory researchers. First, our laboratory’s on-call surgeons are notified by transplant coordinators when a researching consented organ donor meeting our laboratory’s criteria becomes available. Our surgeons are notified of the time of operation and travel to the hospital where the organ donor is located. After the transplant team finishes harvesting organs that are used for life-saving clinical transplantations, the laboratory’s surgeons are allowed to use the same incisions to harvest organs for research purposes. The current protocol and agreement with LiveOnNY allows us to obtain the following tissues: blood, bone marrow, thymus, spleen, lung lymph nodes, mesenteric lymph nodes, inguinal lymph nodes, pancreas, pancreatic lymph nodes, duodenum, jejunum, ileum, colon, appendix, peyer’s patches, lung, salivary glands, tonsils, and fat (Figure 2.1). These organ donor tissues are flushed with cold preservation solution and

transported to the lab in saline, typically arriving within 2-4 hours of organ extraction. Upon arrival in the laboratory, these organs are placed in complete RPMI (RPMI containing 10% FBS, glutamine, and penicillin-streptomycin) at 4°C and are processed immediately, as detailed below.

Isolation of lymphocytes from human tissues

The methods for isolation of lymphocytes described below are based on findings in mice [193, 194] and have been optimized and published by former members of the lab and me over a number of years [13-19, 186]. The basic protocols which were further optimized in this study, including the isolation of lymphocytes without enzymatic digestion are detailed below.

Blood samples were first centrifuged to remove plasma. Blood (after plasma is removed) and bone marrow were diluted 2:1 with complete RPMI and centrifuged through lymphocyte separation medium (LSM, Corning). The lymphocyte containing buffy coat layer was removed and red blood cell lysis was performed using ACK buffer for 5 minutes on ice (Corning).

Spleen samples were chopped into small pieces and placed into 50 ml conical tubes with 25 ml digestion media (RPMI containing 10% FBS, glutamine, penicillin-streptomycin, collagenase D [1 mg/ml], trypsin inhibitor [1 mg/ml], and DNase I [0.1 mg/ml]), and incubated with mechanical shaking at 37°C for 1 hour. Lung and gut tissue were carefully inspected to exclude lymph nodes and then chopped into small pieces and placed in digestion media as above for 2 hours. Digested tissue was disrupted using the gentleMACS tissue dissociator (Miltenyi Biotech) and then passed through a stainless steel tissue sieve (10 to 150 mesh size), followed by pelleting through centrifugation. Residual red blood cells (RBC) were lysed via incubation for 5 min in ACK lysis buffer (Lonza), and dead cells and debris were removed by centrifugation through a solution of RPMI containing 30% Percoll (GE Healthcare Life Sciences). A second RBC

lysis was performed if necessary. Cells were then pelleted and washed with complete RPMI, and the final cell suspension was filtered using a 70 μ m cell strainer (Corning).

For lymph nodes, fat tissue was removed followed by chopping into small pieces and digestion as above for 1 hour. Digested tissue was disrupted using the gentleMACS tissue dissociator (Miltenyi Biotech) and then filtered through a 70 μ m cell strainer (Corning).

Isolation of lymphocytes from solid tissues without enzymatic digestion

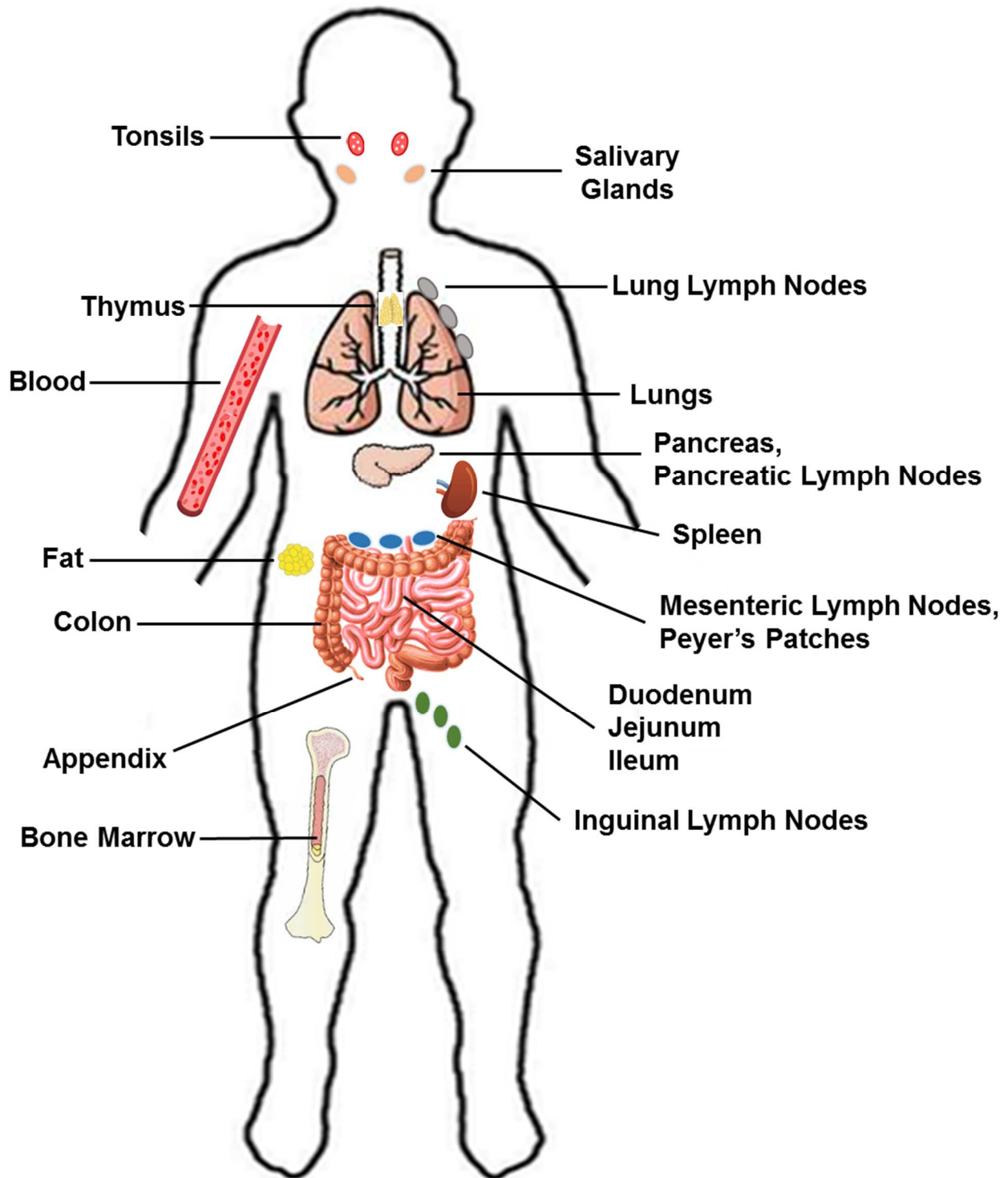
Non-enzymatic isolation was performed using the Bullet Blender Tissue Homogenizer (Next Advance). Tissue samples were chopped into small pieces (<5mm) using scissors and 4-5g of tissue was placed in a 50ml conical tube along with complete RPMI to a total volume of 10ml, followed by addition of 7-8 4.8 mm stain steel beads (Product SSB48). Tissues were homogenized in the bullet blender for 2 minutes at speed setting 3-4. Following homogenization, the mixture was filtered through a 70 μ m Cell Strainer (Corning). ACK buffer was used for RBC lysis, and followed by an additional filtration through a 70 μ m Cell Strainer (Corning).

Cryopreservation of lymphocytes

Lymphocyte suspensions were cryopreserved in Cryogenic Vials (Corning) in a solution of 10% dimethylsulfoxide (DMSO) in FBS at a concentration of 10 million cells/mL per vial. Vials containing the cell suspensions were placed into Mr. Frosty Cryo Freezing Containers (Nalgene) and placed in a -80°C freezer, which allows for cooling a rate of 1°C/min. After reaching -80°C, vials containing frozen cell suspensions were transferred to liquid nitrogen. The frozen lymphocytes are viable for years after storage in liquid nitrogen and the Farber lab has cryopreserved lymphocyte suspensions from multiple tissue sites from over 300 donors.

To thaw cryopreserved cell suspensions, each vial was removed from liquid nitrogen and immediately placed in a 37°C water bath until the cells suspension was fully thawed. Cell suspensions were passed through a 100µm filter paper, and warm complete RPMI was added slowly. This protocol has been demonstrated to optimize cellular viability [195]. Finally, to minimize clumping of cell suspensions, 0.1 mg/mL DNase was added during this step and the solution was allowed to sit at room temperature for 1-2 minutes before centrifugation.

Figure 2.1. Tissue sites received from organ donors.



Note: some organ images taken from Google Image search results.

Section 2.2: Flow cytometric analysis of human T cells

Flow cytometric analysis and cell sorting

For flow cytometry analysis, single-cell suspensions were stained with fluorochrome-conjugated antibodies (See Table 2.1 below for a list of all antibodies used for flow cytometry in this study) in staining buffer (PBS/1% fetal bovine serum/0.1% sodium azide). Control samples included unstained, single fluorochrome-stained compensation beads (UltraComp eBeads, eBioscience) and fluorescence minus one (FMO) controls. Stained cells were acquired using a BD LSRII or BD Fortessa. Data were analyzed using FlowJo software (Tree Star) and FCS Express (De Novo Software). FCS express software was used for generating t-SNE plots from flow cytometry data.

For identification of cytomegalovirus (CMV) specific T cells, samples from HLA-A2 haplotype donors were labeled with IE1-VLE peptide tetramers (Proimmune). For phospho-flow cytometry, cells were first fixed with 4% PFA for 15 minutes followed by permeabilization with ice-cold methanol.

For intracellular staining for detection of cytokines and transcription factors, cells were fixed and permeabilized using the Fixation/Permeabilization Solution Kit (BD Biosciences) for detection of cytokines and Foxp3/Transcription Factor Staining Buffer (Ebiosciences) for detection of transcription factors.

For isolation of subsets by fluorescent-activated cell sorting, lymphocyte suspensions were enriched for T cells using the MojoSort Human CD3 T cell Isolation Kit (Biolegend), stained for surface markers (as described above) in sort buffer (PBS/1% fetal bovine serum), and sorted using a BD Influx high-speed sorter or BD Aria IIu sorter (both from BD Biosciences).

Staining with mitochondrial dyes for detection of efflux(+) T cells

T cells were labeled with Mitotracker Green FM (50nM) or CMXRos (25nM) (Thermo Fischer) for 15 minutes in complete media (10% FBS in RPMI) at 37°C, shielded from light. Dye efflux was blocked by performing fluorescent labeling reactions in the presence of 25-50uM cyclosporine (CSA).

Table 2.1: List of antibodies used for flow cytometry.

Reactivity	Target	Clone	Company
Human	CCR5	J418F1	Biolegend
Human	CCR6	11A9	BD Biosciences
Human	CCR7	G043H7	Biolegend
Human	CCR9	L053E8	Biolegend
Human	CD101	BB27	Biolegend
Human	CD103	ber-ACT8	Biolegend
Human	CD107a	eBioH4A3	eBioscience
Human	CD127	A019D5	Biolegend
Human	CD161	HP-3G10	eBiosciences
Human	CD19	SJ25C1	Biolegend
Human	CD25	BC96	Biolegend
Human	CD27	M-T271	BD Biosciences
Human	CD28	CD28.2	eBiosciences
Human	CD3	OKT3	Biolegend
Human	CD3	SK7	BD Biosciences
Human	CD38	TU66	BD Biosciences
Human	CD39	A1	Biolegend
Human	CD4	OKT4	Biolegend
Human	CD4	RPA-T4	Biolegend
Human	CD45RA	H1100	Biolegend
Human	CD49a	TS2/7	Biolegend
Human	CD57	HNK-1	7Biolegend
Human	CD62L	DREG-56	Biolegend
Human	CD69	FN50	Biolegend
Human	CD8	RPA-T8	Tonbo
Human	CD8	SK1	BD Biosciences
Human	CTLA4	L3D10	Biolegend
Human	CX3CR1	2A9-1	Biolegend
Human	CXCR6	K041E5	Biolegend
Human	Eomes	WD1928	eBiosciences
Human	HLA-DR	LN3	Biolegend
Human	IFN-gamma	B27	BD
Human	IL-10	JES3-9D7	Biolegend
Human	IL-17	BL168	Biolegend
Human	IL-2	MQ1-17H12	BD
Human	Ki67	MKI67	Biolegend
Human	Live/Dead Marker	n/a	Biolegend
Human	Live/Dead Marker	n/a	Biolegend
Human	MDR1	UIC2	Biolegend
Human	PD-1	EH12.1	Biolegend

Human	pSTAT5	pY694	BD Biosciences
Human	Tbet	eBio4B10	eBiosciences
Human	Tim3	B8.2c12	Biolegend
Human	TNF	MAb11	BD
Human	Va7.2	3C10	Biolegend
Human	ZNF683	Sanquin-Hobit/1	BD Biosciences

Section 2.3: Functional Assays

T cell stimulations and cytokine analysis

For quantification of cytokine production by different T cell subsets, sorted cells were plated in 96-well round-bottom plates at 10^5 cells/well in complete RPMI medium and stimulated using anti CD3/CD28/CD2 beads (T cell activation/expansion kit, Miltenyi Biotech) for 48 or 72 hours. Supernatant cytokine levels were measured using the BD Cytometric Bead Array (Human Th1/Th2/Th17 Cytokine Kit) (see details below).

For detection of cytokine production by intracellular staining, CD4⁺ or CD8⁺ T cells from spleen and lung tissues were stimulated with PMA (50ng/ml) + ionomycin (1 μ g/ml) for 3 hours at 37°C in the presence of BD Golgistop (containing Monensin). Cytokine production was assessed by intracellular staining for cytokines as described above. To quantify degranulation (CD107a expression), cells were labeled with anti-CD107a antibody before stimulation with PMA/ionomycin.

Details of Cytometric Bead Array (CBA)

CBA uses the dynamic range of detection in flow cytometry to analyze the levels of multiple cytokines at the same time via detection of fluorophores attached to antibody coated beads [196]. The protocol has two main steps: first, antibody coated beads that bind to cytokines are added to the samples, and second, a fluorochrome conjugated reagent is added that binds to the anti-cytokine beads. Samples are then incubated for 3 hours in the dark, washed to remove beads that did not bind cytokines, and then analyzed by flow cytometry. The APC intensity of the beads is used to identify which cytokine is being detected, and the PE intensity is proportional to the concentration of the cytokine. Finally, a standard curve is created by using serial dilutions of a

sample of known concentration provided by the manufacturer. The Th1/Th2/Th17 kit used in these experiments simultaneously detects the expression of IL-2, IL-4, IL-6, IL-10, TNF, IFN-gamma, and IL-17. Samples were diluted 2:1 with the assay diluent provided in the kit in order to bring the cytokine concentrations within the range of detection.

Proliferation Assays

For proliferation assays, cells were isolated via cell sorting as described above and then were labeled with Cell Trace Violet (Thermo Fisher) according to the manufacturer's instructions. Labelled cells were plated at 100,000 cells/well and stimulated with anti CD3/CD28/CD2 (T cell activation/expansion kit, Miltenyi Biotech) beads for 4 days.

Detection of responses to Il-7 via phospho-flow cytometry

Sorted cells were rested in RPMI medium without serum for 2 hours. Cells were then transferred to complete media supplemented with 50ng/mL IL-7 (PeproTech) and stimulated for 20 minutes before phospho-flow cytometry for detection of p-STAT5 as described above.

Section 2.4: Whole transcriptome profiling by RNA Sequencing

RNA Extraction from T cells and RNA Sequencing

An overview of the workflow for RNA-Sequencing (RNA-Seq) from sample preparation in the laboratory to analysis of data is shown in Figure 2.2. T cell subsets were sorted as described above and RNA was isolated from cell pellets using the RNeasy Mini Kit (Qiagen), according to manufacturer's instructions. RNA concentration and quality was assessed using an Agilent 2100 Bioanalyzer instrument (Agilent Technologies). For the majority of samples, >400ng of total RNA

was submitted for sequencing. RNA-Seq libraries were prepared using standard TruSeq with poly-A pull-down and sequenced them on the Illumina HiSeq 2500 with 101bp single-end reads at the Columbia Genome Center. For samples with less than 100ng total RNA, the Clontech SMART-Seq v4 Ultra Low Input RNA Kit for cDNA amplification was used.

Analysis of Data

RNA-Seq reads were mapped using TopHat [197] with default parameters to the human reference genome build hg19, data quality control performed using RNA-SeQC [198], read counts computed using HTSeq [199], and per-gene Fragment Per Kilobases Per Million reads (FPKM) estimated using Cufflinks [200]. Data are available on GEO (For data presented in Chapter 3, accession: GSE94964).

Downstream statistical analysis was done using R programming language. We used EdgeR [201] for differential gene expression analysis, using donor information as a covariate to control donor-specific effects. We considered genes as significantly differentially expressed between two groups if $FDR \leq 0.05$ and absolute value of \log_2 fold change > 1 . For other analyses and visualization purpose, we first normalized gene read counts with DESeq2 [202], and then removed the donor and sequencing batch effect with function ComBat in sva [203] package. We performed Principal component analysis (PCA) using function *prcomp* in R, with centering, scaling, and cor options on. We plotted heatmap with Z-score of log base 10 normalized read counts with samples clustered by unsupervised hierarchical clustering function *hclust* in R and visualized with heatmap.2 in the *gplots* package. Complete linkage method was used for clustering, with the distance between samples defined by Euclidean distance. For analyses presented in Chapter 4,

DESeq2 was used instead of EdgeR to compute differential expression, and cutoffs for significance were the same as above.

A number of methods were used for biological interpretation of differential expression results. First, pathway analysis was performed using Ingenuity Pathway Analysis software (IPA, Qiagen). For IPA analysis, differential expression data from EdgeR or DESeq2 was uploaded to IPA software. The entire dataset (approximately 25000 genes) was uploaded to IPA, and then within IPA a significance cutoff was set such that the software only analyzes the genes that meet the defined criteria. In general, the top 1000 most significant genes by FDR were used for analysis, based on advice from the company's scientist. The dataset uploaded to IPA contains the gene names, fold changes, expression levels, p-values, and FDR values, and the analysis takes all of these variables into account. Within the analysis results, the canonical pathways and cellular functions tabs were used to interpret data. The canonical pathways function lists pathways that are predicted to be enriched based on the gene expression data, along with a p-value and a z-score that indicates directionality of the pathway. In certain cases, the software is not able to predict the directionality of a pathway, even if the p-value is significant. This situation may arise if several differentially expressed genes are involved in the pathway but the fold changes are not all consistent with up or downregulation of that entire pathway. The cellular functions tab of IPA lists certain functions that are predicted to be enriched based on the differential expression data, and these functions may be for example migration or proliferation.

Pathway analysis was also performed using the Database for Annotation, Visualization and Integrated Discovery (DAVID) [204, 205]. For DAVID online software, the list of differentially expressed genes was first uploaded. In some cases, the list of genes that met our criteria for differential expression was too short for DAVID to do pathway analysis; in this situation, the top

300 differentially expressed genes by FDR value were uploaded. After uploading the dataset, we used the gene ontology function within the functional annotation chart feature. Similar to IPA, this result displays a list of pathways predicted to be enriched based on the differentially expression genes. Unlike IPA however, DAVID only takes into account the actual gene list but not information about fold changes or expression levels. Therefore, pathways results cannot be interpreted in terms of directionality.

The pathways listed by DAVID and IPA were used to determine the functional relevance of the genes that were differentially expressed. However, pathway results produced by these software are often non-specific and sometimes dozens or even 100+ significant pathways are generated. Therefore, biological interpretation of the RNA-Seq data was also based on a manual review of the differentially expressed genes as follows. First, IPA software was used to annotate the list of differentially expressed genes. The dataset uploaded to IPA contains the gene ID, and IPA can create a table that fills in the full gene name, identify the location of the gene product (e.g. nucleus, plasma membrane, etc.), and assign a category that the gene product (e.g. enzyme, cytokine, etc.) This table was exported and served as a basis for manual interpretation. For many genes, IPA was unable to assign a location or category, in which case we would search the literature for data about the gene and its product (and in particular in T cells), and then assign a category. This analysis allowed us to group all of the differentially expressed genes into ~10 broad categories, and then examine the individual genes that contributed to each category. An example of this type of analysis is shown in Chapter 4, where we have manually assigned 133 differentially expressed genes into 9 categories and displayed select genes from these categories. Integrating this analysis with the pathway analysis allows for a more thorough interpretation of the data, particularly when the results from these two analyses are consistent as is the case in Chapter 4. In

that specific example, the categories of genes by manual annotation largely align with the functions associated with the enriched pathways, and visualization of the individual genes contributing to each category provides insight into exactly how the biology of the two groups are different.

Manual interpretation and integration of multiple sources was also used to examine the connectivity between key genes. The diagram in Fig. 3.5B which shows connectivity between genes shown in Fig. 3.5A was created using IPA software, STRING Protein database, GeneCards, and Pubmed literature searches. For IPA, the Networks and Pathways functions were used to examine connections between the gene list in Fig. 3.5A and literature references provided by IPA were checked manually before using predicted or established relationships. For STRING [206], only results in the “Known Interaction” category were used. All of the genes listed in the core signature were put into GeneCards and search results were examined for relationships between genes. For select genes, a PubMed search was conducted to determine if there was an established role of these genes in T cells. Pathways listed in Fig. 3.5B that encompass multiple genes were determined using IPA, ConsensusPathDB [207], and Pathcards.

Identification of lineage- and tissue-specific genes within transcriptional profiles

This section provides a detailed methodology for the analysis that was done for analysis of data presented in Chapter 3 for identification of lineage or tissue specific genes as shown in Figs. 3.13 and 3.14. Among the genes that were differentially expressed in any lineage subset (CD4⁺ or CD8⁺) of 69⁺ vs. 69⁻ cells from any tissue site (spleen or lung), we defined CD4⁺ specific genes by the following criteria: (a) differentially expressed with statistical significance (FDR < 0.05 and absolute value of log₂ fold change >1) in CD4⁺ 69⁺ vs. 69⁻ comparison, (b) log₂ fold change has the same direction in all CD4⁺ 69⁺ vs. 69⁻ comparisons (both spleen and lung samples), and (c)

not differentially expressed with any marginal significance (p -value > 0.05) in CD8⁺ 69+ vs. 69– comparison. We defined CD8⁺ specific genes similarly by switching CD4⁺ with CD8⁺. Among the genes that are differentially expressed in any tissue subset (lung or spleen) of 69+ vs. 69– cells of a certain lineage (CD4⁺ or CD8⁺), we defined lung specific genes by the following criteria: (a) differentially expressed with statistical significance (FDR < 0.05 and absolute value of log₂ fold change > 1) in lung 69+ vs. 69– comparison, (b) log₂ fold change has the same direction in all lung 69+ vs. 69– comparisons (both CD4⁺ and CD8⁺ samples), and (c) not differentially expressed with any marginal significance (p -value > 0.05) in spleen 69+ vs. 69– comparison. We defined spleen specific genes similarly by switching lung with spleen.

Gene set enrichment analysis

We obtained previous published mouse microarray expression data (from Mackay et al., 2013, Wakim et al., 2012) which included TRM and TEM samples as input into GSEA [208], and tested the null hypothesis that genes identified as part of the human TRM signature have uniform distribution in ranks by the absolute value of log fold change between mouse TRM and TEM on the x-axis. We rejected the null hypothesis if the p -value was smaller than 0.05.

Identification of TCR Repertoire Sequences using TRUST

TRUST is a computational method to infer CDR3 sequences of T cell receptors using RNA-seq data based on de novo assembly [209]. The input file used for TRUST was the bam file that was generated using TopHat. The following 3 criteria were applied when parameterizing the aligners: 1) Both mapped reads and unmapped reads were included. 2) Local alignment was

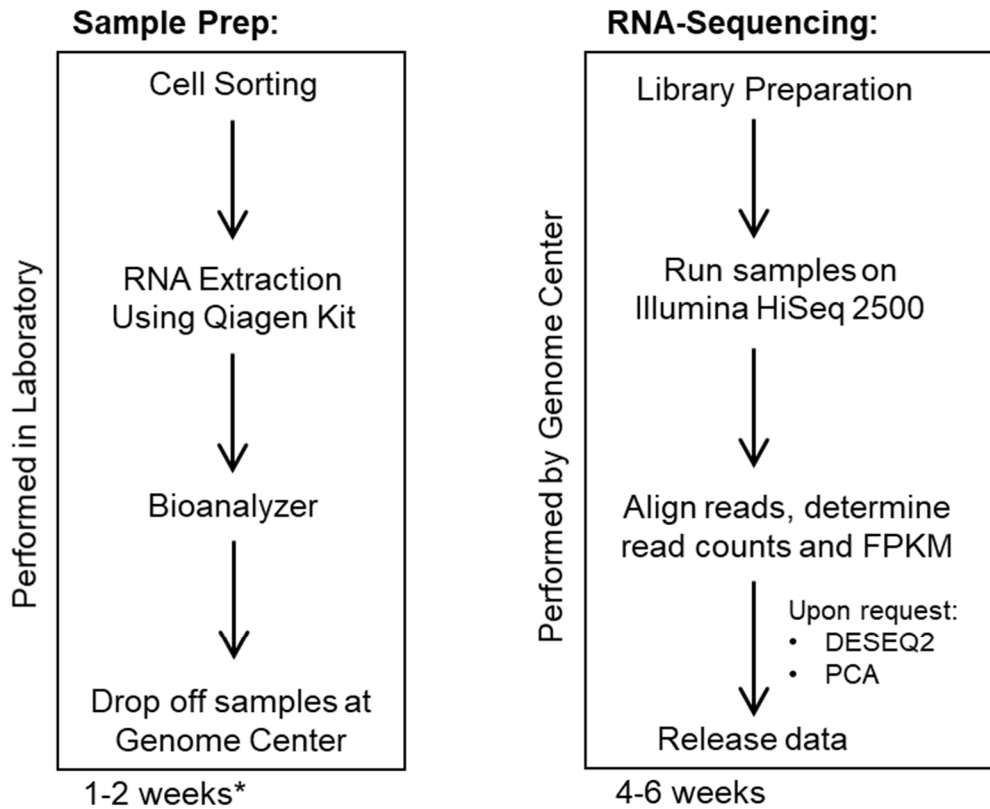
disabled. 3) The number of mismatch tolerated for mapped reads was ≤ 2 . The following command was used: `python TRUST.py -f sample.bam -a -s -H`

Figure 2.2. RNA-Sequencing workflow used in this study.

(A) Left: Workflow for processing samples in laboratory. First, following isolation of lymphocytes from tissues, the cell population of interest was isolated by cell sorting. RNA was extracted from cell pellets using the RNeasy Kit from Qiagen. RNA samples were analyzed for concentration and purity using the Agilent Bioanalyzer, followed by which frozen samples were dropped at the Columbia Genome Center. Right: Workflow for RNA-Sequencing at Columbia Genome Center. First, library preparation and sequencing on the Illumina HiSeq 2500 were performed. Next, read alignment was performed followed by calculation of read counts and FPKM values. Finally, data was released via an online link. Upon request, the Genome Center performed differentiation expression analysis using DESEQ2 as well as PCA analysis.

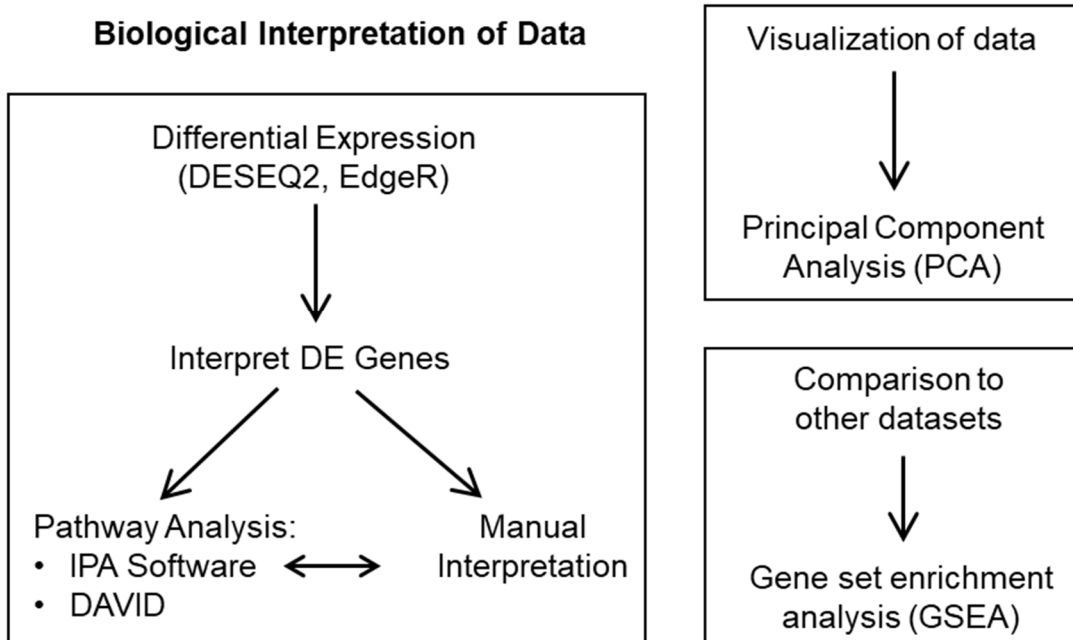
(B) Workflow for biological interpretation of RNA-Seq data. First, differential expression analysis was performed using DESEQ2 or EdgeR. The listed of differentially expressed (DE) genes was interpreted both using pathway analysis or by manual interpretation. Principal Component Analysis (PCA) was used for visualization of samples. Gene set enrichment analysis (GSEA) was used for comparison of data to other datasets.

A.



*Sample processing only. May take months to receive several donors meeting criteria.

B.



Section 2.5: Imaging of human lymphoid tissues

Fresh human LLN isolated from organ donors were fixed immediately in 1.0% paraformaldehyde and PBS (pH 7.4) containing 0.1M L-Lysine (Sigma Aldrich), incubated in 20% sucrose at 4°C, and then embedded in Tissue-Tek OCT compound. 8-10µm thick sections were cut using a Leica CM 1950 cryostat. For staining, sections were first permeabilized using 0.1% Triton X-100 (Sigma-Aldrich). Next, samples were incubated in blocking buffer (PBS + 20% Blocking One reagent) at room temperature. Staining was performed using fluorochrome-conjugated antibodies in blocking buffer at 4°C. Finally, samples were mounted on coverslips with Prolong Diamond Antifade Mountant (Life Technologies). Images were acquired using a EVOS FL Auto 2 Imaging System (Thermo Fischer). Antibodies used for imaging included: CD69 (alexa fluor 647, clone FN50), CD4 (alexa fluor 594, clone OKT4), and CD8 (alexa fluor 488, clone RPA-T8).

Section 2.6: Statistical tests

Descriptive statistics (percent, mean, median, SEM) were calculated using Prism (Graphpad software). Significant differences in frequencies, ratios, gMFI, and density were assessed using a paired *t* test. Statistical analysis of RNA-Sequencing data was described in Section 2.4.

CHAPTER 3: Human tissue-resident memory T cells are defined by core transcriptional and functional signatures in lymphoid and mucosal sites.

ABSTRACT:

Tissue-resident memory T cells (TRM) in mice mediate optimal protective immunity to infection and vaccination, while in humans, the existence and properties of TRM remain unclear. Here, we use a unique human tissue resource to determine whether human tissue memory T cells comprise a distinct subset in diverse mucosal and lymphoid tissues. We identify a core transcriptional profile within the CD69⁺ subset of memory CD4⁺ and CD8⁺ T cells in lung and spleen that is distinct from that of CD69-TEM cells in tissues and circulation, and defines human TRM based on homology to the transcriptional profile of mouse CD8⁺TRM. Human TRM in diverse sites exhibit increased expression of adhesion and inhibitory molecules, produce both pro-inflammatory and regulatory cytokines, and have reduced proliferation compared with circulating TEM, suggesting unique adaptations for *in situ* immunity. Together our results provide a unifying signature for human TRM and a blueprint for designing tissue-targeted immunotherapies.

Chapter expanded from:

Kumar, B.V.*, Ma, W.*, Miron, M., Granot, T., Guyer, R.S., Carpenter, D.J., Senda, T., Sun, X., Ho, S.H., Lerner, H., Friedman, A.L., Shen, Y., and Farber, D.L. (2017). Human Tissue-Resident Memory T Cells Are Defined by Core Transcriptional and Functional Signatures in Lymphoid and Mucosal Sites. *Cell Rep* 20, 2921-2934.

* Co-First Authors

Section 3.1: Introduction

The establishment and maintenance of long term immunity depends on the generation of memory T cells which can populate diverse tissue sites. The effector-memory (TEM) subset [93] is the predominant subset migrating through multiple tissues [210]; however, a significant fraction of TEM phenotype cells persist as non-circulating, tissue-resident subsets (TRM) in multiple sites including lungs, intestines, skin, liver, brain, and other mucosal surfaces (for reviews see [8, 10, 102]). TRM mediate optimal protective responses to site-specific infections through rapid mobilization of immune responses *in situ* [105, 114]. Mouse models have also demonstrated the feasibility of targeting TRM in vaccines for generating protective immunity [117, 118]. Given their potential importance in immune protection and tissue homeostasis, an understanding of TRM identity, function, and regulation in humans is essential for translating strategies to target tissue-specific responses for protection and immunomodulation.

Advances in human TRM biology are limited by the lack of assays to distinguish circulating and resident memory T cells in tissues. In mice, tissue retention demonstrated by parabiosis [103, 104] and *in vivo* antibody labeling [124, 129] identified phenotypic markers associated with tissue residence, including CD69 and CD103. In mice, CD69 is expressed by the majority of CD4⁺ and CD8⁺ TRM cells in multiple sites [103, 105, 134, 135], while CD103 is only expressed by certain subsets of CD8⁺ TRM [10, 133] and not significantly by CD4⁺ TRM [124, 211]. CD69 has also been shown to have tissue-retention functions in lymph nodes through sequestration of the sphingosine-1-P receptor (S1PR) that mediates egress of T cells [131, 138] and is required for TRM retention in the skin [132]. Whether CD69 can delineate TRM from circulating TEM counterparts remains to be established in humans and is a critical outstanding question in the field.

In human tissues, we and others have identified and characterized TRM phenotype cells expressing CD69 and/or CD103 in multiple sites including lungs, liver, lymphoid sites, skin and intestines [8, 17, 18, 142, 155, 157, 159, 163, 185]. However, it is not known whether TRM represent a distinct subset in humans for both CD8⁺ and CD4⁺T cell lineages, with unifying functional, phenotypic, and transcriptional signatures across tissues and individuals.

We have established a unique human tissue resource to obtain blood, multiple lymphoid and mucosal tissues from previously healthy organ donors, enabling novel analysis of T cell compartmentalization and maintenance throughout life [14, 16-18, 212]. We present here transcriptional, phenotypic, and functional analyses which define human TRM as a distinct subset in multiple sites. We show that CD69 is a key marker that distinguishes memory T cells in tissues from those in circulation, while CD103 is expressed only by a subset of tissue memory CD8⁺ and not by CD4⁺ T cells. CD69⁺ tissue memory T cells are transcriptionally and phenotypically distinct from CD69⁻ memory T cells in tissues and blood and exhibit a core gene profile comprising adhesion, migration, and regulatory molecules with homology to mouse TRM. This core signature is shared between human CD4⁺ and CD8⁺TRM and in multiple lymphoid and mucosal tissues. Further, human TRM have an enhanced capacity for production of certain cytokines and regulatory molecules and decreased turnover compared to circulating TEM cells, suggesting long term maintenance *in situ*. Together, our study establishes human TRM as a distinct subset stably maintained in diverse anatomic locations.

Section 3.2: Results

CD69⁺ memory populations exist only in tissues and do not show evidence of activation.

To identify the major phenotypic marker distinguishing tissue from circulating memory T cells, we assessed CD69 and CD103 expression as markers associated with TRM in mice by CD45RA⁻/CCR7⁻ TEM-phenotype CD4⁺ and CD8⁺T cells in blood and 8 additional tissue sites of individual donors (Fig. 3.1A, B). (Table 3.1 shows information about all of the donors used in this study.) We focused on TEM cells as the major memory subset in tissues that is common to both CD4⁺ and CD8⁺ T cells, as previously determined [18]. While blood memory T cells were predominantly CD69⁻/CD103⁻, the majority (>50-90%) of tissue memory CD4⁺ and CD8⁺T cells in all sites examined including lungs, intestines, salivary glands, tonsils, spleen, and various lymph nodes (LN) expressed CD69 (Fig. 3.1A,B). CD103 was expressed predominantly by memory CD8⁺T cells in tissues associated with the oral-gastrointestinal tract (salivary glands, tonsils, intestines) and lung, with significantly lower proportions of CD103⁺CD8⁺ memory T cells in spleen and lymph nodes (10-30%) and few tissue memory CD4⁺ T cells expressing CD103 (<5-10%, Fig. 3.1A, B). Together, these findings indicate that CD69 expression distinguishes tissue from blood TEM across multiple lymphoid and barrier tissues and CD4/CD8 lineages, while CD103 expression is more variable and confined to certain tissue CD8⁺ T cells.

Because CD69 is also a marker of early activation [213], we assessed expression of the activation markers CD25, CD38, and HLA-DR by CD69⁺ and CD69⁻ memory subsets from a representative lymphoid (spleen) and mucosal (lung) tissue. There was uniformly low expression of CD25, CD38, and HLA-DR on CD69⁺ TEM similar to expression levels on resting naïve T cells (Fig. 3.1C). Previously, we also found maintenance of CD28 and CD127 expression by the majority of CD69⁺ tissue memory T cells, indicative of a quiescent state [18]. Together, our results

show that CD69 expression by tissue memory T cells is not associated with markers of recent activation.

Table 3.1. List of all donors used in this study.

Donor	Tissues	Age	Gender
22	Intestines	19	Male
82	Blood	3	Female
87	Lung, Spleen	49	Female
90	Spleen	51	Female
93	Intestines	38	Male
101	Lung	57	Female
103	Lung	25	Male
105	Lung, Intestines	20	Male
108	Spleen	53	Male
109	Lung, Spleen	43	Male
117	Lung	32	Male
142	Spleen, Lung, LLN, MLN, ILN, Intestines	29	Male
146	Lung, Intestines	23	Female
147	Blood, LLN, MLN, ILN	36	Female
149	Lung	55	Male
150	Lung, Blood, MLN, ILN, LLN, Intestines	39	Male
156	Blood, LLN, MLN, ILN, Intestines	40	Female
165	Intestines	29	Female
172	Blood, Tonsils, Salivary Gland	49	Male
174	Spleen	35	Female
175	Lung, Blood, LLN, MLN, ILN, Intestines, Tonsils, Salivary Gland	24	Male
176	Spleen, Lung, LLN, MLN, ILN, Intestines, Tonsils, Salivary Gland	64	Male
177	Spleen, LLN, ILN, Intestines, Tonsils, Salivary Gland	52	Female
178	Spleen, Blood, LLN, MLN, Intestines, Salivary Gland	51	Male
181	Spleen, MLN, LLN, Intestines, Tonsils, Salivary Gland	46	Male
182	Spleen, Lung, LLN, MLN, Intestines, Tonsils, Salivary Gland	46	Male
183	Spleen, Lung, Blood, LLN, MLN, ILN, Intestines, Tonsils, Salivary Gland	69	Female
185	Spleen	57	Male
190	Lung, Spleen	69	Female
191	Lung	29	Male
194	Lung, Spleen	53	Male
195	Lung, Blood, LLN, MLN	37	Female
196	Lung	45	Female
198	Lung	23	Female
199	Spleen, Lung, LLN, MLN, ILN, Intestines	50	Male
200	Spleen, Lung, Blood, LLN, Intestines	55	Male
201	Spleen, Lung, Blood, LLN, MLN, ILN, Intestines, Tonsils, Salivary Gland	21	Male
202	Spleen, Lung, Blood, LLN, MLN, ILN, Intestines, Tonsils, Salivary Gland	50	Male
203	Spleen, Lung, Blood, LLN, MLN, ILN, Tonsils, Salivary Gland	70	Male
204	Lung	30	Male
206	Blood, salivary Gland	50	Male
207	Spleen, Blood, LLN	23	Male
209	Lung, Blood, LLN, MLN, ILN, Intestines, Salivary Gland	59	Male
212	Spleen	48	Male
216	Lung, Blood, MLN, ILN, LLN, Intestines	34	Male
217	Lung, Spleen	49	Male
219	Lung, Spleen	50	Male
220	Lung, Spleen	64	Male
223	Lung, Spleen	29	Female
225	Spleen	54	Male
226	Lung, Spleen	66	Female
227	Lung	26	Male
232	Spleen	53	Male

233	Lung, Spleen	26	Female
235	Spleen	50	Male
236	Lung, Spleen, LLN, Tonsils, Salivary Gland	75	Female
237	Lung, Spleen, Blood, Intestines, MLN, ILN, LLN, Tonsils, Salivary Gland	22	Male
241	Lung	19	Male
244	Lung, Spleen	36	Male
245	Lung, Spleen	50	Female
247	Lung	45	Female
250	Lung, Spleen	39	Female
254	Lung, Spleen, LLN	49	Female
255	Lung, Spleen, Gut	63	Female
257	Lung, Spleen	19	Male
259	Lung, Spleen, LLN	46	Male
262	Lung, Spleen	73	Male
265	Lung, Spleen	24	Male
267	Spleen	70	Female
270	Lung, Spleen	23	Female
273	Lung, Spleen	67	Female
275	Spleen	31	Male
277	Lung	21	Male
285	Lung, Spleen	53	Male
286	Spleen	46	Male
288	Lung, Spleen	32	Male
289	Lung, Spleen	58	Male
291	Lung, Spleen, Gut	26	Female
293	Lung, Spleen, Gut	53	Female
294	Lung, Spleen, Blood	1.5	Female
296	Lung, Spleen, Gut	62	Female
297	Lung, Spleen, Gut	59	Female
298	Lung, Spleen	59	Female
299	Spleen	20	Male
300	Lung	56	Male
302	Lung, Spleen, Blood	56	Male
303	Lung, Spleen, Blood	64	Male
304	Lung	68	Male
305	Spleen	28	Female
306	Spleen	71	Female
308	Lung, Spleen	68	Male
309	Lung, Spleen	45	Female
311	Lung, Spleen	52	Female
312	Spleen	50	Female
315	Lung	63	Male
316	Lung	42	Female
320	Lung, Spleen, Blood	55	Female
321	Lung, Spleen, Blood, Intestines, MLN, Salivary Gland, Tonsils	17	Female
324	Spleen	56	Male
327	Lung, Spleen, Blood, MLN, LLN, Salivary Gland	52	Female
328	Lung, Spleen, Blood, MLN, Salivary Gland, Tonsils	52	Male
332	Spleen, Lung, Blood, MLN, Tonsils, Intestines, ILN, LLN, Salivary Glands	38	Male
Live Donor 1	Blood	30	Male
Live Donor 2	Blood	32	Male
Live Donor 3	Blood	27	Male

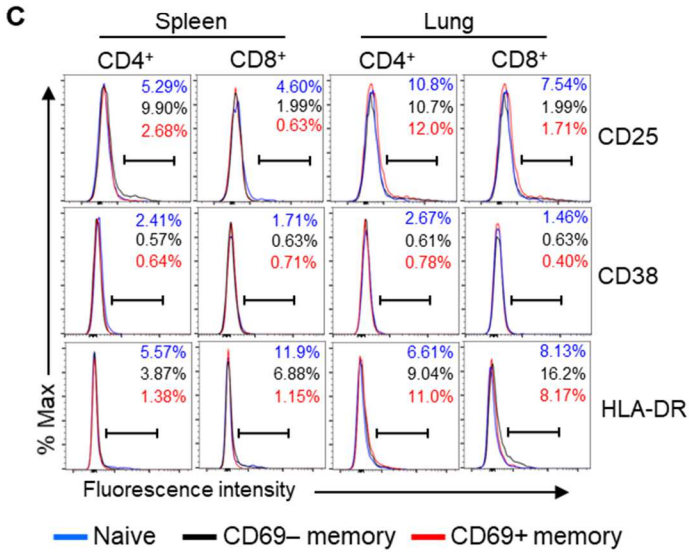
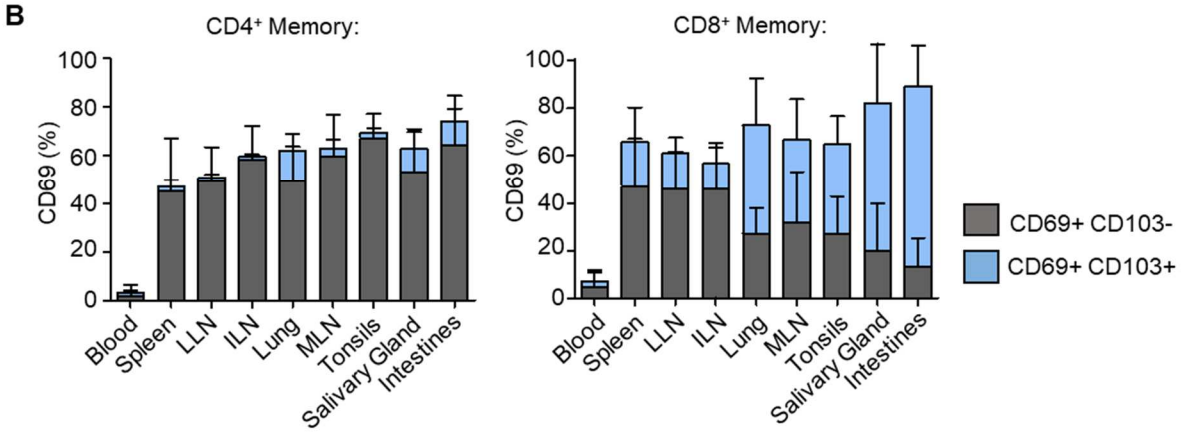
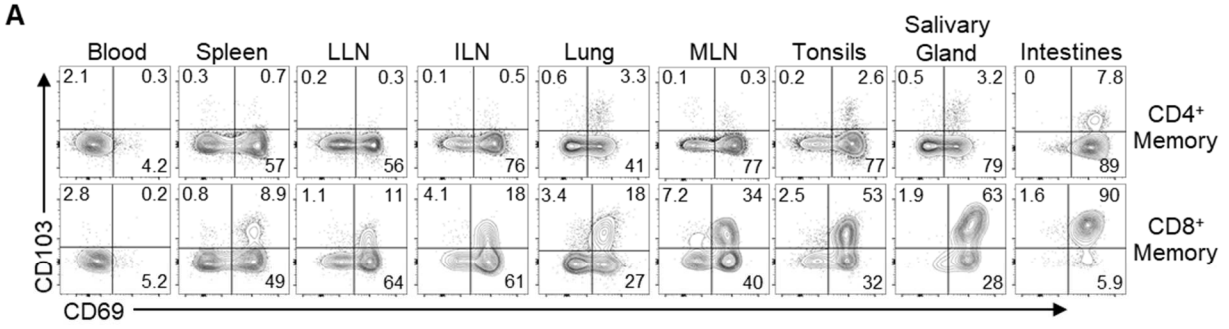
Figure 3.1. CD69+ memory T cells are prevalent in tissues and do not show features of activation.

(A) Expression of CD69 and CD103 by CD4⁺(top) and CD8⁺(lower) memory T cells (CCR7-CD45RA-) within each indicated site from one individual (donor 332) representative of 6 donors.

LLN: Lung lymph node, ILN: inguinal lymph node, MLN: mesenteric lymph node.

(B) Frequency of CD69+CD103+ (grey) and CD69+CD103+ (blue) cells in CD4⁺ (left) and CD8⁺ memory T cells in each tissue compiled from 16-22 donors.

(C) Activation profile of T cells from human tissues. Flow cytometry plots show expression of CD25, CD38, and HLA-DR by naïve T cells (CCR7+ CD45RA+, blue line), and CD69- (black) and CD69+ (red) subsets of memory T cells (CCR7-CD45RA-). Data are representative of 3 donors.



Human CD69⁺ tissue memory T cells comprise a transcriptionally distinct subset with features of tissue residency.

Based on the phenotype analysis above, we hypothesized that human tissue-resident memory T cells could be found within the CD69⁺ subset of tissue memory T cells. We isolated CD4⁺ and CD8⁺ TEM cells from the spleen and lungs of 3 previously healthy organ donors (sorting strategy shown in Fig. 3.2; donor information in Table 3.1), fractionated them into CD69⁺ and CD69⁻ subpopulations for whole transcriptome profiling by RNA-Seq, and analyzed the resultant profiles of CD69⁺ and CD69⁻ subsets for each lineage and tissue. (Quality control summary of all RNA-Seq samples is shown in Table 3.2) Principal component analysis (PCA) revealed that the transcriptome of CD69⁺ cells was distinct from that of the CD69⁻ subset for CD4⁺ and CD8⁺ memory T cells in spleen and lung tissue for all three donors analyzed (Fig. 3.3A). This result indicates that CD69 expression defines a transcriptionally distinct subset of memory T cells in tissues.

Applying the criteria for significance (FDR \leq 0.05 and absolute value of log₂ fold-change \geq 1), for CD4⁺ samples we identified 327 genes differentially expressed between lung CD69⁺ and CD69⁻ subsets and 221 genes differentially expressed between spleen CD69⁺ and CD69⁻ subsets, of which 77 genes (29 upregulated, 48 downregulated) were differentially expressed in both tissues (Fig. 3.3B, C). For CD8⁺ samples we identified 329 genes differentially expressed between lung CD69⁺ and CD69⁻ subsets and 459 genes differentially expressed between spleen CD69⁺ and CD69⁻ subsets, of which 133 genes (39 upregulated, 94 downregulated) were differentially expressed in both tissues (Fig. 3.3B, C). The expression differences in these key genes were similar between three donors (Fig. 3.3C).

The genes differentially expressed by human CD69⁺ and CD69⁻TEM cells (Fig. 3.3C) included key molecules associated with mouse CD8⁺TRM from infection models [108-110, 139]. Notably, downregulation of S1PR1 and its associated transcription factor KLF2 are required for CD8⁺TRM establishment in mice [139], and we found striking downregulation of S1PR1 (8-16-fold) and KLF2 (2-16-fold) transcripts for all CD69⁺ compared with CD69⁻ subsets in every donor for both CD4⁺ and CD8⁺T cells in lung and spleen (Fig. 3.3D). In addition, human CD8⁺CD69⁺ subsets exhibited upregulation of ITGAE (CD103), ITGA1 (CD49a), ICOS, and the transcription factor IRF4, also found to be upregulated by mouse CD8⁺TRM in different systems [148]. Together, these results show that the CD69⁺ tissue memory T cells comprise a transcriptionally distinct subset enriched for features of tissue residency.

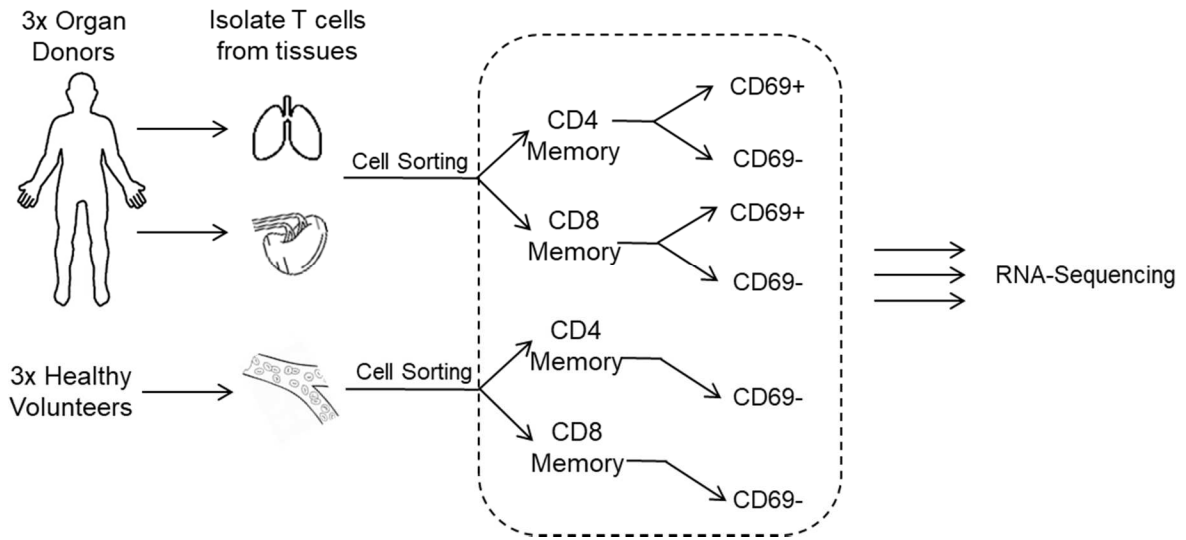
We further compared the transcriptional profiles of tissue memory T cell subsets with circulating TEM cells isolated from the blood of three healthy volunteers. PCA analysis using the gene signature in Fig. 3.3C resulted in clustering of blood TEM with CD69⁻ tissue TEM, distinct from CD69⁺ samples which clustered together (Fig. 3.3E). By contrast, PCA analysis using an equal number of randomly selected genes as a negative control yielded no clustering pattern (Fig. 3.4). This grouping suggests that CD69 expression by memory T cells in tissues distinguishes circulating memory subsets from those retained in tissues.

Figure 3.2. Sorting strategy for RNA-Sequencing.

(A) Schematic shows samples that were isolated for RNA-Sequencing. Cell sorting was used to isolate populations of interest from the spleen and lung of 3 organ donors and from the blood of 3 healthy volunteers. Samples were sent for RNA-Sequencing at the Columbia Genome Center.

(B) Freshly isolated lymphocyte suspensions were enriched for T cells by negative selection to remove B cells, NK cells, monocytes, and other leukocytes using the BD MojoSort kit. T cells were then labelled with fluorophore conjugated antibodies as described in methods. Flow cytometry plots show sorting strategy for isolation of CD45RA-CCR7-CD69⁺ and CD45RA-CCR7-CD69⁻ T cells from a representative spleen, for both CD4⁺ and CD8⁺ lineages.

A.



B.

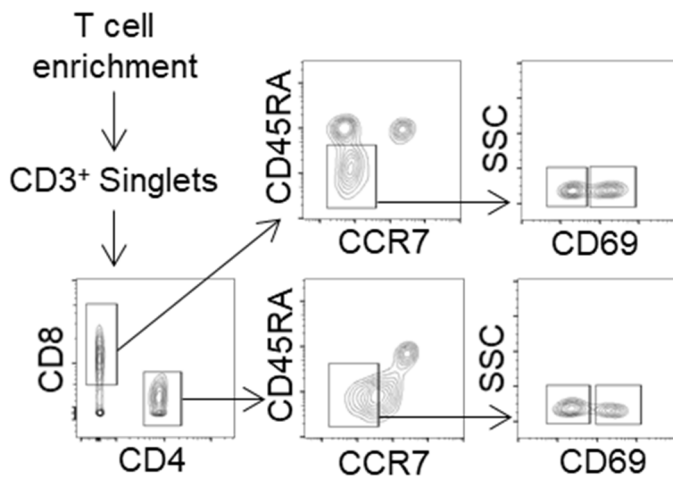


Table 3.2. RNA-Seq QC Summary

Sample Name	Number of Reads	Number of unique Mapped Reads	Median FPKM (isoforms)	Mean FPKM (isoforms)	Num of transcripts (FPKM > 1)	Num of transcripts (FPKM > 0.1)	Num of Genes (FPKM > 1)	Num of Genes (FPKM > 0.1)	Donor	Tissue	T cell lineage	CD69	Batch
BD001	35128448	31505812	0.3	14.2	16708	22127	12629	15984	233	spleen	CD4	-	b1
BD002	38022555	34754087	0.324	14.1	16926	22372	12750	16024	233	spleen	CD4	+	b1
BD003	32218460	29651306	0.356	13.2	17082	22496	12888	16234	233	spleen	CD8	-	b1
BD004	38356407	35458425	0.346	13.2	17016	22406	12775	15995	233	spleen	CD8	+	b1
BD005	32346693	24542330	0.322	16.6	16513	22436	12538	16425	233	lung	CD4	-	b1
BD006	37692355	32861480	0.342	15.6	16608	22850	12581	16452	233	lung	CD4	+	b1
BD007	33819380	30956211	0.363	13.6	16902	22845	12673	16447	233	lung	CD8	-	b1
BD008	24895230	4787100	1.17E-03	1.60E+01	1.57E+04	1.90E+04	1.26E+04	1.53E+04	233	lung	CD8	+	b1
BD009	32632736	28499541	0.347	15.4	16801	22342	12681	16209	226	spleen	CD4	-	b1
BD010	27990247	22016708	0.346	15.9	16953	22372	12892	16444	226	spleen	CD4	+	b1
BD011	30145116	26596999	0.248	16.3	16256	21739	12322	15770	226	spleen	CD8	-	b1
BD012	33916030	30378438	0.303	15.4	16587	22169	12531	15988	226	spleen	CD8	+	b1
BD013	27811140	20844044	0.38	16.1	16778	22864	12791	16907	226	lung	CD4	-	b1
BD014	32406219	25795053	0.364	14.6	16605	23048	12637	16826	226	lung	CD4	+	b1
BD015	25070885	15584406	0.371	16.1	16740	22654	12841	16965	226	lung	CD8	-	b1
BD016	28302772	22382985	0.303	15.3	16170	22422	12361	16462	226	lung	CD8	+	b1
BD017	15491995	9105649	0.0509	30.6	13841	19050	11631	15923	250	spleen	CD4	-	b2
BD018	16938399	14248078	0.369	18.5	16408	24227	12653	19073	250	spleen	CD4	+	b2
BD019	17495605	14309647	0.22	18.5	16274	21201	12504	16154	250	spleen	CD8	-	b2
BD020	22814984	16748291	0.126	19.4	15328	20303	11863	15461	250	spleen	CD8	+	b2
BD021	26232006	20770805	0.266	17.3	16463	21505	12669	16130	250	lung	CD4	-	b2
BD022	34216681	30317405	0.286	15.4	16076	22409	12236	16427	250	lung	CD4	+	b2
BD023	28590077	25954675	0.254	14.6	16399	21649	12331	15841	250	lung	CD8	-	b2
BD024	30669374	27681087	0.238	14.8	16205	21547	12222	15764	250	lung	CD8	+	b2
BD025	22788441	18669677	0.212	12.3	16968	20737	13407	16385	1	blood	CD4	-	b3
BD026	29014993	25437404	0.433	15	17695	22256	13419	16674	1	blood	CD8	-	b3
BD027	23088478	19134440	0.335	17.5	17282	21597	13280	16498	2	blood	CD4	-	b3
BD028	21458544	17375388	0.302	23.8	17049	21557	13061	16387	2	blood	CD8	-	b3
BD029	20881994	17975570	0.418	23.4	17515	22455	13643	17446	3	blood	CD4	-	b3
BD030	20976929	18496160	0.375	16.7	17352	22078	13306	16867	3	blood	CD8	-	b3

Figure 3.3. CD69 expression defines a transcriptionally distinct memory subset in humans with features of tissue residency.

Whole transcriptome profiling by RNA sequencing was performed on CD69⁻ and CD69⁺ subsets of CD4⁺ and CD8⁺ memory T cells from spleen and lungs of 3 donors (Donors 226, 233, 250; see methods).

(A) Principle Component Analysis (PCA) of paired CD69⁺ and CD69⁻ samples from spleen and lung and for CD4⁺ and CD8⁺ subsets, based on the global transcriptome (~20000 genes).

(B) Diagram shows the number of significant differentially expressed genes (FDR \leq 0.05 and log₂ fold-change \geq 1) between CD69⁻ and CD69⁺ samples within each tissue for CD4⁺ and CD8⁺ T cells showing overlap between tissues.

(C) Heat map showing normalized expression levels of the overlap genes identified in (B) for CD4⁺ (77 genes) and CD8⁺ (133 genes) CD69⁻ vs. CD69⁺ subsets from spleen (S) and lung (L).

(D) Transcriptional downregulation of S1PR1 and KLF2 in all CD69⁺ vs. CD69⁻ subsets. Normalized expression levels of S1PR1 (top) and KLF2 (bottom) transcripts in CD69⁻ and CD69⁺ samples from spleen (S) and lung (L) of each donor are shown. Individual donors are indicated by distinct symbols, and lines connect samples from identical donors within a tissue. **** FDR \leq 10⁻⁵, *** FDR \leq 10⁻³.

(E) PCA of CD69⁺ (red) and CD69⁻ (black: tissue, blue: blood) memory subsets based on the genes in (C). S=spleen, L=lung, B=blood. See also Figure 3.4.

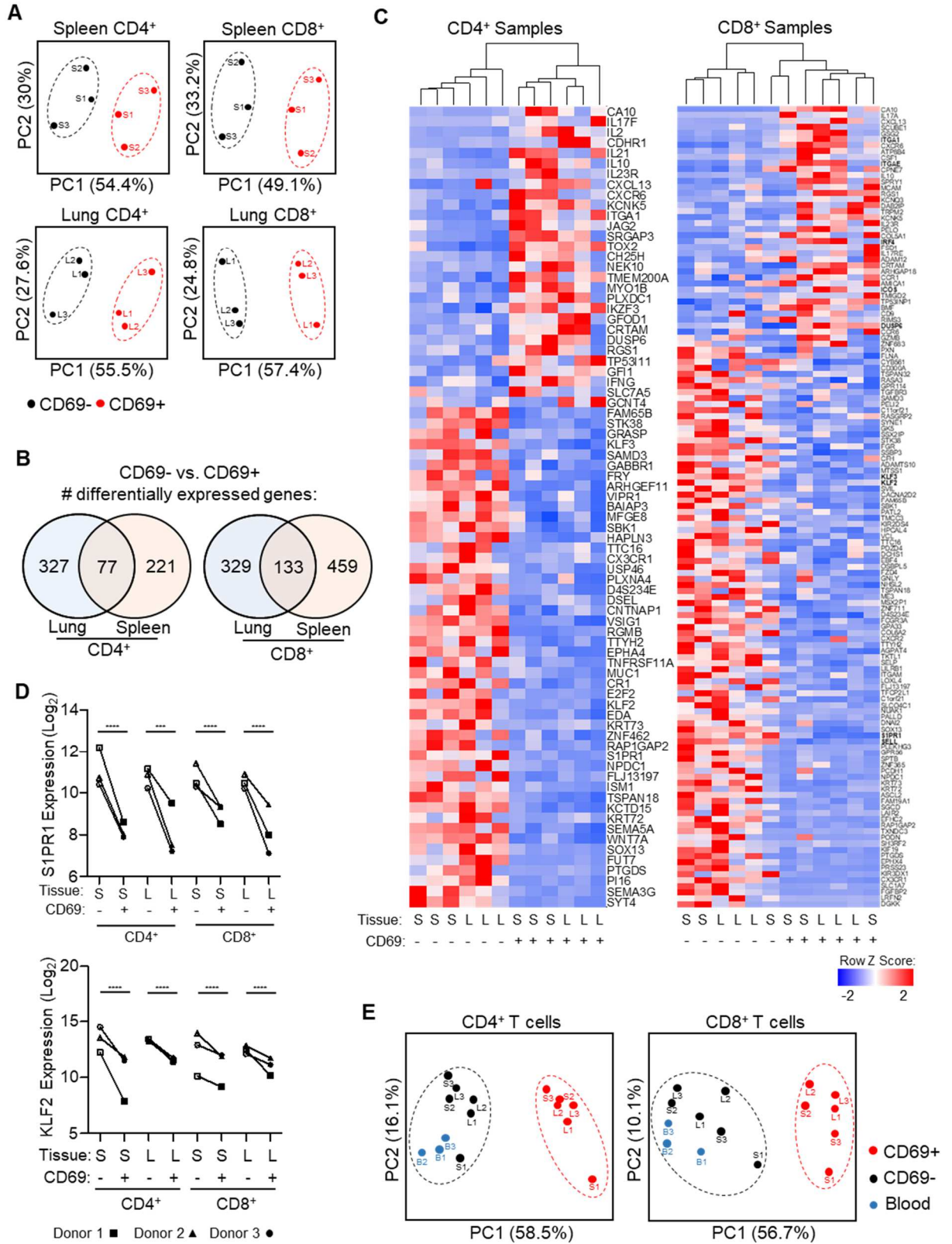
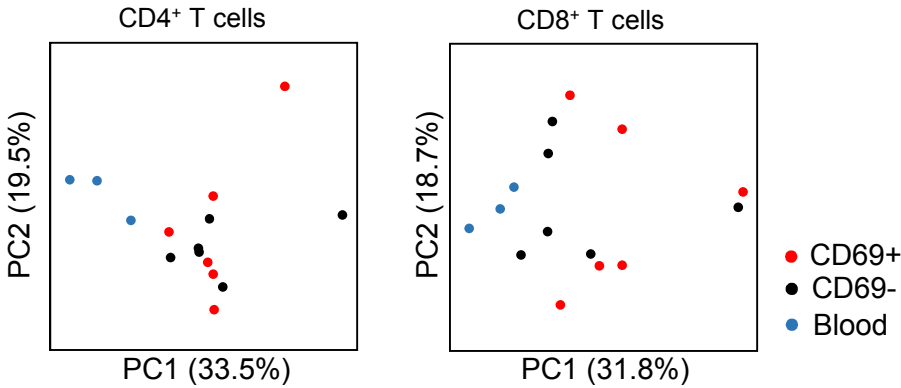


Figure 3.4. PCA of randomly selected genes.

As a negative control, PCA was performed on an equal number of randomly selected genes as the number used to generate the PCA in Figure 3.3E (133 genes for CD8⁺ samples, 77 genes for CD4⁺ samples).



A core gene signature of human CD69⁺ memory T cells.

Based on the gene expression analysis above, we identified 31 core genes with consistent significant differential expression by CD4⁺ and CD8⁺ CD69⁺ compared with the corresponding CD69⁻ subset from lung, spleen, and blood (Fig. 3.5A). (Table 3.3 provides details about the genes identified in Fig. 3.5A). This core signature includes upregulated expression of genes encoding specific integrin and adhesion markers ITGAE (CD103), ITGA1 (CD49a), and CRTAM (cytotoxic and regulatory T cell molecule), chemokine/chemokine-receptors CXCR6 and CXCL13, and molecules with known inhibitory functions in T cells including PDCD1 (PD-1) [214], the dual-specificity phosphatase DUSP6 that turns off MAP Kinase signaling [215], and IL10 (IL-10). Additional cytokine/cytokine receptor genes upregulated in CD69⁺ compared with CD69⁻ samples were IL2 (IL-2) and IL23R, which signals for IL-17 production [216]. Downregulated genes in the core signature include the homing receptors S1PR1 and its associated transcription factor KLF2 which together control T cell homing and tissue retention [139], the related Kruppel-like transcription factor KLF3, the lymph node homing receptor SELL (CD62L), and CX3CR1, the fractalkine receptor shown to be upregulated by mouse CD8⁺ T cells during infection [217]. Other genes in the core signature included controllers of G-protein signaling such as RAP1GAP1 and RGS1, shown to modulate T cell trafficking [218], and the kinase STK38, which regulates MAP kinase and NF- κ B signaling in T cells [219].

Pathways represented within the core signature include those controlling T cell adhesion and migration, proliferation, development, and activation (Table 3.4) that interconnect as diagrammed in Fig. 3.5B. Many of the upregulated genes map downstream of TCR signaling, including CD69, adhesion molecules (ITGA1, ITGAE, CRTAM), and activation-induced molecules IL2 (IL-2), IL10 (IL-10), and PDCD1 (PD-1) that can regulate proliferation and T cell

activation (Fig. 3.5B). Differential upregulation or downregulation of specific chemokines and chemokine receptors (CXCL13, CXCR6, CX3CR1, SELL, S1PR1) and modulation of G-protein mediated signaling (Fig. 3.5B) indicates that tissue residence involves specific tuning of migratory properties. Overall, these results establish that human CD69⁺ tissue memory T cells maintain a core signature impinging on multiple signaling pathways affecting cellular migration, function, and proliferation.

The relative transcript levels of key genes within the core gene signature (ITGA1 (CD49a), CXCR6, ITGAE (CD103), CXCR6, CX3CR1, and PDCD1 (PD-1)) showed differential regulation between CD69⁺ and CD69⁻ subsets that was consistent across tissues, lineages, and diverse donors (Fig. 3.5C-G). We also validated differential surface protein expression by flow cytometry for each marker from 8-20 additional donors (Figs. 3.6, 3.7). Interestingly, for a number of genes (ITGAE, CX3CR1, PDCD1), there was an expression gradient from blood to tissue CD69⁻ to CD69⁺ subsets, with blood memory cells exhibiting lower (ITGAE, PDCD1) or higher (CX3CR1) expression than CD69⁻ subsets from tissues (Fig 3.5D, F-G), suggesting some differences between CD69⁻ subsets in blood and tissues. Together, these data establish CD49a, CD103, CXCR6, CX3CR1, and PD-1 as core surface markers that distinguish human CD69⁺ and CD69⁻ memory subsets across tissues and lineages.

Figure 3.5. A core gene signature defines tissue CD69⁺ memory T cells distinct from circulating CD69⁻ cells in tissues and blood.

(A) Heatmap shows normalized expression of genes with significant differential expression between CD69⁺ and CD69⁻ memory T cells for all subsets (CD4⁺, CD8⁺) and tissues (spleen, lung).

(B) Network analysis of the core gene set in (A) showing known and predicted interactions (activating, inhibitory) between proteins encoded by the core genes that are upregulated (red) or downregulated (green) by TRM compared with TEM with key pathways indicated in the shaded boxes. Relationships were determined using IPA software, String Protein database, GeneCards, and Pubmed literature searches.

(C-G) Normalized mRNA expression levels of ITGA1 (C), ITGAE (D), CXCR6 (E), CX3CR1 (F), and PDCD1 (G) by CD4⁺ and CD8⁺ CD69⁺ and CD69⁻ memory subsets in blood (B), spleen (S) and lung (L) of each individual donor. *FDR≤0.05, ** FDR≤10⁻², ***FDR≤10⁻³, ****FDR≤10⁻⁵. Each donor is represented by a unique shape as indicated. See also Figures 3.6 and 3.7 for flow cytometry validations of the protein expression of select genes shown in this figure.

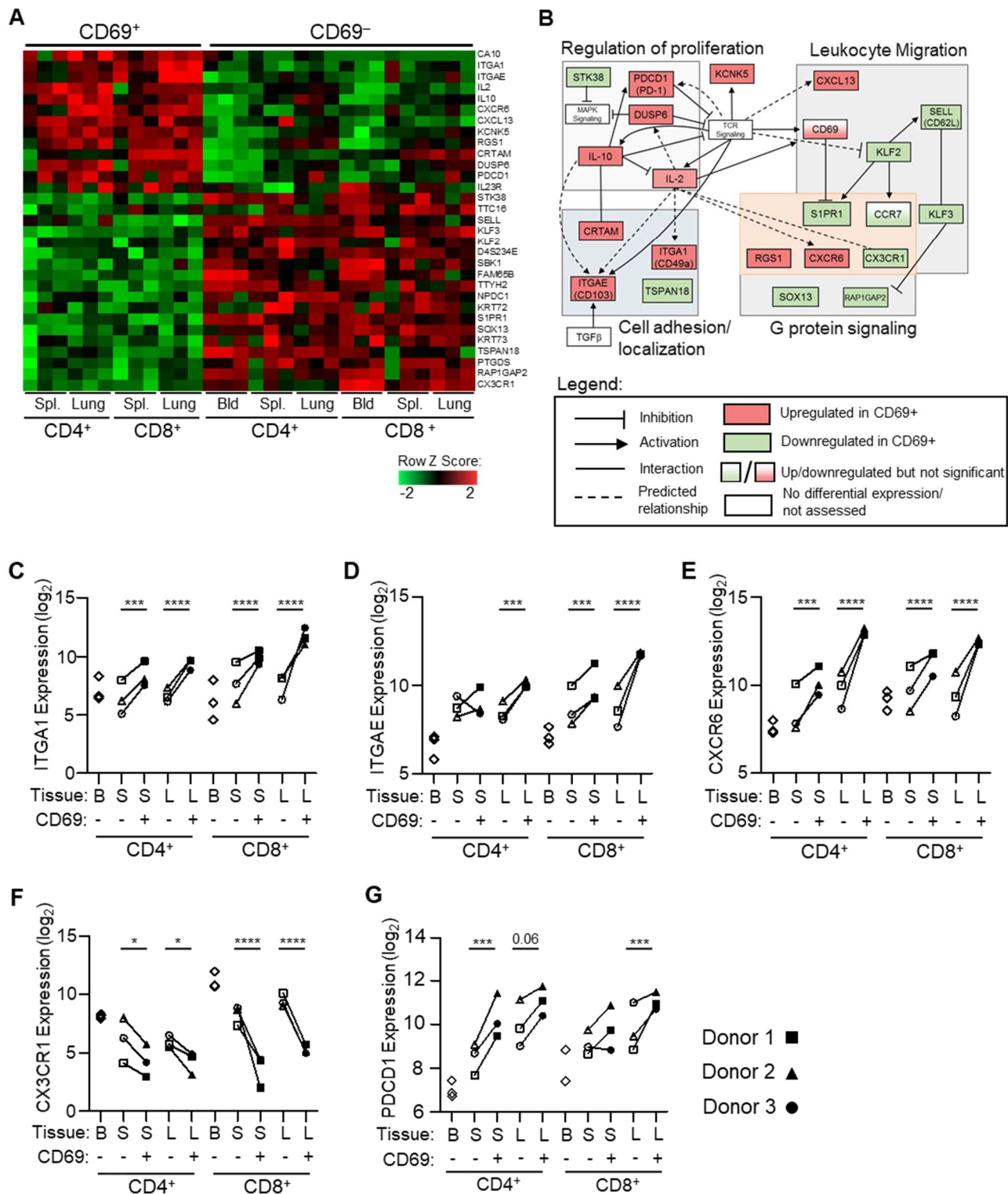
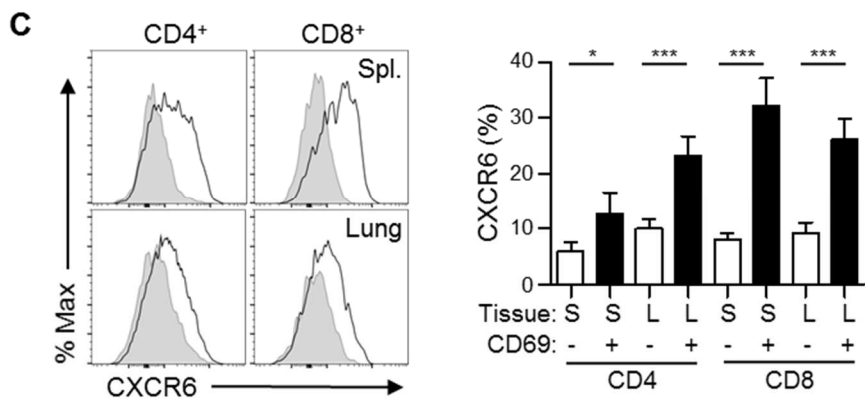
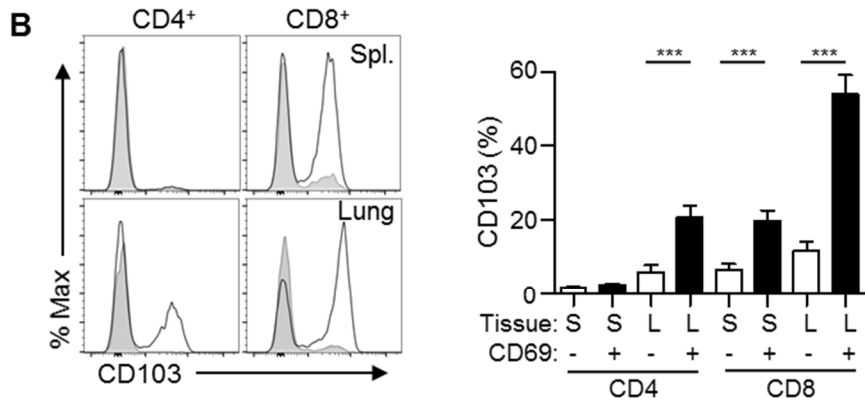
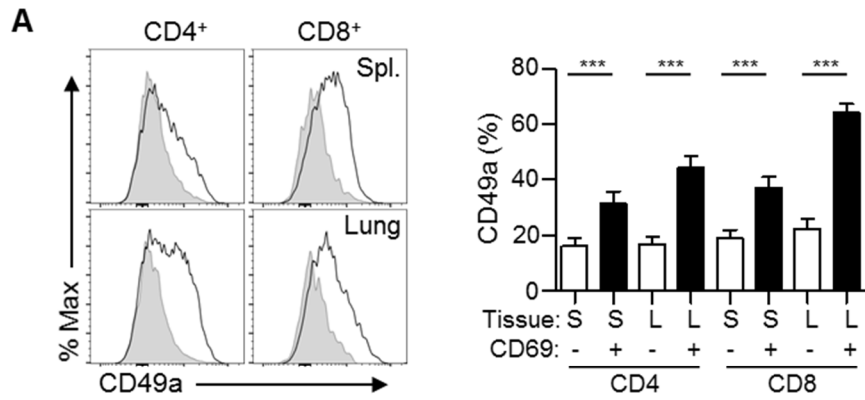


Figure 3.6. Expression of CD49a, CD103, and CXCR6.

Left: Histograms show expression of CD49a (A), CD103 (B), and CXCR6 (C) in CD69+ and CD69- memory T cells from spleen and lung of one representative donor. Right: Graphs show compiled flow cytometry data for CD49a (A, n=15 donors), CD103 (B, n=20 donors), and CXCR6 (C, n=12 donors) depicted as mean frequency of cells expressing each indicated marker \pm SEM. * $p \leq 0.05$, ** $p \leq 10^{-2}$, *** $p \leq 10^{-3}$.



For all histograms:

— CD69+
 — CD69-

For all bar graphs:

□ CD69-
 ■ CD69+

Figure 3.7. Expression of PD-1, CD101, and CX3CR1.

Left: Histograms show expression of CX3CR1 (A), PD-1 (B), and CD62L (C) in CD69+ and CD69- memory T cells from spleen and lung of one representative donor. Right: Graphs show compiled flow cytometry data for CX3CR1 (A, n=8 donors), PD-1 (B, n=15 donors), and CD62L (C, n=4 donors) depicted as mean frequency of cells expressing each indicated marker \pm SEM. * $p \leq 0.05$, ** $p \leq 10^{-2}$, *** $p \leq 10^{-3}$.

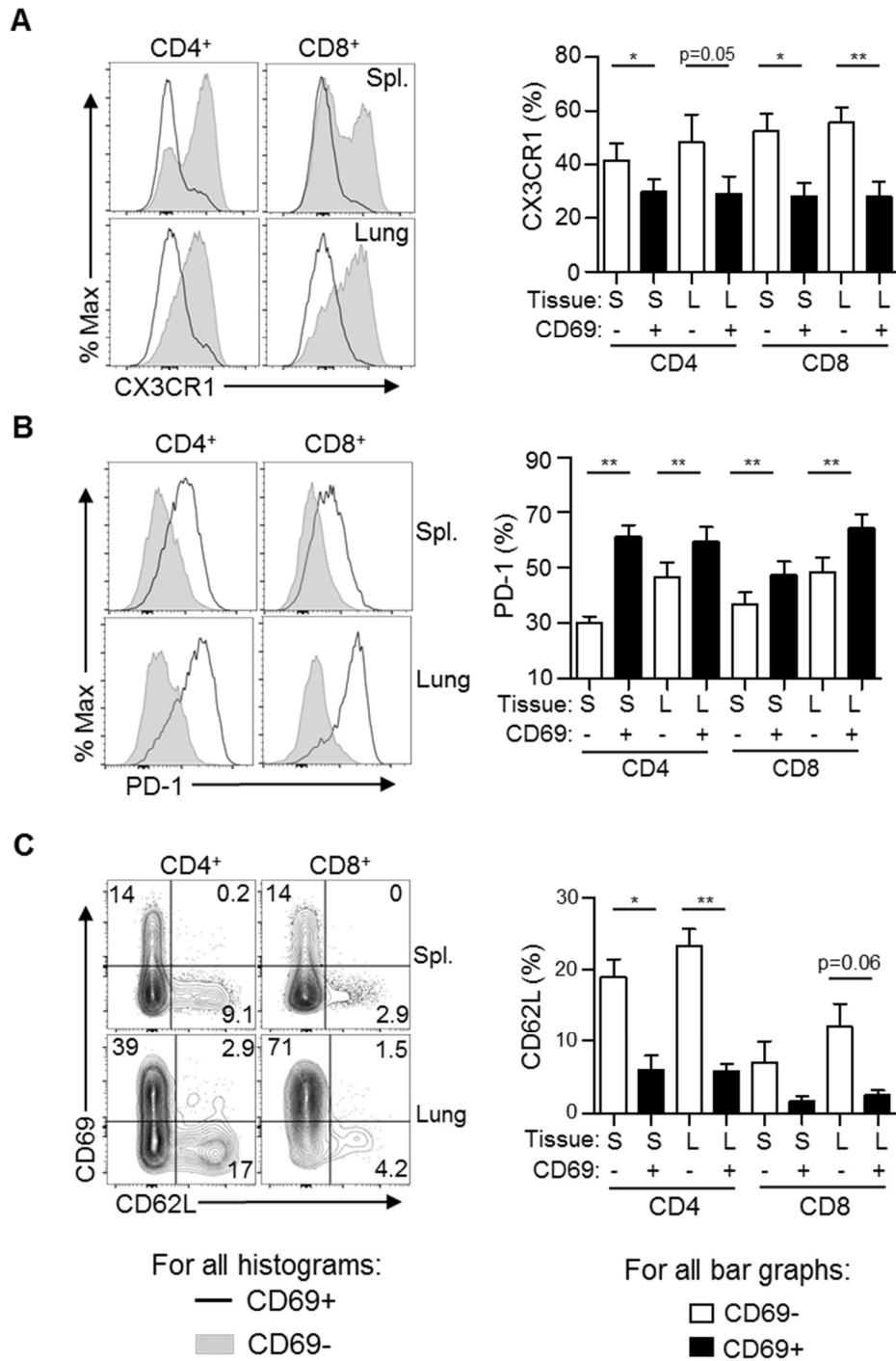


Table 3.3. Details about genes in core signature.

Symbol	Gene Name	Location	Type
CA10	carbonic anhydrase 10	Other	enzyme
CRTAM	cytotoxic and regulatory T-cell molecule	Plasma Membrane	other
CX3CR1	C-X3-C motif chemokine receptor 1	Plasma Membrane	G-protein coupled receptor
CXCL13	C-X-C motif chemokine ligand 13	Extracellular Space	cytokine
CXCR6	C-X-C motif chemokine receptor 6	Plasma Membrane	G-protein coupled receptor
DUSP6	dual specificity phosphatase 6	Cytoplasm	phosphatase
FAM65B	family with sequence similarity 65 member B	Cytoplasm	other
IL2	Interleukin 2	Extracellular Space	cytokine
IL10	interleukin 10	Extracellular Space	cytokine
IL23R	interleukin 23 receptor	Plasma Membrane	transmembrane receptor
ITGA1	integrin subunit alpha 1	Plasma Membrane	other
ITGAE	integrin subunit alpha E	Plasma Membrane	other
KCNK5	potassium two pore domain channel subfamily K member 5	Plasma Membrane	ion channel
KLF2	Kruppel like factor 2	Nucleus	transcription regulator
KLF3	Kruppel like factor 3	Nucleus	transcription regulator
KRT72	keratin 72	Cytoplasm	other
KRT73	keratin 73	Extracellular Space	other
NPDC1	neural proliferation, differentiation and control 1	Extracellular Space	other
PDCD1	programmed cell death 1 (PD-1)	Plasma Membrane	phosphatase
PTGDS	prostaglandin D2 synthase	Cytoplasm	enzyme
RAP1GAP2	RAP1 GTPase activating protein 2	Cytoplasm	other
RGS1	regulator of G-protein signaling 1	Plasma Membrane	other
S1PR1	sphingosine-1-phosphate receptor 1	Plasma Membrane	G-protein coupled receptor
SBK1	SH3 domain binding kinase 1	Other	kinase
SELL	selectin L (CD62L)	Plasma Membrane	transmembrane receptor
SOX13	SRY-box 13	Nucleus	transcription regulator
STK38	serine/threonine kinase 38	Nucleus	kinase
TSPAN18	tetraspanin 18	Other	other
TTC16	tetratricopeptide repeat domain 16	Other	other
TTYH2	tweety family member 2	Other	ion channel

Table 3.4: Significant pathways common to all CD69+ subsets.

Pathway	p-value	Ratio	Direction	Genes from dataset
Sphingosine-1-phosphate Signaling	2.1E-04	0.139	Down	S1PR5,ADCY3,ADCY6,RHOH,PDGFB,S1PR4,PLCD1,S1PR1 +9 more
Integrin Signaling	1.2E-03	0.105	Down	PXN,TSPAN5,ARHGEF7,ABL1,ITGAE,PPP1CB,ITGA5,ITGAL + 16 more
Leukocyte Extravasation Signaling	1.5E-03	0.105	Down	VAV2,VCAM1,PXN,ABL1,ITGA5,NCF4,ITGAL,RHOH,ITGB2 +14 more
Actin Cytoskeleton Signaling	3.1E-02	0.083	Down	VAV2,PXN,ARHGEF12,ARHGEF7,PPP1CB,ITGA5,IQGAP1 +12 more
Cell Cycle: G1/S Checkpoint Regulation	1.7E-03	0.156	n/a	TP53,CDKN2D,FOXO1,CCND3,SMAD3,CDKN1A,ABL1,ATR,E2F2,ATM
Cyclins and Cell Cycle Regulation	7.4E-03	0.128	Up	TP53,CCNH,CDKN2D,CCND3,PPM1L,CDKN1A,ABL1,ATR,E2F2,ATM
Notch Signaling	1.3E-02	0.158	Up	NOTCH4,JAG2,DTX3,RBPJ,NOTCH1,NUMBL
NF-κB Signaling	1.3E-02	0.094	Down	MYD88,TGFBR3,NFKB1,TANK,NTRK2,NTRK3,CARD10,TLR6 +9 more
Tec Kinase Signaling	7.9E-03	0.10	Down	VAV2,ITGA5,NFKB1,RHOH,FAS,BLK,YES1,GNA15,PIK3R6 +8 more
STAT3 Pathway	3.6E-02	0.11	Down	PTPN6,NTRK2,NTRK3,TGFBR3,CDKN1A,IGF1R,FGFRL1,PDGFRB
Protein Kinase A Signaling	3.6E-04	0.095	Up	CAMK4,PTPN13,SMAD3,DUSP6,PDE4A,UBASH3B +29 more
RhoA Signaling	2.6E-02	0.098	n/a	LPAR6,ARHGEF12,ARHGAP9,LPAR2,EPHA1,IGF1R +6 more

Pathway analysis was performed using IPA software and table displays pathways that showed enrichment in all CD69+ vs. CD69– groups. P-values, ratios, and genes from dataset are taken from Lung CD8 CD69+ vs. CD69– as a representative example.

The human CD69+ tissue memory core signature bears key homologies with mouse TRM

To determine whether the core transcriptional profile common to CD69+ memory T cells in spleen and lungs defined a TRM signature, we compared the RNA-Seq profile of the human tissue and blood subsets with that of mouse antigen-specific CD8⁺ TRM isolated from skin and intestines following infection (Mackay et al. 2016). PCA of whole transcriptomes shows species-specific transcriptional differences between human and mouse T cells dominating, with all human samples clustering together distinct from mouse TRM/TEM, with cells from the two mouse infection models also transcriptionally distinct (Fig. 3.8A, left). When analyzed based on the human core gene signature in Fig. 3.5, CD4⁺CD69+ and CD8⁺CD69+ subsets from human spleen and lung cluster together with mouse CD8⁺ TRM from skin and gut in the two different infection models, and are distinct from all TEM/CD69- counterparts (Fig. 3.8A, right). Gene set enrichment analysis (GSEA) [220] also revealed a strong enrichment of the differentially expressed genes in human CD4⁺CD69+ and CD8⁺CD69+ subsets within the gene signatures of TRM from mouse brain [108], and mouse skin and lung [110] (Fig. 3.8B). Taken together, our results show that the gene signature of human CD69+ tissue memory T cells exhibits key features of TRM and likely contain the human TRM subset.

A recent report showed that mouse CD8⁺ TRM in multiple tissues exhibit biased expression of the Hobit (homologue-of BLIMP in T cells) transcription factor, which can drive TRM differentiation *in vivo* [109]. As Hobit was not part of the core gene set in our analysis, we specifically analyzed the expression level of Hobit (ZNF683) by human CD69+ memory T cells compared with mouse TRM. In mouse TRM, Hobit levels were higher than the housekeeping gene GAPDH and comparable to CD69 transcript levels. By contrast, for human CD69+ memory T cells, Hobit transcript levels were below median gene expression and significantly lower than

GAPDH and CD69 levels (Fig. 3.8C). These results suggest distinct molecular control of human and mouse TRM differentiation, despite similar core signatures.

We also measured the levels of the transcription factors Eomes and T-bet, based on data in mice that showed that CD8⁺ TRM downregulate these transcription factors [106, 148]. Consistent with these findings, we found that human within the CD8⁺ lineage, CD69⁺ memory T cells had lower expression of both Eomes and T-bet compared with CD69⁻ memory T cells (Fig. 3.9). Within the CD4⁺ lineage, CD69⁺ memory T cells had lower expression of T-bet compared with CD69⁻ memory T cells (Fig. 3.9B). Both CD69⁺ and CD69⁻ CD4⁺ memory T cells had low (<25%) expression of Eomes with no significant differences. Overall, these data suggest that there may be some similarities in the transcriptional regulation of human and mouse TRM, and that transcription factors controlling CD4⁺ and CD8⁺ TRM in humans may be different.

Figure 3.8. Comparison of the human and mouse TRM transcriptome.

(A) PCA was performed using RNA-Seq data presented here (black symbols) compared to mouse herpes simplex virus (HSV)-specific CD8⁺ TRM from skin and CD8⁺ TEM from spleen (“mouse HSV”, yellow) and LCMV-specific CD8⁺ TRM from intestine and CD8⁺ TEM from spleen (“Mouse LCMV”, red) (Mackay et al. 2016). Left: PCA comparing whole transcriptomes of each dataset comprising 15571 common genes between human and mouse. Right: PCA comparing the human and mouse datasets based on expression of genes in the core signature (Fig. 3.5).

(B) Gene set enrichment analysis (GSEA) comparing our human CD8⁺ (left) and CD4⁺ (left) gene sets to published microarray data of CD103⁺ brain TRM vs. spleen TEM (top row), gut TRM vs. spleen TEM (middle row), and lung TRM vs. spleen TEM (middle row) (Wakim et al. 2012; Mackay et al. 2013). In each plot, the x-axis shows the genes ranked with absolute value of log fold change between TRM vs. TEM and y-axis shows running enrichment score (ES) comparing the ranked list of genes with indicated p values.

(C) Comparison of Hobit gene expression in mouse and human datasets. Violin plots show Z score of gene expression levels from mouse TRM (from Mackay et al. 2016) and human CD69⁺ memory T cells (this study). Red dots represent Hobit, blue dots represent the housekeeping gene GAPDH, green dots represent CD69, and the white dot represents median gene expression.

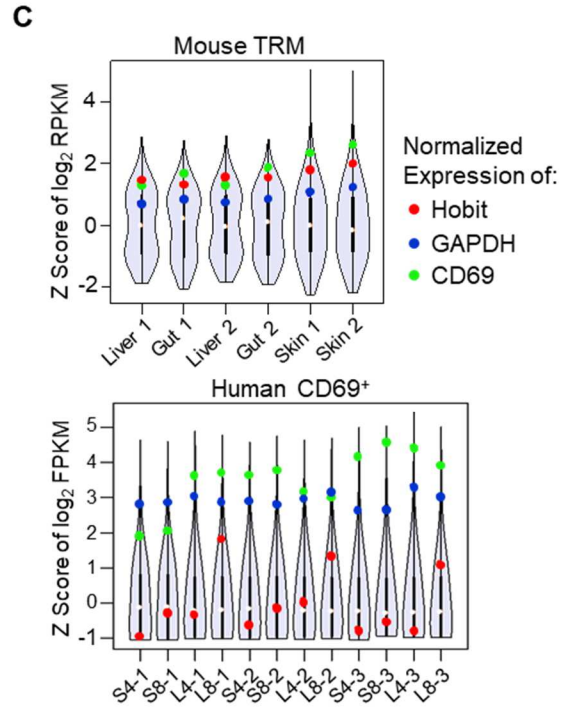
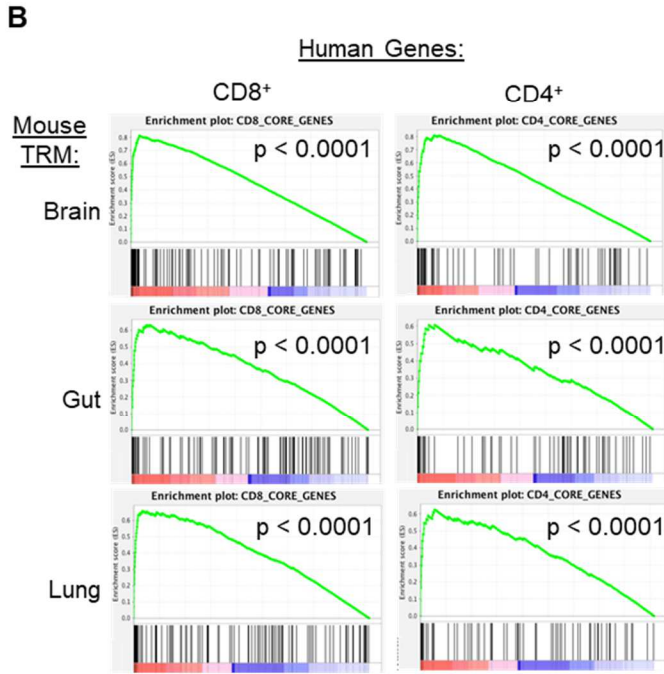
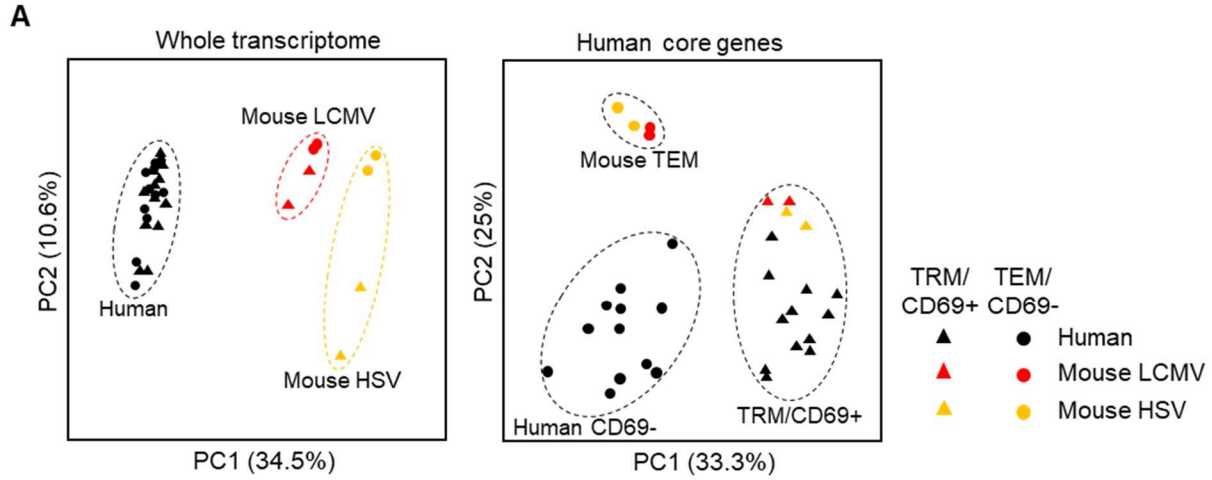
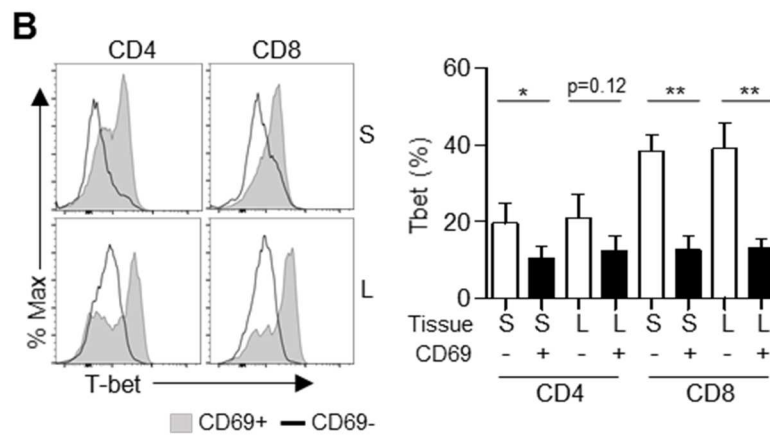
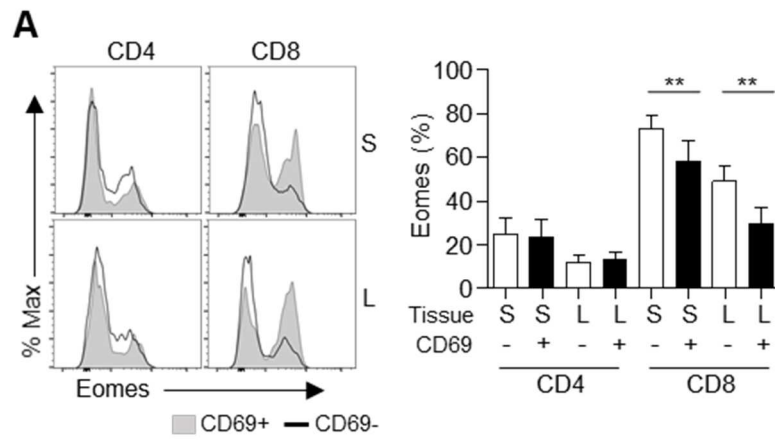


Figure 3.9. T-bet and Eomes expression by human memory T cells.

Flow cytometry was used to measure the expression of Eomes (A) and T-bet (B). Left panels: representative flow cytometry histograms showing of Eomes and T-bet in CD69+ and CD69- memory T cells in the spleen and lung of one representative donor. Right panels: Bar graphs show compiled flow cytometry data as percent positive and SEM. * $p \leq 0.05$, ** $p \leq 0.01$. n=6-8 donors.



Reduced clonal overlap and proliferative turnover of CD69⁺ compared with CD69⁻ memory T cells.

We compared the TCR repertoires of lung and spleen CD69⁺ and CD69⁻ memory T cell subsets using a recently developed algorithm TRUST (TCR repertoire utilities for solid tissue) [209] to extract TCR sequences from the RNAseq reads (see extended methods). Between 0.1% and 0.3% of mapped reads could be assigned to the TCR region (data not shown), with detection of several hundred to over 1000 unique clonotypes per sample (Fig. 3.10). From these data, we measured clonal diversity (# unique clonotypes per mapped reads) and overlap between sites. Overall, CD69⁻ and CD69⁺ cells exhibited similar clonal diversity with CD4⁺ subsets maintaining higher clonal diversity compared to CD8⁺ memory subsets (Fig. 3.11A), consistent with previous findings showing increased clonality of memory CD8⁺ compared to CD4⁺T cells from lymphoid sites [18]. Clonal overlap between sites was minimal (<1%) for CD4⁺ subsets, while CD8⁺CD69⁺ cells exhibited significantly reduced overlap between lung and spleen compared to CD8⁺CD69⁻ cells (Fig. 3.11B), indicating that CD69⁺ memory T cells are more clonally segregated within the tissue compared with CD69⁻ cells. These results provide some additional evidence that CD69⁺ memory T cells may be more retained in tissue site compared with CD69⁻ cells.

We hypothesized that the biased maintenance of CD69⁺ clones in certain sites may indicate reduced turnover. The frequency of CD69⁺ cells expressing Ki67, a marker of proliferating cells, was markedly reduced relative to CD69⁻ cells in both spleen and lung (Fig. 3.11C). Examination of CD57 expression, a marker of replicative senescence and terminal differentiation [221], revealed lower CD57 expression by CD8⁺CD69⁺ compared to CD8⁺CD69⁻ cells in both spleen and lung (Fig. 3.11D). Taken together, these data suggest that human CD69⁺ memory T cells

undergo reduced proliferative turnover and have reduced clonal overlap compared with CD69⁻ cells.

Human CD69⁺ memory T cells have a distinct functional profile

We investigated cytokine production by CD69⁺ and CD69⁻ cells based on differential transcript expression of genes encoding IL-2, IFN- γ , IL-17 and IL-10 identified as significantly upregulated by CD69⁺ versus CD69⁻ memory T cells for both CD4⁺ and/or CD8⁺ subsets (Fig. 3.12; see also 3.3C and 3.5A). IL-2 and IL-10 were produced by a consistently higher proportion of CD69⁺ compared with CD69⁻ memory T cells for both CD4⁺ and CD8⁺ subsets in spleen and lung (Fig. 3.11E-F), consistent with increased IL2 and IL-10 transcription being part of the core signature (Figs. 3.5A, 3.12). IFN- γ was produced by spleen and lung memory CD4⁺ and CD8⁺ T cells, with spleen CD69⁺ memory T cells exhibiting increased IFN- γ production compared with CD69⁻ cells, while lung CD69⁺ and CD69⁻ cells had comparable IFN- γ production (Fig. 3.11G, left). IL-17 was produced more extensively by lung CD4⁺ and CD8⁺CD69⁺ compared with lung CD69⁻ memory T cells, and not significantly by spleen CD69⁺ and CD69⁻ cells (Fig. 3.11G, right). Together these results indicate that the functional capacity of CD69⁺ memory T cells comprise core features (e.g., IL-2, IL-10 production) along with subset and tissue influences.

The functional profile of CD103⁺CD69⁺ memory T cells

CD103 is a cell surface molecule that promotes retention by binding E-Cadherin on epithelial cells [222] and it is often used as a marker of TRM [10]. Therefore, to determine how the functional properties of CD103⁺ and CD103⁻ cells varied within the CD69⁺ fraction, these populations were stimulated with PMA/Ionomycin and cytokine production was measured via

intracellular staining. These experiments were restricted to CD8⁺ cells because of the low percentage of CD103⁺ cells within the CD4⁺ fraction (Fig. 3.1). In both the spleen and lung, a higher fraction of CD103⁺ cells produced IL-2 and IL-17 in response to stimulation compared with CD103⁻ cells (Fig. 3.13). There was no significant difference in the fraction of cells from either group that produced IFN- γ (Fig. 3.13). These results indicate that CD103⁺ cells may have a superior ability to produce certain activating and pro-inflammatory cytokines compared with CD103⁻ cells.

Figure 3.10. TCR repertoire overlap.

RNAseq was performed on CD69+ and CD69– memory T cells and CDR3 sequences were inferred from data using TRUST. Venn diagrams show degree of overlap between samples from each donor. The total number within each oval represents the total number of unique clones within that sample and numbers contained by multiple ovals represent clones that are common to those samples.

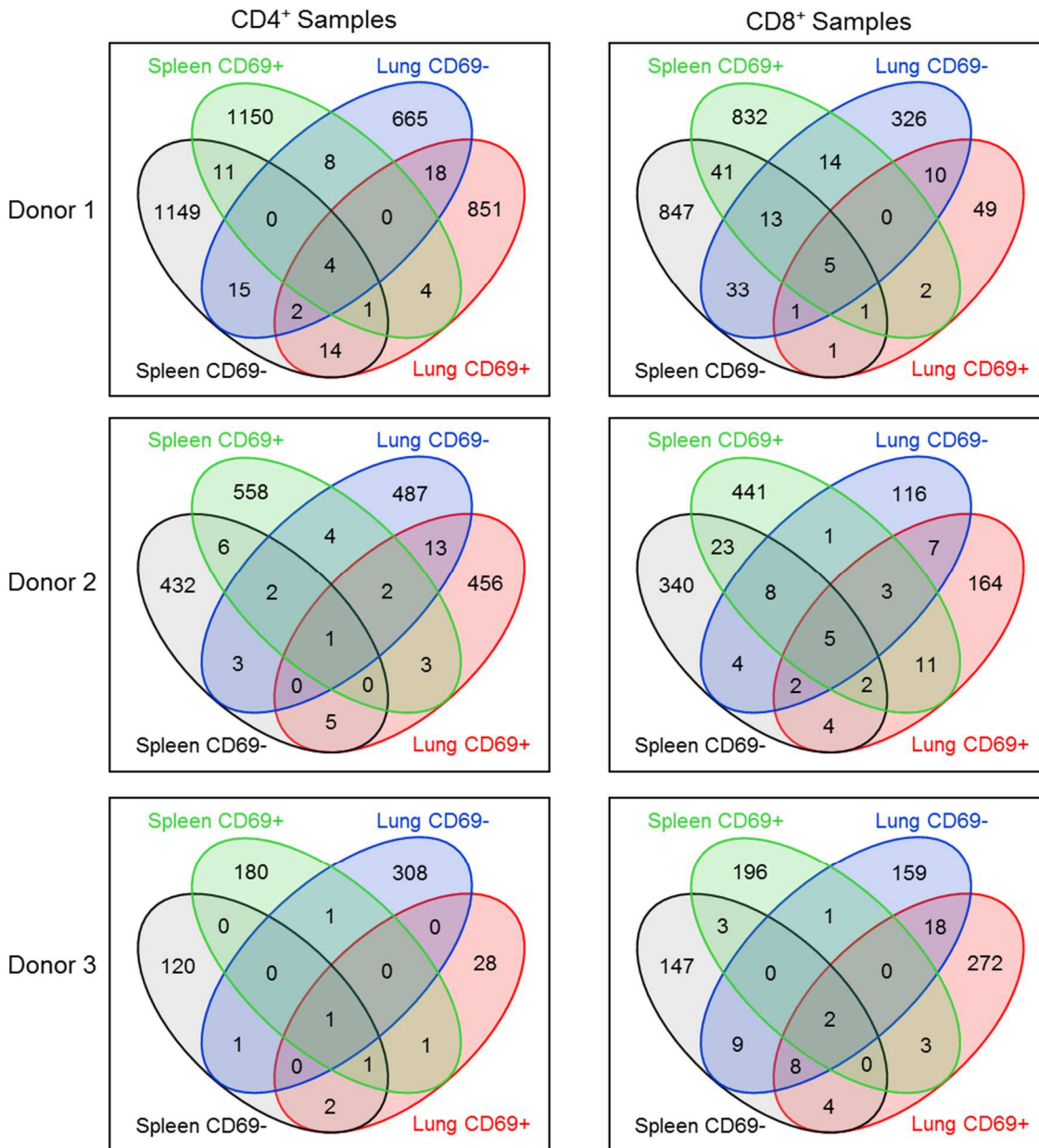


Figure 3.11. TCR clonal analysis, turnover, and function of CD69+ and CD69- cells.

(A) CD8⁺ T cells have reduced TCR repertoire diversity compared with CD4⁺ cells. CDR3 sequences were inferred from RNA-Seq data using TRUST. Graph shows the number of unique CDR3 calls (clonotypes) in each sample per 10³ reads mapped to the TCR region. **(B)** Increased tissue overlap of TCR clones within CD8⁺ CD69- compared to CD69+ memory T cells. Graph shows percentage of overlapping clones between lung and spleen samples from each donor, calculated by dividing the total number of overlapping clones by the total number of unique clones present in both tissues. See also Figure 3.9. **(C)** Reduced proliferative turnover by CD69+ memory T cells. Left: Representative flow cytometry plots of intracellular Ki67 expression from spleen and lungs of one individual donor. Right: Ki67 expression compiled from 10 donors depicted as mean frequency expressing Ki67 ±SEM. **(D)** Increased CD57 expression by CD69- compared with CD69+ cells. Left: CD57 expression by CD69- and CD69+ memory T cell subsets from spleen and lung of one representative donor. Right: CD57 expression compiled from 11 donors displayed as mean percent positive ±SEM. * p≤0.05, ** p≤0.01. **(E-G)** Distinct functional profile of CD69+ cells. CD4⁺ and CD8⁺ CD69- and CD69+ memory T cells isolated from spleens and lungs were stimulated with PMA/Ionomycin and cytokine production was assessed by intracellular cytokine staining (ICS) (for IL-2, IFN-γ, IL-17A), or were stimulated with anti-CD3/CD28 beads (for IL-10) and IL-10 levels in the supernatant were assessed by BD cytokine bead array. **(E)** Graph shows mean frequency of CD69- and CD69+ cells producing IL-2. **(F)** Graph shows mean ±SEM IL-10 production in pg/ml. **(G)** Graph shows mean frequency of CD69- and CD69+ cells producing IFN-γ (left) and IL-17A (right) ±SEM. n=6 donors spleen, 10 donors lung for IL-2, IFN-γ, IL-17A, n=3 donors for IL-10. *p<0.05, **p<0.01, ***p<0.001.

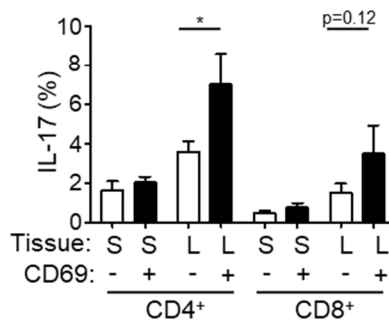
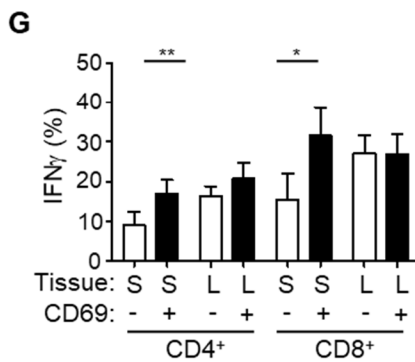
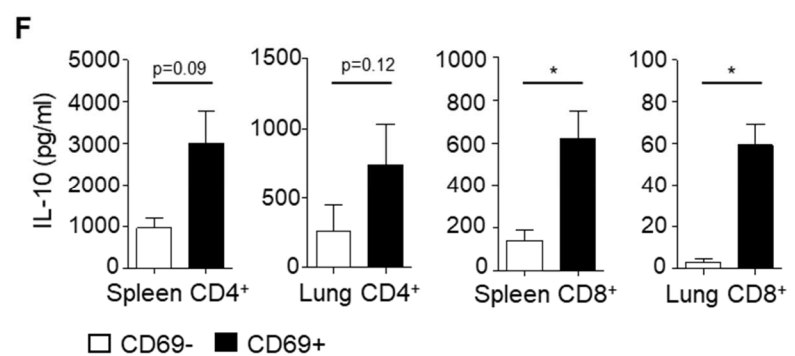
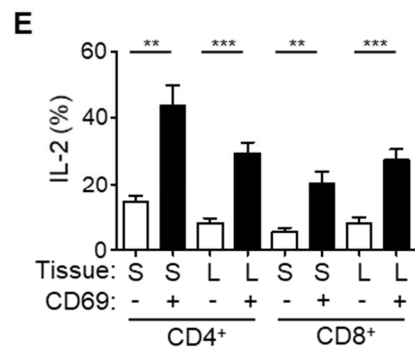
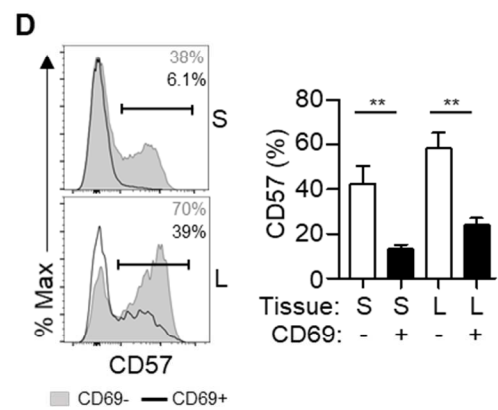
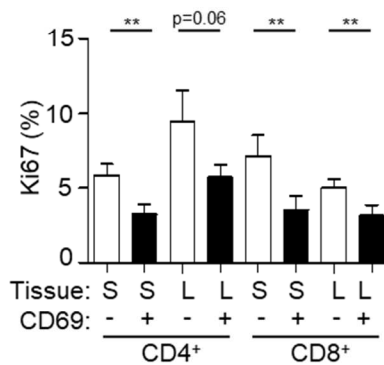
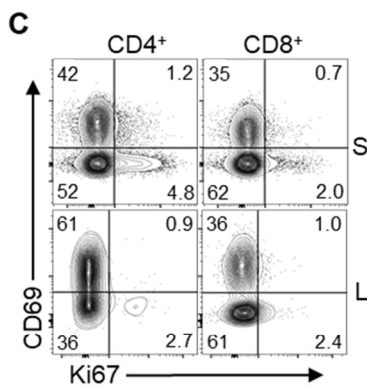
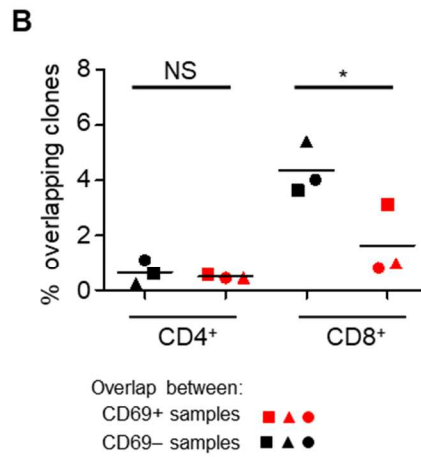
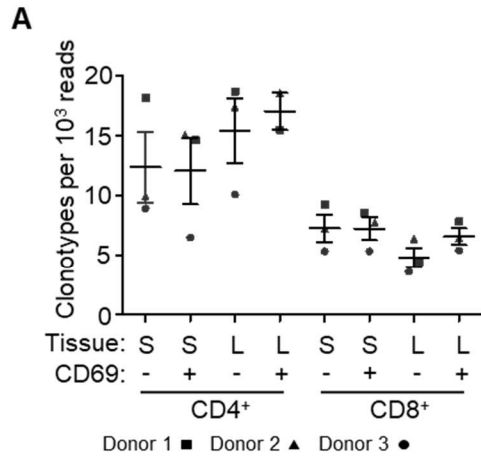


Figure 3.12: Transcript levels of cytokines.

(A) Normalized mRNA expression levels of IL2 (left), IFNG (middle), and IL17A (right) in CD69⁺ and CD69⁻ memory subsets in spleen (S) and lung (L) of each individual donor.

*FDR \leq 0.05, ***FDR \leq 10⁻³.

(B) Normalized mRNA expression levels of IL10 in CD69⁺ and CD69⁻ memory subsets in spleen (S) and lung (L) of each individual donor. *FDR \leq 0.05, ***FDR \leq 10⁻³.

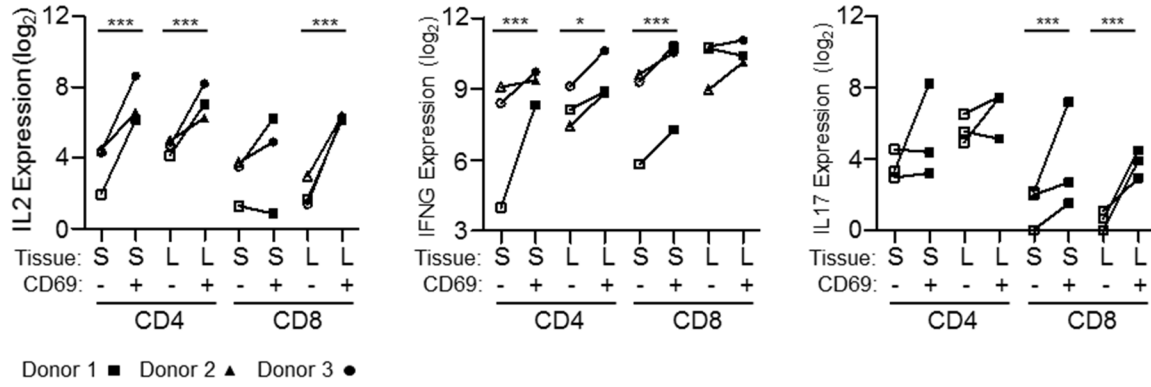
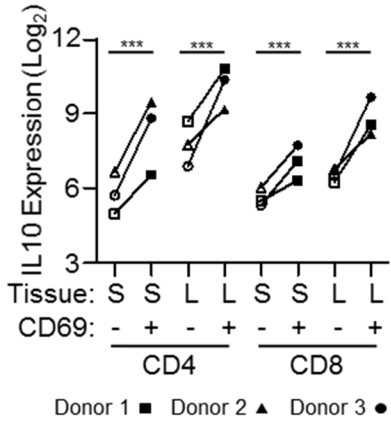
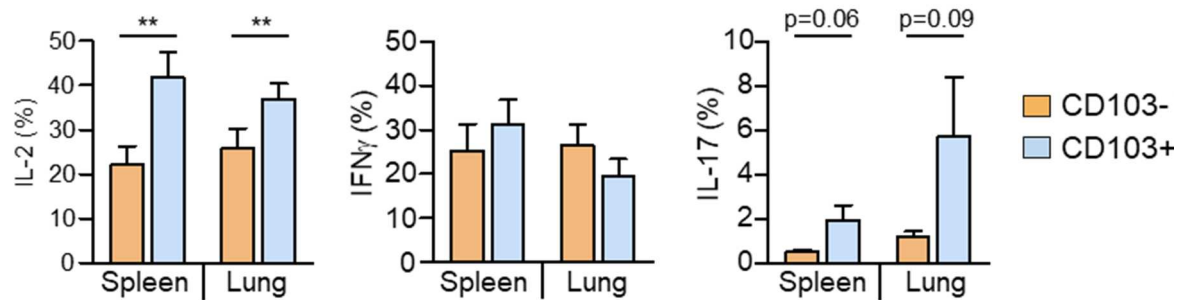
A**B**

Figure 3.13. Cytokine production by CD103+ and CD103- human CD69+ memory T cells.

CD8⁺CD69⁺ memory T cells from spleens (n=6 donors) and lungs (n=10 donors) were stimulated with PMA/Ionomycin for 3 hours and cytokine production was assessed by intracellular cytokine staining. Graphs show production of IL-2 (left), IFN- γ (middle) and IL-17A (Right) depicted as mean frequency expression cytokine \pm SEM, stratified by CD103⁺ (orange) and CD103⁻ (blue) subsets. **p<0.01



The TRM transcriptional profile is conserved across lineages and tissues

Isolation of both CD4⁺ and CD8⁺ memory subsets from two tissue sites of individual donors enabled us to assess lineage- and tissue-specific gene expression patterns. To identify lineage-specific genes, we compared differential gene expression by CD8⁺ CD69⁺ vs. CD69⁻ and CD4⁺ CD69⁺ vs. CD69⁻ subsets for each tissue site. The majority of genes showed similar differential expression in terms of direction and magnitude of fold change when looking at CD69⁺ vs. CD69⁻ subsets from either CD8⁺ or CD4⁺ lineages (Fig. 3.14A). From a total of 907 genes that were differentially expressed by at least one of our CD69⁺ vs. CD69⁻ pairs, there were 4 protein-coding genes that showed differential expression in CD4⁺ but not in CD8⁺ subsets, and 27 genes that showed significant differential expression in CD8⁺ but not in CD4⁺ subsets (Figs. 3.14A and 3.15A-B). Together, these results indicate that human CD4⁺ and CD8⁺ memory T cells have similar overall gene expression profiles.

We applied a similar type of analysis as above to identify genes specific to lung or spleen memory T cells (Fig. 3.14B). Only 10 genes showed differential expression in CD69⁺ vs. CD69⁻ in lung but not spleen samples, and 12 genes that showed significant differential expression in CD69⁺ vs. CD69⁻ in spleen but not lung samples (Fig. 3.14B; 3.15C-D). Notably, CD101 was transcriptionally upregulated in lung compared to spleen memory T cells. CD101 is a cell surface immunoglobulin superfamily protein which inhibits T cell activation and modulates T cell function [223-225]. Examination of CD101 surface expression by flow cytometry revealed increased expression by CD8⁺CD69⁺ compared with CD69⁻ cells in both lung and spleen, with minimal upregulation by CD4⁺ tissue memory subsets (Figs. 3.14C, 3.15E). These results indicate that CD101 could be a new additional marker for CD8⁺TRM.

The chemokine receptor CCR9 emerged as one of the few a spleen-specific genes. As CCR9 has been shown to be critical for homing to the intestine [226], we measured surface expression of CCR9 on intestinal tissue as well as spleen and lung. A significant fraction of intestinal CD4⁺CD69⁺ and CD8⁺CD69⁺ cells ($\geq 20\%$) expressed CCR9, while other samples had lower expression ($< 10\%$) of CCR9 (Fig. 3.16). There was also measurable proportion of splenic CD8⁺CD69⁺ memory T cells that upregulated CCR9 (8-10%) compared to negligible expression by spleen CD8⁺CD69⁻ cells, and low expression by all lung memory T cells (Fig. 3.16). This biased upregulation of CCR9 by splenic CD8⁺CD69⁺ was manifested by an increased ratio of CCR9 MFI in CD8⁺CD69⁺ compared to CD8⁺CD69⁻ cells in spleen but not lung (Fig. 3.16). Our data showing transcriptional upregulation and modest surface expression suggest that CCR9 may have some additional role in splenic T cell retention.

Figure 3.14. Lineage and tissue-specific transcription and phenotypic profiles in human CD69⁺ memory T cells.

(A) Analysis of lineage-specific gene expression in CD69⁺ and CD69⁻ memory T cells. Scatter plots display log₂ fold change of CD4⁺CD69⁺ vs. CD69⁻ on the x axis and CD8⁺ subsets on the y axis from lung (left) and spleen (right). Grey dots represent genes with significant differential expression in any paired CD69⁺ vs. CD69⁻ sample. Orange dots (“CD4 specific”) represent genes with significant differential expression in CD4⁺ CD69⁺ vs. CD69⁻ but not in CD8⁺ samples. Green dots (“CD8 specific”) represent genes with significant differential expression in CD8⁺CD69⁺ vs. CD69⁻ but not in CD4⁺ samples.

(B) Analysis of tissue-specific genes in CD69⁺ and CD69⁻ memory T cells. Scatter plots display log₂ fold change of lung CD69⁺ vs. CD69⁻ samples on the x axis and spleen samples on the y axis for CD4⁺ (left) and CD8⁺ (right) T cells using the same strategy as in (A) with red dots denoting “spleen specific” and blue dots denoting “lung specific” transcripts in the paired analysis.

(C) CD101 expression in human tissues. Representative plots show CD101 expression in CD69⁺ (black outline) and CD69⁻ (shaded) cells from one individual donor. Data are representative of 15 donors (see also Figure 3.14).

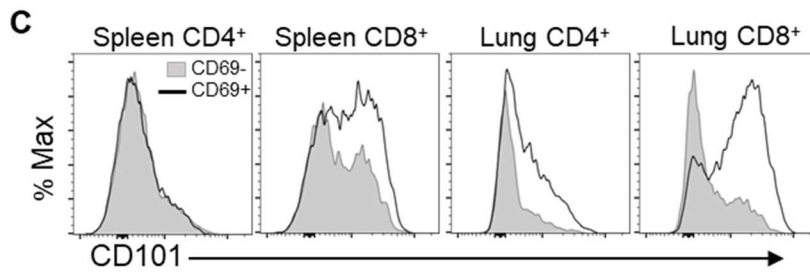
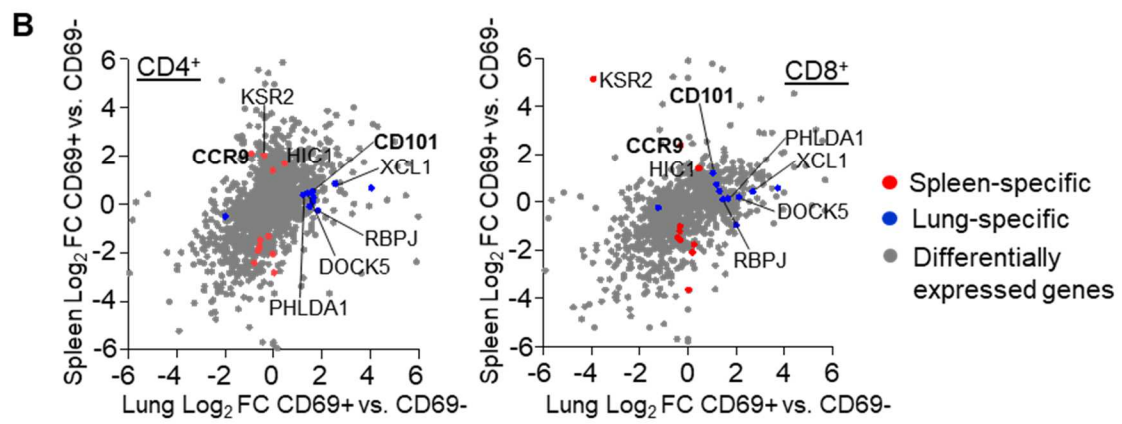
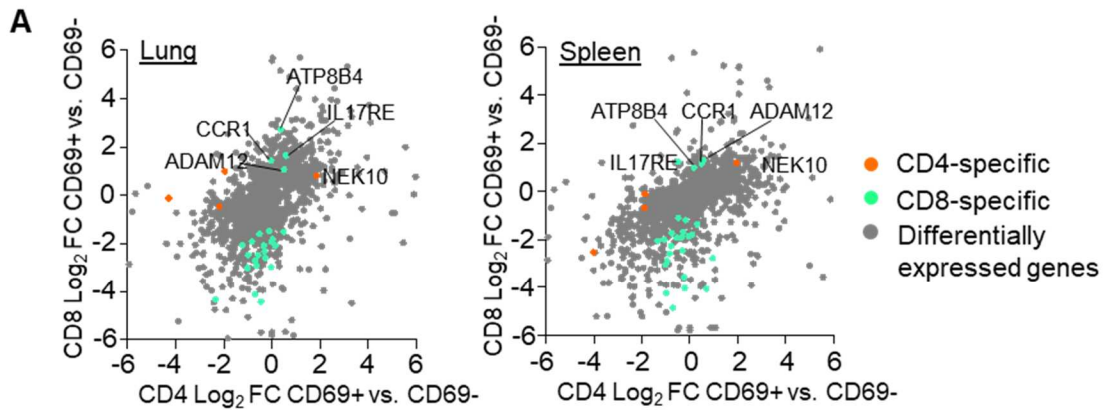


Figure 3.15. Tissue- and lineage- specific genes.

(A-D) Heatmaps show normalized expression of genes that showed differential expression when comparing CD69+ vs. CD69- memory T cell within CD4+ samples but not CD8+ samples (A); comparing CD69+ vs. CD69- memory T cells within CD8+ samples but not CD4+ samples (B); comparing CD69+ vs. CD69- memory T cells within lung samples but not spleen samples (C); and comparing CD69+ vs. CD69- memory T cell within spleen samples but not lung samples (D). (E) Expression of CD101. Graphs show compiled flow cytometry data as mean frequency of cells expressing CD101 ±SEM. * p≤0.05, **p≤10⁻², ***p≤10⁻³. n = 15 donors.

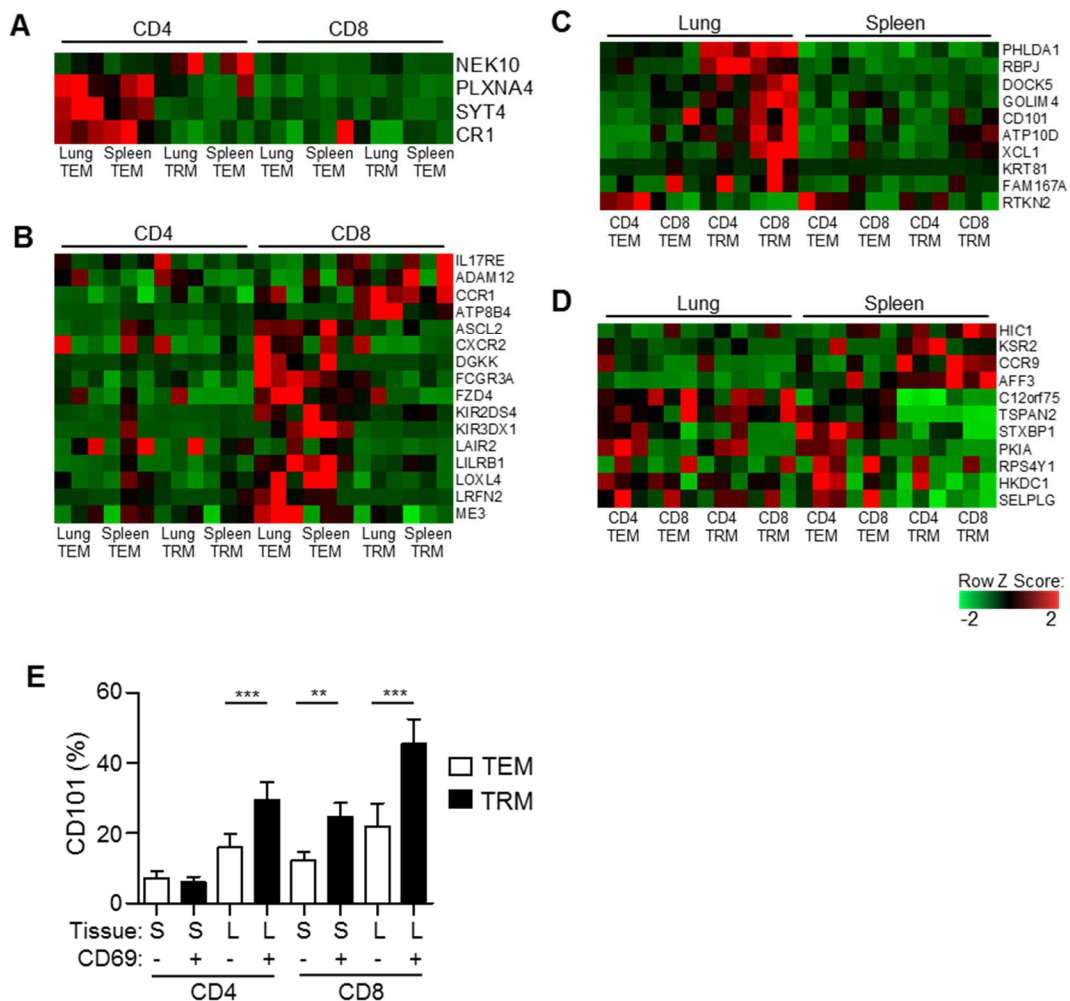
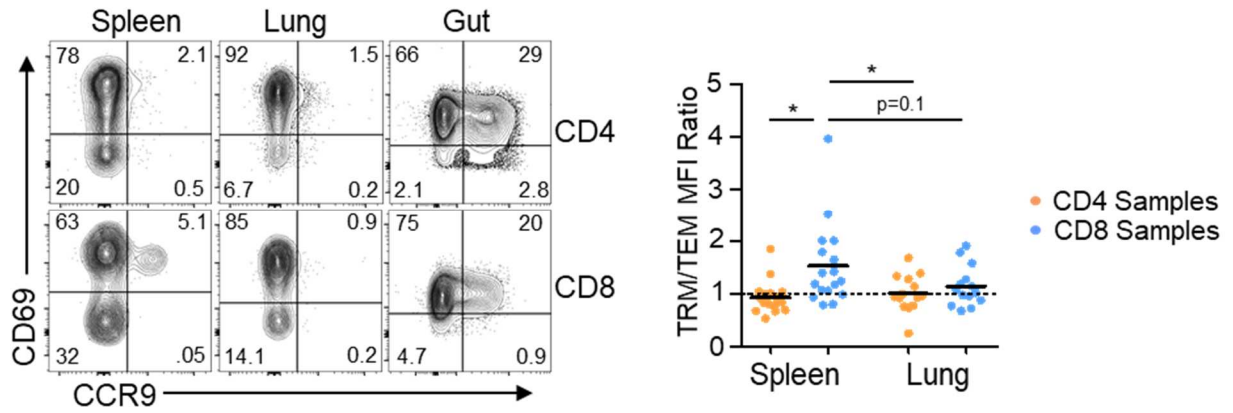


Figure 3.16. CCR9 Expression in CD69+ and CD69- memory T cells.

Left: representative flow cytometry plots show CCR9 expression in the spleen, lung, and gut of one representative donor. Right: Ratio of mean fluorescence intensity (MFI) for CCR9 in CD69+ compared with CD69- negative samples. * $p \leq 0.05$. n= 15 spleen, 13 lung, and 5 gut.



TRM are a phenotypically distinct subset across multiple tissues.

We asked whether multiple elements within the core signature together distinguished tissue memory subsets in spleen and lung using t-distributed stochastic neighbor embedding (t-SNE) analysis [185, 227], a dimensionality reduction method used to visualize high-dimensional data in two dimensions such that cells expressing similar markers will be close to each other. Based on the expression of 6 markers defined as part of the core TRM signature (Fig. 3.5), CD49a, CD103, CXCR6, CX3CR1, PD-1, and CD101, we found that CD69⁺ and CD69⁻ subsets were located in distinct regions of the t-SNE plots for both CD4⁺ and CD8⁺T cells in each tissue (Fig. 3.17A), and in density plots compiled from both sites (Fig. 3.17B, top). Manual gating within each dominant cluster reveals that CD69⁻ subsets exhibit elevated expression of CX3CR1 and low expression of CD49a, PD-1, CD101, CD101, and CXCR6 compared to CD4⁺ and CD8⁺CD69⁺ subsets exhibiting high expression of CD49a, PD-1, and CXCR6, and low expression of CX3CR1, with CD8⁺CD69⁺ subsets having high expression of CD103 and CD101 (Fig. 3.17B). These results further support the designation of tissue CD69⁺ memory T cells as TRM and the CD69⁻ subset as TEM.

We assessed how multiple phenotypic properties of the core signature were distributed in diverse sites within an individual, including in intestines, mesenteric lymph nodes, tonsils, and blood in addition to lung and spleen (Figs. 3.17C-D and 3.18). We initially generated t-SNE plots using concatenated data from all six tissue sites, revealing phenotypically distinct TEM and TRM subsets across multiple tissues (Fig 3.17C). In density plots, CD4⁺ and CD8⁺TEM cells were localized to the same region of the t-SNE, suggesting that TEM phenotypes are conserved across lineages and tissues (Fig. 3.17C). By contrast, CD8⁺TRM and CD4⁺TRM appeared at different regions within the t-SNE density plots distinct from TEM cells, (Fig. 3.17C). Notably, there was

a broader range of phenotypes based on these markers within the CD4⁺TRM subset compared with the tighter clustering of CD8⁺TRM phenotypes, suggesting increased heterogeneity of CD4⁺ tissue memory T cells.

To compare the pattern of subset phenotypes between tissues, we assigned distinct colors to CD8⁺TRM, CD4⁺TRM and TEM populations. Plotting all tissue samples on the same t-SNE reveals the localization of each cell population (Fig. 3.17D, left), with TEM cells and CD4⁺ and CD8⁺TRM cells maintaining their distinct clustering patterns and localization in each site (Figs. 3.17D, right, and 3.18). In blood, TEM cells clustered in a similar pattern as TEM in other tissues (Fig. 3.17D, right), providing additional evidence that TEM in tissues are circulating. Notably, CD8⁺TRM cells exhibit a focused clustering pattern in all tissues, suggesting that human TRM cells represent a unique subset in multiple sites. CD4⁺TRM cells in all tissues exhibited a broader array of phenotypes suggesting increased heterogeneity of CD4⁺TRM compared to CD8⁺TRM cells throughout the body.

Figure 3.17. TRM are a phenotypically distinct subset across multiple tissues.

Simultaneous expression of CD49a, CD103, CD101, CXCR6, CX3CR1, PD-1, and CD69 was visualized using t-SNE analysis.

(A) CD69⁺ and CD69⁻ memory T cells are phenotypically distinct in spleen and lung. Plots show CD69⁺ memory T cells (color coded green) and CD69⁻ memory T cells (color coded black) from spleen and lungs of an individual donor (Donor 321) representative of 5 donors.

(B) Defining the phenotype of TRM and TEM clusters. Regions with high cellular density were manually gated within TEM (CD69⁻), CD4⁺ TRM (CD69⁺), and CD8⁺ TRM (CD69⁺) fractions (top row). Histograms show expression levels of CD49a, CD103, CD101, CXCR6, CX3CR1, and PD-1 within gated regions (bottom row). **(C-D)** The core TRM phenotype is observed across multiple tissues. Phenotype analysis as in **(A)** was performed using lung, intestine, spleen, mesenteric lymph node (MLN), tonsils, and blood samples from one representative donor (Donor 332).

(C) Plots show CD4⁺ (left) and CD8⁺ (right) TRM and TEM subsets from all tissues with cell number density color coded.

(D) Plots shows cells from all tissues (left large plot) or each individual site (Right smaller plots) color coded by cell type (CD4⁺ TRM, red; CD8⁺ TRM, green; TEM, black) of one donor representative of 4 donors. See also Figure 3.16 for t-SNE plot of an additional representative donor.

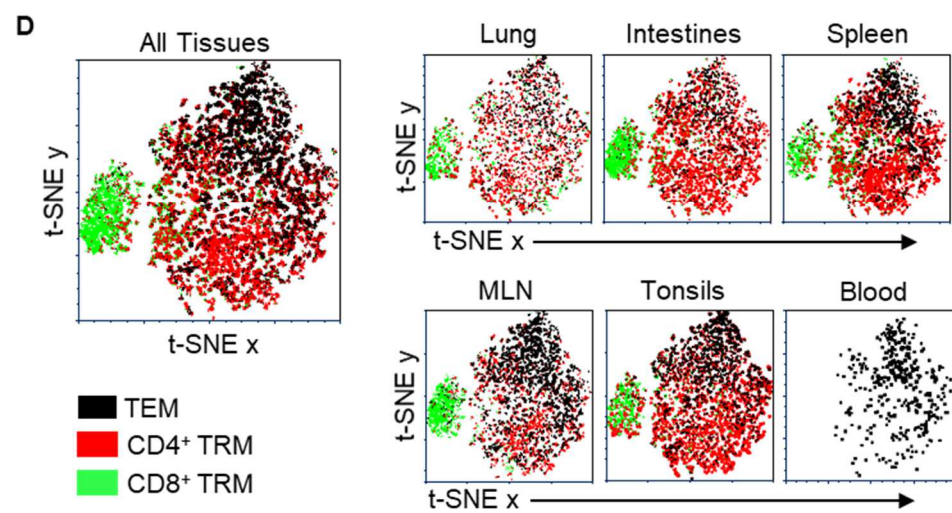
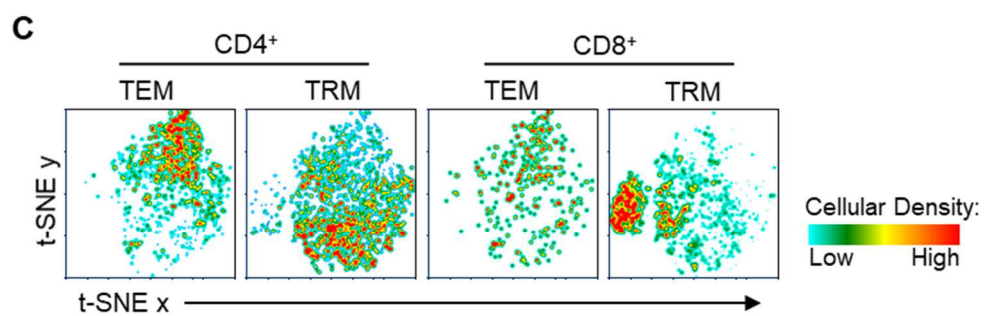
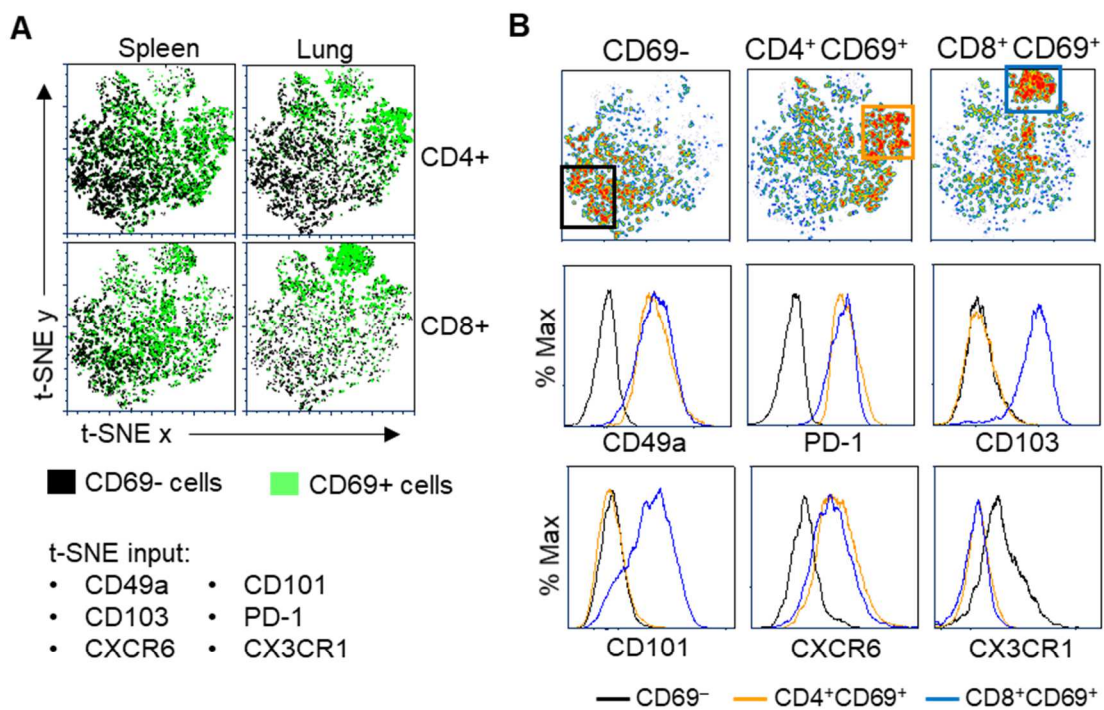
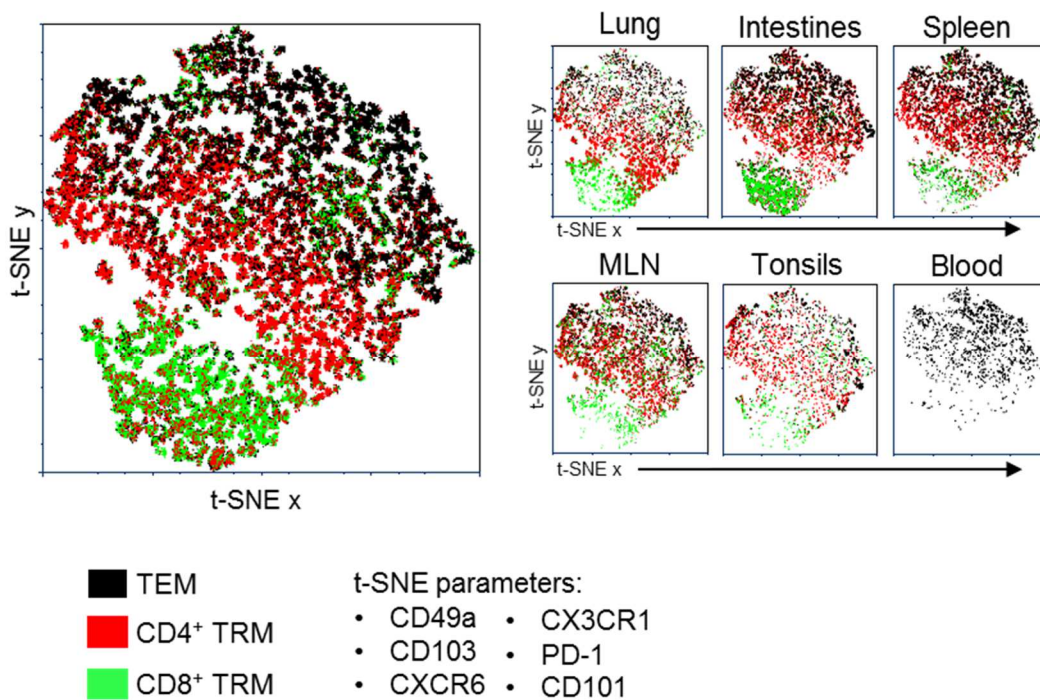


Figure 3.18. t-SNE analysis of TRM and TEM from additional donor.

The expression of CD49a, CD103, CD101, CXCR6, CX3CR1, and PD-1 was analyzed on CD69+ (TRM) and CD69- (TEM) memory T cells from multiple tissues and donors. t-SNE analysis was performed using lung, intestine, spleen, mesenteric lymph node (MLN), tonsils, and blood samples from one representative donor. t-SNEs are color coded by cell type and CD4+ TRM are shaded red, CD8+ TRM are shaded black, and TEM samples are shaded black. Left: t-SNE shows cells from all tissues from one donor. Right: t-SNEs show cells from each individual tissue. t-SNEs are representative of 4 donors.



Section 3.3: Discussion

In this study we provide key insights into TRM biology through a comprehensive analysis of human CD4⁺ and CD8⁺ tissue memory subsets in lymphoid and mucosal tissues within and between multiple human donors. Our results establish that human tissue memory T cells fractionated based on CD69 expression exhibit a core signature of 31 genes conserved across tissues and lineages, with key homologies to the transcriptional profile of mouse TRM. We demonstrate that human TRM persist in multiple lymphoid, mucosal and peripheral tissue sites, exist within both CD4⁺ and CD8⁺ lineages, and exhibit unique functional signatures compared with circulating TEM cells including proinflammatory and regulatory capacities, and low turnover. Together, our results suggest that human TRM are a distinct developmental subset uniquely adapted for in situ immunity.

A definitive phenotypic marker for human TRM has not previously been defined. Transcriptional profiling has been reported for mouse CD8⁺TRM in which CD8⁺ memory T cells isolated from a barrier site (skin, intestine or lung) were compared with spleen [109, 110]. In human studies, CD8⁺TRM isolated based on CD103 expression from individual tissues (lung, skin) have been profiled in comparison to blood subsets [142, 168]. Here, we employed an innovative and comprehensive approach to assess differences in putative circulating and resident populations within tissues by directly comparing CD69⁺ memory subsets from a lymphoid and mucosal site (spleen and lung) with the corresponding CD69⁻ subset from each tissue as well as CD69⁻ TEM from blood for both CD4⁺ and CD8⁺ lineages. While CD103 has been used to define CD8⁺ TRM in mice [102] and humans [142], our results demonstrate that CD69 expression can delineate tissue from circulating memory T cells based on the following results: First, CD69 is the major marker that distinguishes memory T cells in diverse tissues from those in circulation for

CD4⁺ and CD8⁺ T cells, while CD103 expression is limited to a subset of tissue CD8⁺T cells. Second, CD69⁺ tissue memory T cells are a transcriptionally and phenotypically distinct subset that share core features with mouse TRM while human tissue CD69⁻ cells share features with circulatory blood T cells. Finally, core phenotypic markers associated the CD69⁺ subset such as CD49a, PD-1, CXCR6, and CD101 delineate TRM cells across multiple mucosal and lymphoid tissues.

Although we found the TRM signature to be enriched within the CD69⁺ subset of human tissue memory T cells, the role of CD69 in determining tissue residence remains unclear. In mouse models, the majority of TRM cells in barrier sites express CD69; however, TRM cells lacking CD69 expression have been detected [104], and CD69⁺ cells in the thymus were shown to recirculate during homeostasis [228]. However, the extent of CD69 expression by tissue memory T cells appears to be a function of antigen and pathogen exposure. We consistently find higher frequencies of CD69 expression by human tissue memory T cells compared to that found in mouse models maintained in spf conditions, particularly in lymphoid sites [18, 105]. Interestingly, T cells in “dirty” pet store mice had significantly higher frequencies of CD69 expression by T cells in tissues that was similar to humans [229]. In our results, we consistently see separation of transcriptional profiles between CD69⁺ and CD69⁻ subsets (Fig. 3.3), suggesting that delineation between these subsets in humans may be more defined than in mouse spf models due to the history of antigen exposure.

The core TRM gene signature identified here includes canonical genes and proteins associated with tissue residence in mice including downregulation of S1PR1, KLF2, and CD62L, upregulation of specific adhesion molecules (CD49a, CRTAM), modulation of specific chemokine receptors (increased CXCR6, decreased CX3CR1), and upregulation of inhibitory or regulatory

molecules (PD-1, DUSP6, IL-10). We also found TRM to exhibit a distinct functional profile encompassing both pro-inflammatory, activating, and regulatory functions conserved between diverse individuals, tissues, and lineages. This core signature is depicted in Figure 3.19. We further identified a novel marker CD101, with immunomodulatory function that is expressed by CD8⁺ TRM in multiple sites and could be useful in conjunction with other markers to identify TRM. We found phenotypic heterogeneity based on the core markers, particularly among CD4⁺TRM, and additional tissue heterogeneity has been reported in CyTOF profiling of human tissue T cells [185]. CD103 expression by mouse intestinal TRM [133] and CD49a in human skin memory T cells [168], have been shown to delineate distinct functional capacities, and dissecting human TRM heterogeneity will be an important area of focus in future studies.

The dominant presence of TRM in human tissues suggests a key protective role *in situ*. Our results reveal that human TRM possess dichotomous functional capacities, not only being poised for enhanced production of IL-2 and pro-inflammatory cytokines, but also producing IL-10 and exhibiting reduced proliferation and increased expression of inhibitors of T cell activation (i.e., PD-1, CD101). This may enable potent mobilization of immune responses *in situ* through pro-inflammatory cytokines but prevent excessive inflammation and cellular proliferation to limit inflammation-induced tissue damage. Moreover, the quiescent, inhibited state of TRM as assessed by the low turnover could promote longevity and prevent inappropriate activation to non-pathogenic antigens to which many human tissues are continually exposed.

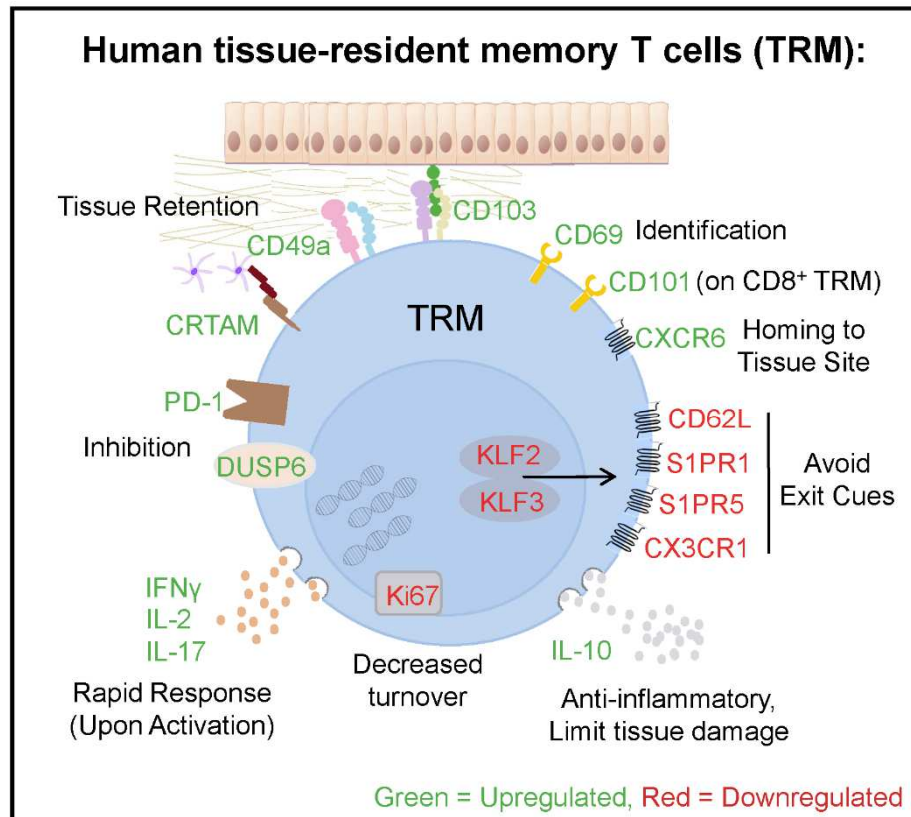
Our findings show that in humans, TRM exist in multiple tissue sites and within CD4⁺ and CD8⁺ T cell lineages. While TRM have been detected in mouse LN [111, 112], the majority of mouse lymphoid memory CD4⁺ and CD8⁺ T cells in mice are circulating, particularly those in the spleen. The predominance of TRM-phenotype cells in all human lymphoid tissues examined here

including spleen, lymph nodes, and tonsils may reflect their long-term persistence over decades and/or continual pathogen exposure, consistent with a recent study identifying memory T cells specific for persistent viruses in human tonsils [157]. TRM persistence in diverse sites may be due to the aggregate experience of numerous antigens over the human lifespan.

Interest in TRM is rapidly expanding to the study of many diseases, from infection to cancer to inflammation and autoimmunity. In humans, it is essential to identify and analyze these cells and determine whether they are functioning aberrantly in disease sites. Our study elucidates major unifying features of all tissue memory T cells in multiple healthy tissue sites within an individual. These results will serve as a valuable baseline from which to detect and study the role of tissue memory T cells in diseases, and for promoting tissue immunity in vaccines, cell- and biologic-based immunotherapies.

Figure 3.19. A core signature of human TRM.

In this study, we identify a core transcriptional, functional, and phenotypic signature of human tissue-resident memory T cells (TRM). This core signature is depicted below and includes a unique profile of homing receptors, which help TRM avoid tissue egress or home to the tissue site; expression of specific adhesion markers, which promote tissue retention; and a unique functional profile, through which TRM have the ability to produce effector cytokines but also secrete anti-inflammatory cytokines and express inhibitory markers.



CHAPTER 4: Dye efflux capacity defines a functionally distinct subset of human CD8⁺ tissue resident memory cells.

ABSTRACT:

Tissue-resident memory T cells (TRM) accelerate pathogen clearance at various tissue sites. However, TRM are heterogeneous, and the functional role of different TRM subsets is not well defined. Here, we describe a functionally distinct subset of CD8⁺ TRM found across human tissues defined by the capacity to efflux fluorescent dyes. Efflux(+) TRM showed evidence of quiescence both transcriptionally and phenotypically, including heightened expression of CD127, reduced turnover, decreased expression of activation and exhaustion markers, and elevated expression of immunosuppressive markers. Further, efflux(+) TRM expressed a unique profile of adhesion and migration markers suggestive of enhanced long-term tissue retention. After TCR stimulation, efflux(+) TRM produced less pro-inflammatory cytokines and underwent less cytotoxic degranulation compared with efflux(-) TRM. Moreover, efflux(+) TRM retained a higher proliferative capacity and exhibited greater responses to IL-7. Notably, efflux(+) also had an enhanced capacity for IL-17 production and showed evidence of Th17-associated signaling transcriptionally. Overall, these results suggest that efflux(+) and efflux(-) TRM may cooperate to mediate tissue immunity in humans; efflux(+) TRM are programmed for longevity and tissue-retention to maintain a reservoir capable of proliferation, while efflux(-) TRM exhibit heightened effector function for generating rapid pro-inflammatory and cytotoxic responses. The identification of these potentially clinically relevant TRM subsets could guide the development of novel vaccination strategies and immunotherapies.

Section 4.1: Introduction

Memory CD8⁺ T cells provide lifelong protection against pathogens. Human memory T cells are heterogeneous, with different subsets exhibiting distinct tissue homing, recirculation, and self-renewal properties [6]. Tissue-resident memory T cells (TRM) are a subset of memory cells residing in peripheral tissues, where they are the key mediators of pathogen protection *in situ* [10]. TRM provide superior protection against invading pathogens compared with circulating memory T cells, and TRM have also emerged as key targets for vaccination strategies [10, 116, 117]. Further, TRM have been specifically implicated in diseases such as psoriasis and vitiligo [121]. These properties make TRM attractive clinical targets; however, recent studies have demonstrated that TRM are highly heterogeneous, encompassing multiple unique subsets [133, 155, 168, 185, 186]. Understanding the role of these different subsets in immune responses is therefore necessary before therapeutic modulation of TRM can be achieved.

In a prior study, we identified substantial phenotypic heterogeneity within human TRM [186]. Indeed, phenotypic variability based on markers such as CD103 and CD49a can identify TRM subtypes with different functional roles [155, 168]. Additionally, TRM subsets identified by these markers are transcriptionally and developmentally distinct and can occupy non-overlapping subanatomic niches [133, 155, 168]; this suggests that the TRM compartment actually comprises multiple distinct subsets that are identified together based on tissue-retention properties. Recently, a subset of memory T cells with the ability to efflux fluorescent dyes has been reported in human tissues including the bone marrow [192], gut [191], and skin [230]. The ability to efflux fluorescent dyes is associated with increased self-renewal properties within hematopoietic stem cells [187, 188], but the role of effluxing TRM is not well characterized. Therefore, we investigated whether

the ability to efflux fluorescent dyes can distinguish a functionally distinct TRM subset with properties of quiescence and self-renewal.

Here, we utilized a unique human tissue resource to investigate heterogeneity of CD8⁺ TRM across multiple tissues obtained from healthy organ donors. We identify a population of CD8⁺ memory T cells in lymphoid and non-lymphoid tissues with the ability to efflux fluorescent mitochondrial dyes. Efflux(+) cells predominated within the TRM compartment, where they expressed a canonical TRM signature including elevated CD103 and CD49a and reduced S1PR1 expression. Further, efflux(+) TRM had reduced expression of Ki67 and exhaustion/senescence markers, as well as a transcriptional profile associated with increased longevity within tissues. Following TCR stimulation, efflux(+) TRM produced less pro-inflammatory cytokines and underwent less cytotoxic degranulation compared with efflux(-) TRM, but retained a greater capacity to proliferate. Uniquely, efflux(+) also had an enhanced capacity for IL-17 production along with transcriptional features of IL-17 signaling following stimulation. Together, these results establish TRM with the ability to efflux dyes as a functionally distinct subset, and suggest that different TRM subsets cooperate for optimal tissue-based immunity.

Section 4.2: Results

Memory CD8⁺ T cells across healthy human tissues efflux fluorescent dyes

We sought to characterize this heterogeneity within the CD8⁺ memory T cell compartment with fluorescent dyes and surface marker phenotyping. The predominant memory (CD45RO⁺) population across human tissues is TEM-phenotype CD45RA-CCR7- [17, 156] (Figure 4.1). T cells isolated from healthy human tissues were labeled with either Mitotracker Green or CMXRos, fluorescent dyes used for mitochondrial labelling (hereafter denoted “Mito Dye”). Two distinct populations, Mito Dye high and low, were observed within memory CD8⁺ T cells across human tissue sites (Figure 4.2A). Equivalent results were obtained with both Mitotracker Green, which labels total mitochondrial mass [231], and CMXRos, which is dependent on mitochondrial membrane potential (Figure 4.3A), suggesting that changes in relative mitochondrial state are not responsible for the observed differences in dye staining. To determine whether the Mito low subset was due to dye efflux, we stained cells in the presence of increasing concentrations of cyclosporine A (CSA), a competitive inhibitor of efflux pumps [232]. Only a single Mito high population was observed when cells were labeled in the presence of CSA (Figure 4.2B). Further, compared with Mito high cells, Mito low cells expressed higher levels of MDR1 (ABCB1) (Figure 4.3B), a cell surface transporter that mediates efflux of fluorescent dyes and xenobiotics in hematopoietic stem cells [233]. Thus, the Mito low subset constitutes a population with dye efflux capacity and will be referred to hereafter as “efflux(+)”, with the corresponding Mito high subset being referred to as “efflux(-).”

We found that the ratio of efflux(+) to efflux(-) populations differed across tissue sites, with the lowest frequency of efflux(+) memory T cells observed in the blood ($\leq 40\%$) and the highest frequency observed in spleen and lung ($>60\%$) (Figure 4.2C). To assess whether efflux(+)

cells specific for clinically relevant human pathogens could be detected, we analyzed cytomegalovirus (CMV)-specific cells with tetramers and dye labeling. Efflux(+) cells were detected amongst tetramer positive cells at similar ratios in multiple tissue sites (Figure 4.2D), indicating that efflux(+) cells are generated following infection and are involved in virus-specific immunity.

Figure 4.1. Identification of Memory T cell subsets in Humans.

Plot shows CCR7 and CD45RA expression in the spleen of one representative donor, after gating for CD3+ CD8+ cells. Labelling within each of the four quadrants denotes the memory T cell subset with that phenotype, as determined by previous studies.

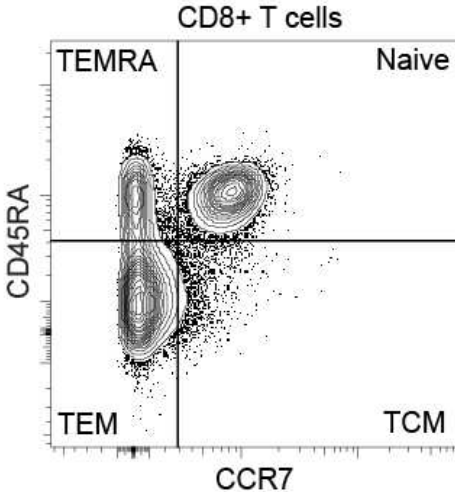


Figure 4.2. A subset of memory CD8⁺ T cells across human tissues effluxes fluorescent dyes.

Human T cells from the indicated tissue sites were loaded with Mito Dye and analyzed by flow cytometry to identify memory (CCR7⁻ CD45RA⁻) CD8⁺ T cells.

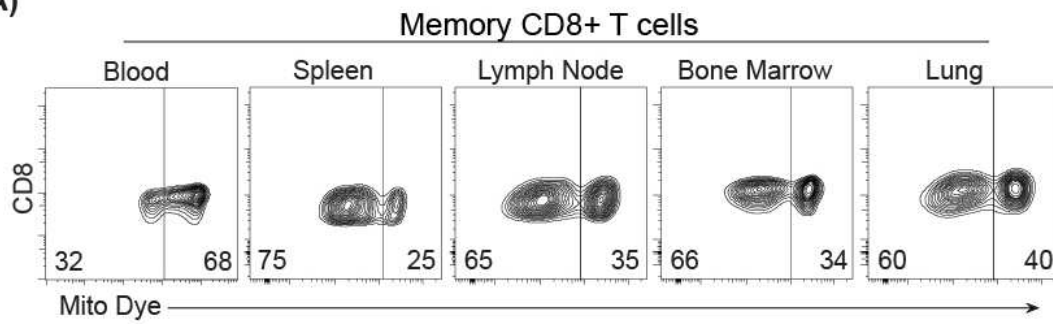
(A) Mitotracker fluorescence within memory CD8⁺ T cells across healthy human tissues. Plots are representative of at least 3 donors per tissue site.

(B) Cyclosporin A (CSA) inhibits Mito Dye efflux. CD8⁺ T cells from spleen were labeled with Mito Dye as in Panel A in the presence or absence of CSA at the indicated concentrations. Results are representative of at least 3 different donors.

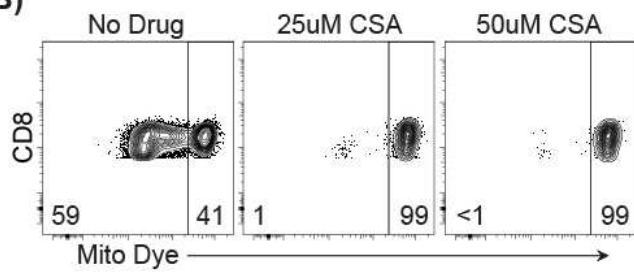
(C) Frequency of efflux(+) and efflux(-) subsets within memory CD8⁺ T cells across tissue sites. Bars indicate standard error of the mean (SEM).

(D) A subset of CMV antigen-specific CD8⁺ T cells across tissues efflux dyes. Upper: Mitotracker fluorescence in memory CD8⁺ T cells from indicated tissue sites labeled with tetramer specific to CMV antigen. Lower: Frequency of efflux(+) cells within tetramer positive population. Results are representative of 2 independent donors.

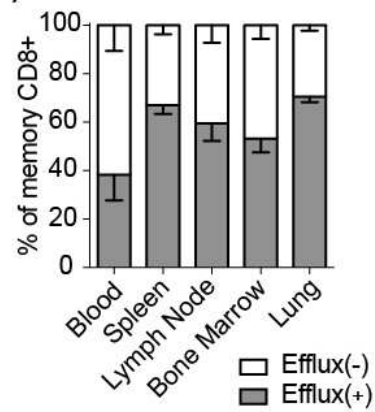
A)



B)



C)



D)

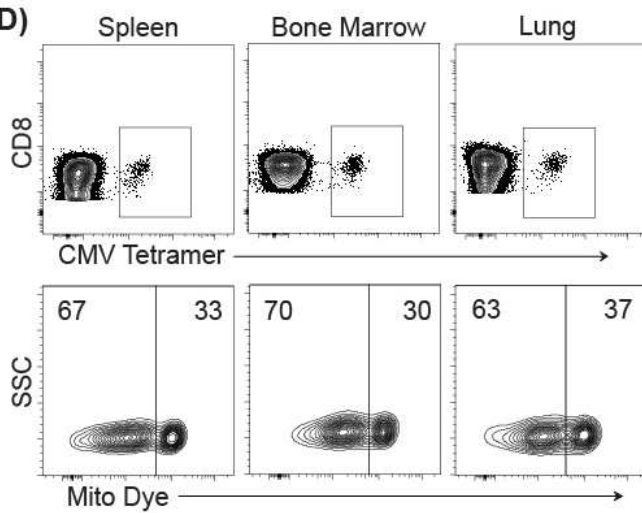
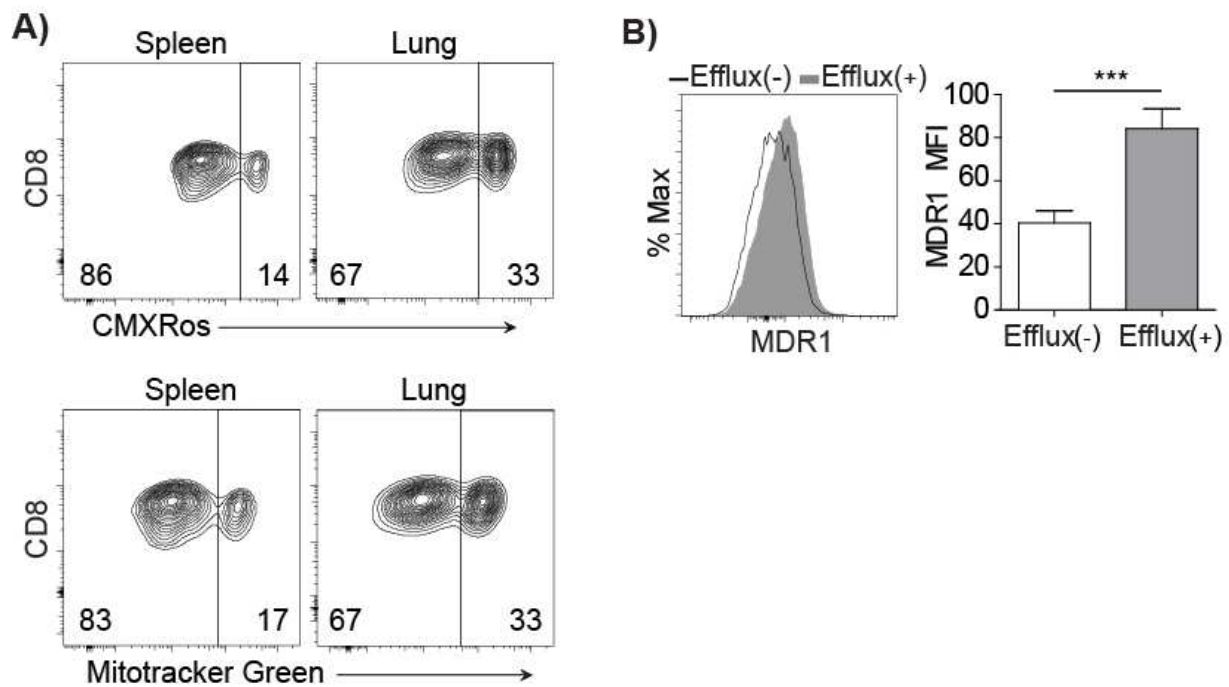


Figure 4.3. Dye efflux yields populations with high and low mitochondrial fluorescence staining.

(A) FACS analysis of CMXRos (upper) and Mitotracker green (lower) staining within CD8⁺ memory T cells from the spleen and lung of the same donor. Numbers within plots indicate percentage of total cells in the Mito dye high or low gates.

(B) Efflux(+) populations have elevated expression of MDR1. Left: Expression of the drug efflux pump MDR1 by MitoDye hi (black line) and low (red line) populations. Right: quantification of MDR1 MFI in MitoDye hi and low memory CD8⁺ T cells. ***p≤0.001.



Tissue resident phenotype of efflux(+) CD8⁺ memory T cells

Based on the finding that tissues contained high fractions of efflux(+) cells, we sought to determine if there was a correlation between efflux capacity and tissue residency. We measured the expression of CD69, a marker commonly used to identify tissue-resident memory T cells (TRM) in both mice [10] and humans [186], on efflux(+) and efflux(-) memory subsets in tissues. (Hereafter, we use TRM and TEM to refer to CD69⁺ and CD69⁻ memory T cells, respectively.) Interestingly, while both TRM and TEM fractions contained efflux(+) cells, TRM were highly enriched for dye-effluxers compared with TEM in multiple human tissues (Figure 4.4A). Across multiple tissues and donors, 60-80% of TRM were efflux(+) and 20-40% of TRM were efflux(-) (Figure 4.4A). This suggests heterogeneity within TRM based on efflux status, with the majority of TRM being efflux(+) but a considerable fraction of efflux(-) TRM being present across donors and tissues.

We further characterized the phenotype of efflux(+) cells for markers that we previously defined as part of a core signature of human TRM [186]. We found that TRM expressing the adhesion markers CD103 and CD49 were predominantly efflux(+) (Figure 4.4B-C). Further, efflux(+) TRM had elevated expression of CD101 (Figure 4.4C), a marker we previously identified on human CD8⁺ TRM [186] that inhibits T cell proliferation [223]. Taken together, the TRM-associated phenotype of efflux(+) cells suggests unique adaptations to maintain residence and longevity within tissues.

Given the previously described association of MAIT cells with dye efflux [189, 190], we sought to confirm that our observations were relevant to the diverse range of polyclonal memory CD8⁺ T cells. MAIT cells, defined by invariant expression of V α 7.2 as well as the marker CD161, have been detected in human liver, gut, and skin, but not in lymph nodes [168, 189], and their

presence in spleen has not been described. Within efflux(+) TRM, only a minor fraction were MAIT cells, and further these MAIT cells were largely CD103 negative (Figure 4.5). Taken together, these results indicate that human polyclonal CD8⁺ TRM comprise the majority of efflux(+) memory cells across healthy human tissues.

Figure 4.4. CD8⁺ TRM have heightened capacity for dye efflux across human tissues.

(A) Top row: Representative plots of CD69 expression by efflux(+) (Mito low) and efflux(-) (Mito high) subsets of memory CD8⁺ T cells in the indicated tissues. Bottom row: Compiled frequency of efflux(+) cells within the TRM (CD69+) and TEM (CD69-) compartments of memory CD8⁺ T cells in each tissue site.

(B) CD69⁺ CD103⁺ TRM have extensive efflux capacity. Upper: Representative plots showing CD103 expression amongst efflux(+) and efflux(-) TRM (CD69⁺) Lower: Quantification of efflux(+) cells amongst CD103⁺ and CD103⁻ TRM (CD69⁺) in the spleen and lung.

(C) Efflux(+) cells are enriched for TRM phenotypic markers. Upper: Representative plots show expression of CD49a and CD101 amongst efflux(+) and efflux(-) TRM (CD69⁺). Lower: Frequency of CD49a and CD101 expressing cells within efflux(+) and efflux(-) TRM. For all: *p≤0.05, **p≤0.01, ***p≤0.001 ****p≤0.0001.

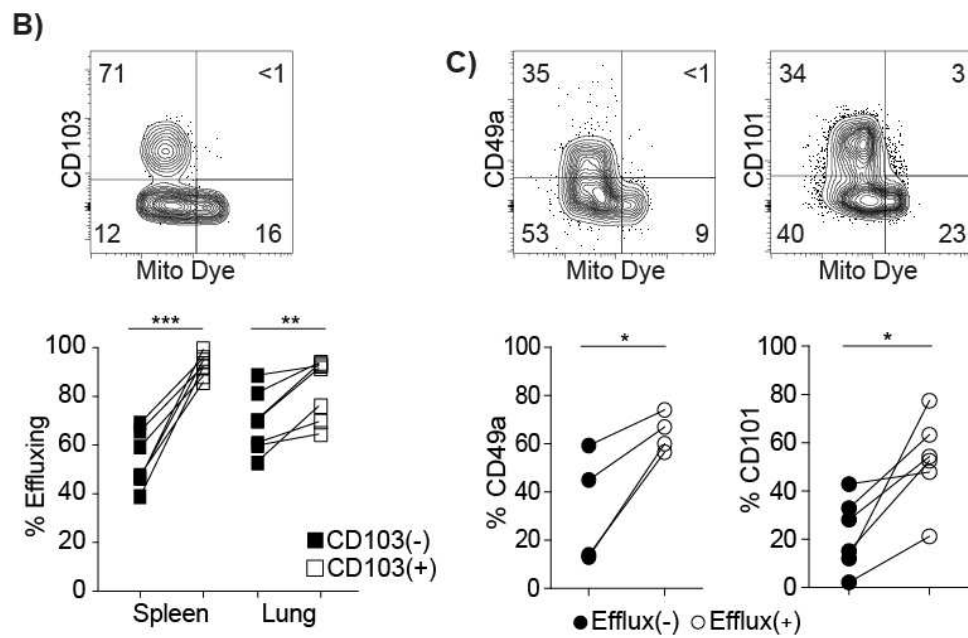
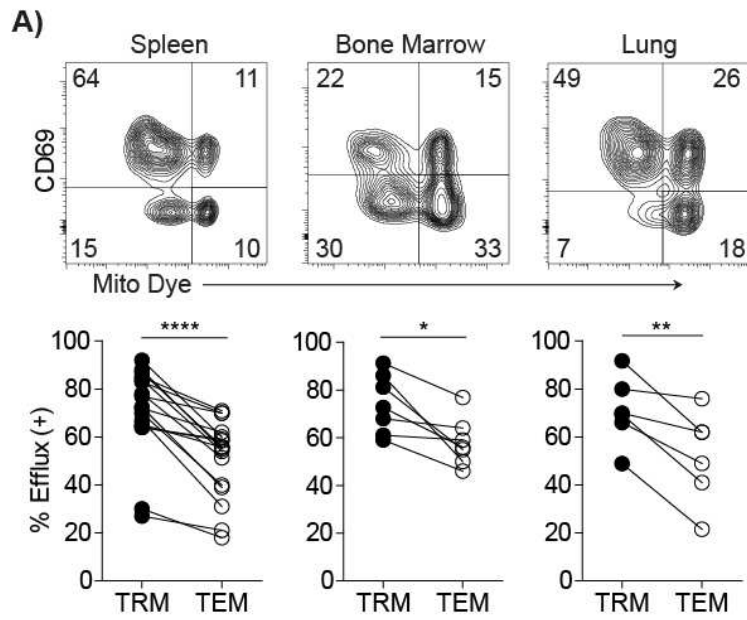
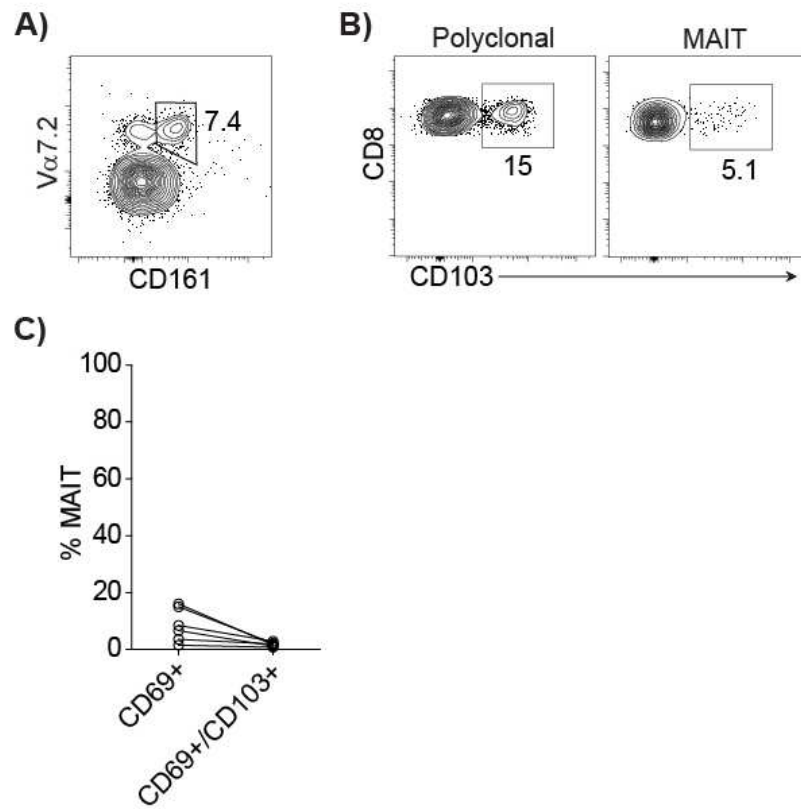


Figure 4.5. MAIT cells are a minor subpopulation of CD69+ human memory CD8+ T cells.

Identification of the MAIT (mucosal associated invariant T cell) populations in spleen. Tissues were stained to identify MAIT CD8+ T cells by CD161 and V α 7.2 TCR clonotype expression. **(A)** Plot shows CD161 and V α 7.2 expression within CD8+ TRM in the spleen of one representative donor.

(B) Plots show CD103 expression within MAIT (CD161+, V α 7.2+) and polyclonal (non-MAIT) T cells.

(C) Compiled frequency of MAIT T cells within CD69+ (TRM) and CD69+CD103+ memory CD8+ T cells in the spleen.



Unique transcriptional characteristics of efflux(+) TRM

Heterogeneity within human TRM has been described based on surface markers [155, 168, 186]. Given that efflux(+) cells represent a significant subset within the TRM compartment (Figure 4.4), we sought to characterize the significance of dye-efflux capability by TRM through whole transcriptome profiling by RNA sequencing (RNA-Seq). Efflux(+) and efflux(-) CD8⁺ TRM (CD69+CD45RA-CCR7-) were isolated by FACS sorting from the spleen of 3 previously healthy organ donors (aged 32, 32, 59) and samples were sent for RNA-Seq at the Columbia Genome Center. (See Table 4.1 for RNA-Seq QC summary.) Principal-component analysis (PCA) revealed that efflux(+) TRM were transcriptionally distinct from efflux(-) TRM (Figure 4.6A). While differences along the first principal component could be attributed to donor variation, consistent differences between efflux(+) and efflux(-) were seen on the second principal component accounting for 21% of the variation in gene expression (Figure 4.6A). This suggests unique transcriptional properties of efflux(+) TRM that are maintained across diverse donors.

Differential expression was assessed using DESeq2 [202], and after applying criteria for significance (false discovery rate [FDR] ≤ 0.05 and absolute value of log₂ fold change > 1), 133 differential expressed genes were detected when comparing efflux(+) and efflux(-) TRM (Figure 4.6B). Notably, this number was smaller than the 300-400 differentially expressed genes we previously reported when comparing the TRM subset to the TEM subset in human tissues [186]. Expression levels of these genes within efflux(+) TRM were consistent across all three donors (Figure 4.6D), suggesting that these represent invariant properties of the efflux(+) TRM subset.

To interpret the biological significance of these differentially expressed genes, we used DAVID online functional annotation analysis [204, 205]. Notably, the pathway with the greatest enrichment within our gene set was phospholipid translocation (Figure 4.6C), consistent with the

ability of efflux(+) TRM to efflux fluorescent dyes. DAVID analysis further revealed that the genes differentially expressed by efflux(+) TRM were implicated in the regulation of key T cell pathways controlling function, cytokine responses, and adhesion and migration (Figure 4.6C-D). Additionally, pathways involved in regulating proliferation were also enriched with significant values (data not shown), although these were not among the top 10 enriched pathways.

TRM exhibit unique adhesion and migration properties, and pathways involved in chemotaxis and cell adhesion were among the top enriched pathways (Figure 4.6C). Consistent with the observed differences in CD49a and CD103 expression (Figure 4.4), efflux(+) cells had increased expression of the genes *ITGAE* (encoding CD103) and *ITGAI* (encoding CD49a), as well as *NCAMI*, *MCAMI*, *CDH4*, and *ANK1*. Efflux(+) cells also had elevated *LAYN* expression, a receptor for hyaluronic acid in the extracellular matrix, recently associated with Tregs and CD8⁺ T cell inhibition [234]. Efflux(+) TRM also exhibited differential expression of a number of homing receptors (Figure 4.6E). Notably, efflux(+) TRM had reduced expression of *SIPRI*, the downregulation of which is required for CD8⁺ TRM differentiation in mice [139], and whose downregulation by human TRM has also been established [142, 186]. Together with increased expression of canonical TRM markers such CD49a and CD103, these results suggests that efflux(+) TRM may have an enhanced capacity for tissue residency compared with their efflux(-) counterparts. Efflux(+) TRM additionally upregulated CCR9, CCR1, and CCR6, and downregulated CCR4 and CCR8 compared with efflux(-) TRM, which could promote differential migratory properties between these subsets.

We observed differential expression of key transcription factors by efflux(+) and efflux(-) TRM (Figure 4.6E), indicative of distinct functional and regulatory pathways in these two subsets. Efflux(+) TRM had increased expression of *TLE1* (Figure 4.6E), a transcriptional regulator

associated with Notch/RBPJ signaling [235], a pathway essential for TRM formation (Hombrink et al., 2016). Notably, efflux(+) cells had elevated *RORC* and *RORA* expression (Figure 4.6E), two transcription factors that drive Tc17-type responses in CD8⁺ T cells [236]. Consistent with an increased capacity for Type 17 responses, efflux(+) cells expressed high levels of *IL17A*, as well as IL23 and IL17 receptors (Figure 4.6E), two critical regulators of Type 17 responses. Efflux(+) TRM also upregulated the adhesion marker *MCAMI* (Figure 4.6E), which has been associated with IL17-producing Tc17 CD8⁺ T cells [237].

Analysis of genes associated with cell cycle and apoptosis control suggested increased quiescence and longevity of efflux(+) TRM compared with efflux(-) TRM. Notably, efflux(+) expressed lower levels of *ZNF365* (Figure 4.6E), encoding a zinc finger protein involved in genome replication and mitotic progression, previously found to be highly expressed by circulating TEM compared with CD103⁺ TRM [142, 238]. Elevated levels of *CD101*, *SPRY1*, and *SPRY2*, genes with documented roles in suppressing T cell proliferation and TCR-mediated calcium signaling [223, 239], coupled with reduced levels of Cyclin B2 (*CCNB2*), further reinforced that efflux(+) may persist in a quiescent state.

In addition to differential expression of a number of genes involved in T cell function, efflux(+) cells expressed higher levels of the newly described, human-specific CD28 analogue *TMIGD2* (CD28H) [240], as well as higher levels of *CD9*, which also delivers costimulatory signals for T cell activation [241, 242] (Figure 4.6E). These data, coupled with lower expression of genes encoding inhibitory receptors *PDCD1* and *CTLA4* (Figure 4.6E), suggest that efflux(+) TRM show less evidence of senescence and exhaustion and thus may respond differentially to TCR stimulation during TRM re-activation.

A number of nutrient, ion, and xenobiotic transporters were expressed at higher levels in efflux(+) TRM, which could be important for homeostasis in barrier tissues and promote longevity via efflux of toxins and waste products and/or import of nutrients (Figure 4.6E). Additionally, consistent with reduced *CTLA4* and *PDCDI* expression, efflux(+) TRM had lower expression of a number of genes encoding MHC class II molecules (Figure 4.7), which mark recent T cell activation [243], further suggesting that efflux(+) TRM are resting within tissues. Finally, efflux(+) TRM upregulated genes encoding killer cell lectin-like receptors (Figure 4.7), which modulate T cell activation [244]. Overall, these data indicate that efflux(+) TRM have a unique transcriptional program that promotes quiescence and longevity within tissues, comprised of genes controlling adhesion and migration, as well as T cell activation, function, and proliferation.

Table 4.1. RNA-Seq QC Summary

Donor	Efflux Status	Stimulation	Number of Reads	Mapped Reads	Mapping Ratio	Mapped Reads Exome
1	+	-	47115590	44261623	93.94%	31724353
1	-	-	48910042	45861860	93.77%	33954253
2	+	-	50373890	47168098	93.64%	31752401
2	-	-	47420384	44770755	94.41%	31054564
3	+	-	26035498	24508180	94.13%	17898923
3	-	-	25419455	23766652	93.50%	16902512
1	+	+	31011637	29086355	93.79%	21959690
1	-	+	28933389	27136830	93.79%	20289527
2	+	+	26957605	25228879	93.59%	19680387
2	-	+	23111752	21714831	93.96%	16286040
3	+	+	22326495	21026323	94.18%	16081927
3	-	+	23048327	21621291	93.81%	15904273

Figure 4.6. Efflux(+) TRM have unique transcriptional properties.

Whole transcriptome profiling by RNA sequencing was performed on efflux(+) and efflux(-) TRM from the spleen of 3 donors.

(A) PCA of efflux(+) and efflux(-) TRM samples, based on the global transcriptome.

(B) Differential expression assessed by DESEQ2. The number of genes with significant different expression is displayed, with the number of genes upregulated in efflux(+) displayed in black, and the number of genes downregulated in efflux(+) TRM shown in white.

(C) Functional annotation analysis by DAVID online software. Select gene ontology (GO) terms with significant adjusted p-Values (adj. p) are displayed, along with fold enrichment. Directionality of pathways was not assessed.

(D) Heatmap shows normalized expression levels of all genes with significant differential expression, as assessed in B.

(E) Log₂ fold changes of select genes when comparing expression in efflux(+) TRM to efflux(-) TRM. Genes are grouped into categories, as indicated by the bold text to the left of each plot. Data from each donor is indicated by a unique shape throughout the plots, as indicated in the legend.

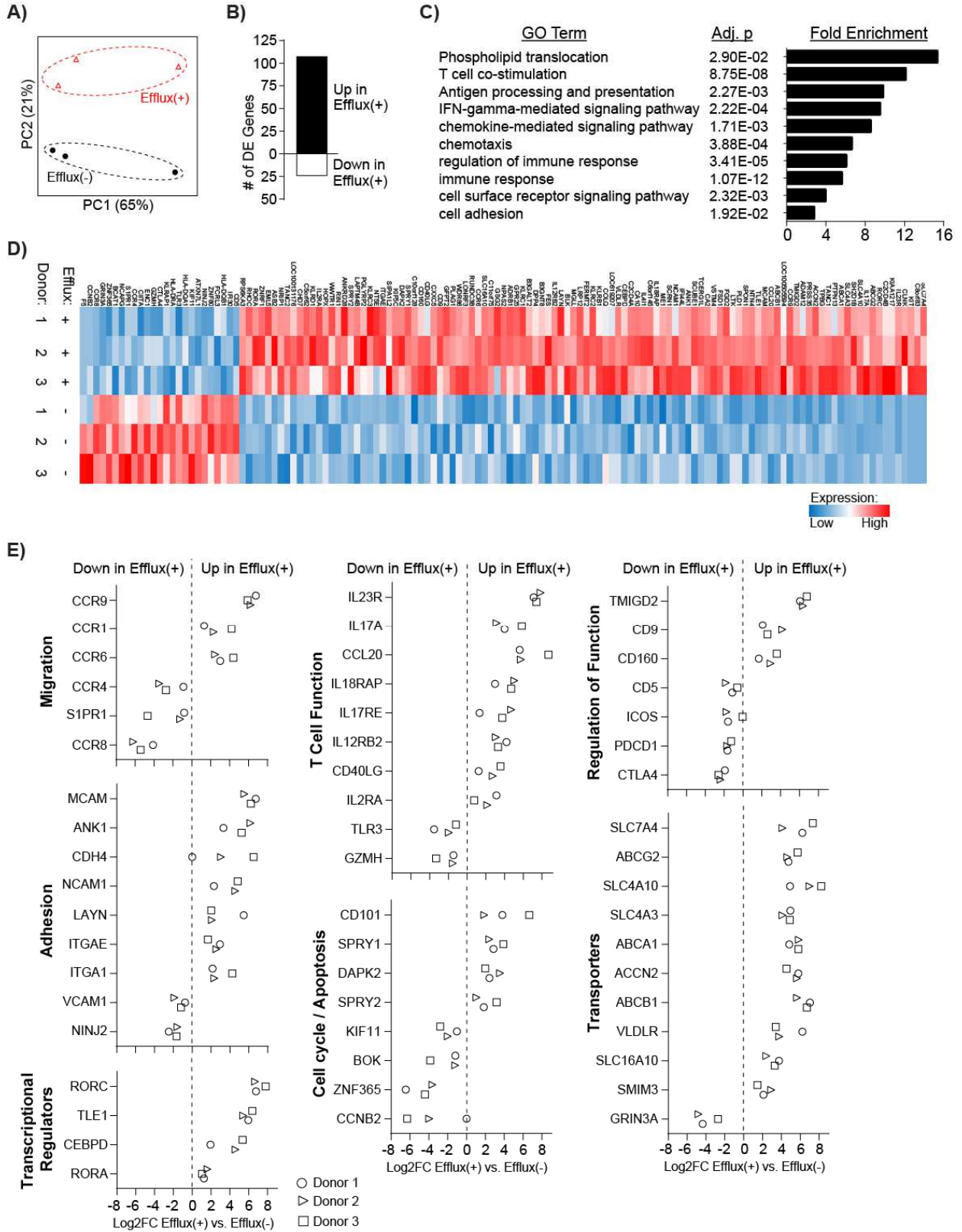
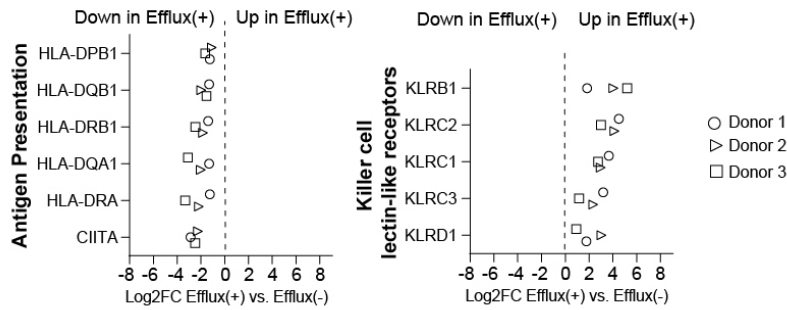


Figure 4.7. Fold Changes of Additional Gene Categories.

Log2 fold changes when comparing expression in efflux(+) TRM to efflux(-) TRM of additional genes not displayed in Figure 4.6. Genes are grouped into categories, as indicated by the bold text to the left of each plot. Data from each donor is indicated by a unique shape throughout the plots, as indicated in the legend.



Efflux(+) TRM Exhibit a Resting Phenotype

We next sought to validate differences observed at the transcriptional level through flow cytometric analysis of steady state efflux(+) and efflux(-) subsets, in particular of markers related to turnover, history of TCR activation and cytokine responses, and functional costimulation. We also determined expression of these markers on TEM to determine if efflux status is associated with unique properties exclusively within TRM or across memory subsets. We first measured the expression of CD127 (IL-7 receptor). IL-7 is critical for memory T cell homeostasis [245], and expression of CD127 delineates memory T cells capable of responding to IL-7 from those with a prior history of IL-7 responses in human tissues [156]. Efflux(+) TRM had elevated CD127 expression compared with efflux(-) TRM (Figure 4.8A), while TEM efflux(+) and efflux(-) cells had similar, lower levels of CD127, suggesting that efflux(+) TRM have elevated capacity for cytokine responses. We then assessed the expression of the co-receptors CD27 and CD28, which are downregulated following TCR stimulation. Within the TRM compartment, efflux(+) TRM had a reduced frequency of CD27+ and CD28+ cells compared with efflux(-) TRM (Figure 4.9). However, dye efflux did not correlate with CD27 or CD28 downregulation for conventional TEM (Figure 4.9).

To confirm the quiescent cell cycle transcriptional profile we observed in RNA-Seq analysis, we analyzed expression of CD57, a marker of replicative senescence and cytotoxicity [246], and Ki67, a marker associated with cellular proliferation. TEM globally expressed more CD57 than TRM, as previously documented (Figure 4.8B) [142, 186]. We found that efflux(+) TRM and TEM both had significantly lower expression of CD57 compared with their efflux(-) counterparts, though for TEM, the difference was only significant in the lung (Figure 4.8B). Further, efflux(+) TRM cells expressed lower levels of Ki67 compared with efflux(-) TRM (Figure

4.8C). This lower proliferative rate was also evident in the efflux(+) TEM subset (Figure 4.8C). These data suggest that efflux(+) subsets are less proliferative at steady-state compared with efflux(-) subsets.

Based on the result that efflux(+) TRM have differential expression of a number of genes encoding exhaustion and inhibitory markers, we measured the expression of PD-1 and CTLA-4. In the lung, spleen and bone marrow, efflux(+) TRM expressed lower levels of PD-1 than efflux(-) TRM from the same tissue (Figure 4.8D). Amongst splenic TRM, efflux(+) cells had lower CTLA4 expression compared with efflux(-) TRM (Figure 4.9C). Finally, efflux(+) TRM also expressed lower levels of the activation marker HLA-DR (Figure 4.9D).

Alongside canonical Foxp3⁺ CD4⁺ T regulatory cells, regulatory CD8⁺ T cells have also been described in humans [247], including one subset that expresses CD39 [248, 249], an ectonucleotidase that catalyzes the production of immunosuppressive adenosine and promotes T cell anti-inflammatory function [250, 251]. We found that CD39 was expressed almost exclusively by efflux(+) TRM, and further that CD39 expressing efflux(+) TRM were almost all CD103⁺ (Figure 4.8E). These findings suggest that a subset of efflux(+) TRM could have additional immunomodulatory functions, and are consistent with CD101 upregulation by efflux(+) TRM (Figure 4.4).

Taken together, these phenotypic differences, coupled with the efflux(+) transcriptome, establishes efflux(+) TRM as a resting subset with less evidence of exhaustion within tissues that retains the ability to respond to cytokine signaling. Further, although some differences were observed between TEM subsets, larger, more consistent differences were found in efflux(+) and efflux(-) TRM, indicating that efflux status delineates a distinct subset primarily within the TRM fraction.

Figure 4.8. Efflux(+) TRM exhibit a resting phenotype at steady-state.

(A) Left: Histograms of CD127 expression by TRM and TEM subsets from the spleen of one representative donor. Right: Compiled frequencies of CD127 efflux(+) and efflux(-) subsets of TEM and TRM from bone marrow (BM) and spleen.

(B) Left: Histograms of CD57 expression by efflux(+) and efflux(-) TRM and TEM subsets from the spleen of one representative donor. Right: Compiled frequencies of CD57+ TRM and TEM from spleen, lung, and bone marrow.

(C) Left: Expression of Ki67 within TRM and TEM subsets from the spleen of one representative donor. Right: Frequency of Ki67+ cells in efflux(+) and efflux(-) TRM and TEM

(D) Left: Expression of PD-1 by TRM and TEM subsets from the spleen of one representative donor. Right: Compiled expression of PD-1 in efflux(+) and efflux(-) TRM and TEM from different tissue sites.

(E) Left: Expression of ectonucleotidase CD39 by splenic TRM and TEM subsets from one representative donor. Middle: Representative plot of CD39 and CD103 expression within TRM. Right: Compiled expression of CD39 in efflux(+) and efflux(-) TRM and TEM from spleen.

* $p \leq 0.05$, ** $p \leq 0.01$, **** $p \leq 0.0001$, ns: not significant. Paired T test.

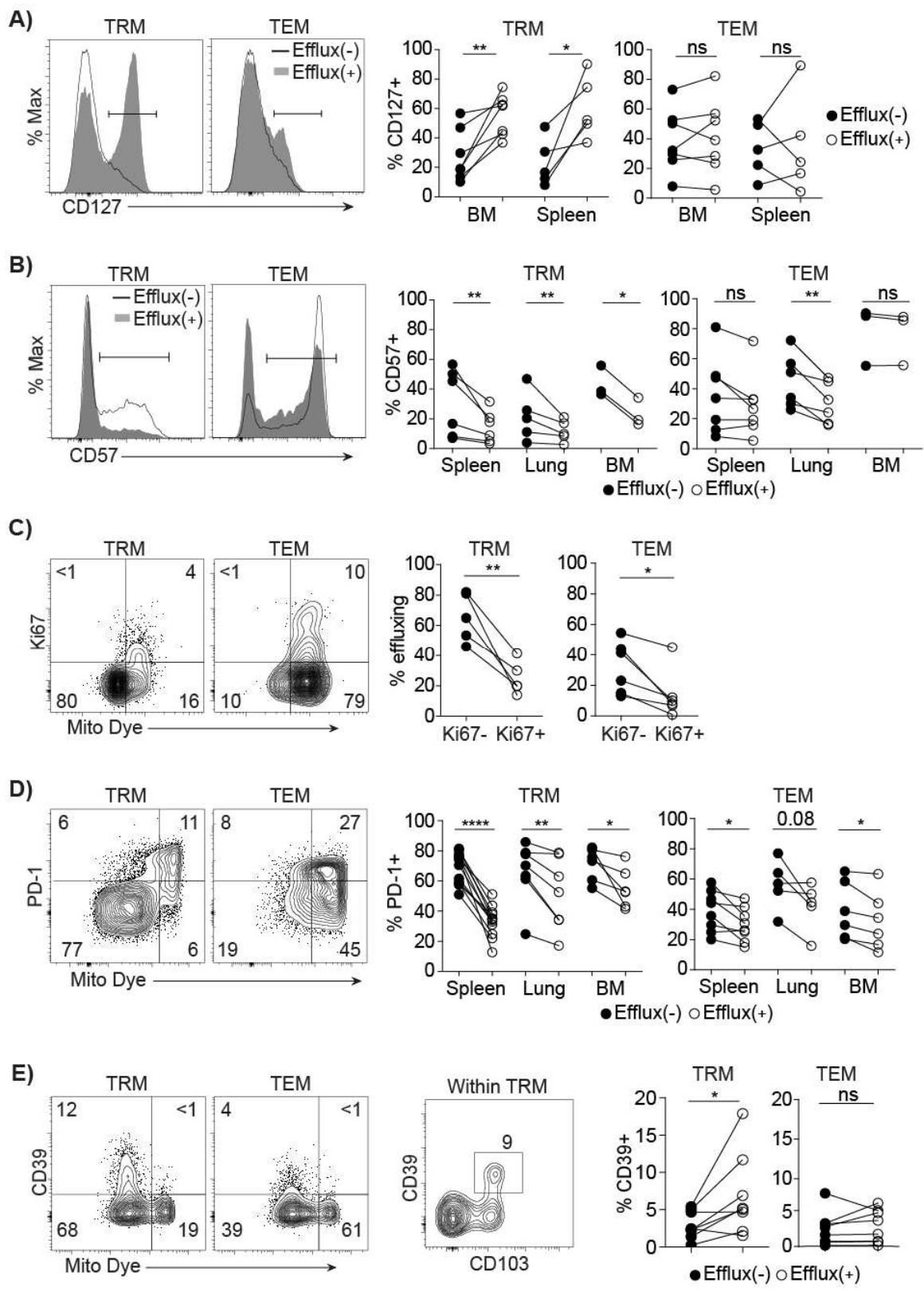
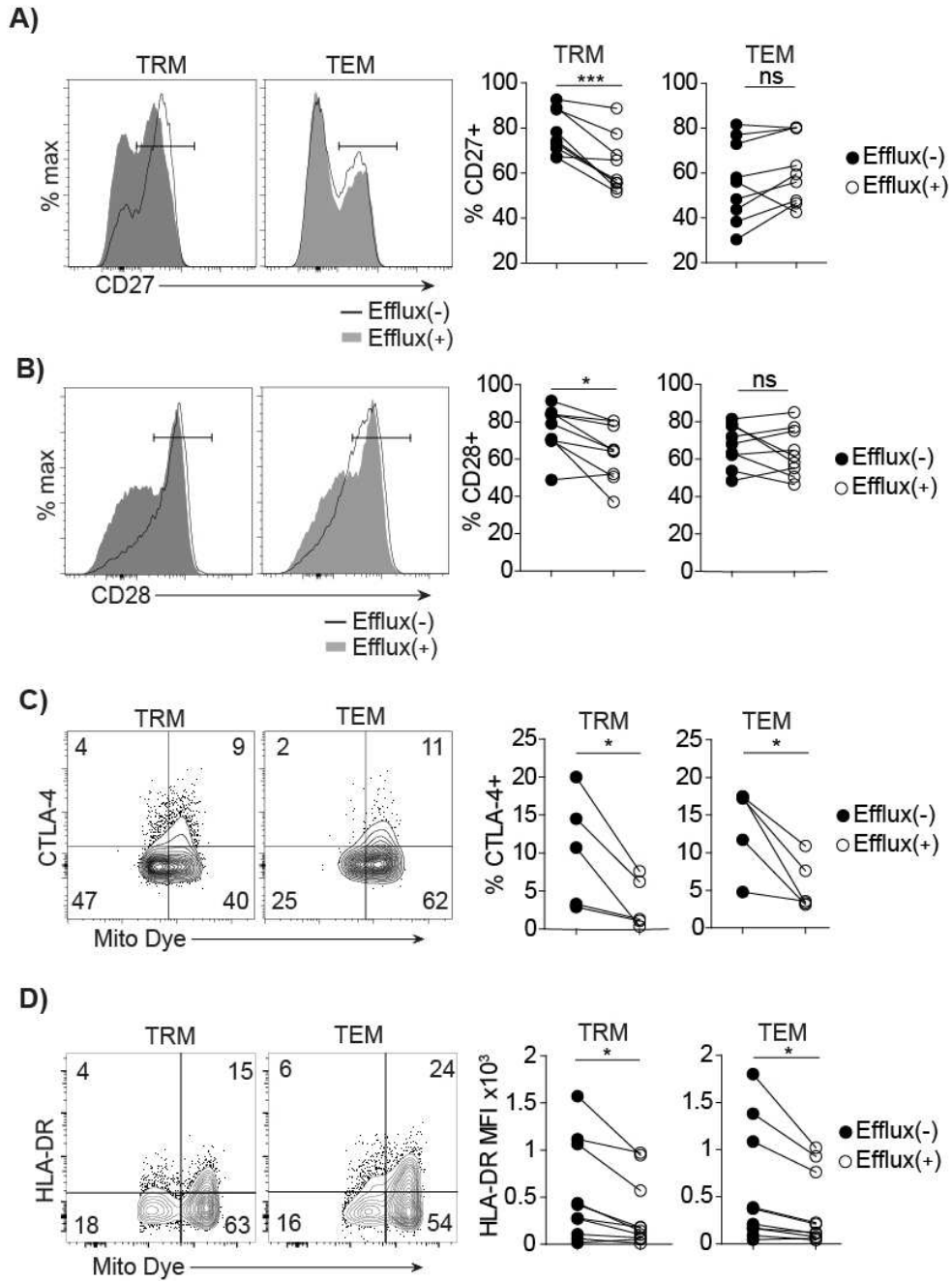


Figure 4.9. Additional phenotypic analysis of efflux(+) CD8⁺ TRM.

(A-B) TCR stimulation history assessed by costimulatory receptor downregulation. Left: Representative histograms of CD27 (A) and CD28 (B) expression in splenic CD8⁺ TRM. Right: Compiled frequencies of CD27⁺ (A) and CD28⁺ (B) cells within efflux(+) and efflux(-) subsets.

(C) Left: Expression of CTLA-4 by TRM and TEM subsets from the spleen of one representative donor. Right: Compiled expression of CTLA-4 in efflux(+) and efflux(-) TRM and TEM.

(D) Left: HLA-DR expression by efflux(+) and efflux(-) TRM and TEM from spleen. Right: Compiled HLA-DR expression by efflux(+) and efflux(-) TRM. * $p \leq 0.05$, *** $p \leq 0.001$, n.s. not significant. Paired T test.



The Transcriptional Response of TRM to TCR stimulation

A number of the genes differentially expressed by efflux(+) TRM at steady-state are closely linked to T cell function (Figure 4.6); therefore, to investigate the unique functional properties of efflux(+) TRM, we performed RNA-Seq after TCR stimulation. However, the transcriptional response of TRM as a whole to stimulation is not well-characterized. Therefore, we first analyzed how TRM respond transcriptionally to short-term 12-hour TCR stimulation before analyzing the individual response of efflux(+) TRM.

Applying the criteria for significance we found 1139 genes to be differentially expressed between stimulated and unstimulated TRM, with these genes showing consistent expression differences across donors (Figure 4.10A-B). Interestingly, more genes were downregulated (789 genes) than were upregulated (340 genes) following stimulation (Figure 4.10A-B). Notably, the number of differentially expressed genes is several fold higher than even the number of genes differentially expressed between memory and naïve T cell subsets [252] or the number genes differentially expressed between TRM and TEM in humans (Figure 4.10C) [186]. These data suggest that TRM are poised for a robust transcriptional response to stimulation on time scales as short as 12 hours.

The magnitude of the transcriptional response to stimulation raises the question is whether TRM lose TRM-like properties after stimulation, and in particular those properties which allow for tissue retention. To address this, we compared the genes that were differentially expressed following stimulations (from our current dataset) to the genes that are differentially expressed between TRM and TEM (using our previously published dataset in [186]). Interestingly, very few genes overlapped between these two datasets (Figure 4.10C), implying that transcriptional changes following stimulation are unrelated to the genes that define the TRM subset. Of the TRM defining

genes that changed following stimulation, the majority changed in a direction such that their expression moved farther away from TEM (Figure 4.10C), suggesting that if anything the TRM transcriptional program was further reinforced during stimulation. TRM are characterized by low expression of the homing receptors S1PR1 and CCR7 and reduced expression of the associated transcription factor KLF2, which together help TRM avoid egress cues [10, 139]. Following stimulation, CD8⁺ TRM further downregulated these genes (Figure 4.10D), implying that the migratory program of TRM is reinforced to allow these cells to carry out functions *in situ*. Taken together, these results suggest that while TRM undergo large transcriptional changes upon activation, these cells remain TRM and do not losing defining features of the subset.

Pathway analysis was done to interpret the biological significance of the transcriptional changes after stimulation. There was significant enrichment of pathways controlling cytokine responses, regulation of cell cycle/proliferation, and metabolism (Figure 4.10E), with the Sirtuin Signaling Pathway emerging as the top result (Figure 4.10E). Sirtuins are a family of NAD(+)-dependent protein deacylases that sense the cellular metabolic state and have critical roles in controlling metabolism, stress responses, and cell cycle progression/apoptosis [253]. The induction of cell cycle and metabolism-related pathways are indicative of a global remodeling of TRM homeostatic programs following TCR stimulation. Other genes related to T cell function and cytokine signaling were also differentially expressed following stimulation (Figure 4.10F), including a number of proinflammatory cytokines (*IL17F*, *LTA* (lymphotoxin alpha), and *IL13*) and the cytotoxic molecule *GZMB* (encoding granzyme B). TRM also upregulated a number of chemokines, consistent with their reported functions of recruiting leukocytes to the site of infection [114, 150, 151].

Figure 4.10. The transcriptional response of TRM to stimulation.

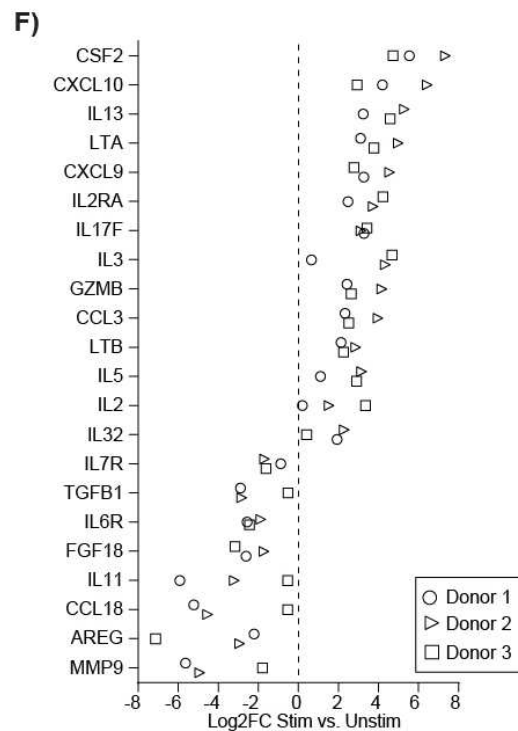
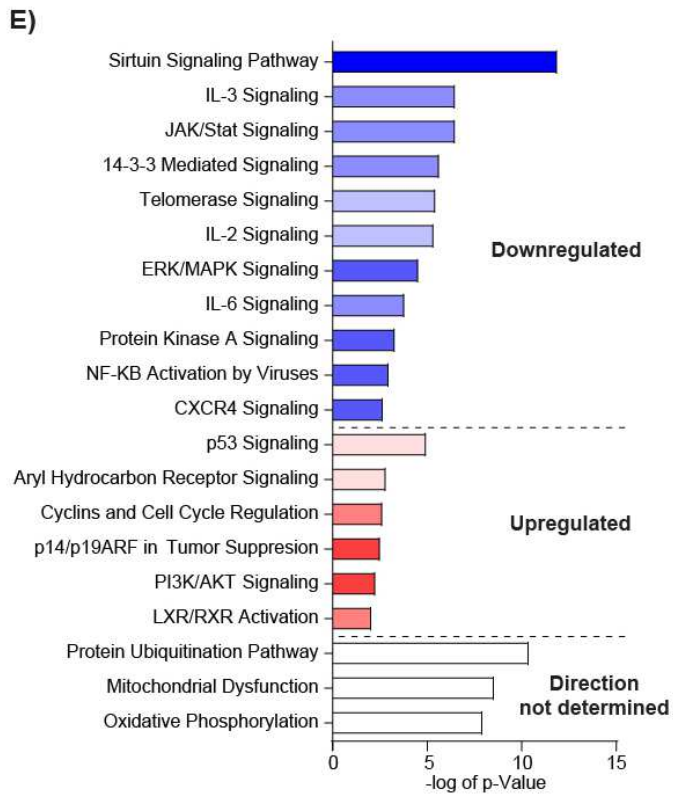
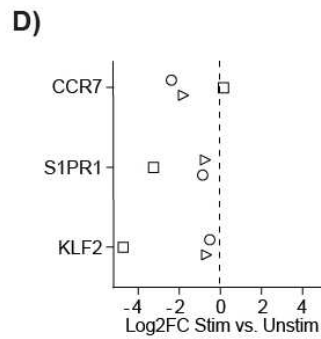
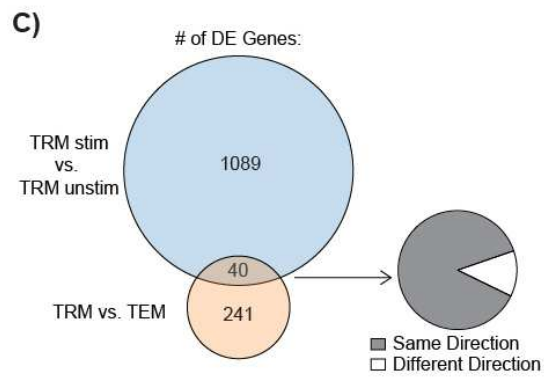
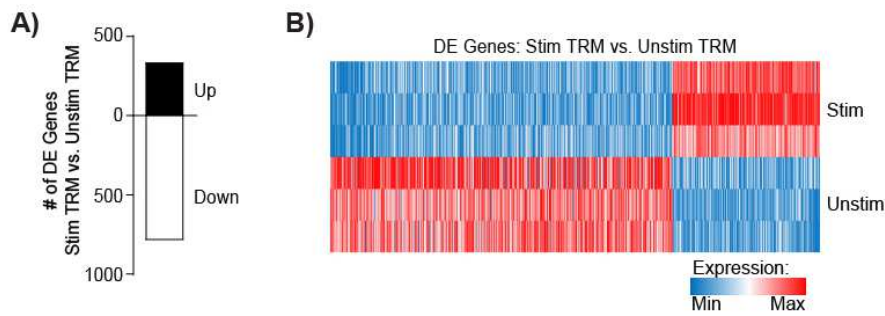
(A) Bar graph shows number differentially expressed (DE) genes when comparing unstimulated TRM with stimulated TRM. Genes upregulated after stimulation are displayed in black, and genes downregulated after stimulation are shown in white.

(B) Heatmap shows normalized expression of all 1129 differentially expressed genes, as assessed in A.

(C) TRM characteristics are preserved after stimulation. Venn diagram shows overlap between genes that are differentially expression when comparing stimulated vs. unstimulated TRM (current dataset) and genes that are differentially expressed when comparing human spleen CD8⁺ TRM and TEM (from Kumar et al., 2017). Pie chart on the right displays proportion of the overlapping genes that change in the same direction comparing stimulated vs. unstimulated TRM and when comparing human spleen CD8⁺ TRM and TEM.

(D) TRM downregulate egress receptors after stimulation. Plot shows log₂ fold changes of CCR7, S1PR1, and KLF2 when comparing stimulated vs. unstimulated TRM samples.

(E) IPA analysis. Select pathways that had significant p-values (≤ 0.01) are displayed. Direction of enrichment in stimulated samples is proportional to the color intensity of each bar. (F) Log₂ fold changes of select genes related to T cell function when comparing stimulated vs unstimulated TRM samples. Data from each donor is indicated by a unique shape, as indicated in the legend.



Transcriptional Response of efflux(+) TRM following TCR stimulation

To determine the contribution of efflux(+) and efflux(-) subsets to the TRM, we compared the gene expression profile of both of these subsets before and after TCR stimulation. Again, stimulated samples were transcriptionally distinct from unstimulated samples in all donors, for both efflux(+) and efflux(-) subsets (Figure 4.11A). Further, consistent with our steady state analysis (Figure 4.10), the transcriptional difference between stimulated and unstimulated samples was greater than the difference between efflux(+) and efflux(-) subsets, such that these two subsets were more transcriptionally similar to each other following stimulation than to their unstimulated precursors (Figure 4.11A). When comparing stimulated with unstimulated samples, 487 and 865 genes had significant differential expression in efflux(-) and efflux(+) subsets, respectively (Figure 4.11B). We then examined these genes to determine which, if any, were unique to the response of either subset. Interestingly, the majority of genes that showed differential expression between stimulated and unstimulated samples in either efflux(-) and efflux(+) subsets had a similar directionality and magnitude of fold change in the other subset, even if the threshold for significance was not met (Figure 4.11C). This suggested that the transcriptional response to stimulation was largely similar between the two subsets, a conclusion that is also supported by PCA analysis (Figure 4.11A). However, a several genes with significant changes in expression exhibited divergent upregulation/downregulation (Figure 4.11D). Of note, efflux(+), but not efflux(-), TRM upregulated expression of *ITGB8*, an integrin critical for local activation of latent TGF- β complexes on Tregs [254]. Efflux(+) TRM also upregulated expression of *TACRI*, encoding neurokinin-1-R, the receptor for substance P, a neuropeptide with a role in Type 17 responses that is potentiated by TGF- β signaling [255]. Taken together, these results implicate

TGF- β signaling and Type 17 responses as a critical node for function TRM that may be differentially regulated by efflux(+)/efflux(-) subsets.

We performed IPA analysis to identify pathways that were enriched when comparing stimulated and unstimulated samples, and stratified to identify those that were significant in either the efflux(+) or efflux(-) subset but not the other, or significant in both but having opposite directional changes (Figure 4.11E). TCR stimulation selectively induced AhR signaling in efflux(+) TRM, a pathway that integrates signals from environmental metabolites and regulates Th17 and Treg-type responses [256, 257]. Crucially, AhR expression is also required for persistence and survival of skin TRM [152]. Consistent with a role in conventional Type 1 responses, efflux(-) cells responded to TCR stimulation with elevated inflammatory HMGB1 signaling [258]. Interestingly, integrin signaling was significantly downregulated in efflux(-) TRM following stimulation (Figure 4.11E), suggesting a loss of certain adhesion properties that could facilitate re- entry into circulation or increased tissue mobility. Finally, a number of pathways related to cell cycle/proliferation as well as mitochondrial metabolism diverged following stimulation (Figure 4.11E), consistent with distinct proliferative and metabolic responses to stimulation. Taken together, these results indicate that although efflux(+) and efflux(-) TRM exhibit overlapping features to TCR stimulation, key differences in pathways related to the nature of the T cell response, including AhR, integrin, and Th17 signaling could mediate unique, non-redundant responses during TRM re-activation.

Figure 4.11. Dissecting the transcriptional response to stimulation by efflux status.

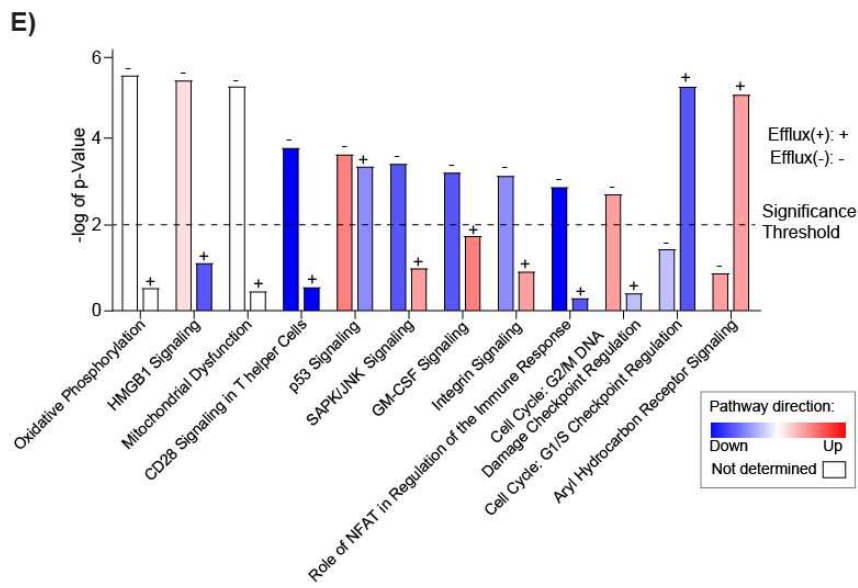
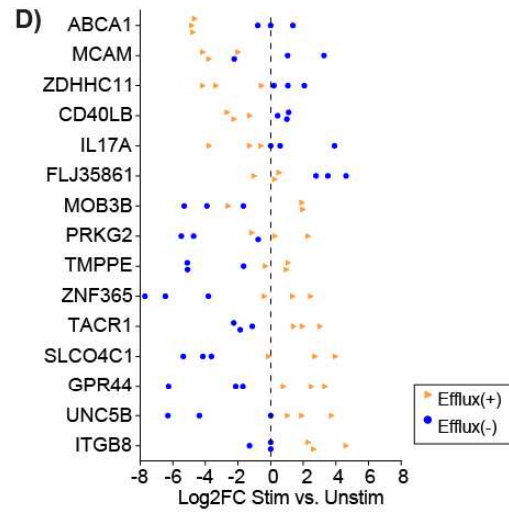
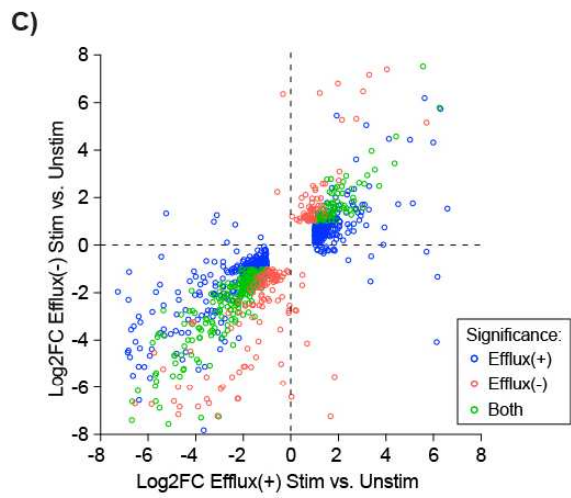
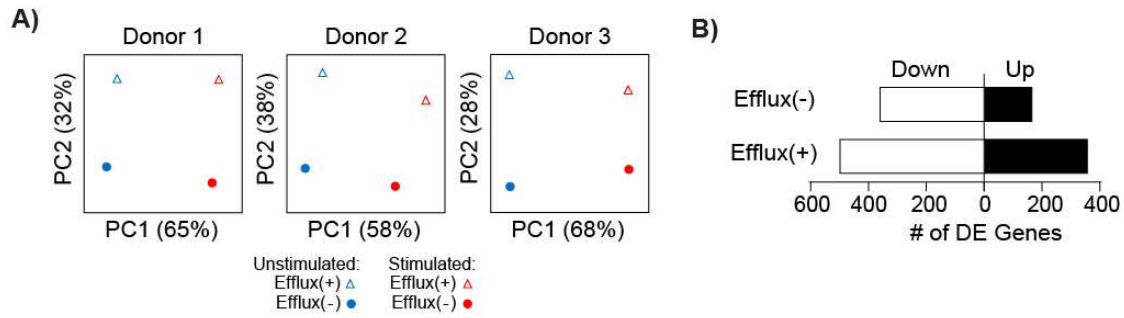
(A) PCA of efflux(+) and efflux(-) TRM from the spleen of 3 donors, based on the global transcriptome.

(B) Differential expression assessed by DESEQ2. Bar graph shows number of differentially expressed (DE) genes when comparing unstimulated and stimulated samples for both efflux(+) and efflux(-) TRM, as indicated.

(C) Scatterplot displays all genes found to have significant differential expression in stimulated vs unstimulated samples as in part B. Value on the X axis represents the log₂ fold change of the gene between stimulated vs unstimulated efflux(+) samples, and the Y axis represents the log₂ fold change of the same gene between stimulated vs unstimulated efflux(-) samples. Samples are color-coded by whether the differential expression was significant in efflux(+) TRM, efflux(-) TRM, or both.

(D) Log₂ fold changes of select genes when comparing expression stimulated vs. unstimulated samples, for both efflux(+) and efflux(-) TRM. Genes were selected by taking all of the genes in part C that has opposite direction changes for efflux(+) and efflux(-) samples after stimulation.

(E) Pathway analysis of the response to stimulation in efflux(+) and efflux(-) TRM. Genes that were differentially expressed between stimulated vs. unstimulated samples were uploaded to IPA, for both efflux(+) and efflux(-) TRM. Bar graph displays select pathways that were significant in efflux(+) or efflux(-) TRM but not the other group, or pathways that had opposite directional changes.



Distinct functional profile of efflux(+) TRM

Differential expression of key genes involved in the cell cycle and Ki67 protein suggested distinct proliferative capacities of efflux(+) and efflux(-) TRM. We sorted efflux(+) and efflux(-) TRM and then labeled with cell proliferation dye to monitor cell division following TCR stimulation. Efflux(+) memory cells were highly proliferative, and a majority underwent >4 divisions by day 4 post-stimulation (Figure 4.12A). Conversely, efflux(-) cells proliferated markedly less, with a large portion undergoing no divisions. TCR stimulation induces metabolic reprogramming and expression of key transcription factors such as IRF4 that regulate proliferation and effector cell differentiation [77-79]. Indeed, following TCR stimulation, both efflux(+) and efflux(-) TRM that proliferated expressed heightened levels of IRF4 (Figure 4.12B). However, while both TRM subsets upregulated IRF4, efflux(-) cells exhibited higher levels of the transcription factor across cell divisions compared with efflux(+) TRM. As IRF4 is associated with effector function, these results suggest that efflux(-) TRM may have heightened effector function following TCR stimulation.

In the skin, reciprocal expression of CCR6 and CD49a defines subsets of CD8⁺ TRM with heightened production of the inflammatory cytokine IL-17 or elevated cytotoxic potential, respectively [168]. We next assessed the capacity of efflux(+) and efflux(-) TRM to producing key cytokines following TCR stimulation. Efflux(+) and efflux(-) TRM were sorted from splenocytes and stimulated with anti-CD3/CD28/CD2 beads for 48 hours. Supernatants were then harvested and assayed for cytokine production (Figure 4.12C). Efflux(-) TRM produced more inflammatory cytokines including IFN- γ and TNF- α , as well as autocrine IL-2. Conversely, efflux(+) TRM produced more IL-17. Interestingly, levels of IL-10 production were comparable between the two subsets (Figure 4.12C). High levels of IFN- γ and TNF- α production suggested that efflux(-) TRM

are primed for activation at steady state. We next assessed the cytotoxicity of TRM subsets as measured by degranulation following PMA/ionomycin stimulation. Efflux(-) TRM exhibited a markedly higher rate of degranulation indicated by retention of CD107a (LAMP1) fluorescence compared to efflux(+) TRM (Figure 4.12D). Both efflux(+) and efflux(-) TEM exhibited equivalent, high levels of degranulation. Thus, efflux(+) TRM have a lower cytotoxic potential as well as decreased proinflammatory cytokine production.

T-box transcription factors, including T-bet and Eomes, regulate cytotoxicity and cytokine production, memory formation, and TRM development in CD8⁺ T cells [73] [106]. We assessed the expression of Eomes and T-bet in TRM and TEM efflux(+) subsets at steady state. While TEM subsets expressed comparable amounts of Eomes, efflux(-) TRM expressed higher levels of this transcription factor (Figure 4.13). Although TRM expressed distinctly less T-bet than TEM, we observed no significant difference between the efflux(+) and efflux(-) subsets (Figure 4.13). These results, along with our RNA-Seq analysis, suggest that dye efflux defines a transcriptionally distinct subset of TRM.

As efflux(+) TRM exhibit evidence of quiescence, we sought to determine whether heightened responses to IL-7 correlated with this functional profile. We sorted efflux(+) and efflux(-) TRM and then stimulated with IL-7 *ex vivo* before assessing phosphorylation of the transcription factor STAT5, a key effector of IL-7 signals [245]. We found that efflux(+) but not efflux(-) TRM responded to IL-7 with potent STAT5 phosphorylation, suggesting an increased capacity to respond to homeostatic cytokines important for memory cell longevity (Figure 4.12E).

Figure 4.12. Dye efflux marks functionally distinct subsets of TRM.

(A-B) Proliferative capacity of TRM subsets. Sorted efflux(+) and efflux(-) TRM were labeled with cell proliferation dye and stimulated with anti-CD3/CD28/CD2 beads. Proliferation was assessed on day 4 of culture. (A) Left: Histogram showing cell proliferation dye dilution at day 4. Results are representative of 4 independent experiments. Middle: Quantification of the percent of proliferating cells. Right: Quantification of the percent of proliferating cells at each division number. * $p \leq 0.05$. ** $p \leq 0.01$ **** $p \leq 0.0001$. Two way ANOVA with Sidak's multiple comparisons test. (B) Heightened IRF4 induction in efflux(-) TRM following TCR-stimulation. Left: Plots show cell proliferation dye dilution and IRF4 expression at day 4. Rectangular gate identifies activated, proliferating cells that have upregulated IRF4. Plots are representative of 3 independent experiments. Middle: Histogram shows IRF4 expression within proliferating cells from efflux(+) and efflux(-) subsets. Right: Quantification of IRF4 MFI amongst activated proliferating cells.

(C) Cytokine production following TCR stimulation. Efflux(+) and efflux(-) TRM were sorted and stimulated with anti-CD3/CD28/CD2 beads for 72 hours, and cytokines in supernatant were quantified using BD CBA.

(D) Cytotoxicity of efflux(+) and efflux(-) TRM subsets. Sorted cells were pulse labeled with CD107a antibody followed by PMA/ionomycin stimulation and flow cytometry analysis. Representative plots and quantification of CD107a+ cells within the indicated populations.

(E) Efflux(+) TRM exhibit increased responses to IL-7. Left: representative histogram of STAT5 phosphorylation following IL-7 stimulation ex vivo. Right: Quantification of %pSTAT5 positive cells amongst efflux(+) and efflux(-) TRM. * $p \leq 0.05$. ** $p \leq 0.01$. **** $p \leq 0.0001$. n.s. not significant. Paired T test.

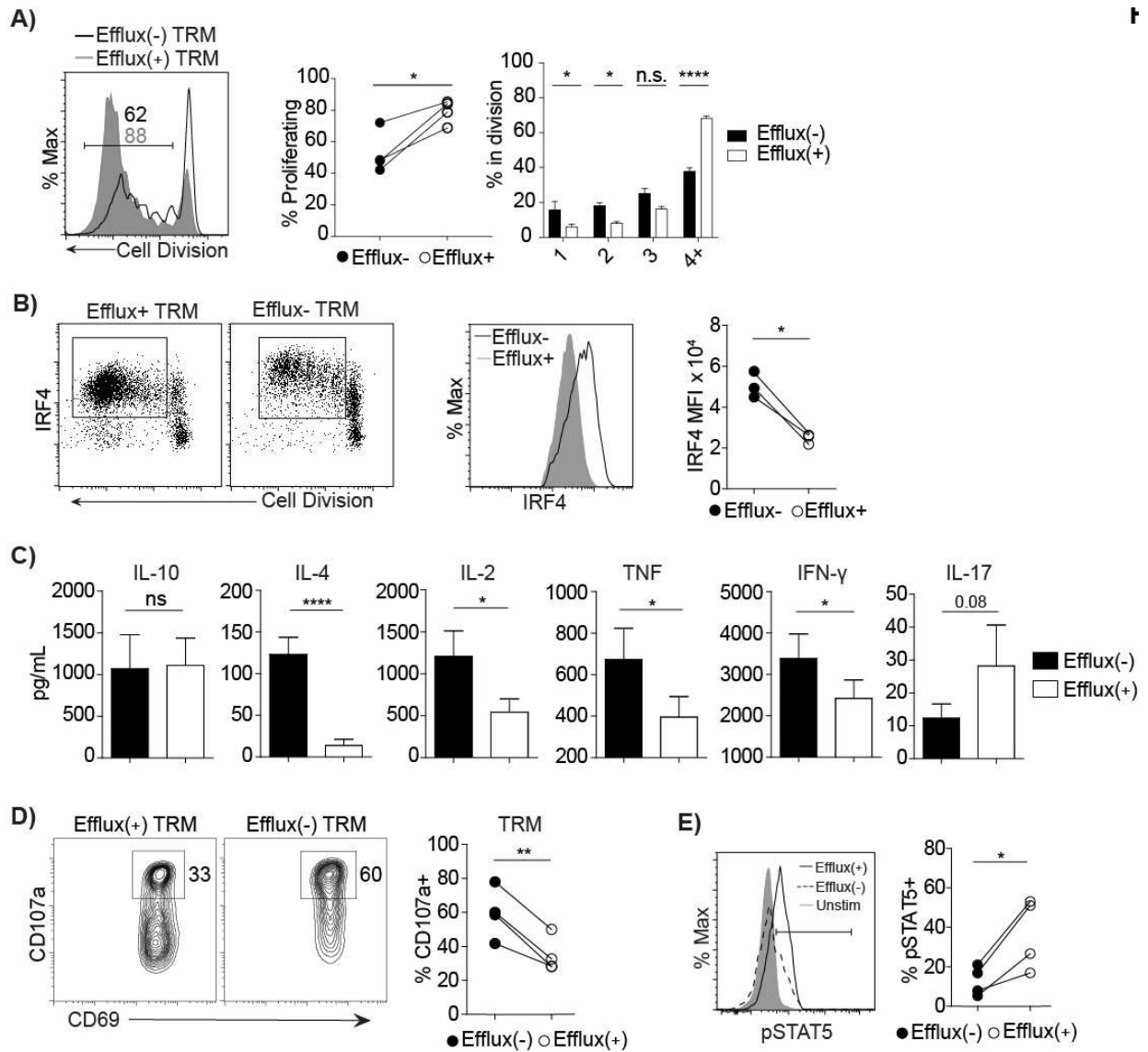
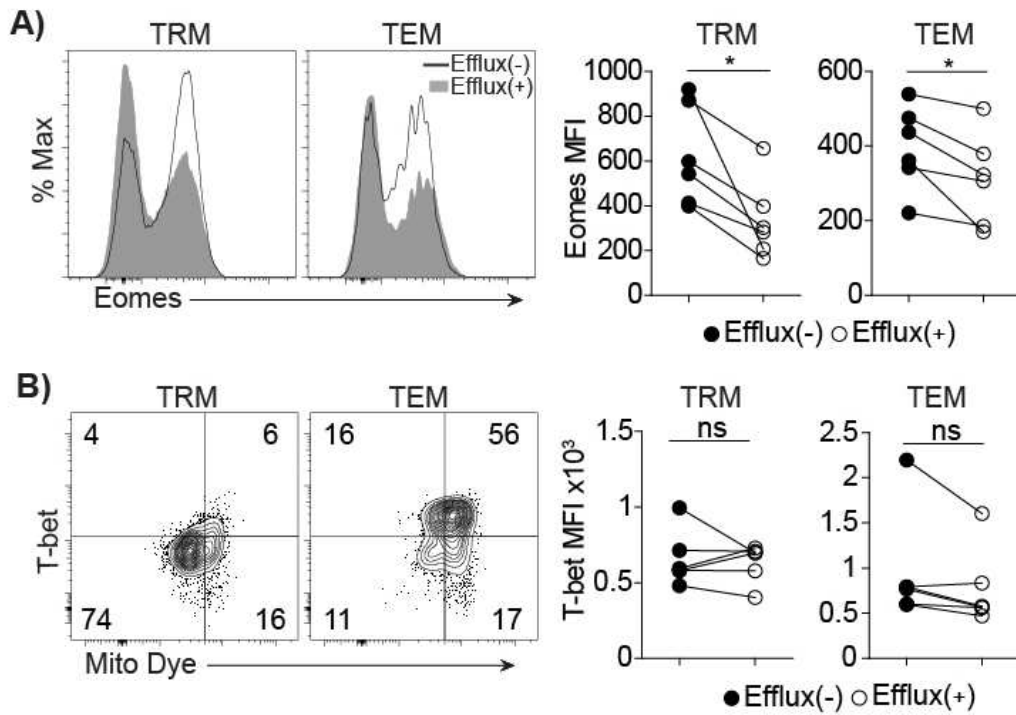


Figure 4.13. T-bet and Eomes expression

(A) Left: Histograms of Eomes expression by efflux(+) and efflux(-) TRM subsets from the spleen of one representative donor. Right: Quantification of Eomes MFI in indicated TRM/TEM subsets.

* $p \leq 0.05$.

(B) Left: T-bet expression in efflux(+) and efflux(-)TRM subsets from the spleen of one representative donor. Right: Quantification of T-bet MFI in indicated TRM subsets. n.s. not significant.



Section 4.3: Discussion

Subsets of memory T cells cooperate to maintain life-long immunity and exhibit unique functional, regulatory, and homing properties. Using healthy primary human tissues, we provide evidence for functional heterogeneity within the CD8⁺ TRM compartment. These subsets were identified by their differential capacity to efflux fluorescent dyes and could be readily extracted and sorted from a variety of tissues for downstream application. Critically, efflux(+) and efflux(-) subsets were functionally distinct, exhibiting key differences both at steady-state and following TCR stimulation. Efflux(+) cells differentially express transcription factors related to Type 1 and Type 17 inflammatory responses, including *Eomes*, *RORC*, and *RORA*, indicating that key regulators of lymphocyte cell fate decisions may also program distinct subsets of TRM. These TRM subsets also exhibited a reciprocal capacity for IFN- γ /TNF or IL-17 cytokine production as well as differential propensity toward degranulation. Given potential differences in TRM localization, this stratification of function suggests that TRM may be programmed toward distinct localized responses tailored to specific pathogens *in situ*.

It is unclear if efflux(+) and efflux(-) subsets can interconvert during physiological homeostasis and immune responses. Efflux(+) cells retain a higher proliferative potential following TCR stimulation and may constitute a resting pool of cells that repopulates the more effector-like efflux(-) subset to promote strong Type 1 inflammatory responses. In support of this, efflux(+) TRM had transcriptional and phenotypic features of quiescence and longevity, including expression of the immunomodulatory receptors CD39 and CD101, reduced expression of activation and exhaustion markers, and expression of genes involved in cell cycle control; efflux(+) TRM also exhibited increased responses to IL-7. Nevertheless, our results demonstrate

that a portion of TRM are not fully terminally differentiated and can undergo substantial proliferation during re-activation.

The stratification of function between TRM subsets suggests that cooperation may mediate complete immunity. Specifically, efflux(-) TRM may be primarily responsible for IFN- γ /TNF secretion and cytotoxic functions, while efflux(+) TRM may mediate Type 17 inflammation and serve as a proliferative reservoir to replenish the TRM compartment. However, transcriptional data also indicates substantial overlapping functions between the subsets, suggesting a model in which certain functions, e.g. IL-10 production, are universal properties of TRM, while others are primarily mediated by a specific TRM subset. The division of labor between TRM subsets may also be driven by subanatomic differences, as suggested by distinct adhesion molecule and migratory receptor expression. Further studies will be necessary to fully determine how TRM subsets cooperate to achieve full immunity.

Our analysis of transcriptional responses to TCR stimulation have implications for TRM biology as a whole. TRM preserve their core profile while undergoing a massive and rapid transcriptional response to TCR stimulation. In fact, TRM further downregulated already low levels of egress receptors like S1PR1 and CCR7, suggesting a reinforcement of tissue retention properties to enforce *in situ* responses to stimulation. Overall, these properties establish TRM as a subset designed for rapid response to pathogens and whose function is exclusively meant to be carried out within the tissue.

Efflux pumps expel of toxic xenobiotics from the cell interior and have been implicated in the persistence of human lymphocytes during chemotherapy [190]. TRM persist in peripheral tissue sites for years or even decades, where they are exposed to a range of foreign agents, particularly in sites such as skin and lung. Given our data that efflux(+) TRM show evidence

quiescence and longevity, heightened expression of functional drug efflux pumps could be crucial for TRM survival and homeostasis in these peripheral tissues. Furthermore, this trait also presents the possibility of therapies that specifically target efflux(+) TRM, as efflux capacity may mediate differential susceptibility to chemotherapy and drug treatments [259]. Given that efflux(+) TRM exhibit increased IL-17 production as well as Th17-associated signaling, specifically targeting efflux(+) cells in psoriasis might be an optimal therapy that spares protective TRM while eliminating pathogenic TRM. Previously, there has been interest in the possibility of “targeted” immune therapies that specifically modulate either TRM or circulatory T cells while leaving other aspects of the immune system undisturbed [121]. Our data suggest that this specificity can be taken further to target specific TRM subsets. Overall, the identification of these distinct subsets could be leveraged toward next generation therapies for infection, cancer, and autoimmunity.

CHAPTER 5: Conclusions

Defining Core Properties of Human TRM

Tissue resident memory T cells (TRM) have been the subject of intense research recently due to a number of reports that these cells offer superior protection compared with other memory subsets [10, 102]. TRM are generated in response to infection at many tissue sites, from which they do not recirculate and remain poised to mediate rapid pathogen clearance [10, 102]. In fact, upon secondary infection TRM are able to clear pathogens without any contribution from circulatory T cells or antibodies. Protective TRM have also been generated in response to vaccination [116, 117], suggesting an immunization strategy to protect against pathogens for which traditional antibody based vaccines have failed. Finally, TRM have been implicated as the drivers of many human illnesses, particularly skin diseases like psoriasis and mycosis fungoides [121].

While these properties make TRM an attractive target for clinical modulation, many gaps exist in our knowledge of human TRM. While TRM have been identified in human tissues, the majority of studies characterizing TRM have been performed in mice. In particular, unifying properties of TRM in humans have not been determined, largely due to the difficulty of obtaining human tissues. Reliable phenotypic markers of TRM in humans have not been established, and it is not known which phenotypic properties allow TRM to maintain tissue retention in humans. The defining transcriptional and functional characteristics that separate TRM from other memory subsets in humans is not known, as well as how these properties vary for CD4⁺ and CD8⁺ TRM and for TRM from different tissues. Finally, the majority of studies in both mice and humans focus on CD8⁺ TRM, meaning that little is known about CD4⁺ TRM in humans.

To address these knowledge gaps, the goal of my current research was to define universal signatures of human TRM and to investigate heterogeneity within human TRM. As TRM are not found in blood, a major barrier to progress in the field has been access to human tissues. Via a novel collaboration with LiveOnNY, the local organ procurement agency, our laboratory is able to obtain >15 tissues from healthy organ donors of all ages. Investigation of blood and 8 additional tissue sites including barrier (lung, intestine), lymphoid (spleen, tonsils, multiple lymph nodes), and exocrine (salivary glands) revealed that CD69 was expressed by CD4⁺ and CD8⁺ memory T cells in tissues but not in blood. CD103 expression, however, was limited primarily to CD8⁺ memory T cells in barrier tissues. A number of other recent studies examining memory T cells in human tissues have confirmed this distribution of CD69 and CD103 expression [14, 157, 158, 163, 164, 185, 260-262]. Coupled with the result that CD69⁺ cells did not show features of activation, these data establish CD69 as the primary marker distinguishing circulatory from tissue memory T cells.

We performed transcriptional, phenotypic, and functional analysis to determine if CD69 identifies TRM in humans and to establish core properties of the TRM subset. RNA-Seq analysis revealed that CD69⁺ memory T cells from tissues shared key transcriptional homologies to mouse TRM and were transcriptionally distinct from CD69⁻ memory T cells. Further, CD69⁻ memory T cells from tissues were transcriptionally similar to memory T cells found in the blood, suggesting that the CD69⁻ in tissues represented circulatory cells. Finally, CD69⁺ memory T cells expressed many canonical TRM features, including transcriptional downregulation of S1PR1 and KLF2 and elevated surface expression of CD49a. Taken together, these results suggest that CD69 expression reliably distinguishes resident from circulatory memory T cells in human tissues.

We analyzed transcriptional data from TRM and TEM subsets from spleen, lung, and blood to establish a core signature of 31 genes that defined human TRM for both CD4⁺ and CD8⁺ subsets across tissues. Notably, this core signature was also preserved when examining transcriptional data from mouse studies, suggesting that it represented universal properties of the TRM subset. This core signature included differential expression of genes that controlled adhesion and migration, which may promote tissue retention, genes involved in T cell function, and finally a number of genes involved in inhibition of T cell function or control of proliferation. We confirmed the expression of many of these at the protein level via flow cytometry. Interestingly, TRM had elevated expression of PD-1, reduced turnover as measured by Ki67, and an enhanced ability to produce IL-10 compared with TEM. Notably, another recent study comparing CD8⁺CD103⁺ lung TRM to blood TEM similarly found that TRM upregulate transcripts encoding TNF, IFN- γ , and granzyme B [142], while simultaneously expressing high levels of PD-1, LAG-3, and CTLA-4. Another study from the same group examining CD4⁺ TRM from human lung also found similar results [263]. We propose that these dual protective and regulatory capabilities are critical for long term maintenance; TRM exist in a quiescent state to promote longevity, have anti-inflammatory/regulatory function to prevent unnecessary activation and tissue damage, but also retain the ability to respond quickly upon pathogen invasion.

Overall these results establish TRM as a distinct memory subset in humans, with unique features to maintain long-term tissue residency. Interestingly, we found that TRM from different tissues sites were similar, and also found many similarities between CD4⁺ and CD8⁺ TRM. This suggests a universal TRM program that is engaged to prevent tissue egress. In the absence of specific targeting features, this reinforces a model in which early effectors enter the tissue during inflammation and engage a TRM program that then promotes residency and prevents exit into the

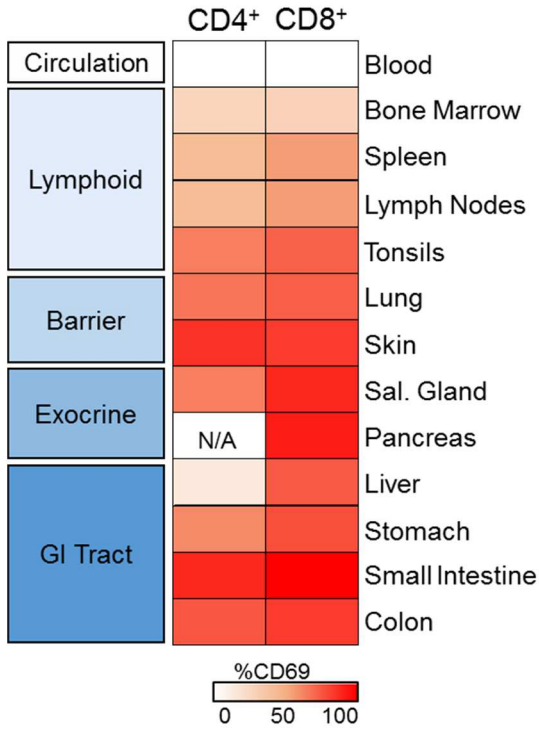
circulation, regardless of the tissue site. This idea is consistent with mice studies examining early TRM development (discussed in Chapter 1). These universal features also suggest that master transcriptional regulators of the human TRM program exist, although these are the subject of future research. Targeting these master regulators or other conserved TRM features may represent a strategy for clinical modulation of TRM and may drive future TRM-based vaccines.

Figure 5.1. Distribution and characteristics of TRM in human tissues.

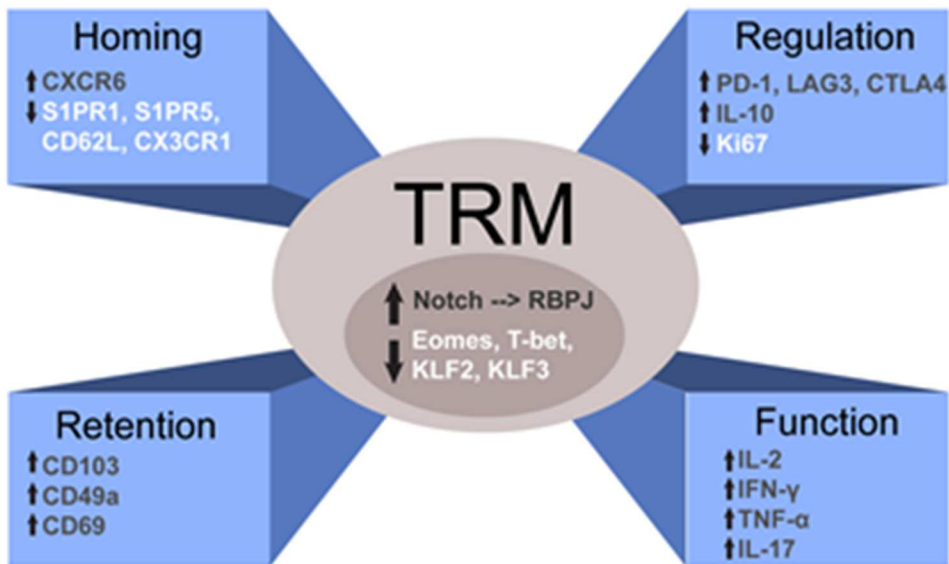
(A) Tissue-resident memory T cells (TRM) are localized to several tissues in humans, and can be distinguished from circulating memory T cells by expression of CD69. Heatmap shows the fraction of memory T cells that express CD69 in specific human tissue sites analyzed.

(B) Unique characteristics of TRM in humans. TRM cells have a unique profile of transcription factor expression, surface expression of homing receptors and adhesion markers to maintain tissue residency, and a distinct functional profile with increased expression and ability to secrete both pro and anti-inflammatory cytokines. TRM also upregulate a number of inhibitory genes and exhibit reduced proliferative turnover compared to circulating memory T cell counterparts.

A.



B.



Defining Heterogeneity within Human TRM

Having established core features of TRM that are preserved across tissues and subsets, we decided to investigate TRM heterogeneity based on the ability to efflux fluorescent dyes. Emerging evidence suggests that TRM as a whole comprise multiple, functionally distinct subsets that may play unique roles in protection and/or immunopathology [133, 155, 168]. These TRM subsets have typically been identified based phenotypic markers. However, it is not known if TRM with the ability to efflux fluorescent dyes exist across human tissues. This question is important because the ability to efflux fluorescent dyes is associated with longevity and stem-like properties in hematopoietic cells [187, 188], and recent evidence suggests that T cells exist with the ability to efflux dyes that have unique properties [230].

We identify a population of CD8⁺ memory T cells with the ability to efflux fluorescent dyes in multiple tissues including spleen, lymph nodes, bone marrow, lung, and blood. Notably the TRM fraction within tissues contained a higher proportion of efflux(+) cells than other memory subsets. Phenotypic and RNA-Seq analysis of efflux(+) and efflux(-) TRM suggested that efflux(+) cells are a unique subset programmed for quiescence and longevity within tissues. Efflux(+) had elevated surface expression of CD127, expressed a number of genes associated with cell cycle control, expressed immunoregulatory markers (CD101, CD39), and had decreased expression of exhaustion and activation markers (CTLA-4, PD-1, CD57, HLA-DR) and decreased turnover. Further, efflux(+) TRM had a unique profile of adhesion and migration markers suggesting an improved ability for tissue retention, including increased expression of CD49a and decreased expression of S1PR1.

Following stimulation, TRM underwent massive transcriptional changes that were largely similar in both efflux(+) and efflux(-) subsets. However, there were notably differences in the

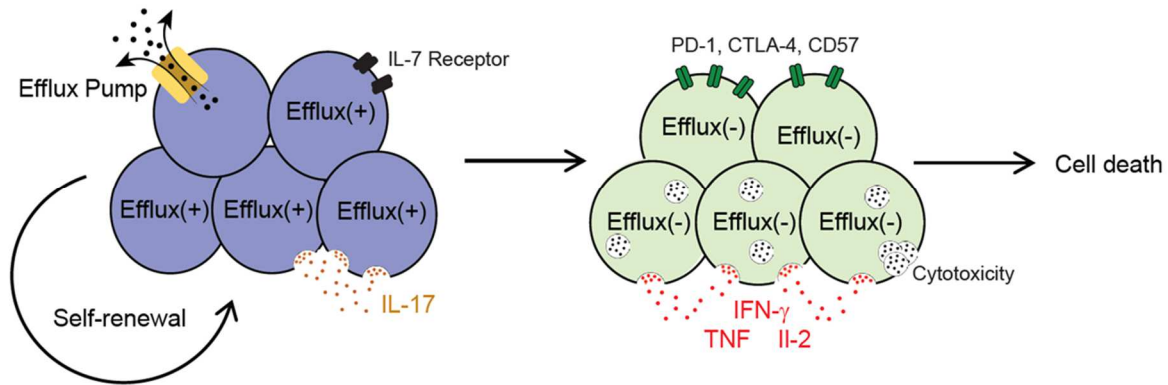
response to stimulation suggesting certain non-redundant functions of these subsets. After TCR stimulation, efflux(+) TRM produced less pro-inflammatory cytokines and underwent less cytotoxic degranulation compared with efflux(-) TRM. Moreover, efflux(+) TRM retained a higher proliferative capacity and exhibited greater responses to IL-7. Notably, efflux(+) also had an enhanced capacity for IL-17 production and showed evidence of aryl hydrocarbon receptor and Th17-associated signaling transcriptionally. Conversely, efflux(-) TRM had decreased integrin signaling and elevated Type 1 inflammatory responses following TCR stimulation. Overall, these results suggest efflux(+) TRM maintain a reservoir capable of proliferation via a program for longevity and tissue retention, while efflux(-) TRM exhibit heightened effector function for generating rapid pro-inflammatory and cytotoxic responses.

Our data suggests cooperation between TRM subsets to achieve complete immunity. Specifically our data suggests that efflux(-) TRM may be primarily responsible for IFN- γ and TNF secretion and cytotoxic functions, while efflux(+) TRM may mediate IL-17 responses and possess immunomodulatory function and proliferative capabilities. However, our transcriptional data also indicates substantial overlapping functions between these two subsets. Further, we found no differences in IL-10 production by these two subsets, suggesting that this anti-inflammatory property may be common to all TRM subsets. Overall, this suggest a model in which certain functions are split between efflux(+) and efflux(-) TRM and in which these two subsets cooperate to achieve full immunity (Figure 5.2). This division of labor may be driven by anatomic differences, as efflux(+) and efflux(-) TRM have notable differences in their expression of adhesion and migration markers. Additional studies are needed to fully determine how TRM subsets cooperate to achieve full immunity.

Previous studies have highlighted the possibility of “targeted” immune therapies that only modulate TRM while leave other aspects of the immune system undisturbed. Our data suggest that this specificity can be taken one step further and that therapies should modulate a specific TRM subset. For example, efflux(+) TRM have a superior ability to produce IL-17 than efflux(-) TRM, and transcriptionally efflux(+) cells upregulate IL17A and other genes associated with IL-17 signaling. This suggests that specifically targeting efflux(+) subset in psoriasis might be an optimal therapy that spares protective TRM while eliminating pathogenic TRM.

Figure 5.2. Proposed cooperativity of TRM subsets.

Our data suggests a model in which efflux(+) and efflux(-) TRM cooperate to mediate immunity. Specifically, efflux(+) TRM represent a subset with greater self renewal capacity. Upon stimulation efflux(+) TRM give rise to both more efflux(+) TRM as well as efflux(-) TRM. The efflux(-) TRM are primarily responsible for viral clearance and may die following infection. Functionally, the efflux(-) are responsible for the bulk of effector cytokine production while efflux(+) TRM are capable of producing IL-17.



Perspectives and outstanding questions

The current research provides two main advances to the TRM field. First, we define universal properties of the TRM subset through simultaneous transcriptional and phenotypic analysis of TRM from multiple tissues and of both CD4⁺ and CD8⁺ lineages. Such a coordinate analysis of multiple TRM subsets had not previously been performed and establishes core features of the dominant memory subset in human tissues. Our core signature may have unique applications for identification of TRM, such as using the gene set to identify TRM in single cell sequencing experiments. Second, we identify a distinct TRM subset not based on a phenotypic marker, but based on the ability to efflux dyes. Importantly, our data puts forth a new model in which TRM subsets cooperate to mediate full immunity. Our data also suggests the potential for a more stem-like TRM that replenishes TRM mediating effector functions. Overall, we establish both core- and subset-specific properties of human TRM (Figure 5.3).

Many outstanding questions remain in the field of TRM. One critical question is the developmental relationship between TRM and other T cell subsets. Similar to recent work that has been done in humans with naïve and certain memory subsets [99-101], epigenetic profiling of TRM compared with other T cell subsets will be critical for establishing the lineage relationships between TRM and other subsets. It is also not known whether TRM have the ability to proliferate *in vivo* in response to infection or if TRM represent a terminally differentiated subset. Our results suggest that TRM retain proliferative capacity, or at least that certain subsets of TRM do. This raises questions about what happens to TRM after stimulation: do TRM remain TRM or do they differentiate into other subsets?

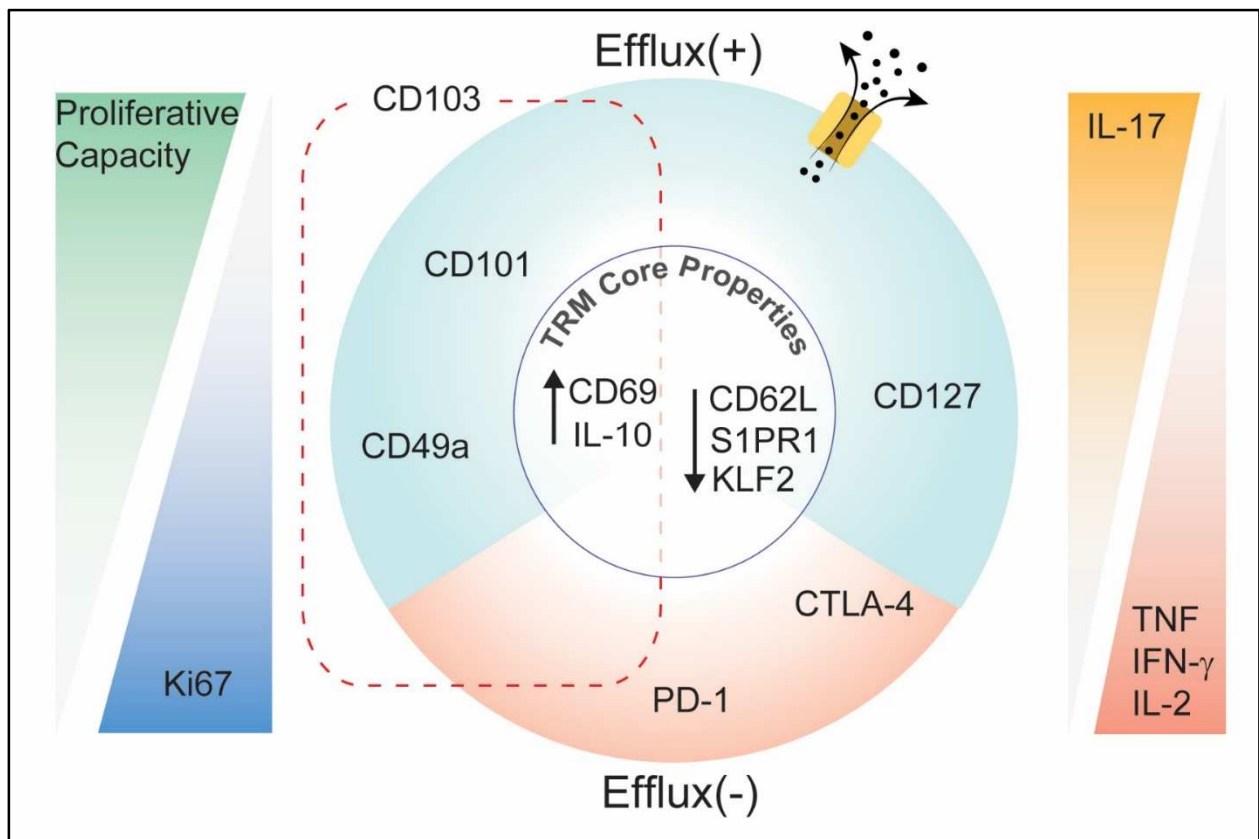
As discussed above, the fact that core features emerge when studying TRM from different sites and across multiple studies suggests a dominant transcriptional program that is engaged to

prevent tissue egress and promote tissue residency. However, it is not known which transcriptional regulators control TRM development in humans. Unlike in mice, evidence does not support a role for Hobit in human TRM development. Human TRM exhibit reduced expression of KLF2, Eomes, and T-bet [142, 186, 263], and downregulation of these transcription factors is required for TRM formation in mice [106, 139]. This suggests that many genes are shut off in the TRM program, consistent with our data that more genes are downregulated than upregulated by TRM compared with circulating memory T cell subset [186]. However, an important question is what transcriptional regulators are upregulated and promote TRM development and maintenance. One potential candidate is RPBJ, as suggested by our data [186] and studies from another laboratory [142]. Overall, an important area of future research is identifying key transcriptional regulators of human TRM development and maintenance.

Dissecting TRM heterogeneity will be a critical area for future research. Initial studies treated TRM as a uniform subset that was distinct from TEM/TCM. However, recent research from our laboratory and others has shown that the TRM compartment is comprised of many functionally distinct TRM subsets. This suggests a model where TRM is an umbrella term encompassing all tissue-retained T cells rather than being a single subset itself. In this model, many distinct TRM subsets are retained within the tissue and the sum of all of their functions mediates complete tissue immunity. Therefore, future studies will need to move beyond treating TRM as one subset to determine the unique role of multiple tissue-retained subsets.

Figure 5.3 Human TRM have core and subset-specific properties.

Our studies have identified both core and subset-specific properties of human TRM. Core features are represented in the middle white circle. Subset specific phenotypic properties are shown on the top (efflux(+)) TRM) and on the bottom (efflux(-)) TRM). Distinct functional and proliferative capabilities are shown on the sides.



REFERENCES

1. Gourley, T.S., et al., *Generation and maintenance of immunological memory*. *Semin Immunol*, 2004. **16**(5): p. 323-33.
2. Kaech, S.M. and E.J. Wherry, *Heterogeneity and cell-fate decisions in effector and memory CD8+ T cell differentiation during viral infection*. *Immunity*, 2007. **27**(3): p. 393-405.
3. Cohen, I.R., *Activation of benign autoimmunity as both tumor and autoimmune disease immunotherapy: a comprehensive review*. *J Autoimmun*, 2014. **54**: p. 112-7.
4. Rosenberg, S.A., *Decade in review-cancer immunotherapy: entering the mainstream of cancer treatment*. *Nat Rev Clin Oncol*, 2014. **11**(11): p. 630-2.
5. Evans, C.J., et al., *Place and cause of death in centenarians: a population-based observational study in England, 2001 to 2010*. *PLoS Med*, 2014. **11**(6): p. e1001653.
6. Farber, D.L., N.A. Yudanin, and N.P. Restifo, *Human memory T cells: generation, compartmentalization and homeostasis*. *Nat Rev Immunol*, 2014. **14**(1): p. 24-35.
7. Lefrancois, L. and D. Masopust, *T cell immunity in lymphoid and non-lymphoid tissues*. *Curr Opin Immunol*, 2002. **14**(4): p. 503-8.
8. Thome, J.J. and D.L. Farber, *Emerging concepts in tissue-resident T cells: lessons from humans*. *Trends Immunol*, 2015. **36**(7): p. 428-35.
9. Zens, K.D., T. Connors, and D.L. Farber, *Tissue compartmentalization of T cell responses during early life*. *Semin Immunopathol*, 2017.
10. Mueller, S.N. and L.K. Mackay, *Tissue-resident memory T cells: local specialists in immune defence*. *Nat Rev Immunol*, 2016. **16**(2): p. 79-89.
11. Clark, R.A., *Skin-resident T cells: the ups and downs of on site immunity*. *J Invest Dermatol*, 2010. **130**(2): p. 362-70.
12. Ganusov, V.V. and R.J. De Boer, *Do most lymphocytes in humans really reside in the gut?* *Trends Immunol*, 2007. **28**(12): p. 514-8.
13. Granot, T., et al., *Dendritic Cells Display Subset and Tissue-Specific Maturation Dynamics over Human Life*. *Immunity*, 2017. **46**(3): p. 504-515.
14. Gordon, C.L., et al., *Tissue reservoirs of antiviral T cell immunity in persistent human CMV infection*. *J Exp Med*, 2017. **214**(3): p. 651-667.
15. Thome, J.J., et al., *Longterm maintenance of human naive T cells through in situ homeostasis in lymphoid tissue sites*. *Sci Immunol*, 2016. **1**(6): p. aah6506.
16. Thome, J.J., et al., *Early-life compartmentalization of human T cell differentiation and regulatory function in mucosal and lymphoid tissues*. *Nat Med*, 2016. **22**(1): p. 72-7.
17. Sathaliyawala, T., et al., *Distribution and compartmentalization of human circulating and tissue-resident memory T cell subsets*. *Immunity*, 2013. **38**(1): p. 187-97.
18. Thome, J.J.C., et al., *Spatial Map of Human T Cell Compartmentalization and Maintenance over Decades of Life*. *Cell*, 2014. **159**: p. 814-828.
19. Carpenter, D.J., et al., *Human immunology studies using organ donors: impact of clinical variations on immune parameters in tissues and circulation*. *Am J Transplant*, 2017.
20. Takahama, Y., *Journey through the thymus: stromal guides for T-cell development and selection*. *Nat Rev Immunol*, 2006. **6**(2): p. 127-35.
21. Qi, Q., et al., *Diversity and clonal selection in the human T-cell repertoire*. *Proc Natl Acad Sci U S A*, 2014. **111**(36): p. 13139-44.
22. Hori, S., T. Nomura, and S. Sakaguchi, *Control of regulatory T cell development by the transcription factor Foxp3*. *Science*, 2003. **299**(5609): p. 1057-61.
23. Watanabe, N., et al., *Hassall's corpuscles instruct dendritic cells to induce CD4+CD25+ regulatory T cells in human thymus*. *Nature*, 2005. **436**(7054): p. 1181-5.
24. Seddiki, N., et al., *Persistence of naive CD45RA+ regulatory T cells in adult life*. *Blood*, 2006. **107**(7): p. 2830-8.

25. Germain, R.N., *T-cell development and the CD4-CD8 lineage decision*. Nat Rev Immunol, 2002. **2**(5): p. 309-22.
26. Klein, L., et al., *Positive and negative selection of the T cell repertoire: what thymocytes see (and don't see)*. Nat Rev Immunol, 2014. **14**(6): p. 377-91.
27. Burt, T.D., *Fetal regulatory T cells and peripheral immune tolerance in utero: implications for development and disease*. Am J Reprod Immunol, 2013. **69**(4): p. 346-58.
28. Haynes, B.F., et al., *Early events in human T cell ontogeny. Phenotypic characterization and immunohistologic localization of T cell precursors in early human fetal tissues*. J Exp Med, 1988. **168**(3): p. 1061-80.
29. Cupedo, T., et al., *Development and activation of regulatory T cells in the human fetus*. Eur J Immunol, 2005. **35**(2): p. 383-90.
30. Michaelsson, J., et al., *Regulation of T cell responses in the developing human fetus*. J Immunol, 2006. **176**(10): p. 5741-8.
31. Dalmaso, A.P., et al., *Studies on the Role of the Thymus in Immunobiology; Reconstitution of Immunologic Capacity in Mice Thymectomized at Birth*. J Exp Med, 1963. **118**: p. 1089-109.
32. Sakaguchi, S., T. Takahashi, and Y. Nishizuka, *Study on cellular events in postthymectomy autoimmune oophoritis in mice. I. Requirement of Lyt-1 effector cells for oocytes damage after adoptive transfer*. J Exp Med, 1982. **156**(6): p. 1565-76.
33. Sakaguchi, S., et al., *Immunologic self-tolerance maintained by activated T cells expressing IL-2 receptor alpha-chains (CD25). Breakdown of a single mechanism of self-tolerance causes various autoimmune diseases*. J Immunol, 1995. **155**(3): p. 1151-64.
34. Mancebo, E., et al., *Longitudinal analysis of immune function in the first 3 years of life in thymectomized neonates during cardiac surgery*. Clin Exp Immunol, 2008. **154**(3): p. 375-83.
35. Wells, W.J., et al., *Neonatal thymectomy: does it affect immune function?* J Thorac Cardiovasc Surg, 1998. **115**(5): p. 1041-6.
36. Prelog, M., et al., *Thymectomy in early childhood: significant alterations of the CD4(+)CD45RA(+)CD62L(+) T cell compartment in later life*. Clin Immunol, 2009. **130**(2): p. 123-32.
37. van den Broek, T., et al., *Neonatal thymectomy reveals differentiation and plasticity within human naive T cells*. J Clin Invest, 2016. **126**(3): p. 1126-36.
38. Silva, S.L., et al., *Autoimmunity and allergy control in adults submitted to complete thymectomy early in infancy*. PLoS One, 2017. **12**(7): p. e0180385.
39. Silva, S.L., et al., *Human naive regulatory T-cells feature high steady-state turnover and are maintained by IL-7*. Oncotarget, 2016. **7**(11): p. 12163-75.
40. Bennett, C.L., et al., *The immune dysregulation, polyendocrinopathy, enteropathy, X-linked syndrome (IPEX) is caused by mutations of FOXP3*. Nat Genet, 2001. **27**(1): p. 20-1.
41. Stritesky, G.L., S.C. Jameson, and K.A. Hogquist, *Selection of self-reactive T cells in the thymus*. Annu Rev Immunol, 2012. **30**: p. 95-114.
42. Hudson, L.L., et al., *Human T cell reconstitution in DiGeorge syndrome and HIV-1 infection*. Semin Immunol, 2007. **19**(5): p. 297-309.
43. Markert, M.L., B.H. Devlin, and E.A. McCarthy, *Thymus transplantation*. Clin Immunol, 2010. **135**(2): p. 236-46.
44. Markert, M.L., et al., *Thymus transplantation in complete DiGeorge syndrome: immunologic and safety evaluations in 12 patients*. Blood, 2003. **102**(3): p. 1121-30.
45. Chinn, I.K., et al., *Thymus transplantation restores the repertoires of forkhead box protein 3 (FoxP3)+ and FoxP3- T cells in complete DiGeorge anomaly*. Clin Exp Immunol, 2013. **173**(1): p. 140-9.

46. Li, B., et al., *Thymic microenvironment reconstitution after postnatal human thymus transplantation*. Clin Immunol, 2011. **140**(3): p. 244-59.
47. Haynes, B.F., et al., *The role of the thymus in immune reconstitution in aging, bone marrow transplantation, and HIV-1 infection*. Annu Rev Immunol, 2000. **18**: p. 529-60.
48. Junge, S., et al., *Correlation between recent thymic emigrants and CD31+ (PECAM-1) CD4+ T cells in normal individuals during aging and in lymphopenic children*. Eur J Immunol, 2007. **37**(11): p. 3270-80.
49. Tanaskovic, S., et al., *CD31 (PECAM-1) is a marker of recent thymic emigrants among CD4+ T-cells, but not CD8+ T-cells or gammadelta T-cells, in HIV patients responding to ART*. Immunol Cell Biol, 2010. **88**(3): p. 321-7.
50. Hazenberg, M.D., et al., *T cell receptor excision circles as markers for recent thymic emigrants: basic aspects, technical approach, and guidelines for interpretation*. J Mol Med (Berl), 2001. **79**(11): p. 631-40.
51. Hazenberg, M.D., et al., *T-cell receptor excision circle and T-cell dynamics after allogeneic stem cell transplantation are related to clinical events*. Blood, 2002. **99**(9): p. 3449-53.
52. Jamieson, B.D., et al., *Generation of functional thymocytes in the human adult*. Immunity, 1999. **10**(5): p. 569-75.
53. Douek, D.C., et al., *Changes in thymic function with age and during the treatment of HIV infection*. Nature, 1998. **396**(6712): p. 690-5.
54. Gurkan, S., et al., *Immune reconstitution following rabbit antithymocyte globulin*. Am J Transplant, 2010. **10**(9): p. 2132-41.
55. den Braber, I., et al., *Maintenance of peripheral naive T cells is sustained by thymus output in mice but not humans*. Immunity, 2012. **36**(2): p. 288-97.
56. Vrisekoop, N., et al., *Sparse production but preferential incorporation of recently produced naive T cells in the human peripheral pool*. Proc Natl Acad Sci U S A, 2008. **105**(16): p. 6115-20.
57. Mold, J.E., et al., *Maternal alloantigens promote the development of tolerogenic fetal regulatory T cells in utero*. Science, 2008. **322**(5907): p. 1562-5.
58. Golding, A., et al., *Deep sequencing of the TCR-beta repertoire of human forkhead box protein 3 (FoxP3)+ and FoxP3- T cells suggests that they are completely distinct and non-overlapping*. Clin Exp Immunol, 2017. **188**(1): p. 12-21.
59. Thiault, N., et al., *Peripheral regulatory T lymphocytes recirculating to the thymus suppress the development of their precursors*. Nat Immunol, 2015. **16**(6): p. 628-34.
60. McGovern, N., et al., *Human fetal dendritic cells promote prenatal T-cell immune suppression through arginase-2*. Nature, 2017. **546**(7660): p. 662-666.
61. Pennock, N.D., et al., *T cell responses: naive to memory and everything in between*. Adv Physiol Educ, 2013. **37**(4): p. 273-83.
62. Crotty, S., *Follicular helper CD4 T cells (TFH)*. Annu Rev Immunol, 2011. **29**: p. 621-63.
63. Prlic, M., M.A. Williams, and M.J. Bevan, *Requirements for CD8 T-cell priming, memory generation and maintenance*. Curr Opin Immunol, 2007. **19**(3): p. 315-9.
64. Magombedze, G., et al., *Cellular and population plasticity of helper CD4(+) T cell responses*. Front Physiol, 2013. **4**: p. 206.
65. Tripathi, S.K. and R. Lahesmaa, *Transcriptional and epigenetic regulation of T-helper lineage specification*. Immunol Rev, 2014. **261**(1): p. 62-83.
66. Zhu, J. and W.E. Paul, *Heterogeneity and plasticity of T helper cells*. Cell Res, 2010. **20**(1): p. 4-12.
67. Campbell, D.J. and M.A. Koch, *Phenotypical and functional specialization of FOXP3+ regulatory T cells*. Nat Rev Immunol, 2011. **11**(2): p. 119-30.
68. Hirahara, K., et al., *Mechanisms underlying helper T-cell plasticity: implications for immune-mediated disease*. J Allergy Clin Immunol, 2013. **131**(5): p. 1276-87.

69. Zhang, N. and M.J. Bevan, *CD8(+) T cells: foot soldiers of the immune system*. *Immunity*, 2011. **35**(2): p. 161-8.
70. Marcet-Palacios, M., et al., *Granzyme B inhibits vaccinia virus production through proteolytic cleavage of eukaryotic initiation factor 4 gamma 3*. *PLoS Pathog*, 2011. **7**(12): p. e1002447.
71. Walch, M., et al., *Cytotoxic cells kill intracellular bacteria through granzysin-mediated delivery of granzymes*. *Cell*, 2014. **157**(6): p. 1309-23.
72. Kaech, S.M. and W. Cui, *Transcriptional control of effector and memory CD8+ T cell differentiation*. *Nat Rev Immunol*, 2012. **12**(11): p. 749-61.
73. Chang, J.T., E.J. Wherry, and A.W. Goldrath, *Molecular regulation of effector and memory T cell differentiation*. *Nat Immunol*, 2014. **15**(12): p. 1104-15.
74. Zhou, X., et al., *Differentiation and persistence of memory CD8(+) T cells depend on T cell factor 1*. *Immunity*, 2010. **33**(2): p. 229-40.
75. Tiemessen, M.M., et al., *T Cell factor 1 represses CD8+ effector T cell formation and function*. *J Immunol*, 2014. **193**(11): p. 5480-7.
76. Lin, W.W., et al., *CD8+ T Lymphocyte Self-Renewal during Effector Cell Determination*. *Cell Rep*, 2016. **17**(7): p. 1773-1782.
77. Yao, S., et al., *Interferon regulatory factor 4 sustains CD8(+) T cell expansion and effector differentiation*. *Immunity*, 2013. **39**(5): p. 833-45.
78. Man, K., et al., *The transcription factor IRF4 is essential for TCR affinity-mediated metabolic programming and clonal expansion of T cells*. *Nat Immunol*, 2013. **14**(11): p. 1155-65.
79. Raczkowski, F., et al., *The transcription factor Interferon Regulatory Factor 4 is required for the generation of protective effector CD8+ T cells*. *Proc Natl Acad Sci U S A*, 2013. **110**(37): p. 15019-24.
80. Akondy, R.S., et al., *Initial viral load determines the magnitude of the human CD8 T cell response to yellow fever vaccination*. *Proc Natl Acad Sci U S A*, 2015. **112**(10): p. 3050-5.
81. Blom, K., et al., *Temporal dynamics of the primary human T cell response to yellow fever virus 17D as it matures from an effector- to a memory-type response*. *J Immunol*, 2013. **190**(5): p. 2150-8.
82. Miller, J.D., et al., *Human effector and memory CD8+ T cell responses to smallpox and yellow fever vaccines*. *Immunity*, 2008. **28**(5): p. 710-22.
83. Wieten, R.W., et al., *17D yellow fever vaccine elicits comparable long-term immune responses in healthy individuals and immune-compromised patients*. *J Infect*, 2016. **72**(6): p. 713-22.
84. DeWitt, W.S., et al., *Dynamics of the cytotoxic T cell response to a model of acute viral infection*. *J Virol*, 2015. **89**(8): p. 4517-26.
85. Wieten, R.W., et al., *A Single 17D Yellow Fever Vaccination Provides Lifelong Immunity; Characterization of Yellow-Fever-Specific Neutralizing Antibody and T-Cell Responses after Vaccination*. *PLoS One*, 2016. **11**(3): p. e0149871.
86. Fuertes Marraco, S.A., et al., *Long-lasting stem cell-like memory CD8+ T cells with a naive-like profile upon yellow fever vaccination*. *Sci Transl Med*, 2015. **7**(282): p. 282ra48.
87. Hammarlund, E., et al., *Duration of antiviral immunity after smallpox vaccination*. *Nat Med*, 2003. **9**(9): p. 1131-7.
88. Larbi, A. and T. Fulop, *From "truly naive" to "exhausted senescent" T cells: when markers predict functionality*. *Cytometry A*, 2014. **85**(1): p. 25-35.
89. Di Benedetto, S., et al., *Impact of age, sex and CMV-infection on peripheral T cell phenotypes: results from the Berlin BASE-II Study*. *Biogerontology*, 2015. **16**(5): p. 631-43.

90. Weiskopf, D., et al., *Dengue virus infection elicits highly polarized CX3CR1+ cytotoxic CD4+ T cells associated with protective immunity*. Proc Natl Acad Sci U S A, 2015. **112**(31): p. E4256-63.
91. Sanders, M.E., et al., *Human memory T lymphocytes express increased levels of three cell adhesion molecules (LFA-3, CD2, and LFA-1) and three other molecules (UCHL1, CDw29, and Pgp-1) and have enhanced IFN-gamma production*. J Immunol, 1988. **140**(5): p. 1401-7.
92. Smith, S.H., et al., *Functional subsets of human helper-inducer cells defined by a new monoclonal antibody, UCHL1*. Immunology, 1986. **58**(1): p. 63-70.
93. Sallusto, F., et al., *Two subsets of memory T lymphocytes with distinct homing potentials and effector functions [see comments]*. Nature, 1999. **401**(6754): p. 708-12.
94. Gattinoni, L., et al., *A human memory T cell subset with stem cell-like properties*. Nat Med, 2011. **17**(10): p. 1290-7.
95. Willinger, T., et al., *Molecular signatures distinguish human central memory from effector memory CD8 T cell subsets*. J Immunol, 2005. **175**(9): p. 5895-903.
96. Campbell, J.J., et al., *CCR7 expression and memory T cell diversity in humans*. J Immunol, 2001. **166**(2): p. 877-84.
97. Pulko, V., et al., *Human memory T cells with a naive phenotype accumulate with aging and respond to persistent viruses*. Nat Immunol, 2016. **17**(8): p. 966-75.
98. Ahmed, R., et al., *The precursors of memory: models and controversies*. Nat Rev Immunol, 2009. **9**(9): p. 662-8.
99. Durek, P., et al., *Epigenomic Profiling of Human CD4+ T Cells Supports a Linear Differentiation Model and Highlights Molecular Regulators of Memory Development*. Immunity, 2016. **45**(5): p. 1148-1161.
100. Abdelsamed, H.A., et al., *Human memory CD8 T cell effector potential is epigenetically preserved during in vivo homeostasis*. J Exp Med, 2017. **214**(6): p. 1593-1606.
101. Moskowitz, D.M., et al., *Epigenomics of human CD8 T cell differentiation and aging*. Sci Immunol, 2017. **2**(8).
102. Schenkel, J.M. and D. Masopust, *Tissue-resident memory T cells*. Immunity, 2014. **41**(6): p. 886-97.
103. Jiang, X., et al., *Skin infection generates non-migratory memory CD8+ TRM cells providing global skin immunity*. Nature, 2012. **483**(7388): p. 227-31.
104. Steinert, E.M., et al., *Quantifying Memory CD8 T Cells Reveals Regionalization of Immunosurveillance*. Cell, 2015. **161**(4): p. 737-49.
105. Teijaro, J.R., et al., *Cutting edge: tissue-retentive lung memory CD4 T cells mediate optimal protection to respiratory virus infection*. J Immunol, 2011. **187**(11): p. 5510-4.
106. Mackay, L.K., et al., *T-box Transcription Factors Combine with the Cytokines TGF-beta and IL-15 to Control Tissue-Resident Memory T Cell Fate*. Immunity, 2015. **43**(6): p. 1101-11.
107. Gebhardt, T., et al., *Memory T cells in nonlymphoid tissue that provide enhanced local immunity during infection with herpes simplex virus*. Nat Immunol, 2009. **10**(5): p. 524-30.
108. Wakim, L.M., et al., *The molecular signature of tissue resident memory CD8 T cells isolated from the brain*. J Immunol, 2012. **189**(7): p. 3462-71.
109. Mackay, L.K., et al., *Hobit and Blimp1 instruct a universal transcriptional program of tissue residency in lymphocytes*. Science, 2016. **352**(6284): p. 459-63.
110. Mackay, L.K., et al., *The developmental pathway for CD103(+)/CD8+ tissue-resident memory T cells of skin*. Nat Immunol, 2013. **14**(12): p. 1294-301.
111. Ugur, M., et al., *Resident CD4+ T cells accumulate in lymphoid organs after prolonged antigen exposure*. Nat Commun, 2014. **5**: p. 4821.

112. Schenkel, J.M., K.A. Fraser, and D. Masopust, *Cutting edge: resident memory CD8 T cells occupy frontline niches in secondary lymphoid organs*. J Immunol, 2014. **192**(7): p. 2961-4.
113. Iijima, N. and A. Iwasaki, *T cell memory. A local macrophage chemokine network sustains protective tissue-resident memory CD4 T cells*. Science, 2014. **346**(6205): p. 93-8.
114. Schenkel, J.M., et al., *T cell memory. Resident memory CD8 T cells trigger protective innate and adaptive immune responses*. Science, 2014. **346**(6205): p. 98-101.
115. Glennie, N.D., et al., *Skin-resident memory CD4+ T cells enhance protection against Leishmania major infection*. J Exp Med, 2015. **212**(9): p. 1405-14.
116. Zens, K.D., J.K. Chen, and D.L. Farber, *Vaccine-generated lung tissue-resident memory T cells provide heterosubtypic protection to influenza infection*. JCI Insight, 2016. **1**(10).
117. Shin, H. and A. Iwasaki, *A vaccine strategy that protects against genital herpes by establishing local memory T cells*. Nature, 2012. **491**(7424): p. 463-7.
118. Zens, K.D., J.-K. Chen, and D.L. Farber, *Vaccine-Generated Lung Tissue-Resident Memory T cells Provide Heterosubtypic Protection to Influenza Infection*. J. Clin. Invest. Insight, 2016. **1** (10): p. e85832.
119. Morawski, P.A., C.F. Qi, and S. Bolland, *Non-pathogenic tissue-resident CD8+ T cells uniquely accumulate in the brains of lupus-prone mice*. Sci Rep, 2017. **7**: p. 40838.
120. Hondowicz, B.D., et al., *Interleukin-2-Dependent Allergen-Specific Tissue-Resident Memory Cells Drive Asthma*. Immunity, 2016. **44**(1): p. 155-66.
121. Clark, R.A., *Resident memory T cells in human health and disease*. Sci Transl Med, 2015. **7**(269): p. 269rv1.
122. Park, C.O. and T.S. Kupper, *The emerging role of resident memory T cells in protective immunity and inflammatory disease*. Nat Med, 2015. **21**(7): p. 688-97.
123. Masopust, D., et al., *Dynamic T cell migration program provides resident memory within intestinal epithelium*. J Exp Med, 2010. **207**(3): p. 553-64.
124. Turner, D.L., et al., *Lung niches for the generation and maintenance of tissue-resident memory T cells*. Mucosal Immunol, 2014. **7**(3): p. 501-10.
125. Zens, K.D., et al., *Reduced generation of lung tissue-resident memory T cells during infancy*. J Exp Med, 2017.
126. Iijima, N. and A. Iwasaki, *A local macrophage chemokine network sustains protective tissue-resident memory CD4 T cells*. Science, 2014.
127. Marriott, C.L., et al., *Retention of Ag-specific memory CD4+ T cells in the draining lymph node indicates lymphoid tissue resident memory populations*. Eur J Immunol, 2017. **47**(5): p. 860-871.
128. Gasteiger, G., et al., *Tissue residency of innate lymphoid cells in lymphoid and nonlymphoid organs*. Science, 2015. **350**(6263): p. 981-5.
129. Anderson, K.G., et al., *Intravascular staining for discrimination of vascular and tissue leukocytes*. Nat Protoc, 2014. **9**(1): p. 209-22.
130. Tomura, M., et al., *Monitoring cellular movement in vivo with photoconvertible fluorescence protein "Kaede" transgenic mice*. Proc Natl Acad Sci U S A, 2008. **105**(31): p. 10871-6.
131. Shioh, L.R., et al., *CD69 acts downstream of interferon-alpha/beta to inhibit S1P1 and lymphocyte egress from lymphoid organs*. Nature, 2006. **440**(7083): p. 540-4.
132. Mackay, L.K., et al., *Cutting edge: CD69 interference with sphingosine-1-phosphate receptor function regulates peripheral T cell retention*. J Immunol, 2015. **194**(5): p. 2059-63.
133. Bergsbaken, T. and M.J. Bevan, *Proinflammatory microenvironments within the intestine regulate the differentiation of tissue-resident CD8(+) T cells responding to infection*. Nat Immunol, 2015. **16**(4): p. 406-14.

134. Masopust, D., et al., *Cutting edge: gut microenvironment promotes differentiation of a unique memory CD8 T cell population*. J Immunol, 2006. **176**(4): p. 2079-83.
135. Schenkel, J.M., et al., *Sensing and alarm function of resident memory CD8 T cells*. Nat Immunol, 2013. **14**(509-13).
136. Sheridan, B.S., et al., *Oral infection drives a distinct population of intestinal resident memory CD8(+) T cells with enhanced protective function*. Immunity, 2014. **40**(5): p. 747-57.
137. Bankovich, A.J., L.R. Shioy, and J.G. Cyster, *CD69 suppresses sphingosine 1-phosphate receptor-1 (S1P1) function through interaction with membrane helix 4*. J Biol Chem, 2010. **285**(29): p. 22328-37.
138. Matloubian, M., et al., *Lymphocyte egress from thymus and peripheral lymphoid organs is dependent on S1P receptor 1*. Nature, 2004. **427**(6972): p. 355-60.
139. Skon, C.N., et al., *Transcriptional downregulation of S1pr1 is required for the establishment of resident memory CD8+ T cells*. Nat Immunol, 2013. **14**(12): p. 1285-93.
140. Pan, Y., et al., *Survival of tissue-resident memory T cells requires exogenous lipid uptake and metabolism*. Nature, 2017. **543**(7644): p. 252-256.
141. Zhao, S., et al., *Comparison of RNA-Seq and microarray in transcriptome profiling of activated T cells*. PLoS One, 2014. **9**(1): p. e78644.
142. Hombrink, P., et al., *Programs for the persistence, vigilance and control of human CD8+ lung-resident memory T cells*. Nat Immunol, 2016. **17**(12): p. 1467-1478.
143. Mackay, L.K., et al., *Long-lived epithelial immunity by tissue-resident memory T (TRM) cells in the absence of persisting local antigen presentation*. Proc Natl Acad Sci U S A, 2012. **109**(18): p. 7037-42.
144. Liang, S., et al., *Heterosubtypic immunity to influenza type A virus in mice. Effector mechanisms and their longevity*. J Immunol, 1994. **152**(4): p. 1653-61.
145. Hogan, R.J., et al., *Protection from respiratory virus infections can be mediated by antigen-specific CD4(+) T cells that persist in the lungs*. J Exp Med, 2001. **193**(8): p. 981-6.
146. Cuburu, N., et al., *Intravaginal immunization with HPV vectors induces tissue-resident CD8+ T cell responses*. J Clin Invest, 2012. **122**(12): p. 4606-20.
147. Davies, B., et al., *Cutting Edge: Tissue-Resident Memory T Cells Generated by Multiple Immunizations or Localized Deposition Provide Enhanced Immunity*. J Immunol, 2017. **198**(6): p. 2233-2237.
148. Mackay, L.K. and A. Kallies, *Transcriptional Regulation of Tissue-Resident Lymphocytes*. Trends Immunol, 2017. **38**(2): p. 94-103.
149. Teijaro, J.R., et al., *Memory CD4 T cells direct protective responses to influenza virus in the lungs through helper-independent mechanisms*. J Virol, 2010. **84**(18): p. 9217-26.
150. Ariotti, S., et al., *T cell memory. Skin-resident memory CD8(+) T cells trigger a state of tissue-wide pathogen alert*. Science, 2014. **346**(6205): p. 101-5.
151. Schenkel, J.M., et al., *Sensing and alarm function of resident memory CD8(+) T cells*. Nat Immunol, 2013. **14**(5): p. 509-13.
152. Zaid, A., et al., *Persistence of skin-resident memory T cells within an epidermal niche*. Proc Natl Acad Sci U S A, 2014. **111**(14): p. 5307-12.
153. Ariotti, S., et al., *Tissue-resident memory CD8+ T cells continuously patrol skin epithelia to quickly recognize local antigen*. Proc Natl Acad Sci U S A, 2012. **109**(48): p. 19739-44.
154. Clark, R.A., et al., *Skin effector memory T cells do not recirculate and provide immune protection in alemtuzumab-treated CTCL patients*. Sci Transl Med, 2012. **4**(117): p. 117ra7.

155. Watanabe, R., et al., *Human skin is protected by four functionally and phenotypically discrete populations of resident and recirculating memory T cells*. *Sci Transl Med*, 2015. **7**(279): p. 279ra39.
156. Thome, J.J., et al., *Spatial map of human T cell compartmentalization and maintenance over decades of life*. *Cell*, 2014. **159**(4): p. 814-28.
157. Woon, H.G., et al., *Compartmentalization of Total and Virus-Specific Tissue-Resident Memory CD8+ T Cells in Human Lymphoid Organs*. *PLoS Pathog*, 2016. **12**(8): p. e1005799.
158. Booth, J.S., et al., *Characterization and functional properties of gastric tissue-resident memory T cells from children, adults, and the elderly*. *Front Immunol*, 2014. **5**: p. 294.
159. Purwar, R., et al., *Resident memory T cells (T(RM)) are abundant in human lung: diversity, function, and antigen specificity*. *PLoS One*, 2011. **6**(1): p. e16245.
160. Zhu, J., et al., *Immune surveillance by CD8 α α + skin-resident T cells in human herpes virus infection*. *Nature*, 2013. **497**(7450): p. 494-7.
161. Gebhardt, T., et al., *Different patterns of peripheral migration by memory CD4+ and CD8+ T cells*. *Nature*, 2011. **477**(7363): p. 216-9.
162. Zhu, J., et al., *Virus-specific CD8+ T cells accumulate near sensory nerve endings in genital skin during subclinical HSV-2 reactivation*. *J Exp Med*, 2007. **204**(3): p. 595-603.
163. Pallett, L.J., et al., *IL-2high tissue-resident T cells in the human liver: Sentinels for hepatotropic infection*. *J Exp Med*, 2017. **214**(6): p. 1567-1580.
164. Okhrimenko, A., et al., *Human memory T cells from the bone marrow are resting and maintain long-lasting systemic memory*. *Proc Natl Acad Sci U S A*, 2014. **111**(25): p. 9229-34.
165. Campbell, J.J., et al., *Sezary syndrome and mycosis fungoides arise from distinct T-cell subsets: a biologic rationale for their distinct clinical behaviors*. *Blood*, 2010. **116**(5): p. 767-71.
166. Bhushan, M., et al., *Anti-E-selectin is ineffective in the treatment of psoriasis: a randomized trial*. *Br J Dermatol*, 2002. **146**(5): p. 824-31.
167. Boyman, O., et al., *Spontaneous development of psoriasis in a new animal model shows an essential role for resident T cells and tumor necrosis factor-alpha*. *J Exp Med*, 2004. **199**(5): p. 731-6.
168. Cheuk, S., et al., *CD49a Expression Defines Tissue-Resident CD8+ T Cells Poised for Cytotoxic Function in Human Skin*. *Immunity*, 2017. **46**(2): p. 287-300.
169. Laidlaw, B.J., et al., *CD4(+) T Cell Help Guides Formation of CD103(+) Lung-Resident Memory CD8(+) T Cells during Influenza Viral Infection*. *Immunity*, 2014. **41**(4): p. 633-45.
170. Nakanishi, Y., et al., *CD8(+) T lymphocyte mobilization to virus-infected tissue requires CD4(+) T-cell help*. *Nature*, 2009. **462**(7272): p. 510-3.
171. Gaide, O., et al., *Common clonal origin of central and resident memory T cells following skin immunization*. *Nat Med*, 2015. **21**(6): p. 647-53.
172. El-Asady, R., et al., *TGF- β -dependent CD103 expression by CD8(+) T cells promotes selective destruction of the host intestinal epithelium during graft-versus-host disease*. *J Exp Med*, 2005. **201**(10): p. 1647-57.
173. Zhang, N. and M.J. Bevan, *Transforming growth factor-beta signaling controls the formation and maintenance of gut-resident memory T cells by regulating migration and retention*. *Immunity*, 2013. **39**(4): p. 687-96.
174. Casey, K.A., et al., *Antigen-Independent Differentiation and Maintenance of Effector-like Resident Memory T Cells in Tissues*. *J Immunol*, 2012. **188**(10): p. 4866-75.
175. Iijima, N. and A. Iwasaki, *Tissue instruction for migration and retention of TRM cells*. *Trends Immunol*, 2015. **36**(9): p. 556-64.

176. Slutter, B., et al., *Lung airway-surveilling CXCR3(hi) memory CD8(+) T cells are critical for protection against influenza A virus*. *Immunity*, 2013. **39**(5): p. 939-48.
177. Khan, T.N., et al., *Local antigen in nonlymphoid tissue promotes resident memory CD8+ T cell formation during viral infection*. *J Exp Med*, 2016. **213**(6): p. 951-66.
178. Zens, K.D., et al., *Reduced generation of lung tissue-resident memory T cells during infancy*. *J Exp Med*, 2017. **214**(10): p. 2915-2932.
179. Surh, C.D. and J. Sprent, *Homeostasis of naive and memory T cells*. *Immunity*, 2008. **29**(6): p. 848-62.
180. Panduro, M., C. Benoist, and D. Mathis, *Tissue Tregs*. *Annu Rev Immunol*, 2016. **34**: p. 609-33.
181. Clark, R.A. and T.S. Kupper, *IL-15 and dermal fibroblasts induce proliferation of natural regulatory T cells isolated from human skin*. *Blood*, 2007. **109**(1): p. 194-202.
182. Sanchez Rodriguez, R., et al., *Memory regulatory T cells reside in human skin*. *J Clin Invest*, 2014. **124**(3): p. 1027-36.
183. Feuerer, M., et al., *Lean, but not obese, fat is enriched for a unique population of regulatory T cells that affect metabolic parameters*. *Nat Med*, 2009. **15**(8): p. 930-9.
184. Peters, J.H., et al., *Human secondary lymphoid organs typically contain polyclonally-activated proliferating regulatory T cells*. *Blood*, 2013. **122**(13): p. 2213-23.
185. Wong, M.T., et al., *A High-Dimensional Atlas of Human T Cell Diversity Reveals Tissue-Specific Trafficking and Cytokine Signatures*. *Immunity*, 2016. **45**(2): p. 442-56.
186. Kumar, B.V., et al., *Human Tissue-Resident Memory T Cells Are Defined by Core Transcriptional and Functional Signatures in Lymphoid and Mucosal Sites*. *Cell Rep*, 2017. **20**(12): p. 2921-2934.
187. Goodell, M.A., et al., *Isolation and functional properties of murine hematopoietic stem cells that are replicating in vivo*. *J Exp Med*, 1996. **183**(4): p. 1797-806.
188. Goodell, M.A., et al., *Dye efflux studies suggest that hematopoietic stem cells expressing low or undetectable levels of CD34 antigen exist in multiple species*. *Nat Med*, 1997. **3**(12): p. 1337-45.
189. Dusseaux, M., et al., *Human MAIT cells are xenobiotic-resistant, tissue-targeted, CD161hi IL-17-secreting T cells*. *Blood*, 2011. **117**(4): p. 1250-9.
190. Turtle, C.J., et al., *A distinct subset of self-renewing human memory CD8+ T cells survives cytotoxic chemotherapy*. *Immunity*, 2009. **31**(5): p. 834-44.
191. Fergusson, J.R., et al., *CD161(int)CD8+ T cells: a novel population of highly functional, memory CD8+ T cells enriched within the gut*. *Mucosal Immunol*, 2016. **9**(2): p. 401-13.
192. Kudernatsch, R.F., et al., *Human bone marrow contains a subset of quiescent early memory CD8(+) T cells characterized by high CD127 expression and efflux capacity*. *Eur J Immunol*, 2014. **44**(12): p. 3532-42.
193. Klein, A.B., et al., *Impact of different cell isolation techniques on lymphocyte viability and function*. *J Immunoassay Immunochem*, 2006. **27**(1): p. 61-76.
194. Holt, P.G., et al., *Preparation of interstitial lung cells by enzymatic digestion of tissue slices: preliminary characterization by morphology and performance in functional assays*. *Immunology*, 1985. **54**(1): p. 139-47.
195. Ramachandran, H., et al., *Optimal thawing of cryopreserved peripheral blood mononuclear cells for use in high-throughput human immune monitoring studies*. *Cells*, 2012. **1**(3): p. 313-24.
196. Defoort, J.P., et al., *Simultaneous detection of multiplex-amplified human immunodeficiency virus type 1 RNA, hepatitis C virus RNA, and hepatitis B virus DNA using a flow cytometer microsphere-based hybridization assay*. *J Clin Microbiol*, 2000. **38**(3): p. 1066-71.
197. Trapnell, C., L. Pachter, and S.L. Salzberg, *TopHat: discovering splice junctions with RNA-Seq*. *Bioinformatics*, 2009. **25**(9): p. 1105-1111.

198. Wang, L., S. Wang, and W. Li, *RSeQC: quality control of RNA-seq experiments*. Bioinformatics, 2012. **28**(16): p. 2184-2185.
199. Anders, S., P.T. Pyl, and W. Huber, *HTSeq—a Python framework to work with high-throughput sequencing data*. Bioinformatics, 2014: p. btu638.
200. Trapnell, C., et al., *Transcript assembly and quantification by RNA-Seq reveals unannotated transcripts and isoform switching during cell differentiation*. Nature biotechnology, 2010. **28**(5): p. 511-515.
201. Robinson, M.D., D.J. McCarthy, and G.K. Smyth, *edgeR: a Bioconductor package for differential expression analysis of digital gene expression data*. Bioinformatics, 2010. **26**(1): p. 139-140.
202. Love, M.I., W. Huber, and S. Anders, *Moderated estimation of fold change and dispersion for RNA-seq data with DESeq2*. Genome biology, 2014. **15**(12): p. 550.
203. Leek, J.T., et al., *The sva package for removing batch effects and other unwanted variation in high-throughput experiments*. Bioinformatics, 2012. **28**(6): p. 882-883.
204. Huang da, W., B.T. Sherman, and R.A. Lempicki, *Systematic and integrative analysis of large gene lists using DAVID bioinformatics resources*. Nat Protoc, 2009. **4**(1): p. 44-57.
205. Huang da, W., B.T. Sherman, and R.A. Lempicki, *Bioinformatics enrichment tools: paths toward the comprehensive functional analysis of large gene lists*. Nucleic Acids Res, 2009. **37**(1): p. 1-13.
206. Szklarczyk, D., et al., *STRING v10: protein-protein interaction networks, integrated over the tree of life*. Nucleic Acids Res, 2015. **43**(Database issue): p. D447-52.
207. Kamburov, A., et al., *The ConsensusPathDB interaction database: 2013 update*. Nucleic Acids Res, 2013. **41**(Database issue): p. D793-800.
208. Suárez-Fariñas, M., et al., *Evaluation of the psoriasis transcriptome across different studies by gene set enrichment analysis (GSEA)*. PloS one, 2010. **5**(4): p. e10247.
209. Li, B., et al., *Ultrasensitive detection of TCR hypervariable-region sequences in solid-tissue RNA-seq data*. Nat Genet, 2017. **49**(4): p. 482-483.
210. Masopust, D., et al., *Preferential localization of effector memory cells in nonlymphoid tissue*. Science, 2001. **291**(5512): p. 2413-7.
211. Thom, J.T., et al., *The Salivary Gland Acts as a Sink for Tissue-Resident Memory CD8(+) T Cells, Facilitating Protection from Local Cytomegalovirus Infection*. Cell Rep, 2015. **13**(6): p. 1125-36.
212. Thome, J.J., et al., *Longterm maintenance of human naive T cells through in situ homeostasis in lymphoid tissue sites*. Sci Immunol, 2016. **1**(6).
213. Cibrian, D. and F. Sanchez-Madrid, *CD69: from activation marker to metabolic gatekeeper*. Eur J Immunol, 2017. **47**(6): p. 946-953.
214. Barber, D.L., et al., *Restoring function in exhausted CD8 T cells during chronic viral infection*. Nature, 2006. **439**(7077): p. 682-7.
215. Bertin, S., et al., *Dual-specificity phosphatase 6 regulates CD4+ T-cell functions and restrains spontaneous colitis in IL-10-deficient mice*. Mucosal Immunol, 2015. **8**(3): p. 505-15.
216. Qu, N., et al., *Pivotal roles of T-helper 17-related cytokines, IL-17, IL-22, and IL-23, in inflammatory diseases*. Clin Dev Immunol, 2013. **2013**: p. 968549.
217. Bottcher, J.P., et al., *Functional classification of memory CD8(+) T cells by CX3CR1 expression*. Nat Commun, 2015. **6**: p. 8306.
218. Gibbons, D.L., et al., *Cutting Edge: Regulator of G protein signaling-1 selectively regulates gut T cell trafficking and colitic potential*. J Immunol, 2011. **187**(5): p. 2067-71.
219. Enomoto, A., et al., *Negative regulation of MEKK1/2 signaling by serine-threonine kinase 38 (STK38)*. Oncogene, 2008. **27**(13): p. 1930-8.

220. Subramanian, A., et al., *Gene set enrichment analysis: a knowledge-based approach for interpreting genome-wide expression profiles*. Proc Natl Acad Sci U S A, 2005. **102**(43): p. 15545-50.
221. Kared, H., et al., *CD57 in human natural killer cells and T-lymphocytes*. Cancer Immunol Immunother, 2016. **65**(4): p. 441-52.
222. Schon, M.P., et al., *Mucosal T lymphocyte numbers are selectively reduced in integrin alpha E (CD103)-deficient mice*. J Immunol, 1999. **162**(11): p. 6641-9.
223. Soares, L.R., et al., *V7 (CD101) ligation inhibits TCR/CD3-induced IL-2 production by blocking Ca²⁺ flux and nuclear factor of activated T cell nuclear translocation*. J Immunol, 1998. **161**(1): p. 209-17.
224. Schey, R., et al., *CD101 inhibits the expansion of colitogenic T cells*. Mucosal Immunol, 2016. **9**(5): p. 1205-17.
225. Jovanovic, D.V., et al., *CD101 expression and function in normal and rheumatoid arthritis-affected human T cells and monocytes/macrophages*. J Rheumatol, 2011. **38**(3): p. 419-28.
226. Mora, J.R., et al., *Selective imprinting of gut-homing T cells by Peyer's patch dendritic cells*. Nature, 2003. **424**(6944): p. 88-93.
227. van der Matten, L. and G. Hinton, *Visualizing data using t-SNEJ*. Mach. Learn. Res. , 2008. **9**: p. 2579-2605.
228. Park, S.L., L.K. Mackay, and T. Gebhardt, *Distinct recirculation potential of CD69+CD103- and CD103+ thymic memory CD8+ T cells*. Immunol Cell Biol, 2016. **94**(10): p. 975-980.
229. Beura, L.K., et al., *Normalizing the environment recapitulates adult human immune traits in laboratory mice*. Nature, 2016. **532**(7600): p. 512-6.
230. Boddupalli, C.S., et al., *ABC transporters and NR4A1 identify a quiescent subset of tissue-resident memory T cells*. J Clin Invest, 2016. **126**(10): p. 3905-3916.
231. Pendergrass, W., N. Wolf, and M. Poot, *Efficacy of MitoTracker Green and CMXrosamine to measure changes in mitochondrial membrane potentials in living cells and tissues*. Cytometry A, 2004. **61**(2): p. 162-9.
232. Takeguchi, N., et al., *Inhibition of the multidrug efflux pump in isolated hepatocyte couplets by immunosuppressants FK506 and cyclosporine*. Transplantation, 1993. **55**(3): p. 646-50.
233. Zhou, S., et al., *The ABC transporter Bcrp1/ABCG2 is expressed in a wide variety of stem cells and is a molecular determinant of the side-population phenotype*. Nat Med, 2001. **7**(9): p. 1028-34.
234. Zheng, C., et al., *Landscape of Infiltrating T Cells in Liver Cancer Revealed by Single-Cell Sequencing*. Cell, 2017. **169**(7): p. 1342-1356 e16.
235. Larabee, J.L., et al., *Increased cAMP in monocytes augments Notch signaling mechanisms by elevating RBP-J and transducin-like enhancer of Split (TLE)*. J Biol Chem, 2013. **288**(30): p. 21526-36.
236. Curtis, M.M., S.S. Way, and C.B. Wilson, *IL-23 promotes the production of IL-17 by antigen-specific CD8 T cells in the absence of IL-12 and type-I interferons*. J Immunol, 2009. **183**(1): p. 381-7.
237. Dagur, P.K., et al., *Secretion of interleukin-17 by CD8+ T cells expressing CD146 (MCAM)*. Clin Immunol, 2014. **152**(1-2): p. 36-47.
238. Zhang, Y., et al., *ZNF365 promotes stalled replication forks recovery to maintain genome stability*. Cell Cycle, 2013. **12**(17): p. 2817-28.
239. Akbulut, S., et al., *Sprouty proteins inhibit receptor-mediated activation of phosphatidylinositol-specific phospholipase C*. Mol Biol Cell, 2010. **21**(19): p. 3487-96.
240. Zhu, Y., et al., *B7-H5 costimulates human T cells via CD28H*. Nat Commun, 2013. **4**: p. 2043.

241. Tai, X.G., et al., *A role for CD9 molecules in T cell activation*. J Exp Med, 1996. **184**(2): p. 753-8.
242. Kobayashi, H., et al., *The tetraspanin CD9 is preferentially expressed on the human CD4(+)CD45RA+ naive T cell population and is involved in T cell activation*. Clin Exp Immunol, 2004. **137**(1): p. 101-8.
243. Holling, T.M., E. Schooten, and P.J. van Den Elsen, *Function and regulation of MHC class II molecules in T-lymphocytes: of mice and men*. Hum Immunol, 2004. **65**(4): p. 282-90.
244. Vivier, E. and N. Anfossi, *Inhibitory NK-cell receptors on T cells: witness of the past, actors of the future*. Nat Rev Immunol, 2004. **4**(3): p. 190-8.
245. Mazzucchelli, R. and S.K. Durum, *Interleukin-7 receptor expression: intelligent design*. Nat Rev Immunol, 2007. **7**(2): p. 144-54.
246. Brenchley, J.M., et al., *Expression of CD57 defines replicative senescence and antigen-induced apoptotic death of CD8+ T cells*. Blood, 2003. **101**(7): p. 2711-20.
247. Noble, A., A. Giorgini, and J.A. Leggat, *Cytokine-induced IL-10-secreting CD8 T cells represent a phenotypically distinct suppressor T-cell lineage*. Blood, 2006. **107**(11): p. 4475-83.
248. Bai, A., et al., *NADH oxidase-dependent CD39 expression by CD8(+) T cells modulates interferon gamma responses via generation of adenosine*. Nat Commun, 2015. **6**: p. 8819.
249. Noble, A., et al., *IL-12 and IL-4 activate a CD39-dependent intrinsic peripheral tolerance mechanism in CD8(+) T cells*. Eur J Immunol, 2016. **46**(6): p. 1438-48.
250. Deaglio, S., et al., *Adenosine generation catalyzed by CD39 and CD73 expressed on regulatory T cells mediates immune suppression*. J Exp Med, 2007. **204**(6): p. 1257-65.
251. Antonioli, L., et al., *CD39 and CD73 in immunity and inflammation*. Trends Mol Med, 2013. **19**(6): p. 355-67.
252. Weng, N.P., Y. Araki, and K. Subedi, *The molecular basis of the memory T cell response: differential gene expression and its epigenetic regulation*. Nat Rev Immunol, 2012. **12**(4): p. 306-15.
253. Vachharajani, V.T., et al., *Sirtuins Link Inflammation and Metabolism*. J Immunol Res, 2016. **2016**: p. 8167273.
254. Kitamura, H., et al., *Mouse and human lung fibroblasts regulate dendritic cell trafficking, airway inflammation, and fibrosis through integrin alphavbeta8-mediated activation of TGF-beta*. J Clin Invest, 2011. **121**(7): p. 2863-75.
255. Beinborn, M., et al., *TGF-beta regulates T-cell neurokinin-1 receptor internalization and function*. Proc Natl Acad Sci U S A, 2010. **107**(9): p. 4293-8.
256. Gagliani, N., et al., *Th17 cells transdifferentiate into regulatory T cells during resolution of inflammation*. Nature, 2015. **523**(7559): p. 221-5.
257. Mezrich, J.D., et al., *An interaction between kynurenine and the aryl hydrocarbon receptor can generate regulatory T cells*. J Immunol, 2010. **185**(6): p. 3190-8.
258. Lotze, M.T. and K.J. Tracey, *High-mobility group box 1 protein (HMGB1): nuclear weapon in the immune arsenal*. Nat Rev Immunol, 2005. **5**(4): p. 331-42.
259. Dimeloe, S., et al., *Human regulatory T cells lack the cyclophosphamide-extruding transporter ABCB1 and are more susceptible to cyclophosphamide-induced apoptosis*. Eur J Immunol, 2014. **44**(12): p. 3614-20.
260. Trimble, C.L., et al., *Human papillomavirus 16-associated cervical intraepithelial neoplasia in humans excludes CD8 T cells from dysplastic epithelium*. J Immunol, 2010. **185**(11): p. 7107-14.
261. Swaims-Kohlmeier, A., et al., *Progesterone Levels Associate with a Novel Population of CCR5+CD38+ CD4 T Cells Resident in the Genital Mucosa with Lymphoid Trafficking Potential*. J Immunol, 2016. **197**(1): p. 368-76.

262. Radenkovic, M., et al., *Characterization of resident lymphocytes in human pancreatic islets*. Clin Exp Immunol, 2017. **187**(3): p. 418-427.
263. Oja, A.E., et al., *Trigger-happy resident memory CD4+ T cells inhabit the human lungs*. Mucosal Immunol, 2017.
264. Zhu, J., et al., *Immune surveillance by CD8alphaalpha skin-resident T cells in human herpes virus infection*. Nature, 2013.
265. Arase, N., et al., *Heterotypic interaction of CRTAM with Necl2 induces cell adhesion on activated NK cells and CD8+ T cells*. Int Immunol, 2005. **17**(9): p. 1227-37.
266. Cortez, V.S., et al., *CRTAM controls residency of gut CD4+CD8+ T cells in the steady state and maintenance of gut CD4+ Th17 during parasitic infection*. J Exp Med, 2014. **211**(4): p. 623-33.
267. Takeuchi, A., et al., *CRTAM confers late-stage activation of CD8+ T cells to regulate retention within lymph node*. J Immunol, 2009. **183**(7): p. 4220-8.
268. Hong, D.K., et al., *Cationic lipid/DNA complex-adjuvanted influenza A virus vaccination induces robust cross-protective immunity*. J Virol, 2010. **84**(24): p. 12691-702.
269. Verhoeven, D., J.R. Teijaro, and D.L. Farber, *Pulse-oximetry accurately predicts lung pathology and the immune response during influenza infection*. Virology, 2009. **390**(2): p. 151-6.

Appendix A. The functional profile of naïve and memory T cells with aging.

Only data resulting from experiments that I performed is presented in this section, and this data is taken from:

Thome, J.J.C.*, Grinshpun, B*, **Kumar, B.V.**, Kubota, M., Ohmura, Y., Lerner, H., Sempowski, G.D., Shen, Y., Farber, D.L. (2016) Long-term maintenance of human naïve T cells through in situ homeostasis in lymphoid tissue sites. *Sci Immunol* Dec;1(6).

Naïve T cells develop in the thymus and coordinate immune responses to new antigens; however, mechanisms for their long-term persistence over the human life span remain undefined. We investigated human naïve T cell development and maintenance in primary and secondary lymphoid tissues obtained from individual organ donors aged 2 months to 73 years. In the thymus, the frequency of double-positive thymocytes declined sharply in donors >40 years of age, coincident with reduced recent thymic emigrants in lymphoid tissues, whereas naïve T cells were functionally maintained predominantly in lymph nodes (LNs). Analysis of T cell receptor clonal distribution by CDR3 sequencing of naïve CD4⁺ and CD8⁺ T cells in spleen and LNs reveals site-specific clonal expansions of naïve T cells from individuals >40 years of age, with minimal clonal overlap between lymphoid tissues. We also identified biased naïve T cell clonal distribution within specific LNs on the basis of VJ usage. Together, these results suggest prolonged maintenance of naïve T cells through in situ homeostasis and retention in lymphoid tissue.

As detailed in Chapter 1, there is a marked decline in thymic function with aging in humans, such that there is virtually no output of naïve T cells from the thymus by age 40. However, naïve populations are still maintained even into the seventh and eight decade of life, particularly in lymphoid tissues. As maintenance of naïve populations shifts from thymic to peripheral production, an important question is whether the function of naïve populations is affected.

To determine how cessation of thymic output affects T cell function, naïve (CCR7+CD45RA+) T cells were isolated by cell sorting from donors with active thymic output (35 years of age or younger) or from donors without thymic output (50 years of age or older). As a comparison group, memory T cells (CCR7-CD45RA-) were also isolated from the same donors and tissues. Isolated T cells were stimulated with anti CD3/CD28/CD2 beads for 48 hours and cytokine secretion was measured via BD Cytometric Bead Array (for detailed methods, see Chapter 2).

Naïve T cells from all tissue sites from multiple donors above the age of 50 retained the capacity to produce IL-2 upon stimulation but produced low levels of IFN- γ , IL-4, and IL-10 (Figs. A.A.1, A.A.2 and Table A.A.1). Further, the functional properties of naïve T cells did not vary by age. Memory T cells on the other hand were able to produce more substantial levels of IFN- γ , IL-4, and IL-10 compared with naïve T cells. However, some age related changes were noted, with memory T cells from older individuals producing reduced amounts of IL-10 (Fig. A.A.2 and Table A.A.1). Overall, these results suggest that CCR7+CD45RA+ phenotype naïve T cells retain naïve-like function even after cessation of thymic output.

Figure A.A.1. Naïve T cells retain function with age.

Naïve and memory CD4⁺ and CD8⁺ T cells were isolated from spleen, inguinal lymph nodes (ILN), and lung lymph nodes (LLN), stimulated for 48 hours using anti-CD3/CD28/CD2 beads, and the cytokine content in supernatants was assessed using the BD Cytometric Bead Array kit.

(A) IL-2 and IFN- γ production (in pg/ml; means \pm SEM) isolated from donors <35 years of age (white bars) and >50 years of age (black bars). n=2-4 donors except spleen CD4⁺ >50, for which n=1.

(B) Heatmap shows IL-2 and IFN- γ production by naïve and memory CD4⁺ and CD8⁺ T cells from the LLN of four individual donors <35 years of age (aged 29, 25, 26, and 34) and four donors >50 years of age (aged 54, 56, 52, and 59). Cytokine levels are normalized by donor and indicated by Z score [(cytokine level – mean cytokine level)/SD].

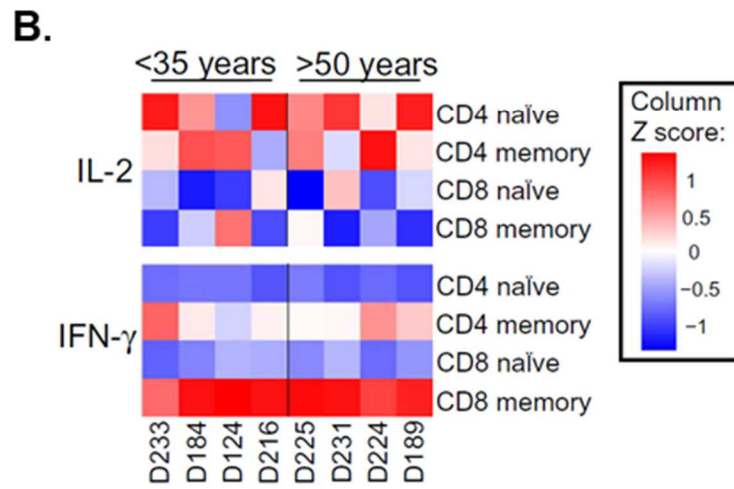
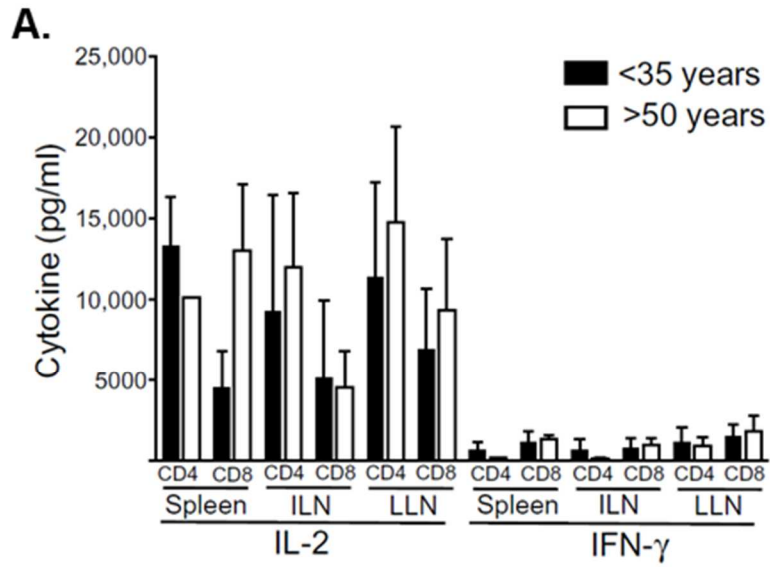


Figure A.A.2. IL-4 and IL-10 Production by Naïve and Memory T cells

Naïve and memory CD4⁺ and CD8⁺ T cells were sorted from spleen, ILN, and LLN and stimulated for 48h using anti CD3/CD28/CD2 beads, and the cytokine content in supernatants was assessed using the BD Cytometric Bead Array kit for 48 hours (see methods in Chapter 2). IL-4 (A) and IL-10 (B) production (pg/ml, mean± SEM) by naïve and memory T cells isolated from tissues of donors under age 35 years of age (white bars, n=2-5 donors) and over 50 years of age (black bars, n=2-4 donors except for spleen naïve CD4 T cells for which n=1).

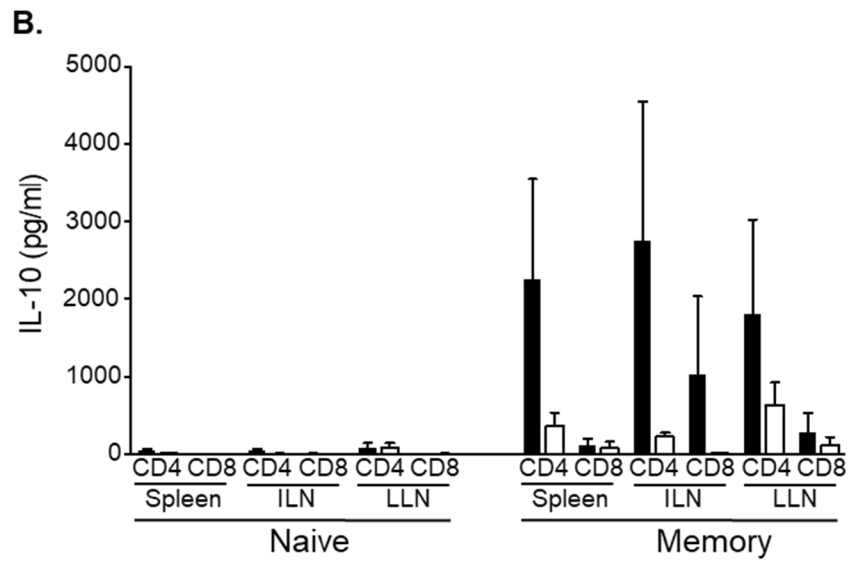
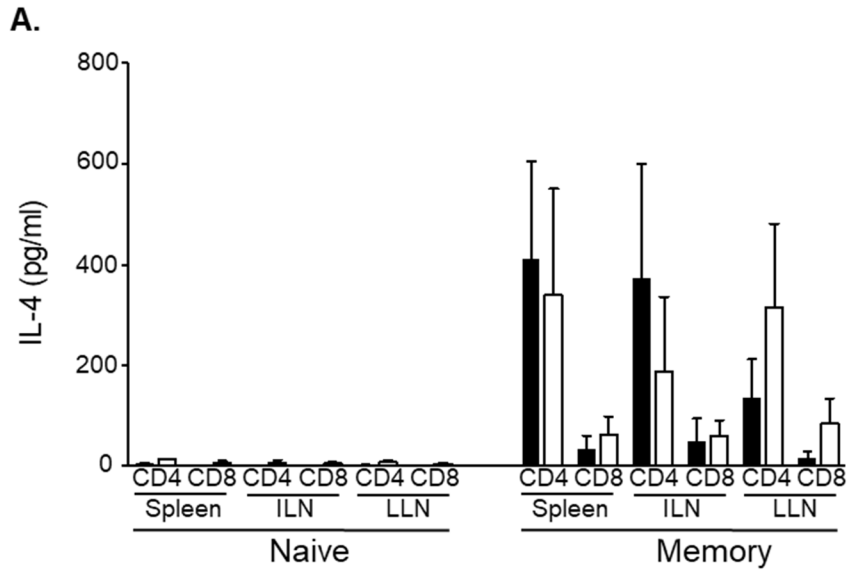


Table A.A.1: Tabular data for all cytokines measured in this study

IL-2 (pg/ml)	Donor	D175	D233	D184	D124	D216	D225	D231	D224	D189
	Age	24	26	25	26	34	54	56	52	59
	Spleen CD4 Naïve		19146	9164	4753	11550			10152	
	Spleen CD4 TEM		15836	3370	3592	5924	19329	1974	7682	
	Spleen CD8 Naïve		8449	401	1039	4684	17078		8990	
	Spleen CD8 TEM		2064	190	199	272	5956	97	2647	
	ILN CD4 Naïve		23441	4222	259		15921	17161	2880	
	ILN CD4 TEM		15425	3058	1511		12135	10569	2681	
	ILN CD8 Naïve		9965	306			8008	5390	203	
	ILN CD8 TEM		2132	224			10034	693	646	
	LLN CD4 Naïve		21653	2442	245	21235	9423	23041	744	25811
	LLN CD4 TEM	5030	12753	2943	1004	8390	9572	12542	1461	18952
	LLN CD8 Naïve		8093	38	8	12686	3565	16928	55	16723
LLN CD8 TEM	179	2530	1325	939	4442	7692	4099	354	10891	

IFN γ (pg/ml)	Donor	D175	D233	D184	D124	D216	D225	D231	D224	D189
	Age	24	26	25	26	34	54	56	52	59
	Spleen CD4 Naïve		1703	122	66	212			193	
	Spleen CD4 TEM		12127	2137	1246	2244	9513	101	5112	
	Spleen CD8 Naïve		2456	251	326	740	1583		1161	
	Spleen CD8 TEM		11422	1140	1098	654	10746	76	6872	
	ILN CD4 Naïve		1347	67	4		206	160	50	
	ILN CD4 TEM		12952	1592	182		3180	1738	845	
	ILN CD8 Naïve		1393	220			1281	1544	108	
	ILN CD8 TEM		10922	599			12332	914	867	
	LLN CD4 Naïve		3032	29	2	349	164	984	34	2516
	LLN CD4 TEM	2626	13164	1090	185	3357	4529	3489	990	8798
	LLN CD8 Naïve		2602	120	123	1791	605	2363	41	4362
LLN CD8 TEM	670	12961	2565	784	7047	12148	6645	1295	13432	

IL-4 (pg/ml)	Donor	D175	D233	D184	D124	D216	D225	D231	D224	D189
	Age	24	26	25	26	34	54	56	52	59
	Spleen CD4 Naïve		4	3	0	2			11	
	Spleen CD4 TEM		884	576	77	110	282	5	731	
	Spleen CD8 Naïve		0	0	0	0	0		8	
	Spleen CD8 TEM		116	0	4	0	122	0	62	
	ILN CD4 Naïve		0	0	0		0	0	14	
	ILN CD4 TEM		800	297	20		83	0	481	
	ILN CD8 Naïve		0	0			0	0	8	
	ILN CD8 TEM		93	0			109	4	62	
	LLN CD4 Naïve		1	0	0	0	0	0	11	11
	LLN CD4 TEM	89	432	0	13	139	74	162	806	221
	LLN CD8 Naïve		0	0	0	0	0	0	8	0
LLN CD8 TEM	0	66	0	0	6	59	21	19	231	

IL-10 (pg/ml)	Donor	D175	D233	D184	D124	D216	D225	D231	D224	D189
	Age	24	26	25	26	34	54	56	52	59
	Spleen CD4 Naïve		114	38	6	9			16	
	Spleen CD4 TEM		5819	2532	437	203	573	46	492	
	Spleen CD8 Naïve		8	0	0	1	0		8	
	Spleen CD8 TEM		405	0	23	3	12	0	244	
	ILN CD4 Naïve		77	69	0		0	8	14	
	ILN CD4 TEM		6179	1998	28		138	283	267	
	ILN CD8 Naïve		10	0			0	2	4	
	ILN CD8 TEM		2028	12			8	6	28	
	LLN CD4 Naïve		280	13	0	23	0	113	6	240
	LLN CD4 TEM	256	6569	1463	28	698	222	658	231	1442
	LLN CD8 Naïve		14	0	0	0	0	2	4	22
LLN CD8 TEM	0	1312	0	0	60	12	37	13	429	

Appendix B. Imaging of frozen sections of human lymph nodes

The localization of TRM within tissues in mice has been investigated in several studies by our lab [124] and others [103, 107, 111, 112, 133, 153]. However, the localization of TRM within human tissues has not been fully investigated. After HSV infection in humans, resident T cells were found to cluster around infected cells [162, 264], however these cells were CD8 $\alpha\alpha$ T cells and not canonical TRM that express $\alpha\beta$ TCR. Another human study examined the localization of both CD103⁺ and CD103⁻ TRM in spleen and tonsils [157]. Altogether, these studies show that CD8⁺ TRM are localized to distinct regions within tissues compared with non-resident T cells, consistent with their unique retention capabilities and function to intercept pathogens at sites of entry. However, the localization of CD4⁺ TRM and of CD8⁺ TRM in other tissue sites such as lymph nodes has not been investigated.

To identify the localization of TRM within lymphoid tissues, we performed fluorescence imaging frozen sections of human lung lymph nodes (LLN) and stained for CD4, CD8, and CD69 (see Chapter 2 for detailed methods). We found that T cells not expressing CD69 were primarily located towards the edges of the lymph node, while T cells expressing CD69 were located towards the inside of the lymph node (Figure A.B.1). These data suggest a unique localization for TRM within lymphoid tissues. However, it should be noted that these data were only based on staining a small number of donors (n=3). Further, no memory markers (i.e. CD45RA) were included in the staining. This means that CD69⁺ T cells being detected could represent naïve or TCM cells, or even activated T cells, and may not be true TRM.

Figure A.B.1. Localization of CD69⁺ and CD69⁻ T cells within human lymph nodes.

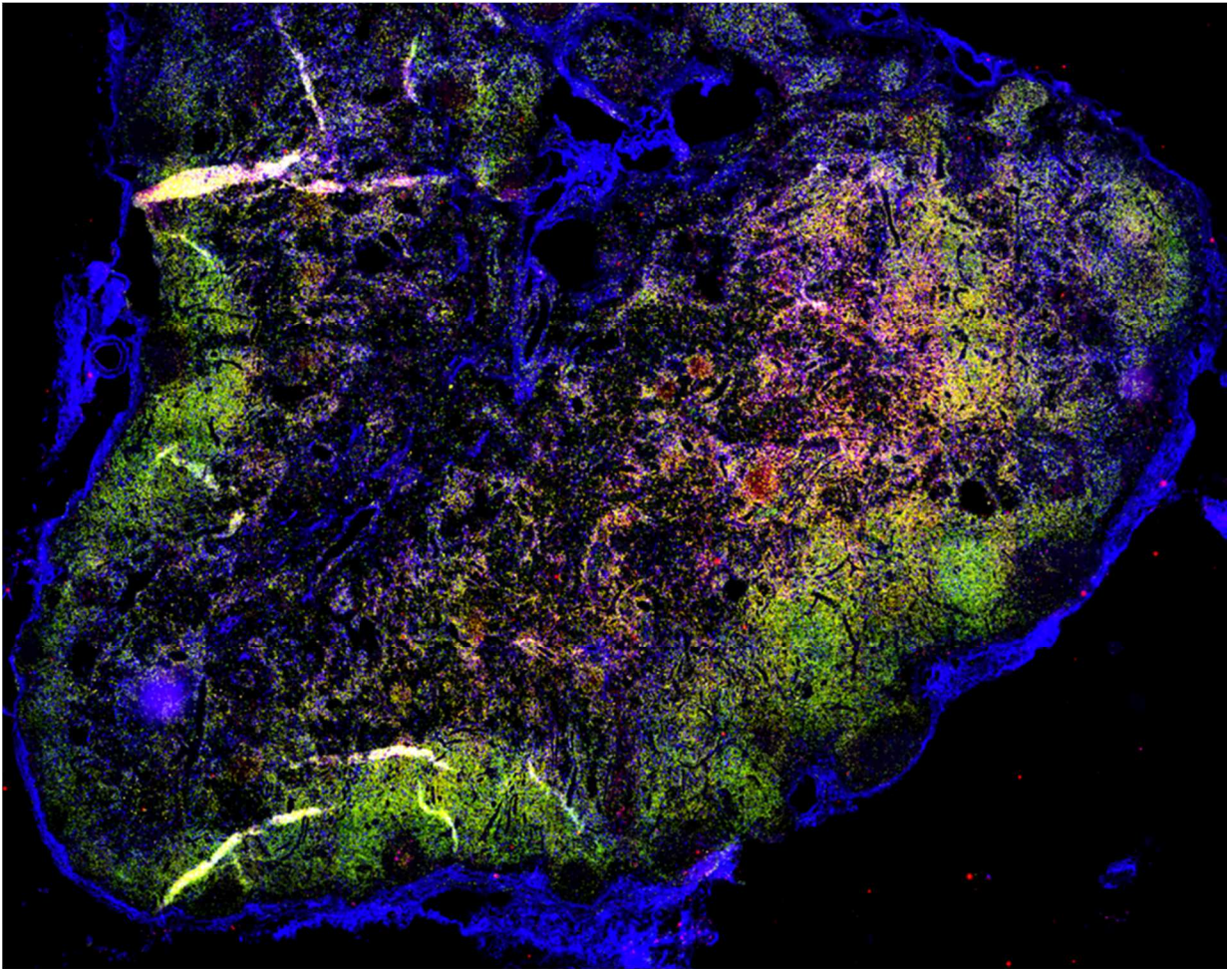
Fixed human LLN was stained for CD4 (green), CD8 (blue), and CD69 (red). Image shown is from a single representative donor (donor 229, age 43) at 10x magnification, representative of 3 donors.

(A) Image shows full LLN.

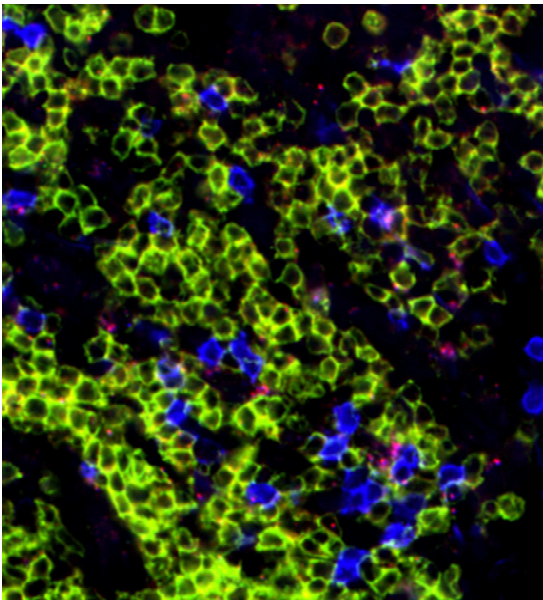
(B) Magnification on outer area containing single positive CD4⁺ and CD8⁺ T cells.

(C) Magnification on inner area containing double positive CD4⁺CD69⁺ and CD8⁺CD69⁺ T cells.

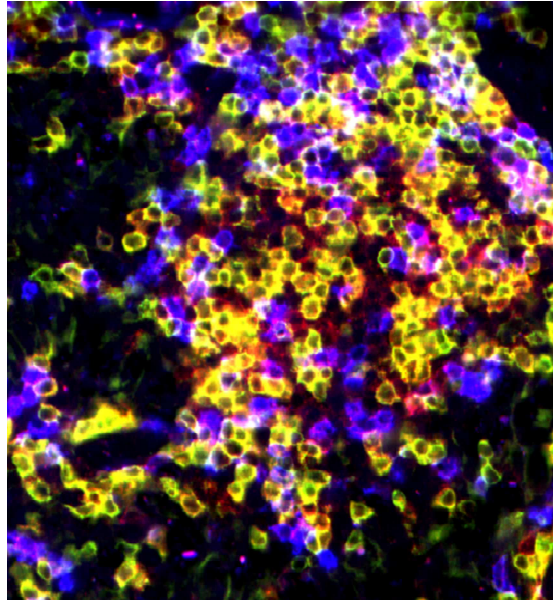
A.



B.



C.



Appendix C. Role of CRTAM in lung TRM: preliminary data and project proposal

(Mouse experiments performed by Daniel Paik)

Preliminary Data and Rationale

Transcriptionally, the gene CRTAM was one of the most significantly upregulated genes in human lung TRM in both CD4⁺ and CD8⁺ subsets, showing over 2-fold increase in TRM compared with TEM in all donors (Data from Chapter 3, Fig. A.C.1). *Crtam* (cytotoxic and regulatory T cell molecule) is a cell surface adhesion molecule that is expressed by T cells and other leukocytes such as NK cells [265-267]. *Crtam* binds *Cadm1*, which is found on the surface of dendritic cells and other cell types such as epithelial cells, and it has been shown that *Crtam* may play a role in the retention of T cells to certain locations [265-267]. *I hypothesize that Crtam is required for the generation, retention, and optimal function of lung TRM.* Preliminary data also indicate that *Crtam* is expressed exclusively by lung TRM in mouse following influenza infection (Fig. A.C.2). Further, *Crtam*⁺ cells in mouse have a TRM-like phenotype, being CD49a⁺ and CD62L⁻ (Fig. A.C.2).

Experimental Plan

The requirement of *Crtam* for generation of TRM in the lung can be determined using a well-established mouse model for generating and tracking influenza-specific CD4⁺ T cells that has been used by our laboratory to study TRM in the lung (Fig. A.C.3) [105, 116, 124, 125]. To generate antigen specific TRM, purified CD45.2⁺ ovalbumin (OVA)-specific TCR transgenic OT-II CD4⁺ cells are transferred into naïve CD45.1⁺ B6 host mice which are subsequently infected with the OVA-expressing recombinant influenza strain PR8-OVA, leading to an expansion of transferred OT-II cells that migrate to the infected lungs (Fig. A.C.3). After 4-8 weeks, the recovered flu-memory mice will contain OT-II lung TRM which can be differentiated from host

polyclonal TRM by their CD45.2⁺ congenic marker. In vivo antibody labeling can be used to distinguish TRM from circulatory T cells, and this technique that has been extensively validated in different labs including our own [104, 105, 116, 124, 125, 129]. A fluorescently labeled antibody is injected into a mouse which distributes in the blood and specifically binds to circulating leukocytes. Non-circulating leukocytes such as TRM are protected from antibody labeling and fall into the negative population, which distinguishes them from fluorescently labeled TEM.

As lung TRM in mice express Crtam (Fig A.C.2), Crtam knockout mice can be crossed with OT-II mice, and the OT-II Crtam^{-/-} T cells can be used investigate the need for Crtam in generation of CD4⁺ lung TRM. (OT-I Crtam^{-/-} T cells can be used to investigate CD8 TRM generation.) OT-II Crtam^{-/-} and wild-type OT-II cells can be transferred into host mice and TRM generation by these two cells types will be assessed after infection.

To assess the role of Crtam in protection against secondary infection, host mice containing either OT-II CRTAM^{-/-} or wild-type OT-II cells can be infected with PR8-OVA. After 4-8 weeks, these mice can be challenged with H3N2 virus X31-OVA to assess heterosubtypic protection. A different strain is used to measure protection mediated by T cells, and removes the effect of antibodies that are generated during primary infection. Mice can be evaluated for differences in weight loss, viral clearance, mortality, and lung injury. Lung viral titers can be calculated as described previously [268]. To assess tissue damage, lung histology can be performed using hematoxylin and eosin (H&E) to observe necrosis, changes to the lung architecture, and immune infiltrates. Changes in lung function can be measured using a mouse-specific pulse oximeter to calculate differences in blood oxygen levels [269]. Finally, to assess specifically protection due to TRM rather than all T cells, mice can be challenged in the presence of FTY720, which limits

leukocyte migration into tissue, and thus restricts the protective response to TRM as we have previously shown [116, 124].

Figure A.C.1. Elevated CRTAM expression by human lung TRM.

Graph displays normalized mRNA expression levels of CRTAM in blood and lung samples from three donors. Lines connect samples from identical donors. Differential expression was assessed by EdgeR and * FDR<0.05, ****FDR<10⁻⁵. Tissue abbreviations: B=blood, L=lung. Solid squares: lung TRM, open squares: lung TEM, triangle: blood TEM.

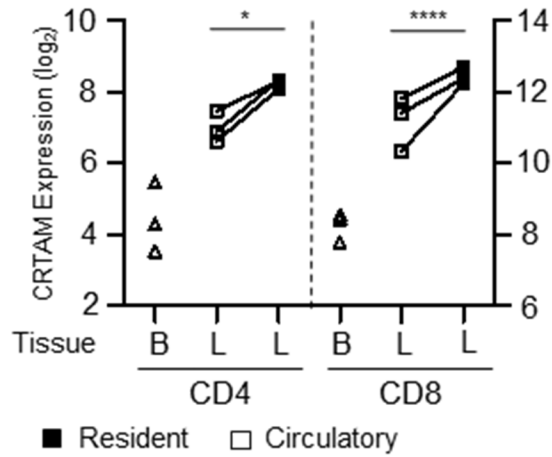


Figure A.C.2. Crtam is expressed exclusively by Lung TRM in mice.

Mice were infected with PR8 (H1N1) influenza and 10 weeks later memory (CD44⁺) T cells from lung and spleen were analyzed for Crtam expression.

(A) Representative flow cytometry plots showing Crtam expression in circulatory (in vivo labelled) and resident (in vivo unlabeled) memory T cells.

(B) Representative flow cytometry plots showing Crtam coexpression with ITGA1 and CD62L in lung memory T cells. Plots are representative of 3 experiments. Only data for CD4⁺ T cells shown.

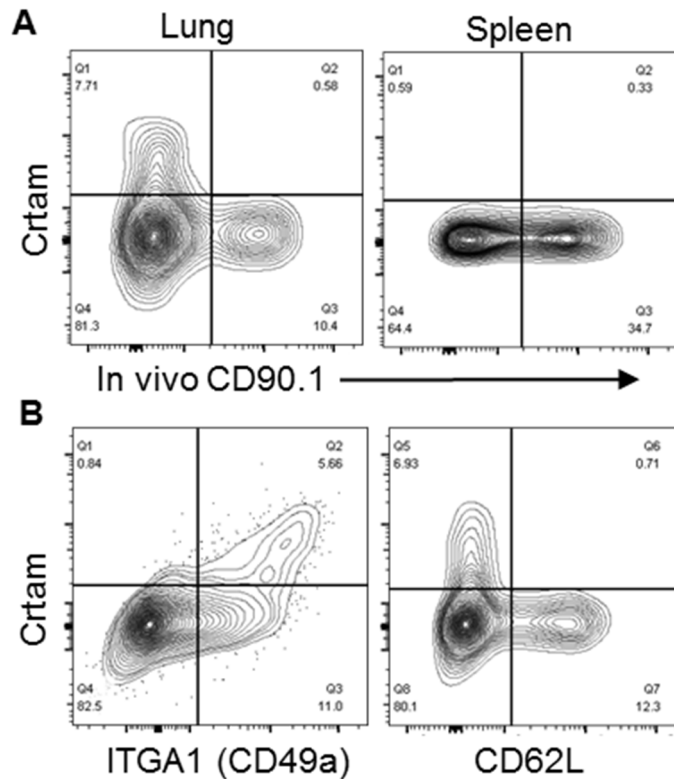
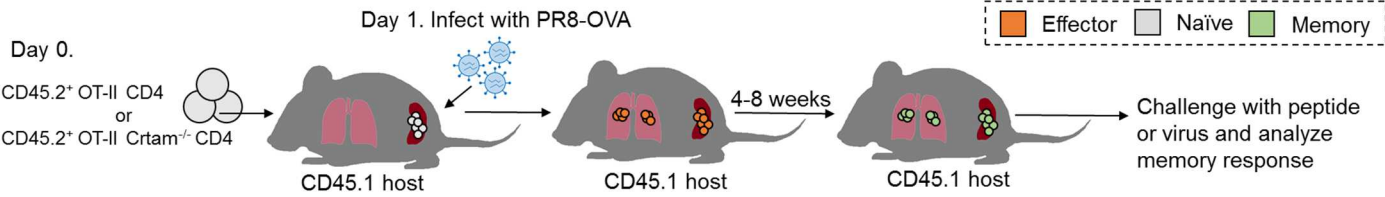


Figure A.C.3. Schematic of OT-II Flu Memory Model



Appendix D. Accepted Abstracts

2016 Oral Presentation: **A core transcriptional and functional profile distinguishes resident memory T cells in human.**
Middle-European Societies for Immunology and Allergology (MESIA)
2016 Annual Meeting in Budapest, Hungary
Travel Award Recipient

Authors: **Brahma V. Kumar**, Wenji Ma, Michelle Miron, Tomer Granot, Dustin J. Carpenter, Takashi Senda, Yufeng Shen, and Donna L. Farber.

Abstract:

Tissue-resident memory T cells (TRM) are a non-circulatory subset of T cells that mediate rapid responses to secondary infection. TRM have been shown to provide superior protective responses compared with circulating memory T cells in mouse studies, and TRM are implicated in tissue-specific inflammatory diseases in humans. Targeting TRM could be an effective strategy for vaccination or immunomodulation; however, little is known about TRM in humans and access to tissues is a critical barrier to advances in this field. Here, we investigate whether TRM can be identified in human tissue sites and whether TRM represent a distinct memory subset in humans. Through our collaboration with the New York organ procurement organization, we obtained lymphoid and mucosal tissues from healthy organ donors and used these to isolate cells bearing the phenotypic markers of TRM (CCR7⁻, CD45RA⁻, CD69⁺) and effector memory (TEM; CCR7⁻, CD45RA⁻, CD69⁻) subsets. We performed whole transcriptome profiling by RNA Sequencing of TRM and TEM from the lung and spleen of 3 donors, as well as blood TEM from 3 donors, for both CD4 and CD8 subsets. CD69⁺ human TRM were transcriptionally similar to mouse CD8 TRM, showing downregulation of KLF2 and S1PR1 and upregulation of ITGA1 and ITGAE, and all TRM samples clustered together in PCA analysis while spleen and lung TEM clustered with circulatory populations from blood, suggesting that the putative marker CD69 identifies TRM in humans. We compiled differential expression results between TRM and TEM and identified a core transcriptional signature of 80 and 142 genes that define CD4 and CD8 human TRM, respectively. TRM show differential expression of genes involved in migration and adhesion, upregulation of genes involved in the effector response, and upregulation of several inhibitory genes. Ex vivo functional studies support these results and show that TRM have a superior ability to rapidly produce IL-2 and effector cytokines such as IFN- γ and TNF compared with TEM. Using flow cytometry, we validated the expression of several adhesion markers and homing receptors including ITGA1, CXCR6, and CX3CR1, which may mediate tissue residency and could be used for identification of human TRM. Pathway analysis suggests that TRM are responding to TCR stimulus, cytokine signaling, and chemokine signaling in situ. Finally, by comparing differential expression in our dataset to publicly available ChIP-Seq data, we identified transcription factors that could represent upstream regulators of the TRM gene signature in both CD4 and CD8 subsets and validated the expression of select transcription factors by qPCR and flow cytometry. Overall, our data comprehensively characterize the transcriptional and functional properties of both CD4 and CD8 human TRM and provide insight into mechanisms of tissue targeting and retention in the human immune system.

2017 Oral Presentation: **Human tissue-resident memory T cells are defined by core transcriptional and functional signatures in lymphoid and mucosal sites.**
Federation of Clinical Immunology Societies (FOCIS)
2017 Annual Meeting in Chicago, IL
FCE Fusion Award Recipient

Authors: **Brahma V. Kumar**, Wenji Ma, Michelle Miron, Tomer Granot, Rebecca Guyer, Dustin J. Carpenter, Takashi Senda, Harvey Lerner, Yufeng Shen, and Donna L. Farber

Abstract:

Resident memory T cells (TRM) have been identified in mouse models as having rapid protective capacities to site-specific pathogens and are key targets for vaccine-mediated protection. TRM-phenotype cells are detected in human tissues but defining characteristics of human TRM for CD4 and CD8 T cells including how TRM differ from circulatory subsets and potential mechanisms for site-specific targeting are not defined. We performed whole transcriptome profiling of memory T cell subsets from the lung, spleen and blood of 3 donors, for both CD4 and CD8 subsets, as well as in-depth phenotypic and functional profiling of memory T cells from 63 additional donors. Our results show that TRM are a transcriptionally distinct memory T cell subset in humans that can be identified by CD69 expression. We identify 30 core genes that define human TRM including the adhesion markers ITGA1 and ITGAE and homing receptors CXCR6 and CX3CR1, and we confirmed the surface expression of these genes and others by flow cytometry. TRM upregulated several cytokines transcriptionally and had a superior ability to produce IL-2, IL-17, and IFN-gamma during stimulations compared with circulatory memory T cells. Interestingly, TRM showed enrichment of cell cycle inhibition pathways, a result which was supported by reduced Ki67 expression in TRM. TRM also upregulated IL-10, DUSP6, and PD-1, together suggesting that TRM may exist in an inhibited state to prevent inflammation-mediated tissue damage. Overall, our data comprehensively characterize CD4 and CD8 human TRM and provide new insights into how TRM establish residency and mediate protection in humans.

Appendix E. Abstracts of contributing author manuscripts

Miron, M., **Kumar B.V.**, Meng, W., Granot, T., et al. Human lymph nodes maintain a distinct subset of TCF-1hi resident memory T cells throughout life. *Science*. Submitted.

Tissue resident memory T cells (TRM) predominate in barrier sites and mediate protective immunity, while their role in lymphoid tissues is undefined. Here we analyzed human memory CD8⁺T cells in different lymphoid compartments including bone marrow, spleen, and lymph nodes (LN) relative to lung within diverse individuals. We identify an organ-specific subset in human LN (designated TLN) not found in blood or other tissues, expressing high levels of TCF-1 and transcriptionally enriched for signatures of quiescence, self-renewal, and follicular-helper cells. High dimensional CyTOF analysis reveals TLN as intermediate in differentiation between naive and TRM cells, with circulating TEM cells the most differentiated. TLN exhibit higher TCR diversity, lower in vivo turnover, yet higher proliferative responses compared to memory cells in other lymphoid or mucosal sites. These findings establish human LN as reservoirs for diverse memory T cells poised for high expansion and TLN as important targets for in vivo immunotherapies.

Carpenter, D.J., Granot, T., Matsuoka, N., Senda, T., **Kumar, B.V.**, Thome, J.J.C., Gordon, C.L., Miron, M., Weiner, J., Connors, T., et al. (2017). Human immunology studies using organ donors: impact of clinical variations on immune parameters in tissues and circulation. *Am J Transplant*. doi: 10.1111/ajt.14434

Organ donors are sources of physiologically healthy organs and tissues for life-saving transplantation, and have been recently used for human immunology studies which are typically confined to the sampling of peripheral blood. Donors comprise a diverse population with different causes of death and clinical outcomes during hospitalization, and the effects of such variations on immune parameters in blood and tissues are not known. We present here a coordinate analysis of innate and adaptive immune components in blood, lymphoid (bone marrow, spleen, lymph nodes), and mucosal (lungs, intestines) sites from a population of brain-dead organ donors (2 months-93 years; n = 291) across eight clinical parameters. Overall, the blood of donors exhibited similar monocyte and lymphocyte content and low serum levels of pro-inflammatory cytokines as healthy controls; however, donor blood had increased neutrophils and serum levels of IL-8, IL-6, and MCP-1 which varied with cause of death. In tissues, the frequency and composition of monocytes, neutrophils, B lymphocytes and T cell subsets in lymphoid or mucosal sites did not vary with clinical state, and was similar in donors independent of the extent of clinical complications. Our results reveal that organ donors maintain tissue homeostasis, and are a valuable resource for fundamental studies in human immunology.

Granot, T., Senda, T., Carpenter, D.J., Matsuoka, N., Weiner, J., Gordon, C.L., Miron, M., **Kumar, B.V.**, Griesemer, A., Ho, S.H., et al. (2017). Dendritic Cells Display Subset and Tissue-Specific Maturation Dynamics over Human Life. *Immunity*, 46(3), 504-515. doi: 10.1016/j.immuni.2017.02.019

Maturation and migration to lymph nodes (LNs) constitutes a central paradigm in conventional dendritic cell (cDC) biology but remains poorly defined in humans. Using our organ donor tissue resource, we analyzed cDC subset distribution, maturation, and migration in mucosal tissues (lungs, intestines), associated lymph nodes (LNs), and other lymphoid sites from 78 individuals ranging from less than 1 year to 93 years of age. The distribution of cDC1 (CD141^{hi}CD13^{hi}) and cDC2 (Sirp- α ⁺CD1c⁺) subsets was a function of tissue site and was conserved between donors. We identified cDC2 as the major mature (HLA-DR^{hi}) subset in LNs with the highest frequency in lung-draining LNs. Mature cDC2 in mucosal-draining LNs expressed tissue-specific markers derived from the paired mucosal site, reflecting their tissue-migratory origin. These distribution and maturation patterns were largely maintained throughout life, with site-specific variations. Our findings provide evidence for localized DC tissue surveillance and reveal a lifelong division of labor between DC subsets, with cDC2 functioning as guardians of the mucosa.

Thome, J.J.*, Grinshpun, B.*, **Kumar, B.V.**, Kubota, M., Ohmura, Y., Lerner, H., Sempowski, G.D., Shen, Y., and Farber, D.L. (2016). Longterm maintenance of human naïve T cells through in situ homeostasis in lymphoid tissue sites. *Sci Immunol*, 1(6). doi:10.1126/sciimmunol.aah6506

Naïve T cells develop in the thymus and coordinate immune responses to new antigens; however, mechanisms for their long-term persistence over the human life span remain undefined. We investigated human naïve T cell development and maintenance in primary and secondary lymphoid tissues obtained from individual organ donors aged 2 months to 73 years. In the thymus, the frequency of double-positive thymocytes declined sharply in donors >40 years of age, coincident with reduced recent thymic emigrants in lymphoid tissues, whereas naïve T cells were functionally maintained predominantly in lymph nodes (LNs). Analysis of T cell receptor clonal distribution by CDR3 sequencing of naïve CD4⁺ and CD8⁺ T cells in spleen and LNs reveals site-specific clonal expansions of naïve T cells from individuals >40 years of age, with minimal clonal overlap between lymphoid tissues. We also identified biased naïve T cell clonal distribution within specific LNs on the basis of VJ usage. Together, these results suggest prolonged maintenance of naïve T cells through in situ homeostasis and retention in lymphoid tissue.

Appendix F. Curriculum Vitae

Education:

M.D./Ph.D.
(Anticipated 2019)

Columbia University, New York, NY
PhD in Immunology.
Advisor: Donna L. Farber, PhD.
Thesis: Identification and characterization of tissue-resident memory T cells in humans.

B.A.
(2011)

Johns Hopkins University, Baltimore, MD
Bachelor of Arts in Economics

Research:

July 2015– Present

Ph.D. Graduate Student

Laboratory of Donna L. Farber, PhD
Department of Immunology, Columbia University

Currently, I am studying tissue-resident memory T cells (TRM) in humans. TRM play an important role in defending against pathogens at peripheral sites; however, most of our knowledge about TRM comes from studies in mice. We obtain human tissues through a collaboration with the organ procurement agency, and in my project I isolate TRM and compare these cells to other memory subsets to determine defining characteristics of human TRM. My data show that TRM are a distinct memory T cell subset in humans and can be identified by CD69 expression. I further identified unique functional and phenotypic properties of TRM in humans. In this project we also compare human and mouse TRM and identify a core signature of 31 genes common to TRM from both species and common to TRM from multiple tissues sites.

In subsequent projects, I am now investigating TRM heterogeneity based on the ability to efflux fluorescent dyes. Our data suggest that effluxing TRM transcriptionally and functionally distinct TRM subset with features of quiescence. Our data also suggest that effluxing TRM may represent a less differentiated subset that gives rise to more effector-like non-effluxing TRM after stimulation.

2011–2012

Research Assistant

Laboratory of Attila Bacsı, PhD
Institute of Immunology, University of Debrecen, Hungary

Although ragweed pollen is one of the most common triggers of allergic asthma, whole pollen grains are too large to reach the lower airways. Dr. Bacsi's group previously demonstrated the release of subpollen particles (SPP) from ragweed pollen, which are small enough to penetrate the lower airways, and one of my main projects was to investigate mechanisms of SPP induced inflammation. Briefly, we found that dendritic cells (DCs), which exist in large numbers beneath the airways, are triggered by antigens and enzymes found in SPPs. SPPs trigger DC maturation, pro-inflammatory cytokine release by DCs, and these DCs are capable of priming T cells. We found that the mechanism of DC activation is largely a result of reactive oxygen species produced by enzymes contained within the SPPs.

2010–2011

Undergraduate Research Assistant

Johns Hopkins Hospital, Baltimore

I worked on two clinical projects related to Huntington's disease (HD). In the first project, we examined factors that contribute to institutionalization in HD, and in the second project we examined how CAG repeat length contributes to disease progression in HD. For these projects, I compiled patient data by chart review and created databases of patients that were used for studies. I performed statistical analyses using these databases. I am a coauthor on two publications resulting from these projects (listed below).

Publications:

Kumar, B.V., Connors, T., and Farber D.L. (2017) Human T cells and immune responses: impact of place and time. *Immunity*. In press.

Kumar, B.V., Ma, W., Miron, M., Granot, T., Guyer, R.S., Carpenter, D.J., Senda, T., Sun, X., Ho, S.H., Lerner, H., Friedman, A.L., Shen, Y., and Farber, D.L. (2017). Human Tissue-Resident Memory T Cells Are Defined by Core Transcriptional and Functional Signatures in Lymphoid and Mucosal Sites. *Cell Rep* 20, 2921-2934.

Carpenter, D.J., Granot, T., Matsuoka, N., Senda, T., **Kumar, B.V.**, Thome, J.J.C., Gordon, C.L., Miron, M., Weiner, J., Connors, T., et al. (2017). Human immunology studies using organ donors: impact of clinical variations on immune parameters in tissues and circulation. *Am J Transplant*. doi: 10.1111/ajt.14434

Granot, T., Senda, T., Carpenter, D.J., Matsuoka, N., Weiner, J., Gordon, C.L., Miron, M., **Kumar, B.V.**, Griesemer, A., Ho, S.H., et al. (2017). Dendritic Cells Display Subset and Tissue-

Specific Maturation Dynamics over Human Life. *Immunity*, 46(3), 504-515. doi: 10.1016/j.immuni.2017.02.019

Thome, J.J., Grinshpun, B., **Kumar, B.V.**, Kubota, M., Ohmura, Y., Lerner, H., Sempowski, G.D., Shen, Y., and Farber, D.L. (2016). Longterm maintenance of human naive T cells through in situ homeostasis in lymphoid tissue sites. *Sci Immunol*, 1(6). doi: 10.1126/sciimmunol.aah6506

Szabo, A., T. Fekete, G. Koncz, **B. V. Kumar**, K. Pazmandi, Z. Foldvari, B. Hegedus, T. Garay, A. Bacsi, E. Rajnavolgyi and A. Lanyi (2016). "RIG-I inhibits the MAPK-dependent proliferation of BRAF mutant melanoma cells via MKP-1." *Cell Signal* 28(5): 335-347.

Csillag, A., **B. V. Kumar**, K. Szabo, M. Szilasi, Z. Papp, M. E. Szilasi, K. Pazmandi, I. Boldogh, E. Rajnavolgyi, A. Bacsi and J. F. Laszlo (2014). "Exposure to inhomogeneous static magnetic field beneficially affects allergic inflammation in a murine model." *J R Soc Interface* 11(95): 20140097.

Pazmandi, K., Z. Agod, **B. V. Kumar**, A. Szabo, T. Fekete, V. Sogor, A. Veres, I. Boldogh, E. Rajnavolgyi, A. Lanyi and A. Bacsi (2014). "Oxidative modification enhances the immunostimulatory effects of extracellular mitochondrial DNA on plasmacytoid dendritic cells." *Free Radic Biol Med* 77: 281-290.

Pazmandi, K., **B. V. Kumar**, K. Szabo, I. Boldogh, A. Szoor, G. Vereb, A. Veres, A. Lanyi, E. Rajnavolgyi and A. Bacsi (2012). "Ragweed subpollen particles of respirable size activate human dendritic cells." *PLoS One* 7(12): e52085.

Szabo, A., R. M. Osman, I. Bacskai, **B. V. Kumar**, Z. Agod, A. Lanyi, P. Gogolak and E. Rajnavolgyi (2012). "Temporally designed treatment of melanoma cells by ATRA and polyI: C results in enhanced chemokine and IFNbeta secretion controlled differently by TLR3 and MDA5." *Melanoma Res* 22(5): 351-361.

Rosenblatt, A., **B. V. Kumar**, A. Mo, C. S. Welsh, R. L. Margolis and C. A. Ross (2012). "Age, CAG repeat length, and clinical progression in Huntington's disease." *Mov Disord* 27(2): 272-276.

Rosenblatt, A., **B. V. Kumar**, R. L. Margolis, C. S. Welsh and C. A. Ross (2011). "Factors contributing to institutionalization in patients with Huntington's disease." *Mov Disord* 26(9): 1711-1716.

Oral and Poster Presentations:

2017 Title: **Human tissue-resident memory T cells are defined by core transcriptional and functional signatures in lymphoid and mucosal sites.**
Federation of Clinical Immunology Societies (FOCIS)
2017 Annual Meeting in Chicago, IL
FCE Fusion Award Recipient

- 2017 Oral Presentation: **Core transcriptional and functional signatures define human resident memory T cells in lymphoid and mucosal sites.**
Columbia Center of Translational Immunology (CCTI) Seminar Series
Columbia University, New York, NY
- 2016 Oral Presentation: **A core transcriptional and functional profile distinguishes resident memory T cells in human.**
Middle-European Societies for Immunology and Allergology (MESIA)
2016 Annual Meeting in Budapest, Hungary
Travel Award Recipient
- 2016 Oral Presentation: **Profiling resident memory T cells in the human body.**
Biannual retreat for the Integrated Graduate Program
Columbia University, New York, NY

Other Professional Experience:

2012-2013

Psychiatric Technician

Montgomery County Emergency Services, Norristown, PA

I worked at an inpatient psychiatric hospital and that receives all involuntary commitments in Montgomery County, PA. I was responsible for interviewing and monitoring a group of approximately 8 patients each shift in order to write detailed notes about their behavior, responses to medication, and general progress. My other responsibilities included obtaining vital signs, feeding and bathing low-functioning patients, performing one-on-one observations for assaultive or suicidal patients, assisting group activities, and admitting new patients.